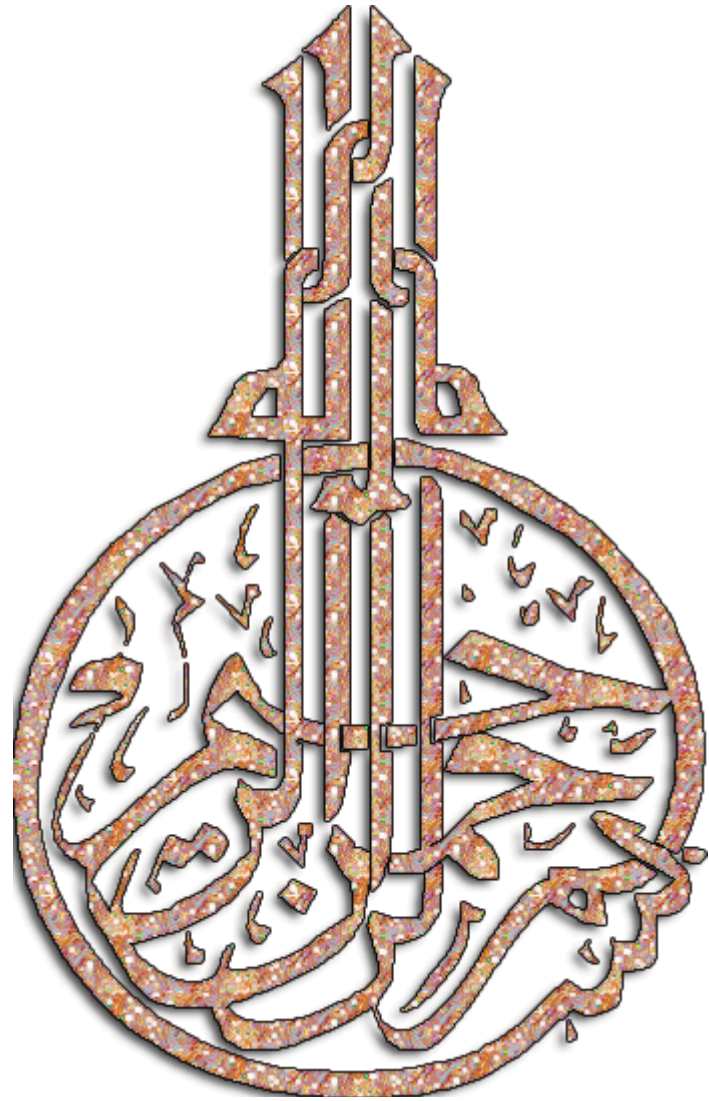


**Preconcentration, Determination and Chemical
Speciation of Trace Concentrations of some
Inorganic Pollutants in Aqueous Media**

Amal Ali Mohammed Bahafi

**A thesis submitted for the requirements of the degree of Doctor of Philosophy
(Analytical Chemistry)**

**FACULTY OF SCIENCE
KING ABDULAZIZ UNIVERSITY
JEDDAH – SAUDI ARABIA
Rajeb, 1434 H – May, 2013 G**



**Preconcentration, Determination and Chemical
Speciation of Trace Concentrations of some
Inorganic Pollutants in Aqueous Media**

By

Amal Ali Mohammed Bahafi

**A thesis submitted for the requirements of the degree of Doctor of
Philosophy (Analytical Chemistry)**

Supervised By

Prof.Dr. Abdulghani Hamza

Prof. Dr. Ameera Al-Attas

Rrof.Dr. Mohammed S. El-Shahawi

**FACULTY OF SCIENCE
KING ABDULAZIZ UNIVERSITY
JEDDAH – SAUDI ARABIA
Rajeb,1434H – May, 2013G**

Preconcentration, Determination and Chemical Speciation of Trace Concentrations of some Inorganic Pollutants in Aqueous Media

By

Amal Ali Mohammed Bahafi

This thesis has been approved and accepted in partial fulfillment of the requirements for the degree of Doctor of Philosophy in Chemistry (Analytical Chemistry)

EXAMINATION COMMITTEE

	Name	Rank	Field	Signature
Internal Examiner	Prof. El-Sayed Mahmoud Mabrouk	Full Professor	Electro-Analytical Chemistry	
External Examiner	Prof.Ekram Yousif Danish	Full Professor	Electro-Analytical Chemistry	
Advisor	Prof Abdulghani.Hamza	Full Professor	Analytical Chemistry	
Co-Advisor	Prof.Ameera Alattas	Full Professor	Analytical Chemistry	
Co-Advisor	Prof.Mohammed S. El-Shahawi	Full Professor	Analytical Chemistry	

**KING ABDULAZIZ UNIVERSITY
Rajab,1434H - , May, 2013G**

Dedicated to

My great parents
My sister and brother
My dear friends

Acknowledgement

In the name of Allah, most gracious, most merciful

My profound gratitude to **Prof. A.H. Soliman and Prof Amira Al-Attas** for his support, and kind advices during the experimental work and preparation of the thesis

I would like to thank my supervisor **Prof. M.S. El-Shahawi** for suggesting the point of research, valuable and expert supervision, guidance, helpful critiques, and encouragement throughout the experimental work and preparation of thesis.

I would like to express my sincere gratitude to **Professor Aisha Alturkustani** Chairman of the Department of Chemistry Department, Faculty of Education for Girls, Jeddah Branch. Special thanks to, all Chemistry staffs at Faculty of Education for their help and support during the work of this thesis.

I wish to express my heartfelt gratitude to my parents for their excellent support and encouragement.

Amal A. M. Bahafi

Preconcentration, Determination and Chemical Speciation of Trace Concentrations of some Inorganic Pollutants in Aqueous Media

Amal Ali Mohammed Bahfi

Abstract

There has been considerable interest in developing low cost methods for removal and precise determination of trace concentrations of heavy metal ions in aqueous media. Hence the in the present study is focused on: :Developing of a simple, low cost and sensitive square wave adsorptive cathodic stripping voltammetry (DP-CSV) method for trace mercury (II) determination using the reagent 4-(2-Thiazolylazo) - resorcinol (TAR). Plot of mercury (II) concentration *versus* cathodic peak current ($I_{p,c}$) was linear over a range of concentration ($1-12 \mu\text{g L}^{-1}$). The method was applied successfully for the analysis of mercury (II) in water samples. The method was validated by comparison with reported methods; ii. Deploying a precise and selective SQ -CSV method for the analysis of trace concentrations of palladium (II) based upon the adsorptive accumulation of the resulting palladium(II)-TAR complex on the HMDE, followed by the stripping voltammetric measurements of the resulting $i_{p,c}$ of the adsorbed complex vs. Ag/AgCl electrode. The method was applied for the analysis of palladium(II) in various water samples and compared successfully with the standard ICP-MS method. The method provide good correlation with the ICP-MS data for the analysis of trace concentration of palladium(II) complex species and finally iii. Studying the retention profile, kinetics, and thermodynamic characteristics of arsenic(III) uptake by the local clay. A dual retention mechanism for arsenic (III) sorption involving a “weak base anion ion exchanger” and/ or “solvent extraction” of

the $[\text{AsCl}_4]^-_{\text{aq}}$ and an added component for surface adsorption was proposed.
retention onto the sorbent The sorption isotherm.

List of Contents

	Page
Acknowledgment	ii
Abstract	iv
List of Figures	ix
List of Tables	xiii
English Summary	xiv
List of Abbreviations	xi
Preliminary Postgraduate Courses	xvii

Chapter I

General Introduction

	Page
1.1 Introduction	2
1.2 Occurrence, toxicity and determination of mercury.	4
1.3 Occurrence and determination of palladium	13
1.4 Occurrence and determination of arsenic.	19
1.5 Aim of current study	26
1.6 References	29

Chapter II

Chemical Speciation and Determination of Mercury Species by Adsorptive Differential Pulse Cathodic Stripping Voltammetry using 4-(2-Thiazolylazo) resorcinol Reagent

	Page
2.1 Introduction	40
2.2 Experimental	45
2.2.1 Reagents and materials	45

2.2.2	Apparatus	45
2.2.3	General DP-CSV procedures for mercury (II) – TAR complex Recommended procedures for mercury(II) determination	46
2.2.4	Recommended procedure for mercury determination	47
2.2.5	Analytical applications	48
2.2.5.1	Analysis of mercury in certified reference material (<i>CRM, Soil 7- IAEA</i>) by the developed DP-CSV method	48
2.2.5.2	Analysis of labile mercury (II) complex in tap- and drinking water samples by the developed DP-CSV method	49
2.2.5.3	Chemical speciation of labile and complexed fractions of mercury (II) in water samples by the developed DP-CSV method Results and discussion	49
2.3	Characterization of Hg-TAR	50
2.3.1	Electrochemical behaviour of Hg (II) – TAR complex:	50
2.3.2	Analytical parameters	55
2.3.3	Analytical performance of the developed DP-CSV procedure	63
2.3.4.	Reference study	69
2.3.5	Analytical application	73
2.3.6	Analysis of certified reference material (<i>IAEA Soil-7</i>)	73
2.3.6.1	Analysis of mercury (II) in tap- and drinking water samples	73
2.3.6.2	Chemical speciation of mercury in drinking	74
2.3.6.2	Conclusions	75
2.4	References	76

Chapter III

Direct Determination of Trace Concentrations of Palladium in wáter by Square adsorptive cathodic stripping voltammetry using using the 4-(2-Thiazolylazo) – resorcinol

	Page	
3.1	Introduction	82
3.2	Experimental	87
3.2.1	Reagents and materials	87
3.2.2	Apparatus	87
3.2.3	Recommended analytical procedure	88
3.2.4	Analytical applications	89
3.2.4.1	Analysis of certified reference materials	89
3.2.4.2	Analysis of palladium in water samples	90
3.3.	Results and discussion	90
3.3.1	Characteristics of the Palladium (II) – TAR	90
3.3.2	Electrochemical behaviour of palladium(II) – TAR complex	93
3.3.3	Influence of analytical parameters	101
3.3.4	Analytical performance of the developed SW-CSV method	109
3.3.5	Influence of diverse ions on the sensitivity of the developed method	112
3.3.6	Analytical applications	113
3.3.6.1	Analysis of Pd in CRM (<i>IAEA Soil-7</i>)	113
3.3.6.2	Analysis of palladium in water sample	114
3.4	Conclusions	115
3.5	References	116

Chapter IV

Chemical Speciation of Trace Concentrations of Arsenic(III & V) in Water and Wastewater Samples by Local Clay of Saudi Arabia Prior inductively coupled plasma–optical emission spectrometry

	Page	
4.1	Introduction	120
4.2	Experimental	126
4.2.1	Reagents and materials	126
4.2.2	Apparatus	127
4.2.3	Clay deposits	129
4.2.4	Preparation of clay packed column	135
4.2.5	General batch experiments	136
4.2.6	Flow experiments	137
4.2.6.1	Retention and recovery of arsenic (III)	137
4.2.6.2	Extraction procedures of arsenic (V) species	138
4.2.7	Analytical applications	138
4.2.7.1	Analysis of arsenic(III) in tap and wastewater samples	138
4.2.7.2	Analysis of arsenic (V) in tap and wastewater samples	139
4.2.7.3	Analysis of arsenic (V) in tap and wastewater samples	130
4.3	Results and discussion	140
4.3.1	Characterization of clay minerals	140
4.3.2	Retention profile of arsenic(III) on local clay minerals	145
4.3.3	Kinetic behavior of arsenic (III) sorption onto local clay sorbent	150
4.3.4	Sorption isotherms of arsenic(III) species onto clay sorbent	154
4.3.5	Thermodynamic characteristic of arsenic(III) retention onto clay sorbent	161
4.3.6	Chromatographic separation of arsenic (III) by clay packed column	164
4.3.7	Analytical performance of the developed clay packed columns	167
4.3.8	Analytical applications of clay packed column	169
4.4	Conclusion	170
4.5	References	171
	Conclusion and concluding remarks	177
	Future work	178
	Publications	179

LIST OF FIGURES

CHAPTER I: General Introduction

- 1.1 The biogeochemical mercury cycle. 10

CHAPTER II: Chemical Speciation and Determination of Mercury

Species by Adsorptive Differential Pulse Cathodic Stripping

Voltammetry using 4-(2-Thiazolylazo) resorcinol Reagent

- 2.1 Structure of TAR 42
- 2.2. Electronic spectra of TAR and its mercury(II) complex in aqueous medium. 51
- 2.3 FTIR spectra of TAR (A) and its mercury(II) complex (B). 54
- 2.4 Proposed chemical structural formula of mercury(II) – TAR complex. 54
- 1.5 DP-CSVs of TAR(9.8×10^{-7} M) in presence of mercury (II) ions(4.9×10^{-7} M) at various B-R buffer solutions at the HMDE vs. Ag/AgCl reference electrode at 50 mVs^{-1} scan rate and 50 mV pulse amplitude. 56
- 2.6 Plot of cathodic peak potential ($E_{p,c}$) of mercury (II)-TAR complex vs. solution pH at HMDE. 57
- 2.7 Cyclic voltammograms of mercury (II)-TAR at pH 6-7 at various scan rates (20-1000 mVs^{-1}) at HMDE vs. Ag/AgCl electrode. 58
- 2.8 Plot of $E_{p,c1}$ vs. $\log v$ of Hg-TAR complex at pH 6-7 at HMDE vs. Ag/AgCl reference electrode. 59
- 2.9 Plot of $E_{p,c1}$ vs. $\log v$ of Hg-TAR complex at pH 6-7 at HMDE vs. Ag/AgCl reference electrode. 59

- 2.10 Plot of $\log i_{p,c1}$ vs. $\log v$) of Hg-TAR complex at pH 6-7 at 60
HMDE vs. Ag/AgCl reference electrode.
- 2.11 Plot of current function ($i_{p,c} / v^{1/2}$) vs. scan rate at HMDE vs. Ag/AgCl 61
electrode.
- 2.12 Plot of CV cathodic peak current ($i_{p,c1}$) vs. scan rate at HMDE vs. 63
Ag/AgCl electrode at pH 6-7 of Hg(II)-TAR complex.
- 2.13 Effect of pH on peak current of Hg(II)-TAR. Conditions: [TAR], 64
 9.8×10^{-7} M; $[Hg^{II}]$, 4.9×10^{-8} M; 50 mVs^{-1} scan rate and 50 mV pulse
tude.
- 2.14 Plot of Effect of the cathodic peak current of Hg(II)-TAR 65
vs. Accumulation time (s). Conditions: TAR concentration
 $=9.8 \times 10^{-7}$ M; $Hg^{2+} = 4.9 \times 10^{-11}$ M; deposition potential
 $=-0.45$ V, scan rate 60 mVs^{-1}
and pulse amplitude of 60 mV.
- 2.15 Plot of the cathodic peak current of Hg(II)-TAR vs. Deposition 66
potential (V) Conditions: TAR concentration $=9.8 \times 10^{-7}$ M; $Hg^{2+} =$
 4.9×10^{-11} M; deposition time $=-60$ s, scan rate 60 mVs^{-1} and pulse
amplitude of 60 mV.
- 2.16 Effect of scan rate on the cathodic peak current of Hg(II)-TAR vs. 67
Accumulation time (s). Conditions: TAR concentration $=9.8 \times 10^{-7}$ M;
 $Hg^{2+} = 4.9 \times 10^{-7}$ M; deposition potential $=-0.04$ V, scan rate 60 mVs^{-1}
and pulse amplitude of 60 mV.
- 2.17 Effect of pulse amplitude on peak current. Conditions: [TAR] 9.8×10^{-7} 68
M; $[Hg^{II}]$, 4.9×10^{-11} M; deposition potential, -0.04 V.

- 2.18 Influence of TAR concentration on the $i_{p,c}$ at -0.38 V of the DP-CSV of mercury(II)-TAR complex at pH 6-7 at HMDE vs. Ag/AgCl . 69
Mercury (II) ions ($1.5 \times 10^{-5} \text{ M}$); E_{acc} -40 mV; t_{acc} of 60 s; V of 60 mVs⁻¹ and 60 mV pulse amplitude.
- 2.19 DP-CSVs of Hg(II)-TAR complex in the presence of various concentrations of mercury ($7.5 \times 10^{-9} - 5.25 \times 10^{-7}$) mol L⁻¹) at HMDE vs. Ag/AgCl electrode at pH 6-7 under the optimum operational parameters. 71
- 2.20 Calibration plot of Hg(II) -TAR complex in the presence of various concentrations of mercury ($7.5 \times 10^{-9} - 5.25 \times 10^{-7}$) mol L⁻¹) at HMDE vs Ag/AgCl electrode at pH 6-7 under the optimum operational parameters. 72

CHAPTER III: Direct Determination of Trace Concentration of Palladium in water by Square Wave Adsorptive Cathodic Stripping Voltammetry Using 4-(2-Thiazolylazo)-Resorcinol Reagent

- 3.1 Visible spectra of the reagent TAR and its Pd(II)-TAR complex 91
- 3.2 IR spectrum of palladium-TAR chelate 92
- 3.3 Proposed chemical structure of Pd(II)-TAR complex. 93
- 3.4 Square wave -CSV of palladium (II)-TAR complex species in various B-R buffers of pH 4, 5, 6, 7.04 and 8.1 at the HMDE vs. Ag/AgCl. P, [TAR] = $8.9 \times 10^{-8} \text{ M}$; [Pd^{II}], $1.6 \times 10^{-8} \text{ M}$; scan rate = 100 mV/s; pulse amplitude of 60 mV 95
- 3.5 Plot of cathodic peak potential of palladium (II)-TAR with pH 7 at 100 mVs⁻¹ scan rate and 50 mV pulse amplitude 96

3.6	Cyclic voltammograms of palladium (II) - TAR at various scan rates (30 – 100 mV s ⁻¹) at pH 7 at HMDE vs. Ag/AgCl. [TAR] = 4.9 x 10 ⁻⁷ mol L ⁻¹ and palladium (II) concentration = 9 x 10 ⁻⁸ mol L ⁻¹	97
3.7	Plot of E _{p,c} vs. log v of Pd(II)-TAR complex at pH 7-8 at HMDE vs. Ag/AgCl reference electrode	98
3.8	Plot of log i _{p,c} vs. log v of Pd-TAR complex at pH 7-8 at HMDE vs. Ag/AgCl reference electrode.	99
3.9	Plot of i _{p,c} vs. square root of scan rate (v) of palladium (II)-TAR complex at pH 7-8 at HMDE and Ag/AgCl reference electrode	100
3.10	Plot of current function (i _{p,c} / v ^{1/2}) vs. scan rate of Pd(II)-TAR complex at HMDE vs. Ag/AgCl electrode.	101
3.11	Influence of pH effect on the cathodic peak current of Pd(II)-TAR complex at HMDE vs. Ag/AgCl reference electrode. Conditions: [TAR], 9x10 ⁻⁸ M; [Pd ^{II}], 1.6x10 ⁻⁸ M; deposition potential, -0.1V; deposition time, 180 s; pulse amplitude, 0.05 V; scan rate, 50 mV s ⁻¹ .	103
3.12	Influence of deposition potential on the cathodic peak current of Pd(II)-TAR complex at HMDE vs. Ag/AgCl reference electrode. Conditions: [TAR] = 8.9x10 ⁻⁸ M, [Pd ^{II}], 1.6x10 ⁻⁸ M, accumulation time, 180 s, pulse amplitude = 50 m V and scan rate of 50 mV s ⁻¹	104

- 3.13 Influence of deposition potential on the cathodic peak current of Pd(II)-TAR complex at HMDE vs. Ag/AgCl reference electrode. Conditions: [TAR] = 8.9×10^{-8} M, [Pd^{II}], 1.6×10^{-8} M, accumulation time, 180 s, pulse amplitude = 50 mV and scan rate of 50 mV s^{-1} . 105
- 3.14 Plot of pulse amplitude on the cathodic peak current. Conditions: [TAR] = 8.9×10^{-8} M, [Pd^{II}] = 1.6×10^{-8} M, deposition potential = 0.15 V, deposition time = 200 s and 55 mV/s scan rate. 106
- 3.15 Effect of scan rate (mV/s) on the cathodic peak current. Conditions: [TAR], 8.9×10^{-8} M; [Pd^{II}], 1.6×10^{-8} M; deposition potential, 0.15 V; deposition time, 180 s; pulse amplitude, 0.05 V. 107
- 3.16 Plot of TAR concentrations versus cathodic peak potential at pH 7-8 at HMDE vs. Ag/AgCl reference electrode. Conditions: Deposition potential = 0.15 V, deposition time = 200 s; scan rate 50 M/s and pulse amplitude of 50 mV. 109
- 3.17 SW-CSVs of Pd(II)-TAR complex in the presence of various concentrations of palladium (5.0- – 53 $\mu\text{g/L}$) at HMDE vs. Ag/AgCl electrode at pH 6-7 under the optimum operational parameters 111
- 3.18 Calibration plot of palladium(II) -TAR complex in the presence of various concentrations of palladium (7.5×10^{-9} – 5.25×10^{-7}) at HMDE vs. Ag/AgCl electrode at pH 6-7 under the optimum operational parameters. 112

3.19	Typical calibration plot for the analysis of palladium (II) in drinking water at pH 7-8 at HMDE vs. Ag/AgCl reference electrode.	114
------	--	-----

CHAPTER IV: Chemical Speciation of Trace Concentrations of Arsenic(III & V) in Water and Wastewater Samples by Local Clay of Saudi Arabia Prior inductively coupled plasma–optical emission spectrometry

4.1	Preparation of polyurethane foam packed column.time.	128
4.2	Simplified geological and location map of the sedimentary clay deposits in Makkah and Rabigh quadrangles.	130
4.3	A landsat image showing Al – Khyat clay quarry, Khulays area. Basalt flows at the top (dark black areas).	131
4.4	Bedded clay deposits with Harrat basalt at the top (Right top)..	132
4.5	Bedded multicolored clay deposits with montmorillonite rich beds (chocolate brown)..	133
4.6	Chemical structures of clay minerals (Montmorillonite (I), Kaolinite (II) and illite (III)).	141
4.7	XRD pattern of bulk sample number 1.	142
4.8	XRD pattern of bulk sample number 2.	142

4.9	XRD pattern of bulk sample number 3.	143
4.10	XRD pattern of bulk sample number 4.	143
4.11	XRD pattern of bulk sample number 5.	144
4.12	XRD pattern of untreated (Red); glycolated (Violet) and heated sample 3 at 550 °C (Green).	144
4.13	XRD pattern of untreated (Red); glycolated (Violet) and heated sample5 at 550 °C (Green).	145
4.14	Effect of pH on the sorption percentage of arsenic(III) from the aqueous solutions onto clay minerals at 25±1 °C after 1 h shaking time.	147
4.15	Influence of shaking time on the percentage uptake (%) of arsenic (III) from the aqueous solutions at pH 6-7 onto clay minerals at 25±1 °C.	148
4.16	Rate of arsenic(III) retention from the test aqueous solution of pH 6-7 onto clay minerals at 25±1 °C.	149
4.17	Weber-Morris plots of the sorbed arsenic(III) concentration from aqueous solution of pH 6-7 vs. square root of shaking time onto clay minerals at 25±1 °C .	151
4.18	Lagergren plot of the kinetics of arsenic (III) sorption from the aqueous solution of pH 6-7 onto unlo clay minerals at 25 ±0.1°C	152
4.19	Bhattacharya- Venkobachar plots of arsenic(III) uptake from aqueous solution of pH 6-7 onto clay sorbent at 25±0.1°C.	154

4.20	Sorption isotherms of arsenic (III) uptake from the aqueous solution of pH 6-7 onto clay sorbent at $25\pm 0.1^\circ\text{C}$.	155
4.21	Plot of D of arsenic sorption vs. As concentration in the bulk aqueous solutions of pH 6-7 onto clay minerals at $25\pm 0.1^\circ\text{C}$.	156
4.22	Freundlich sorption isotherm of arsenic(III) retention from the aqueous solution of pH 6-7 onto clay minerals at $25\pm 0.1^\circ\text{C}$.	158
4.23	Langmuir sorption isotherms of arsenic(III) uptake from the aqueous solutions of pH 6-7 onto clay sorbent at $25\pm 0.1^\circ\text{C}$.	159
4.24	Plot of $\ln K_c$ of arsenic(III) sorption versus $1000/T$ (K^{-1}) from the aqueous solutions of pH 6-7 onto clay sorbent.	162
4.25	Vant-Hoof plot of the distribution ratio ($\log D$) vs. $1000/T$ (K^{-1}) for arsenic (III) retention onto clay sorbent.	163
4.26	Chromatogram of recovery of arsenic (III) recovery from the aqueous solution by clay packed column using nitric acid as eluating agent at 3 mL min^{-1} flow rate.	168

LIST OF TABLES

CHAPTER I: General Introduction

- 1.1 Concentration ranges of total mercury in different natural waters 8

CHAPTER II: Chemical Speciation and Determination of Mercury

Species by Adsorptive Differential Pulse Cathodic Stripping

Voltammetry using 4-(2-Thiazolylazo) resorcinol Reagent

- 2.1 Voltammetric method of Mercury (II) determination 43
- 2.2 Analysis of mercury spiked to drinking water samples (n=6) by the developed methods 75

CHAPTER III: Direct Determination of Trace Concentration of Palladium in water by Square Wave Adsorptive Cathodic Stripping Voltammetry Using 4-(2-Thiazolylazo)–Resorcinol Reagent

- 3.1 Voltammetric methods for palladium (II) determination 85

CHAPTER IV: Chemical Speciation of Trace Concentrations of Arsenic(III & V) in Water and Wastewater Samples by Local Clay of Saudi Arabia Prior inductively coupled plasma–optical emission spectrometry

- 4.1 Represented major and trace constituents of bulk samples (1-3) from Khulays Formation (KH) [63] 135
- 4.2 Represented major and trace constituents of bulk samples (1-3) from Khulays Formation (KH) [63] 165
- 4.3 Average recovery percentage (%) of arsenic(V) ions from deionized water by the developed clay packed column at 5 mL min⁻¹ flow rate[†] 166

English Summary

Recently great attention has been focused on developing low cost and efficient procedures for removal and / or minimization of inorganic contaminants in water e.g. arsenic, mercury, lead, antimony etc. On the other hand, improving the sensitivity and selectivity of trace metals analysis represents an important task. Thus, many research papers have been focused on the development of novel analytical methods of high sensitivity and selectivity for trace and ultra trace contaminants . Moreover, the direct determination of trace and ultra trace metal ions usually requires an efficient preconcentration step in order to bring the concentration of the analyte within the dynamic measuring range of detection and to eliminate the matrix effect and interference that can not be manipulated by the measuring device. Therefore, the overall work in this thesis can be summarized as follows:

1. Chapter one includes an excellent literature survey on the source, occurrences, mode of action, toxicity, methods of removal and / or subsequent determination of heavy metal ions in water at trace and ultra trace concentrations. The survey also involves the sources, occurrences, mode of action, toxicity and analysis of heavy metals and food colorants.
2. Chapter two includes the following:
 - i. Developing of a simple, low cost and sensitive square wave adsorptive cathodic stripping voltammetry (DP-CSV) method for trace determination of mercury (II) using the reagent 4-(2-Thiazolylazo) - resorcinol (TAR). The method was based upon the adsorptive deposition of mercury (II) –TAR complex at hanging mercury drop electrode (HMDE), followed by the reduction of the adsorbed complex at -0.45 V versus Ag/AgCl reference electrode in Britton- Robinson (B-R) buffer at the optimum pH. The mechanism of the electrode reaction was discussed using cyclic

voltammetry at HMDE and Pt working electrode. The optimum conditions for the analysis of mercury (II) include 2.3×10^{-8} mol L⁻¹ (TAR), accumulation potential of – 0.5 V (versus Ag:AgCl), accumulation time of 150 s, scan rate of 60 mV/s and pulse amplitude of 70 mV.

ii. Plot of mercury (II) concentration *versus* cathodic peak current ($I_{p,c}$) was linear over a range of concentration (1-12 µg L⁻¹). The values of the lower limits of detection (LOD) and quantification (LOQ) of the developed method were calculated from calibration curve as 0.15 µg L⁻¹ and 0.49 µg L⁻¹, respectively. A relative standard deviation (RSD) of 1.054% was achieved for mercury (II) at specific concentration. The method was applied successfully for the analysis of mercury (II) in water samples and the recovery was in the range of 98% - 101%. The method was validated by comparison with reported methods.

3. Chapter three covered the following:

i. The redox behavior of the palladium(II) –TAR chelate in B-R buffer at different pH. The nature and mechanism of the electrode reaction were assigned at the HMDE. The dependence of the CV response of the observed cathodic peaks on the scan rates was typical of an irreversible reaction mechanism. The calculated value of the electron transfer coefficient (α) and the linear plot of $E_{p,c}$ vs. $\log v$ at the optimum pH confirmed the irreversible nature of the developed cathodic peak. The plots of the $i_{p,c}$ and $i_{p,c} / v^{1/2}$ vs. v were linear confirming that, the reduction step is diffusion controlled process and the reduction process favors the well known chemical reaction of the type EE mechanism.

ii. Deploying a precise and selective SQ -CSV method for the analysis of trace concentrations of palladium (II) in complicated matrixes. The method was based upon the adsorptive accumulation of the resulting palladium(II)-TAR complex on

the HMDE, followed by the stripping voltammetric measurements of the resulting $i_{p,c}$ of the adsorbed complex vs. Ag/AgCl electrode. The lower limits of detection, lower limits of quantification and the linear dynamic range of the developed method were determined. The method was applied for the analysis of palladium(II) in various water samples and compared successfully with the standard ICP-MS method. The method provide good correlation with the ICP-MS data for the analysis of trace concentration of palladium(II) complex species.

4. Chapter four was focused on:

i. The retention profile of arsenic(III) species in aqueous media onto local clay in an attempt to develop an efficient procedure for removal and subsequent determination of arsenic(III) in aqueous media using clay packed column. The method was also used for the retention of arsenic(V) after reduction to arsenic(III) using SO_2 gas.

ii. The kinetics, and thermodynamic characteristics of arsenic(III) uptake by the local clay were critically investigated and are properly assigned. The most probable retention mechanism for arsenic (III) sorption involving a “weak base anion ion exchanger” and/ or “solvent extraction” of the $[\text{AsCl}_4]_{\text{aq}}$ retention onto the sorbent. The sorption isotherm of arsenic (III) over wide rang of equilibrium concentrations was also studied and the system was modeled by Langmuir, the Dubinin – Radushkevich (D – R), and Freundlich isotherms. The capacity of clay towards arsenic (III) calculated from sorption isotherm was determined.

Preliminary Postgraduate Courses

Besides the work carried out in this thesis, the candidate Miss. Amal Ali Mohammed Bahafi has attended and successfully passed the following postgraduate courses:

- 1. Advanced Computational Chemistry**
- 2. Advanced Computer Science**
- 3. Selected Topics in Analytical Chemistry**
- 4. Advanced Instrumental Analysis**
- 5. Selected Topics in Analytical Chemistry**

Prof. Aisha Alturkustani.

Chairman of Chemistry Department

List of Abbreviations

H ₂ Dz	Dithizone
HMDE	Hanging mercury dropping electrode
SCE	Standard Calomel Electrode
HG-ICP-AES	Hydride generation inductively coupled plasma atomic emission spectrometry
HPLC	High - performance liquid chromatography
ASV	Anodic Stripping Voltammetry
CVS	Catodic Stripping voltammetry
SQ-CSV	Square wave cathodic stripping voltammetry
DP-CSV	Differential pulse cathodic voltammetry
LOD	Lower limit of detection
LOQ	Lower limit of quantification
I _{p, c}	Cathodic peak current
E _{p, c}	Cathodic peak potential
I _{p, a}	Anodic peak current
E _{p, a}	Anodic peak potential
ν	Sweep rate mV/s
N _{α}	Number of electron transfer
A	Electron transfer coefficient
AAS	Atomic Absorption spectrometry
Ag/AgCl	Standard silver - silver chloride electrode
B-R	Britton Robinson buffer
ET-AAS	Electrothermal atomic absorption spectrometry
ICP-MS	Inductively coupled plasma mass spectrometry
L-L	Liquid-liquid extraction
PGEs	Platinum group elements
XRD	X -ray diffraction

Chapter1

General Introduction

1.1 Introduction

Our environment contains countless numbers of toxic metal ions e.g. arsenic, antimony, mercury, lead, cadmium, etc and platinum group elements (PGEs) e.g. Pt, Pd etc and compounds which influence on natural components of the environment e.g. soil, water and air. The pollution of environment with metal ions represents one of the most serious environmental problems because of their high stability in contaminated site and complexity of mechanism in biological toxicity. Nowadays, the contamination of water by toxic metal ions through the discharge of industrial and municipal wastewater is a worldwide environmental problem. The term “heavy metal” refers to the metallic elements having density greater than or equal to 6.0 g mL^{-1} . Heavy metals are introduced into environment through dumping wastes, effluents leading to heavy metals runoff of terrestrial system and geological weathering [1, 2].

Arsenic, mercury, bismuth, lead, cadmium, antimony, copper, and others have the ability to accumulate in bottom sediments. Due to various processes of remobilization, these metals may be released and moved into the biological or food chain and concentrate in fish and other edible organisms, thereby, reaching humans and causing chronic or acute diseases [2]. This class of chemicals occurs in a minute concentration in natural biological systems and exerts a beneficial or harmful effects on plant, animal and human life. Moreover, biomagnifications, i.e. the tendency of some chemicals e.g. heavy metals to pass through the food chain resulting in progressive increase of its levels at each tropic level may occur and enter into the environment [3]. The toxicity and the bioavailability of heavy metals in water depend on its pH, conductivity, and dissolved substances [3]. Moreover, it is found that the

edges, feeding habits of fish or aquatic animals and their retention time in polluted water affect the accumulation of the heavy metals ions such class of organisms [4, 5]. Therefore, the subsequent survey will briefly discuss occurrence, toxicity, determination methods of toxic pollutants under study e.g. Hg and cyanide.

Pollution with heavy metals, toxic anions and others has been a matter of great concern for human health and animals [6-10]. Mercury, arsenic (III, V), chromium(VI), lead, cadmium, bismuth(III, V), antimony(III, V) species are one of the most elements affecting the environment. Thus, recent years have seen an upsurge of interest in monitoring and controlling environmental pollution from trace elements [6, 7]. Therefore, great attention has been oriented towards developing precise and low cost methods for removal and determination of heavy metal ions in various matrices including industrial water effluents [9 -10].

Water pollution occurs when pollutants are discharged into water bodies without adequate treatment to remove harmful compounds [11]. There are many causes for water pollution but two general categories exist: direct and indirect contaminant sources. Direct sources include effluent outfalls from factories, refineries, mining and waste treatment plants. Indirect sources include contaminants that enter the water supply from soils/groundwater systems and from the atmosphere via rain water. Soils and ground waters contain the residue of human agricultural practices and improperly disposed of industrial wastes [11, 12]. Atmospheric contaminants are also derived from human practices (such as gaseous emissions from automobiles and factories) [11,12]. Heavy metal ions toxicity are in significant in human body and are

capable of causing ecological risk to aquatic organisms. Heavy metal ions could also gradually accumulate in human body through food chain and cause damage to human health [14]. Thus, the determination of trace metals in the environmental samples including food materials has been continuously performed in order to designate the level of pollution as the number of ecological and health problems associated with environmental contamination continue to rise. Direct instrumental analysis of these samples is difficult because of complex formation and significant matrices, which invariably influence normal instrumental analysis. In addition, some metals have low concentrations, which are near or below the limit of detection of the instrument, hence effective preconcentration step can solve the above two problems and leads to simple determination of heavy metal ions in complicated matrices[15].

1.2 .Occurrence, toxicity and determination of mercury.

Mercury is a highly toxic element and the large scale production, uses mostly in chloralkali and electrical industries and its release from the fossil fuels combustion give rise to serious environmental concerns [16].Mercury (II) has a toxicity nature and harmful effects even at low level of concentrations in environmental, industrial, agriculture and biological fields. The toxicological effects of mercury include neurological damage, irritability, paralysis, blindness and insanity. Mercury (II) enters the environment from a large number of miscellaneous sources related to human use. Mercury metal exists in two oxidation states I and II, the latter being is more stable. The almost unique dimeric Hg^{2+} disproportionates readily to mercury (II) and elemental mercury

(Hg⁰). Mercury (II) forms strong complexes with halides and sulphur donors. Many mercury compounds are covalent but water soluble. Volatilization of Hg⁰ is the most widely used separation technique prior to atomic spectroscopy determination. The use of NaBH₄ or NaBEt₄ to convert mercury into volatile species is popular as it enables a simultaneous derivatization of organo-mercury compounds [17]. The most widely used reductants include SnCl₂ and NaBH₄ [18-20], usually applied in acid media. The advantages of NaBH₄ include rapid reaction kinetics, lower susceptibility to interferences, applicability to slurries and the ability to reduce organic Hg compounds to Hg⁰ (not all the compounds are reduced) Electrolytic reduction of Hg(II) using Cr(II) ions produced from Cr(III) in a flow-type cell has been reported [21].

preconcentration and trace determination of Hg(II) based on the total fluorescence quenching using a 1,10-phenanthroline (1,10-phen) and dichlorofluorescein (DCF) ternary complex after homogeneous liquid-liquid extraction of the metal complex has been developed by Panichlertumpi and Chanthai , 2013 [22]. Hg(II) ions were dissolved in acid and the sample was complexed with an excess amount of diethyldithio -carbamate (DDTC). The complex of Hg(II)-DDTC formed in an aqueous phase has been extracted into a layer of perfluorooctanoic acid dissolved in lithium hydroxide solution, resulting in 100 μL of the sediment liquid phase prior to analysis of the ternary complex by spectrofluorophotometry [22]. Under the optimized conditions with a preconcentration factor between 15 and 20 using a mixture of 0.2 mol L⁻¹ acetate buffer pH 4.5, 2.5 × 10⁻³ mol L⁻¹ 1,10-phen, 1% (v/v) Triton X-100 and 2.9 × 10⁻⁶ mol L⁻¹ DCF in 15 mL final volume, the decrease in fluorescence intensity of the ternary complex was measured against the reagent

blank, in the absence of Hg(II) ions, at the excitation and emission wavelengths of 504.0 and 525.0 nm, respectively. The calibration curve was widely linear over the range of 4.0 $\mu\text{g L}^{-1}$ to 2.0 mg L^{-1} with a correlation coefficient greater than 0.997. The method recovery of Hg(II) was about 76.9 to 98.2% at a concentration of 250 $\mu\text{g L}^{-1}$. The relative standard deviation (RSD) was below 5.5% with a detection limit of 1.0 $\mu\text{g L}^{-1}$.

Graphite furnace AAS offers a detection limit of about 2 ng ml^{-1} . As all mercury compounds are extremely volatile, losses occur above 2000C even in the presence of modifiers. Palladium as $\text{Pd}(\text{NO}_3)_2$, was found to be the most efficient matrix modifier [23, 24]. Cationic interferences are unlikely owing to the stability of the Pd-Hg compound [25]; chloride, sulphate, iodide and cyanide interfere by forming stable and volatile compounds in the condensed and/or gas phase [25]. Inductively coupled plasma atomic emission spectrometry (ICP-AES) is one of the techniques used for Hg determination nowadays. It offers a detection limits about 20-50 ng m^{-1} at the most sensitive 253.65 and 194.23 nm lines. The 253.65 nm line is overlapped by Fe and Co. Despite its freedom from non-specific background absorption of volatile organic species ICP AES is seldom used. Mercury has seven stable isotopes ^{196}Hg (0.15%), ^{198}Hg (10.02%), ^{199}Hg (16.83%), ^{200}Hg (23.13%), ^{201}Hg (13.22%), ^{202}Hg (29.80%), ^{204}Hg (6.85%) and thus it is readily amenable to isotope dilution. Detection limits reported for inductively coupled plasma mass spectrometry (ICP-MS) were 30 pg ml^{-1} with direct injection nebulization [26]. The sensitivity is increased by vapour introduction of Hg.

The toxicity of mercury species is highly dependent on its chemical form. The determination of organic and inorganic Hg in addition to total Hg is important

for quality control taking into account the risk for human health (e.g., ingestion of Hg contaminated food like fish practically all organic mercury content is found as methyl mercury (a highly toxic species)). In natural water, Hg concentrations are typically in the low-ng/L range[27]. The well known concentration ranges of mercury species in various natural and contaminated water samples are summarized in Table 1.1 [28, 29]. Trace concentration ranges of mercury species makes their reliable determination a major analytical challenge. In fresh waters e.g., lake water about 94– 99% of inorganic Hg and 72–97% of organic Hg are complexed by dissolved humic matter [30], whereas, in seawater, the proportion of Hg bound to humic matter is very low due to high chloride-ion concentrations that stabilize Hg species in solution by ionic interactions. Furthermore, the proportion of organic Hg species in marine waters is typically less than 5% of the total Hg concentration [31] (although Mediterranean waters show an “Hg anomaly” with an organic Hg content of up to 30% of total Hg [32]), while, in freshwater systems, the organic Hg fraction is typically 30% of the total Hg, which is in the range 1–5 ng Hg/L [33].

Table 1.1. Concentration ranges of total mercury in different natural waters

[28,29]

Natural water	Concentration of total Hg
Open ocean water	below 1 ng/L
Estuarine water	0.5–5 ng/L
Humic lakes and particle-rich river water	10–20 ng/L
Contaminated natural water	up to 1g/L

A wide range of instrumentations are known for the detection and quantification of mercury are known. Chemical speciation of mercury species (Hg_{inorg} , Hg_{org} and Hg_{total}) in some selected type of fish tissues has been carried out by electrothermal atomic absorption spectrometry (ET-AAS) [34]. The selectivity of extraction has been evaluated using liquid chromatography coupled to chemical vapor generation and the determination has been successfully achieved by inductively coupled plasma mass spectrometry (ICP-MS) [35]. A new method, based on single-drop micro extraction (SDME) combined with electrothermal vaporization atomic absorption spectroscopy (ETV-AAS) has been developed for the trace determination of mercury in water samples [36]. The detection limit of the method was $0.01 \mu\text{g L}^{-1}$ and the relative standard deviation was 6.1% ($n = 7$). The proposed method has been successfully applied to the determination of Hg in two river water samples. The effects of the most common interfering species such as Pt, Pd, Cu, Au, and Bi, having the tendency to form complexes with the chromogenic reagent

dithizone at two concentration levels (100 and 1000 $\mu\text{g L}^{-1}$) have been critically investigated [36]. Cloud point extraction process using the nonionic surfactant Triton X-114 for extracting mercury from aqueous solutions have been used for spectrophotometric determination of mercury [37]. The method has been based upon the complexation reaction of Hg(II) with Thio-Michler's Ketone (TMK) and micelle-mediated extraction of the complex [38].

Drinking water represents the main source for incorporation of mercury to human body [38]. Thus, in recent years mercury determination in drinking water becomes very important task. A total mercury concentration in water ranging from 0.006 to 3 $\mu\text{g L}^{-1}$ has been reported [38]. The upper limit for total mercury concentration in drinking water has been recommended by European Community as 1.0 $\mu\text{g/L}$ [39]. Determination of mercury (II) species has been reported using the non-ionic surfactant polyethyleneglycolmono-*p*-nonylphenylether (PONPE 5) [39]. The method has been based upon extraction of mercury (II) species- mediated by Micelles of the non-ionic surfactant polyethyleneglycolmono-*p*-nonylphenylether (PONPE 5) in combination with 2-(5-bromo-2-pyridylazo)-5-diethylaminophenol [Hg(II)-2(5-Br-PADAP)] complex at pH 9.2 [39]. In this method, cold vapor generation has been developed from 100 μl of the extracted surfactant-rich phase by means of a stannous chloride (SnCl_2) solution as reductant. Liquid-liquid extraction procedure (L-L) based on room temperature ionic liquid (RTIL) has also been developed for the preconcentration and determination of mercury in different water samples [40]. The analyte has been extracted quantitatively with 1-butyl-3-methylimidazolium hexafluorophosphate ($[\text{C}_4\text{mim}][\text{PF}_6]$) under the form Hg-2(5-Br-PADAP) complex. The limit of detection (LOD) obtained under the

optimal conditions was 2.3 ng L^{-1} and the relative standard deviation (RSD) for 10 replicates at $1 \text{ } \mu\text{g L}^{-1} \text{ Hg}^{2+}$ was 2.8% [41].

In natural waters, the most common and well known three main mercury species found in the dissolved phase are: i inorganic mercury Hg^{2+} and its Hg(II) complexes; ii organic mercury e.g. monomethylmercury and dimethylmercury and finally iii elemental mercury (Hg^0). All of these mercury species are highly mobile by the biogeochemical cycle of mercury as demonstrated in Fig.1.1 [42].

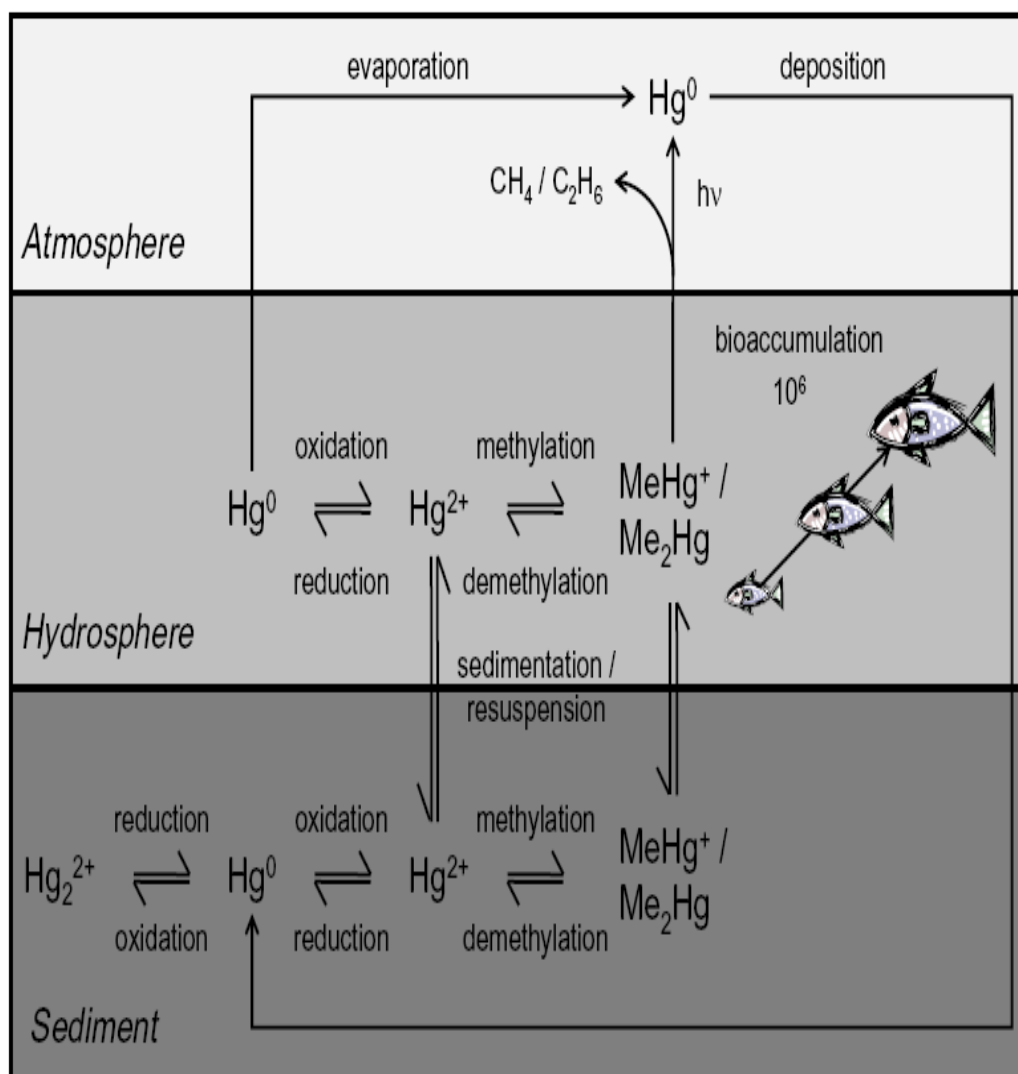


Fig. 1.1 Biogeochemical cycle of mercury.

Mercury in dental - unit wastewater ranges from large sized amalgam particles to submicron mercury containing colloidal particulates. Thus, Hamza et al [42] have reported an excellent method for mercury determination in dental – unit wastewaters as an important source of environment pollution with mercury. Wastewater samples taken directly from the dental chair is mainly in the form of elemental mercury (Hg^0) bound to particulate in addition to ionic mercury species (Hg^{2+}), dissolved elemental and organic forms [42]. The average concentrations of mercury from settled wastewater collected directly from the dental chair are: total mercury $21.438 \mu\text{g mL}^{-1}$, Hg^0 $24.06 \mu\text{g L}^{-1}$, Hg^{2+} $54.00 \mu\text{g L}^{-1}$ and Hg^0 bound to amalgam particulates $21.360 \mu\text{g mL}^{-1}$ [42]. Absorption of inorganic Hg (also known as ionic Hg) by the gastrointestinal tract in humans is relatively limited and approximates 7% of the ingested dose [42]. Kidney tissue contains the highest concentration of Hg after exposure to inorganic salts and elemental Hg [43]. It has been demonstrated that elemental Hg in human saliva can be oxidized to ionic Hg which may be protective since ionic Hg is a less toxic species: both Hg and ionic Hg were present in saliva of all study subjects but only patients with amalgam restorations had detectable elemental Hg levels in their saliva [43].

The chromogenic reagent dithizone (diphenylthiocarbazon, H_2Dz) has been reported as a selective chelating agent for mercury determination [44]. The developed method was based upon formation of soluble orange – yellow complex, $\text{Hg}(\text{Dz})_2$, in CCl_4 or CHCl_3 [44]. The method was rapid and sensitive for mercury determination. Although this method was sensitive and precise, it is suffered from the interferences of silver, copper, palladium and other ions. Therefore, many of sensitive, selective and precise spectrophotometric

methods based on the chromogenic reaction between mercury (II) and some organic or inorganic compounds have been developed. Rapid spectrophotometric procedure for the mercury determination in environmental, biological, soil, and plant samples has been proposed. The method has been based upon the reaction of the chelating agent 2-hydroxy – 5 – sulfobenzenediaminoazobenzene (HSDAA) with Hg^{2+} in an acidic aqueous solution. The sensitivity of the method has been improved by adding a non – ionic surfactant (TX – 100) to the reaction medium. Under the optimum experimental conditions, the effective molar absorptivity (ϵ) was $1.67 \times 10^5 \text{ L mol}^{-1} \text{ cm}^{-1}$ at $\lambda_{\text{max}} = 518$ [44]. Simultaneous spectrophotometric determination of mercury (II) and palladium (II) has been proposed by El-Sayed, 1998 [45]. The method has been based upon the use of technique of first – derivative spectrophotometry to resolve the absorption electronic spectra of Hg^{2+} and Pd^{2+} complexes with the chromomeric reagent 5-(3,4-methoxyhydroxyphenylmethylene)-2-thioxo-1,thiazolidine[5-(3,4-methoxyhydroxy benzylidene) - rhodamine].

A novel spectrophotometric method has been reported for the determination of trace amounts of mercury in verity of samples after carrying out pre concentration process [46]. The method was based upon cloud point extraction (CPE) using the non – ionic surfactant e.g. TX – 114 for pre concentration of mercury prior to its spectrophotometric determination. The method has been based upon the complex formation of mercury (II) with Thio – Mickler's Ketone(TMK) and micelle – mediated extraction of the formed complex. The linearity and the detection limit were 5 – 80.0 and $0.83 \mu\text{g L}^{-1}$, respectively [46]. The developed method was a rapid for preconcentration of

mercury prior to its determination. A good method has been reported for mercury determination. The method has been based upon flotation of the ion – associate of HgI_4^- and ferrion followed by subsequent extraction into n-heptane interface at pH 5 [47]. The method has provided linearity and detection limit in the range $6 - 190 \mu\text{g L}^{-1}$ and $1.24 \mu\text{g L}^{-1}$, respectively [47]. The method has been applied successfully for the analysis of mercury(II) species in complicated matrices e.g. marine and seawater samples.

1.3 Occurrence and determination of palladium

The importance of the palladium metal has grown many fold in the recent years due to the increasing applications for the production of dental and medicinal devices, jewellery, automobile and catalytic converters. Palladium occurs together with the other PGEs at very low concentrations ($<1 \mu\text{g/kg}$) in the Earth's crust. Economically important sources exist in Russia, South Africa and North America [48]. Palladium and its alloys have been used as catalysts in the (petro)chemical and, above all, the automotive industries. Applications for electronics and electrical technology include use in metallization processes (thick film paste), electrical contacts and switching systems. Palladium alloys are also widely used in dentistry (e.g., for crowns and bridges). Recently, ^{103}Pd has been used for cancer (e.g., prostate) brachytherapy, a form of cancer radiation therapy in which radioactive sources are implanted directly into a malignant tumor [49, 50]. Therefore having in mind the highest bioavailability of Pd among PGE [51] and its cytotoxicity and mutagenic effects in living

organisms [52] the need for reliable methods for analysis and the necessity for its determination in environmental samples becomes obvious.

The general population is primarily exposed to palladium through dental alloys, jewellery, food and emissions from automobile catalytic converters [53, 54]. Concentrations of palladium in surface water generally ranged from 0.4 to 22 ngL⁻¹ in fresh water and from 19 -70 pgL⁻¹ in salted water [54]. The development of analytical techniques for analysis of platinum group metals (PGMs) comprises Pt, Pd, Rh, Ir, Os and Ru is growing because of their applications in chemical engineering, micromechanics and medicine. Palladium has been used in different areas of science and technology, including agents, brazing alloys, petroleum, electrical industries, and catalytic chemical reactions [55, 56]. Pd also has been used in catalytic converters in motor vehicles and in some industrial processes [57], hence its concentration in the environment has been rapidly increasing. Because of Pd toxicity [58], its monitoring at trace level in surface waters, soil surfaces, plant and particular matter samples has been getting increasingly important. However, Pd concentration remains at a relatively low level that is why the methods used for Pd determination should be of highly sensitivity.

The determination of trace Pd(II) ions in environmental samples with an inexpensive method is one of the principal challenges facing scientists [59]. Several methods have been described for the separation and determination of Pd(II). These methods include precipitation, solvent extraction, chelating resin and ion exchange. Many types of adsorbents e.g. calcium alginate, silica gel and, Dowex 1-X8, fiber, polyvinyl pyridine, alumina and polyurethane

foam) have been developed for the recovery of palladium from aqueous media.

Flame atomic absorption spectrometry (FAAS), GF-AAS, electrothermal AAS, AAS, ICP -OES ICP MS and electrospray ionization mass spectrometry (ESI-MS) after dispersive liquid - liquid microextraction represent the most popular and modern spectrometric analytical tools used for Pd analysis at trace levels [60-70]. The main disadvantages of these techniques are the complexity, the high cost of the instruments, preconcentration step and the need of some degree of expertise for their proper operation. Therefore, the development of low cost, easy to operate, highly sensitive and reliable method for routine analysis of Pd e.g. stripping voltammetry is of great concern in recent years [71].

Stripping voltammetry represents the most popular, thanks to such unquestionably features as excellent sensitivity and selectivity, low detection limits, good accuracy and precision, and inexpensive and portable instrumentation [71 -74].

Adsorptive stripping voltammetry (AdSV), which is based upon the accumulation of the analyte on a suitable working electrode by potential controlled adsorption and subsequent electrochemical reduction of the preconcentrated species has been reported for sensitive determination of Pd [75 -78]. In the vast majority of these methods, dimethylglyoxime (DMG) has been applied as the complexing reagent [79-84]. The reagent α -(2-benzimidazolyl)- α' , α'' -(N-5-nitro-2-pyridyl hydrazonotoulene [85] has been tested as potential ligand for Pd. A summary from the literature of Pd concentrations in different wastes and sediments from different cities that have been found to contain

artificially introduced environmental Pd has been reported by Shaidarova, et al., 1994 [86]. Palladium chemistry plays an extremely active part of coordination and organometallic chemistry; palladium complexes occupy a special position of pivotal importance in the field of catalysis for different chemical transformations particularly in carbon–carbon bonds formation in organic syntheses [87].

Recently, Graphite furnace atomic absorption spectrometry (GF AAS), mass spectrometry with the ICP ionisation (ICP-MS), voltammetric methods and neutron activation analysis (NAA) represent the most suitable analytical techniques for palladium determination at trace concentration level [88 -100]. However, direct determination by all these techniques is restricted owing to the interferences caused by environmental sample matrices and, usually, a preliminary palladium separation and enrichment is required. A novel method for the determination of palladium in environmental samples is done by using low temperature ETV-ICP-OES (Inductively coupled plasma/optical emission spectrometry) with dimethylglyoxime (DMG) as an extractant and chemical modifier has been developed [90]. It was found that palladium can form complexes with dimethylglyoxime(0.05%, mass fraction) at pH 6. 0 and can be extracted into chloroform quantitatively. The complexes can be evaporated into plasma at a suitable temperature(1400°C) for ICP-OES detection. Under the optimized conditions, the detection limits of palladium are 0. 40 ng/mL, while the RSD values is 3. 1% [90]. Graphite furnace atomic absorption represents another method for palladium determination after their separation from environmental samples. The sample was digested by aqua regia and the analyte element was separated on the dithizone sorbent, the low limit of detection was

established as 0.2 ng g^{-1} for palladium [91]. Dispersive liquid–liquid microextraction preconcentration coupled with graphite furnace atomic absorption spectrometry detection have been successfully used for Pd determination [92]. Diethyldithiocarbamate (DDTC) has been used as a chelating agent, and carbon tetrachloride and ethanol have been selected as extraction and dispersive solvent. The detection limit for palladium was 2.4 ng L^{-1} (3σ), and the relative standard deviation (R.S.D.) was 4.3% ($n = 7$, $c = 1.0 \text{ ng mL}^{-1}$). This method was successfully applied for the determination of trace amount of palladium in water samples [92].

Determination of palladium in food additive, sea water, tea and biological samples has been carried out by modified cold-induced aggregation microextraction (M-CIAME) [100]. This method was found fast and simple for extraction and preconcentration of metal ions from samples with high salt content. Furthermore, this technique is much safer in comparison with the organic solvent extraction. The extraction of palladium (Pd) was performed in the presence of Michler thioketone (TMK) as the complexing agent. In this method, sodium hexafluorophosphate (NaPF_6) was added to the sample solution containing small amounts of 1-hexyl-3-methylimidazolium tetrafluoroborate [$\text{Hmim}][\text{BF}_4]$. A relative standard deviation (RSD) of 1.7% for 40 ng mL^{-1} of palladium ($n = 5$) has been achieved [93-101]. The synthesized indicator 2,2-bis-[3-(2-thiazolylazo)-4-hydroxyphenylpropane], (TAPHP) has been used for the selective palladium determination in acidic media. It was applied in the flow cell for the selective detection of palladium cations in a trans illuminating configuration. This technique offers an alternative way to the classical colorimetric determination of metal cations,

involving flow-through measurements with the possibility of the automated sequential sample injection [102].

In 2009 a new simple and reliable method for rapid and selective extraction and determination of the trace levels of Pd²⁺ ion was developed by dispersive liquid–liquid microextraction preconcentration and flame atomic absorption spectrometry detection. In this method, thioridazine HCl (TRH) was used as a Pd²⁺ ion selective complexing agent. The effective parameters on the extraction recovery were studied and optimized utilizing two decent optimization methods; factorial design and central composite design (CCD). Through factorial design the best efficiency of extraction acquired using of ethanol and chloroform as dispersive and extraction solvents respectively. CCD optimization resulted in 1.50 mL of dispersive solvent; 0.15 mL of extraction solvent; 0.45 mg of TRH and 250 mg of potassium chloride salt per 5 mL of sample solution. Under the optimum conditions the calibration graph was linear over the range 100–2000 µg L⁻¹. The average relative standard deviation was 0.7% for five repeated determinations. The limit of detection was 90 µg L⁻¹. The average enrichment factor and recovery reached 45.7% and 74.2%, respectively [103].

1.4. Occurrence and determination of arsenic

Arsenic is pervasive in nature. As cited throughout the literature, arsenic is the 20th most abundant mineral in the earth's crust and 12th most abundant mineral in the human body. Arsenic in the environment is of considerable concern to countries whose population obtains a majority of their drinking water from wells, specifically tube wells. Inorganic arsenic species are toxic and found in ground water around the globe at levels higher than the maximum contaminant level of $10 \mu\text{g L}^{-1}$ (10 ppb) recommended by the World Health Organization (WHO) [104]. Drinking of arsenic contaminated water for a long time causes illnesses such as hyperkeratosis on the palm or feet, fatigue, and cancer of the bladder, skin or other organs. Arsenic is a naturally occurring element widely distributed in the earth's crust. Inorganic arsenic compounds are mainly used to preserve wood [104, 105]. Organic arsenic compounds are used as pesticides, primarily on cotton fields and orchards. Exposure to lower levels can cause nausea and vomiting, decreased production of red and white blood cells, abnormal heart rhythm, damage to blood vessels, and a sensation of "pins and needles" in hands and feet [104].

Arsenic and its compounds are toxic pollutants for the environment and all living organisms and the toxicity of arsenic derived from several natural phenomena and anthropic activities [106, 107]. Arsenic mainly reaches humans through water supplies where it generally occurs as arsenic (III) and (V), depending on the solution pH and redox conditions [108, 109]. Typical concentration of arsenic in natural water can rise up to 3mg L^{-1} [110]. Arsenate species predominate in aerobic and oxidizing conditions while, arsenite species prevail in anaerobic and moderately reducing conditions [111]. Due to their

high toxicity and to the widespread of their emissions, arsenic and its compounds are strictly controlled by environmental regulations [112]. Arsenic (III) is reported to be 25–60 times more toxic than arsenic (V) and several hundred times as toxic as organoarsenic at least in the case of the mono and dimethylated forms) [113, 114].

Speciation of As is of particular interest because different species exhibit wide-ranging levels of toxicity to various organisms. Under aerobic conditions in water, sediments and soils arsenic exists mainly in inorganic forms (mainly arsenate), while in biota it occurs primarily in organic forms. Methylated forms, such as monomethylarsonic acid (MMAA) and dimethylarsinic acid (DMAA), are the most common forms of organic As, but arsenobetaine (AB) is the main As species found in marine organisms. In general, inorganic forms of arsenic e.g. arsenite [As(III)] and arsenate [As(V)] are known to be toxic As species especially to mammals and also to invertebrates[115].

The technical feasibility of various low-cost adsorbents for heavy metal removal from contaminated water has been employed as replacements for commercial activated carbon. Researchers have worked on inexpensive materials, such as chitosan, zeolites, and other adsorbents, which have high adsorption capacity and are locally available. It is evident from our literature survey of many papers that low-cost adsorbents have demonstrated outstanding removal capabilities for certain metal ions as compared to activated carbon. Adsorbents that stand out for high adsorption capacities are chitosan (815, 273, 250 mg/g of Hg(II), Cr(VI), and Cd(II), respectively), zeolites (175 and 137 mg/g of Pb(II) and Cd(II), respectively), waste slurry (1030, 560, 540 mg/g of Pb(II), Hg(II) and Cr(VI), respectively), and lignin (1865 mg/g of Pb(II)).

These adsorbents are suitable for inorganic effluent treatment containing the metal ions mentioned previously. It is important to note that The adsorption capacities of such solid adsorbents are mainly depend on the characteristics of the individual adsorbent, the extent of chemical modifications, and the concentration of adsorbate [116].

Clay minerals have different adsorption capacities for metal ions, such as mesoporous silica⁷ and montmorillonite clay for Hg(II) [117] which depend on the absorption conditions as they have been found to be very effective, economical, versatile and simple [118]. The removal of metal ions using kaolinite clay is based on ion exchange and adsorption mechanisms. Kaolinite is known to have has a relative low cation-exchange capacity (CEC) [3–15 meq/100 g of clay] and smaller surface area ranged from 10 to 20 m²/g [119]. Heavy metals, such as Pb(II), Cd(II) and Ni(II) in aqueous medium removed by kaolinite was also reported [120]. Similarly, kaolinite has been used as adsorbents for the removal of Fe(III), Co(II) and Ni(II) in aqueous medium for removal of Cu(II) [121] and Pb(II) [122].

Recently, the use of clay for sorption or elimination of arsenite and arsenate species in effluents has been object of study in a great deal of research due to its several economic advantages [123, 124]. The cost of these adsorbents is relatively low when compared to other alternative adsorbents, including activated coal, natural and synthetic zeolites, ion-exchange resins and other adsorbent materials. Clay and minerals as montmorillonite, vermiculite, illite, caulinite and bentonite are some natural materials that are being studied as heavy metal adsorbents. Another advantage of using clay as an adsorbent is related to its intrinsic properties such as: great specific surface area, excellent

physical and chemical stability and several other structural and surface properties [125]. Some types of clay (especially montmorillonite and bentonite) are also widely utilized as barriers in order to avoid contamination of underground water and soil in embankments as a result of lixiviation with heavy metals. The performance of Na-montmorillonite towards Cd, Cr, Cu, Mn, Ni, Pb or Zn even when organic substances (bonds) are present have been reported [126]. Most of these metal ions have been adsorbed in mineral clays simultaneously from solutions with several concentrations.

Most of the pollutants and heavy metals discharged in industrial effluents ultimately find their way to aquatic ecosystems, i.e., rivers, ponds, and lakes. The presence of heavy metal pollutants in waterbodies poses risk to the health of humans and ecosystems. In recent years, there has been increased global concern over the deteriorating state of water bodies due to heavy metal pollution [127]. Several techniques have been developed to remove heavy metals from the water bodies with mixed success. Most techniques proved to be partially effective and too costly to be adopted in feasible manner. Most of the modern technologies used to treat wastewaters have their own implications, as these technologies are quite costly, concomitantly, posing threats to aquatic life [128].

Most developing countries may not be able to afford the huge expenditure required to treat the heavy metal pollution by modern technologies [129]. In the recent past, utilization of aquatic plants for the wastewater treatment has been reported as an economical device for the treatment of heavymetal-contaminated wastewater. Several research works demonstrated heavy metal removal under artificial conditions. There is still a paucity of data on the

comparative efficiency of different aquatic plants for heavy metal removal under natural conditions, especially in tropical regions.

A wide variety of methods e.g. ultraviolet spectrophotometer; atomic absorption spectrometric methods (AAS), mainly coupled to hydride generation (HG-AAS); electrothermal-AAS in graphite furnace (ETAAS); atomic fluorescence spectrometry (AFS); inductively coupled plasma optical emission spectrometry (ICP-OES); inductively coupled plasma-mass spectrometry (ICP-MS); X-ray spectrometry; neutron-activation analysis (NAA); and capillary electrophoresis have been published for the determination of arsenic [130]. However, most of these methods require expensive instrumentation, complicated procedures and special sample pre-treatment and not applicable for routine work. Besides, most of these methods are essentially sensitive to total arsenic. The developed method by Minakata, et al., 2009 [131] has shown excellent sensitivity for arsenic (III) and (V) determination after reduction of the latter with thiosulfate to arsenic (III) . The total inorganic arsenic (III) and (V) has also been determined in urine samples. The limit of detection of As was $0.22 \mu\text{g L}^{-1}$ using $10 \mu\text{L}$ of sample solution, and it is far below the permissible limit of As in drinking water, $10 \mu\text{g L}^{-1}$, recommended by the WHO [105].

Recent years have seen an upsurge of interest on the application of electrochemical methods for the analysis of trace arsenic [118 -119]. The electrochemical techniques offer many advantages e.g. simple instrumentation and operation; low cost; high sensitivity and excellent selectivity which allow the chemical speciation of trace metal ions including arsenic. Direct current polarography (DCP) has shown a detection limit of approximately 0.7 mg L^{-1}

for arsenite species in water [120]. An excellent and novel method has been reported by Xu et al., 2008 [132] for the determination of trace or ultra trace concentrations of arsenic (III) on highly ordered platinum-nanotube array electrodes. Generally stripping analysis technique has been reported to be better suited than the direct polarography for trace determination of toxic metal ions in particular arsenic (III and V) in real samples because the substance of interest was first pre-concentrated on the working electrode [122]. The most common and efficient electro - chemical methods for determining arsenic (III) involved the use of cathodic and /or anodic stripping voltammetry using a pulsed wave form [123, 124]. Several papers have been published for the analysis of arsenic (III) at low ppb levels at hanging mercury dropping electrode (HMDE) [125]. An excellent stripping voltammetric method has been developed for determination of arsenic (III) and or arsenic (V) in seawater by Sun et al. [133]. Gold film and a rotating glassy carbon electrode with a gold film deposited from a gold plating solution have been used as working electrodes in the voltammetric cell. And the relative standard deviation of multiple measurements was 8% at 1.0×10^{-9} mol L⁻¹ arsenic (III) solution. A square wave cathodic stripping voltammetric and a portable electrochemical device for the measurement of arsenic (III) and (V) in water at a gold film deposited on a platinum wire as a working electrode have been reported for arsenic analysis in water [127, 128]. The developed methods been applied for the analysis of total arsenic in river and sea water samples and soils using DP-CSV [128].

The determination of total As in sea water by hydride generation atomic fluorescence spectrometry has been investigated [134]. The influence of the

chemical, flow and instrumental parameters were investigated and optimized. The pre-reduction of As(V) to As(III) was performed using KI plus ascorbic acid in 3.5 mol L^{-1} HCl medium. No multiplicative interference was present and external aqueous calibration could be used. The limit of detection was 36 ng L^{-1} , while the repeatability was 2% ($n = 10$), at a 500 ng L^{-1} concentration level. The sample throughput was 15 h^{-1} if triplicate measurements were made. The accuracy was assessed by the analysis of a seawater certified reference material and excellent agreement between the obtained and certified values was verified. Analysis of sea water offshore samples collected at the Brazilian coast was ranged from 860 to 1200 ng L^{-1} were found [135].

A method for separation and pre-concentration in alumina, followed by direct analysis of the alumina is evaluated. Quantification was performed using the Al-K α and Co-K α lines as internal standard in samples prepared on an alumina matrix, and compared to a calibration with aqueous standards. Artificial water samples of As (III) and As (V) were analyzed after the treatment. Fifty milliliters of the sample at ppb concentration levels were mixed with 10 mg of alumina. A pre-concentration factor of 100 was found, with detection limit of $0.7 \text{ }\mu\text{g L}^{-1}$. The percentage of recovery was 98% for As (III) and 95% for As (V) demonstrating the suitability of the procedure [136]. The inductively-coupled plasma-mass spectrometry method was applied as the analytical method for the determination of the arsenic concentration in water. The governing factors for the ion exchange/sorption of arsenic on resins in a batch and a fixed bed flow system were analyzed and compared [137].

1.5. Aim of the current study

The problem of pollution control and environmental pollution of Hg and arsenic has become one of the modern preoccupations of the human and is attracting a growing attention worldwide. On the other hand, increasing area of palladium applications stimulates the development of analytical methods to characterize materials containing this noble metal. Various methods involving the use of a series of chromogenic reagents have been used for the assay of Hg, Pd and As . Thus, recent years have seen an upsurge of interest in developing novel methods and low cost for precise analysis and / or removal of trace and ultra concentrations of such class of metal ions in various matrices e.g. drinking, and marine waters represents a vital task in recent years. Chemical speciation of these metal ions in different matrixes is also of great importance. Thus, the overall goals of the work presented in this thesis will be focused on:

1. Reviewing the essential background information's on the occurrence, mode of action, various sources, migration and movement to food chains and analytical methodology for the determination of trace concentrations of inorganic pollutants and food colorants. Special attention will be oriented towards the various methods used for the analysis of ultra trace concentrations of cations, anions and molecules understudy. The need of reliable, sensitive, selective, and rapid technique for analysis of these metal ions in environmental samples with emphasis upon the types of chemical information represent important tasks for human health and environment.

2. Developing of a low cost, precise and highly selective differential pulse cathodic stripping voltammetry (DP-CSV) method for trace analysis of

mercury species at the hanging mercury drop electrode (HMDE) in different matrices. The nature and mechanism of the electrochemical reduction step of mercury chelate at the surface of HMDE will be discussed. On the other a proper assigning of the most probable reduction mechanism of the Hg-TAR at HMDE will also discussed.

3. Deploying of a precise, selective and low cost square wave differential pulse cathodic stripping voltammetry (SQ-CSV) method for determination of palladium using HMDE in various water samples. In this account, the most effective electrochemical parameters controlling SQ-CSV and cyclic voltammetry (CV) at hanging mercury dropping electrode (HMDE) and Pt electrodes will be discussed in more details. Such kind of investigations will contribute significantly to further developments and refinement in the field of material science, and geological analysis for analysis of palladium in its alloys and minerals, respectively .

4. Recently, the use of clay minerals such as montmorillonite, vermiculite, illite, caulinite, bentonite un treated or physically immobilized with some chelating agents for sorption and / or elimination of heavy metal ions from industrial effluent e.g. wastewater has been object of study in a great deal of research due to its several economic advantages. The cost of clay adsorbent is relatively low when compared to other alternative adsorbents e.g. activated coal, synthetic zeolites, ion-exchange resins and other adsorbent materials. Thus, the work was also focused mainly on developing simple, convenient, and low cost procedure, involving clay as sorbent for preconcentration, and sequential chemical speciation of arsenic (III) and (V). The influence of several parameters that controlling As removal of trace and

ultra trace concentrations by clay will be discussed. A clay packed column will also be considered and they are going to be used for retention and recovery of traces of arsenic (III) and (V) in different water samples. The kinetic and thermodynamic characteristics of arsenic(III) sorption by clay will be studied and the most probable retention mechanism will be assigned.

The fulfillment of the overall objectives of the present investigation will contribute significantly to further developments and refinement in the field of environmental pollution by hazardous chemical.

1.6. References

- 1.M. P. Urquiza, R. Ferrer, J.L. Beltrain, *J. Chromatography A* 883 (2000) 277 – 283.
- 2.R.A. Hoodles, K.G. Pitman, T.E. Stewart, J.M. Thompson, J.E. Arnold, *J. Chromatography* 54 (1971) 393 – 404.
- 3.M. P. Urquiza, M.D. Part, J.I. Beltrain, *J. Chromatography A* 871 (2000) 227 – 234.
- 4.A. A. Barros, J.A., *Electroanalysis* 3 (1991) 243 – 245.
- 5.S. Armenta, S. Garrigue, M.D. Guardia, *Trends in Analytical Chemistry (TRAC)* 27 (2008) 497 – 511.
- 6.X. Yang, Y. Feng, Z. He, P.J. Stofeela, *J. Trace Elements in Medicine and Biology* 18 (2005) 339-345.
- 7.T.R. Dulsk, *Trace Elemental Analysis of Metals, Methods and Techniques*, Marcel Dekker Inc., (1999).
- 8.M.M Abou-Mesalam, I.M. El-Naggar, M.S. Abdel-Hai, M.S. El-Shahawi, *J. Radioanalytical and Nuclear Chemistry* 258 (2003) 619-626.
- 9.M.S. El-Shahawi, M.A. Othman, M.A. Abdel-Fadeel, *Anal. Chim. Acta*, 546 (2004) 221-226.
10. M.S. El-Shahawi, M.A. Othman, M.I. Nassef, M.A. Abdel-Fadeel, *Anal. Chim. Acta*, 536 (2005) 227-131.
11. U. Fötstner, U. (1984) Cadmium. In: Hutzinger, O., edn., *The Handbook of Environmental Chemistry, VoL. 3, Part A, Anthropogenic Compounds*, New York, Springer-Verlag, pp. 59-107.
12. J.H. Duffus *Pure and Applied Chemistry* 74 (2002)793-807.

13. S.A. Counter, L. Buchanan A Review, *Toxicology and Applied Pharmacology* 198 (2004): 209-230.
14. D. Chen, B.H. Bin Hu, C. Huang *Talanta* 78 (2009) 491–497.
15. R. Lobi, N. Ski, Z. Marczenko, *Spectrochemical Trace Analysis for Metals and Metalloids*, Elsevier Science (1997).
16. S. Rapsomanikis, *Analyst*, 119 (1994) 1429-1439
17. B. Welz and M. Melcher, *Anal. Chem.*, 57 (1985) 427.
18. M. Goto, E. Munaf and D. Ishii, *Fresenius' Z. Anal. Chem.*, 332 (1988) 745.
19. S.B. Adeloju, H.S. Dhindsa and R.K. Tandon, *Anal. Chim. Acta*, 285 (1994) 359.
20. H. Tanaka, M. Kouno, H. Morita, K. Okamoto and S. Shimomura, *Anal. Sci.*, (1992) 851.
21. B. Panichlertumpi, S. Chanthai Bhuchonk *Anal. Methods*, 2013,5, 987-997
22. Z. Grobanski, W. Erler and U. Völlkopf, *At. Spectrosc.*, 6 (1985) 91.
23. L. Ping, K. Fuwa and K. Matsumoto, *Anal. Chim. Acta*, 171 (1985) 279.
24. B. Welz, G. Schlemmer and J.R. Mudakavi, *J. Anal. At. Spectrom.*, 7 (1992) 499.
25. M.J. Powell, E.S.K. Quan, D.W. Boomer and D.R. Wiederin, *Anal. Chem.*, 64 (1992) 2253.
26. M. Ghaedi, A. Shokrollahi, A.H. Kianfar, A. Pourfarokhi, N. Khanjari, A.S. Mirsadeghi, M. Soylak *J. Hazardous Material*. 162 (2009) 1408–1414.

27. M.J. Shaw, P.R. Haddad, , *Environment International* 30 (2004) 403–431.
28. K. Leopold, M. Foulkes, P.J. Worsfold, *Trends in Analytical Chemistry* 28 (2009) 426-435.
29. R.P. Mason, K.R. Rolffhus, W.F. Fitzgerald, *Mar. Chem.* 61 (1998) 37.
30. R.J.M. Hudson, A.S. Gherini, C.J. Watras, D.B. Procella, in: C.J. Watras, J.W. Huckabee, (Editors), "Mercury pollution – Integration and synthesis" Lewis publishers, Boca Raton, FL, USA, (1994) 473 – 523.
31. R.P. Mason, K.A. Sullivan, *Deep – Sea Res, Part II Top. Stud. Oceanography.* 46 (1999) 937.
32. D. Cossa, M. Coquery, in: A. Saliot (Editor), *Handbook of Environmental Chemistry*, 5 Springer, Berlin, Germany (2005) 177 – 208.
33. N. Bloom, C.J. Fish, *Aquat. Sci.* 46 (1989) 1131.
34. E.M. Soliman, M.B. Saleh, S.A. Ahmed, *Talanta* 69 (2006) 55.
35. H. Jiang, B. Hu, Z. Jiang, Y. Qin, *Talanta* 70 (2006) 7.
36. E.L. Seibert, V.L. Dressler, D. Pozebon, A.J. Curtius, *Spectrochim. Acta, Part B* 56 (2001) 1963.
37. F.A. Duarte, C.A. Bizzi, F.G. Antes, V.L. Dressler, E.M. *Spectrochimica Acta Part B: Atomic Spectroscopy* 64 (2009) 513–519.
38. H. Bagheri, M. Naderi, *J. Hazard. Mater.* 165: (2009)353–358.
39. A. Niazi, T. Momeni-Isfahani, Z. Ahmari, *J. Hazard. Mater.* 165 (2009)1200-1203.
40. J.C. Wuilloud, R.G. Wuilloud, M.F. Silva, R.A. Olsina, L.D. Martinez, *Spectrochimica Acta Part B: Atomic Spectroscopy* 57: (2002)365-374.

41. E.M. Martinis, P. Bertón, R.A.Olsina, J.C. Altamirano, R.G. Wuilloud, J. Hazard. Mater. 167 (2009) 475–481.
42. . S.M. Ulrich, T.W. Tanton, S.A. Abdrashitova, Crit. Rev. Env. Sci. Technol. 31 (2002) 241.
43. A. Hamza, A.S. Bashammakh, A.A. Al-Sibaai, H.M. Al-Saidi, M.S. El-Shahawi J. Hazard. Mater, 178 (2010) 287 -292.
44. Agency for toxic substance and Disease Registry (ATSDR) Toxicological profile for mercury Atlanta, GA, (1999).
45. L. Liang, R.J. Brooks, Water Air and Soil Pollution. 80 (1995) 103 – 107.
46. Z. Marczenko "Separation and Spectrophotometric Determination of Elements" 2nd edn. John Wiley and Sons (1986).
47. X.A. Cao, Y.H. Chen, H.M. Lin, P.U. Guang Fen, 24 (2004) 474 – 476.
48. A.Y. El-Sayed, Analytical Letters, 31 (1998) 1905 – 1916.
49. A. Niazi, T. Momeni-Isfahani, Z. Ahmari, J. Hazardous Materials, 165 (2009) 1200 – 1203.
50. M.S. Hussein, H.H. Moghaddan, Analytical Science, 20 (2004) 1449.
51. Dulsk, T.R. Trace Elemental Analysis of Metal, Methods and Techniques, Marcel Dekker Inc., 1999.
52. Sharkey, J., Chovnick, S.D., Behar, R.J., Perez, R., Otheguy, J., Solc, Z., Huff, W. and Cantor, A. (1998) Urology, 51(5), 796-803.
53. Finger, P.T., Berson, A. and Szechter, A. (1999) Ophthalmology, 106(3), 606-613.

54. Schäfer, J., Hanner, D., Eckhard, J.D. and Stüben, D. (1998) *Sci. Total Environ.*, , 215,59-67.
55. Gómez, M.B., Gomez, M.M. and Palacios, M.A. (2000) *Anal. Chim. Acta.*, 404, 285-294.
56. C. Locatelli, *Electroanalysis* 19 (2007) 2167 and references therein.
57. G. Asimellis, N. Michos, I. Fasaki, M. Kompitsas, *Spectrochim. Acta B* 63 (2008) 1338.-1349.
58. Z. Marczenko, M. Balcerzak, *Separation, Preconcentration and Spectrophotometry in Inorganic Analysis*, El- Sevier, Amsterdam, 2000.
59. G. Asimellis, N. Michos, I. Fasaki, M. Kompitsas, *Spectrochim. Acta B* 63 (2008) 1338.
60. D. Afzali, R. Jamshidi, S. Ghaseminezhad, Z. Afzali, *Arabia. J. Chem* 5 (4) (2012) 461- 466.
61. E.A. Moawed, *Analytica Chimica Acta* Vol. 580 (2006) 263–270.
62. M. Mohamadi, A. Mostafavi, *Talanta* 81 (2010) 309.
63. S. Atilgan, S. Akman, A. Baysal, Y. Bakircioglu, T. Szigeti, *Spectrochim. Acta B* 70 (2012) 33 – 38.
64. B. Majidi, F. Shemirani, *Talanta* 93 (2012) 245.
65. P. Liang, E. Zhao, F. Li, *Talanta* 77 (2009) 1854.
66. T.A. Kokya, K. Farhadi, *J. Hazardous Materials* 169 (2009) 726.
67. N. Kovachev, A. Sanchez, K. Simitchiev, V. Stefanova, V. Kmetov, A. Canals, *International J. Environ. Anal. Chem.* 92 (9) (2012)1106.
68. C. Puls, A. Limbeck, S. Hann, *Atmospheric Environment* 55 (2012) 213.

69. P.G. Jaison, P. Kumar, V.M. Telmore, S.K. Aggarwal, *Rapid Communications in Mass Spectrometry* 26 (17) (2012)1971.
70. Y-Q. Ye, X.-Z Yang, X-S.Li, F.-Q Yao, Q.-F Hu, *Asian Journal of Chemistry* 24 (11) (2012) 4967.
71. C. Van Der Horst, B. Silwana, E. Iwuoha, V. J. Environ. Sci. Health - Part A Toxic/Hazardous Substances and Environmental Engineering 47 (13) (2012)2084.
72. S.I. Kim K.W. Cha *Talanta* 57(4) (2002) 675.
73. A.A. Ensafi, T. Khayamian, M. Atabati, M.M. Ardakani, *Can. J. Anal. Sci. Spectro* 49 (1) (2004) 8.
74. M. Georgieva, B. Pihlar, *Electroanalysis* 8 (1996) 1155.
75. C. Locatelli, *Electroanalysis* 17 (2005) 140-146.
76. C. Locatelli, D. Melucci, G. Torsi, *Anal. Bioanal. Chem.* 382 (2005) 1567-1572.
77. C. Locatelli, *Anal. Chim. Acta* 557 (2006) 70.
78. M. Georgieva, B. Pihlar, *Fresenius J. Anal Chem.* 357 (1997) 874.
79. J. Wang, K. Varughese, *Anal. Chim. Acta*, 199 (1987) 185.
80. Z. Q. Zhang, H. Liu, H. Zhang, Y. F. Li, *Anal. Chim. Acta*, 333 (1-2) (1996) 119.
81. G. Raber, K. Kalcher, C.G. Neuhold, C. Talaber, G. Kolbl, *Electroanalysis*, 7 (2005) 138.
82. L.G. Shaidarova, M.A. Al-Gakhri, N.A. Ulakhovich, N.G. Zabirov, G.K. Budnikov, *Z. Anal. Khimii*, 49 (5) (1994) 501.
83. M.T. Jackson, J. Sampson, H.M. Prichard, *The Science of the Total Environment* 385 (2007)117–131.

84. K. Saikia, B. Deb, B.J. Borah, P.P. Sarmah, D.K. Dutta, *Journal of Organometallic Chemistry* 696 (2012) 4293-4297.
85. L. Pan, Y. Qin, H. Hu, Z. Jiang, *Chemical Research in Chinese Universities* 23 (2007) 399-403.
86. J. Chwastowska, W. Skwara, E. Sterlińska, L. Pszonicki, L. Talanta 64 (2004) 224-229.
87. P. Liang, E. Zhao, F. F. Li, *Talanta* 77 (2009) 1854-1857.
88. M. Vaezzadeh, F. Shemirani, B. Majidi, *Food and Chemical Toxicology* 48 (2010)1455–1460.
89. M. Arndt, I. Zadrożna, A. Dybko, K. Wróblewski, K. Kasiura, *Sensors and Actuators B: Chemical* 90 (2003) 332–336.
90. T.A, Kokya, K. Farhadi, *J. Hazard. Mater.* 169 (2009)726–733.
91. E.A. Moawed, *Analytica Chimica Acta* 580 (2006) 263–270.
92. M.T. Jackson, J. Sampson, H.M. Prichard, *The Science of the Total Environment* 385 (2007)117–131.
93. K. Saikia, B. Deb, B.J. Borah, P.P. Sarmah, D.K. Dutta, (2012) *Journal of Organometallic Chemistry* 696 (2012) 4293-4297.
94. L. Pan, Y. Qin, B. Hu, Z. Jiang, *Chemical Research in Chinese Universities* 23 (2007) 99-403.
95. J. Chwastowska, W. Skwara, E. Sterlińska, L. Pszonicki, *Talanta* 64 (2004)224-229.
96. S. Mallick, New London, BBC News, Retrieved July, 2012.
97. Atsdr (2007), *Division of Toxicology and Environmental Medicine Tox FAQs™*, Atlanta, GA: U.S. Department of Public Health and Human Services, Public Health Service.

98. C.K. Jain, I. Ali, *Water Res.*, 34 (2000) 4304.
99. D.B. Singh, G. Prasad, D.C. Rupainwar, V.N. Singh, *Water, Air, Soil Poll.* 42 (1988) 373.
100. R. Piech, B. Bas, E. Niewiara, W.W. Kubiak, *J. Talanta* 72 (2007) 762.
101. R. Piech, W.W. Kubiak, *J. Electroanal. Chem.* 599 (2007) 59.
102. P. Mondal, C.B. Majumder, B. Mohanty, *J. Hazard. Mater. B*, 137 (2006) 464.
103. L. Lorenzen, J.S.J. Van Deventer, W.M. Landi, *Mineral Eng.* 8 (4) (1995) 557.
104. D. Mohan, C.U. Pittman, *J. Hazard. Mater.* 142 (2007) 1.
105. M. Kumaresan, P. Riyazuddin, *Curr. Sci.* 80 (2001) 837.
106. Z.L. Gong, X.F. Lu, M.S. Ma, C. Watt, X.C. Le, *Talanta* 58 (2002) 77.
107. H. Shibata, R. Brand, G. Mul, J.A. Moulijn, *Studies in Surface Science and Catalysis* 172 (200) 249-252.
108. A.R. Almeida, J.A. Moulijn, G. Mul, *J. Physical Chemistry C* 2008, 112, 1552-1561.
109. O. Berg, M.S. Hamdy, T. Maschmeyer, J.A. Moulijn, J.M. Bonn, G. Mul, *J. Physical Chemistry C* 112 (2008) 5471-5475.
110. P. Du, A. Bueno-Lopez, M. Verbaas, A.R. Almeida, M. Makkee, J.A. Moulijn, G. Mul, *J. Catalysis* 260 (2008) 75-80.
111. P. Du, J.T. Carneiro, J.A. Moulijn, G. Mul, *Applied Catalysis, A: General* 334 (2008) 119-128.
112. S. Eijsbouts, J.A.R. Van Veen, E.J.M. Hensen, G. Mul, *Catalysis Today* 130 (2008) 1-2.

113. G. Mul, G. M. Hamminga, J.A. Moulijn, *Petroleum Chemistry*, 53 (2008) 120-122.
114. X. Jing, W. Feng, P. Hong, *Research J. Chemistry and Environment*, 17 (2013) 41-46.
115. A. Anjum, P. Lokeswari, M. Kaur, M. Datta, *J. Anal. Sci, Methods and Instrumentation*, 1 (2011) 25-30.
116. J.T. Carneiro, A.R. Almeida, J.A. Moulijn, G. Mul, *Physical Chemistry Chemical Physics* 12 (2010) 2744-2750.
117. J.T. Carneiro, T.J. Savenije, J.A. Moulijn, G. Mul, *J. Physical Chemistry C* 114 (2010) 327-332.
118. S. Telalovic, A. Ramanathan, G. Mul, U.J. Hanefeld, *J. Materials Chemistry* 20 (2010) 642-658.
119. G. Mul, M.A. Banares, G. Garcia Cortez, B. van der Linden, S. J. Khatib, J.A. Moulijn, *Physical Chemistry Chemical Physics* 5 (2003) 4378-4383.
120. G. Mul, I.E. Wachs, A.S. Hirschon *Catalysis Today* 78 (2003) 327-337.
121. Ruokolainen, M., Panssar-Kallio, M., Haapa, A., Kairesalo, T. *Science of the Total Environment*. 258(2000) 139-147.
122. N. Dirilgen, N. Dogan, H. Ozbal, *Anal. Lett.* 39 (2006) 127.
123. R.A. Meyers "Encyclopedia of Environmental Analysis and Remediation", John Wiley and Sons Inc. 1998.
124. R. Feeney, S.P. Kounaves, *Talanta*, 58 (2002) 23.
125. E. Munoz, S. Palmero, *Talanta* 65 (2005) 613.

126. G. Ceprić, N. Alexa, E. Cordos, J.R. Castillo, J.R., *Talanta* 66 (2005) 875..
127. H. Huang, P.K. Dasgupta, *Anal. Chim. Acta* 380 (1999) 27.
128. H. Li, R. Smart, *Anal. Chim. Acta* 325 (1996) 25.
129. I. Eguiarte, R. Alonso, R. Jimenez, *Analyst* 121 (1996) 1835.
130. D.E. Mays, A. Hussam, *Analytica Chimica Acta* 64 (2009) 6–16.
131. K. Minakata, M. Suzukib, O. Suzukia, O., *Anal. Chim. Acta* 631 (2009) 87.
132. H. Xu, L. Zeng, S. Xing, G. Shi, J. Chen, Y. Xian, L. Jin, *J. Electrochem. Commun.* 10 (2008) 1893.
133. Y. Sun, J. Mierzwa, M. Yang, *Talanta* 44 (1997) 1379.
134. N.B. Arain, T.G. Kazi, J.A. Baig, M.K. Jamali, H.I. Afridi, A.Q. Shah, N. Jalbani, R.A. Sarfraz, *Food and Chemical Toxicology* 47(2009) 242–248.
135. C.L.T. Correia, R.A. Gonçalves, M.S. Azevedo, M.A. Vieira, R.C. Campos, *Microchemical Journal* 96 (2010) 157–160.
136. H. Barros, L.M. Parra, L. Bennun, E.D. Greaves, *Spectrochimica Acta Part B: Atomic Spectroscopy* 65 (2010) 489–492.
137. N.B. Issa, V.N. Rajaković-Ognjanović, B.M. Jovanović, L.V. Rajaković, *Analytica Chimica Acta* 673(2010)185–193.

Chapter II

Chemical Speciation and

Determination of Mercury Species by

Adsorptive Differential Pulse Cathodic

Stripping Voltammetry using 4-(2-

Thiazolylazo) resorcinol Reagent

2.1. Introduction

Mercury is one of the most toxic heavy metal in the earth and it exists in nature at trace and ultra trace amounts in three valence states (0, II, III). Mercury species are able to combine with most inorganic and organic complex species to form various complexes and methyl mercury [1]. Mercury can enter into human body through the food chain causing damage of central nervous because of its high tendency to accumulate in animals and plants [2]. Human activities have greatly increased the emissions of mercury into the environment over the past century. In the atmosphere, mercury mainly exists in the form of Hg⁰ which is considered one of the major reservoirs [3]. Because of the toxicological effects and potential accumulation of mercury onto human bodies and aquatic organisms, the determination of mercury (II) or organo mercury (II) has seen great interest in the last few years [3, 4].

According to the World Health Organization (WHO), the allowed limit of mercury in drinking water is less than 1.0 μg L⁻¹ as a maximum contaminant level (MCL) for mercury in drinking water [5, 6]. Mercury element, without charge is a volatile gas that may be transferred for long distances by air. Mercury is chemically or biologically transformed into methylmercury and dimethylmercury. Mercury is not essential for plant or animal life and the main human exposure to mercury via inhalation of the vapor of a gas and the ingestion of mercury. Hence, analysis of mercury at trace and/ or ultra trace levels is a vital task for diagnostics and prognostics purposes. Therefore, considerable efforts and progress are required for developing accurate, low cost and reliable methods for mercury determination in contaminated samples without any complicated processing steps.

Several sensitive methods have been reported for analysis of mercury in natural samples e.g. spectrophotometry [7], inductively coupled plasma –mass spectrometry (ICP-MS) [8-10]; atomic fluorescence [11-14]; cold vapour atomic absorption [15-18]; GC [19]; stripping voltammetry [20, 21]; X-ray fluorescence spectrometry [22] and neutron activation analysis [23]. The determination, and chemical speciation of mercury (II) and/ or methyl mercury in a series of complicated matrices e.g. Mushroom from Tokat – Turkey, water and fish have been reported by Tuzen et al., [24, 25]. Moreover, the use of Lichen (*Xanthoparmelia conspersa*) biomass and *Streptococcus pyogenes* loaded Dowex optipore SD-2 have been reported as efficient materials for the removal of mercury (II) and methylmercury from aqueous media [26-32]. Most of these methods are suffered from the lack of sensitivity due to the significant interference of the excess of chromogenic reagent with the analyte at λ_{\max} .

Recently, numerous voltammetric methods have been reported for detection and determination of aqueous Hg from different matrices either alone or in conjunction with emerging technologies such as piezoelectric sensors (Table 4. 1) [33-39].

Stripping voltammetry in particular adsorptive cathodic stripping voltammetry has been the most popular, because of the unquestionably features e.g. excellent sensitivity and selectivity, low detection limits, good accuracy, precision, inexpensive and portable instrumentation [40-43]. The technique is based upon the accumulation of the analyte on a suitable working electrode by potential controlled adsorption and subsequent electrochemical reduction of the preconcentrated species [41]. The sensitivity in stripping voltammetry is

enhanced by increasing the accumulation time and modification of the working electrode [42, 43].

Recent literature has revealed no study on the use of the chelating agent 4-(2-thiazolylazo) resorcinol (TAR) as chelating agent (Fig. 2.1) for chemical speciation and determination of mercury using CSV technique. Thus, the work in this chapter is focused on: i redox characteristics of mercury (II) - TAR chelate in aqueous media; ii assigning the probable electrochemical mechanism and nature of electrode reactions and finally developing of a low cost, and simple cathodic stripping voltammetry method for chemical speciation and determination of mercury in complex matrices e.g. water samples and certified reference materials.

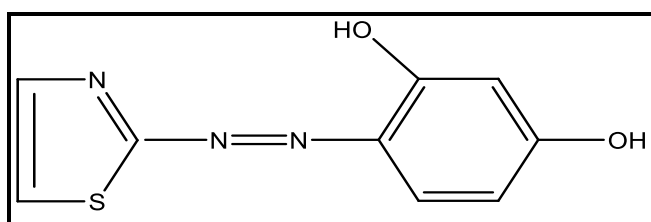


Fig. 2.1 . Structure of TAR

Table 2.1 Voltammetric method of Mercury (II) determination

Technique	Complexing agent	Working electrode	Limit of detection, (LOD)	Referen
DPASV		Twin Au electrode	1 ng L ⁻¹	[33]
Open circuit adsorption stripping voltammetry		Pt disk electrode	1.2 × 10 ⁻⁸ mol L ⁻¹	[34]
Subtractive ASV	—	Rotating Au disk electrode	50 pM	[35]
ASV	Poly(ethylenimine) (PEI)	Carbon electrodes	1.1 × 10 ⁶ mol L ⁻¹	[36]
Cyclic voltammetry		Modified GCE	4.4 × 10 ⁻¹¹ mol L ⁻¹	[37]
ASV	—	Solid Au electrode	0.40 μg L ⁻¹	[38]
ASV	On-line medium exchange	Au film electrode	0.17 μg L ⁻¹	[39]

Table 2.1 Continued

quare wave anodic stripping voltammetry		Screen-printed Au electrodes	1.1 ng mL ⁻¹	[40]
Anodic stripping square wave voltammetry	In highly acidic medium of 1 M hydrochloric acid	Sb Film-CPE	1.3 ppb	[41]
(DPASV) In-situ differential pulse anodic stripping voltammetry	hollow fiber-based liquid-three phase micro	AuNPs–modified Pt-wire	0.06 nmol L ⁻¹	[42]
SWASV		AuNPs modified GC electrodes	0.40 nM	[43]

2.2.2. Experimental

2.2.1. Reagents and materials

Analytical – reagent grade (A.R) chemicals were used except otherwise specified. A stock solution of mercury ($1000 \mu\text{g mL}^{-1}$) was prepared from mercury (II) chloride (BDH, Poole, England). More diluted standard ($0.05\text{--}20 \mu\text{g mL}^{-1}$) solutions were then prepared by dilution and were stored in low density poly ethylene (LDPE) bottles. An accurate weight (0.01 g) of the pure reagent 4-(2-thiazolylazo) resorcinol (TAR) (Fig.2.1) was dissolved in a minimum volume of ethanol), followed by dilution with absolute ethanol (100 mL). A series of Britton- Robinson (B-R) buffer (pH2-11) was prepared by mixing equal proportions of BDH acetic (0.04 mol L^{-1}), phosphoric (0.04 mol L^{-1}) and boric (0.04 mol L^{-1}) acids in deionized water and the pH of the solutions were then adjusted to the required pH by adding various volumes of NaOH (0.2 mol l^{-1}) solution as reported earlier [44].

2.2.2. Apparatus

The cyclic, linear and differential pulse cathodic stripping voltammetric measurements were performed on a Metrohm 757 VA trace analyzer and 747 VA stand (Basel, Switzerland). A Perkin Elmer inductively coupled plasma- mass spectrometer (ICP-MS) (Sciex model Elan DRC II, USA) was used for measuring the trace and ultra trace concentrations of mercury as a standard method and for the validation of the developed DP-CSV method for arsenic determination. A Perkin Elmer (Lambda EZ-210) double beam spectrophotometer ($190\text{--}1100 \text{ nm}$) with 1 cm (path width) quartz cell was used for recording the electronic spectra of the reagent TAR and its mercury(II) complex. A Perkin Elmer FTIR spectrometer 100 series (Beaconsfield, Bucks, and UK) was used for recording the IR spectra of TAR and its mercury(II) complex. A Bruker

advance DPX 400 MHz model using TMS as an internal standard was used for recording the ^1H NMR spectra of TAR and its mercury (II) complex on deuterated DMSO. A CEM microwave system (Mars model, 907500, USA) was used for the digestion of the certified reference material (CRM, *IAEA-soil-7*).

A three-compartment borosilicate (Metrohm) voltammetric electrochemical cell (10 mL) configuration incorporating hanging mercury dropping electrode (HMDE, drop surface area 5 mm^2) as a working electrode, double-junction Ag/AgCl,(3M) KCl, as a reference and platinum wire (BAS model MW-1032) as counter electrodes, respectively. Platinum (Pt, surface area 2 mm^2) and gold (Au, surface area 2 mm^2) were also used separately as working electrodes for recording the cyclic voltammetry. A digital-micro-pipette 10 - 100 μL (Volac) was used for transferring the sample solutions to the electrochemical cell. The electrochemical data were then recorded at room temperature and the peak current heights were measured using the "tangent fit method". Digital pH-meter (model MP220, Mettler Toledo) was used for pH measurements with absolute accuracy limits at the pH measurements being defined by NIST buffers. De-ionized water was obtained from Milli-Q Plus system water purification system (Milford, MA, USA).

2.2.3 General DP-CSV procedures for mercury (II) –TAR complex

The electrochemical cell was pre cleaned by soaking in nitric acid (10% v/v) and washed with de ionized water. The general procedure used to obtain differential pulse – adsorptive cathodic stripping voltammetry (DP-CSV) was as follows. An accurate volume (10 mL) of an aqueous solution containing B-R buffer as supporting electrolyte at the required pH (2.1-11.5) and the required volume (20 μL) of the TAR reagent ($1.0 \times 10^{-2}\text{ mol L}^{-1}$) were transferred into the voltammetric cell by micropipette. The solution was stirred and purged with nitrogen gas for at least 15 min. The stirrer was then stopped

and after 10 s quiescence time, the background voltammogram of the supporting electrolyte and the reagent were then recorded by applying a negative going potential scan from 0.0 – to -1.5 V vs. Ag/AgCl at a deposition potential of – 0.4 V, accumulation time of 60 s; starting potential 0 V; scan rate of 50 mVs⁻¹ and 60 mV pulse amplitude. After recording the voltammogram of the reagent solution, an accurate volume (30 μ L) of mercury (II) solution (8.21x 10⁻³ mol L⁻¹) was added. The DP-CSV voltammogram was repeated with new mercury drop under the same experimental conditions of the reagent (TAR). The solution was stirred and purged with nitrogen gas for 5 min and the stirrer was then stopped. After 10 s quiescence time, the voltammogram of the mercury(II)-TAR complex was finally recorded by applying a negative going potential scan from 0.0 to –1.5 V vs. Ag/AgCl reference electrode. Following these procedures, the influence of the operational parameters e.g. deposition time, accumulation potential, starting potential, concentration of the reagent and pulse amplitude was critically investigated. The influence of the scan rate ($v = 0.02\text{--}2 \text{ Vs}^{-1}$) on the cyclic voltammograms of palladium (II) – SQ-OH complex at pH 10 was also carried out in the same cell under the experimental conditions.

2.2.4 Recommended procedures for mercury(II) determination

An accurate volume (10 mL) of an aqueous solution containing B-R buffer as supporting electrolyte at pH 7-8 was placed in the voltammetric cell. An accurate volume of the TAR reagent solution was transferred into the electrochemical cell to provide final concentrations of $9.8 \times 10^{-6} \text{ mol L}^{-1}$. The sample solution was then stirred and purged with pure nitrogen gas for at least 5 min before recording the voltammograms. The stirrer was then stopped and after 10 seconds equilibration time, the voltammograms were recorded by applying a negative potential scan from 0.0 to -1.5

V vs. Ag/AgCl at 60 s accumulation time, -0.4 V deposition potential, 0.0 V starting potential; 60 mV pulse amplitude and finally 50 mVs⁻¹ scan rate. After recording the voltammogram of the blank solution, an accurate volume (20 µl) of mercury(II) was then added. The DP-CSV voltammogram was then repeated with new mercury drop under the same experimental conditions. The peak current for mercury(II) was measured at about -0.52 V vs. Ag/AgCl reference electrode. Mercury concentration was then determined from the difference between the cathodic peak current corresponding cathodic peak current at -0.52 V before and after adding mercury to the reagent solution.

2.2.5 Analytical applications

2.2.5.1. Analysis of mercury in certified reference material (CRM, Soil 7- IAEA) by the developed DP-CSV method

An accurate weight (0.10 ±0.001g) of the CRM sample was transferred into a Teflon beaker (50.0 mL) containing HF (7.0 mL), concentrated HCl (2.0 mL), and concentrated HNO₃ (5.0 mL), (7:2:5 v/v) and left at room temperature for 24 h. The reaction mixture was heated gently for 1h at 100-150°C on a hot plate. After evolution of the NO₂ fumes had ceased, the reaction mixture was evaporated almost to dryness. The solid residue was then re dissolved in dilute nitric acid (10.0 mL, 10%v/v). The resulting mixture was filtered through a Whatman 41 filter paper. The filtrate and the washings were then collected, transferred quantitatively to volumetric flask (25.0 mL) and completed to the mark with de ionized water. The mercury content in the test solution was then analyzed following the recommended procedures for mercury(II). The validation of the method was tested by comparing the data obtained with the antimony content in the CRM sample determined by the standard ICP-MS and the claimed value.

2.2.5.2. Analysis of labile mercury (II) complex in tap- and drinking water samples by the developed DP-CSV method

Tap – and / or drinking water samples were collected and filtered through 0.45 μm cellulose membrane filters and stored in low density polyethylene bottles (500 mL). The recommended electrochemical procedures used for the standard curve of mercury (II) determination at pH 7-8 were then followed. Labile mercury concentration was finally determined from the calibration plot using the equation:

$$\text{Mercury concentration} = C_{\text{istd}} \times i_{\text{samp}} / A_{\text{istd}} \quad (2.1)$$

where, C_{istd} is the standard concentration of analyte and i_{samp} and A_{istd} are the current heights of the sample and standard in nA at -0.52 V, respectively.

Alternatively, the standard addition (spiking) method was used as follows: transfer volume (2.0 mL) of the test water samples adjusted to pH 7-8 into the electrochemical cell in the presence of TAR at the optimum experimental conditions. The change in the current heights displayed by the test solution before and after addition of various volumes of the standard mercury (II) ions was then computed from the corresponding DP-CSVs. The concentration of mercury (II) ions was finally determined from the calibration curve of the standard addition.

2.2.5.3 Chemical speciation of labile and complexed fractions of mercury (II) in water samples by the developed DP-CSV method

Tap and / or treated wastewater samples were collected from municipal discharge station samples, Jeddah city, KSA using a battery powered and peristaltic pump. The sample solutions were immediately filtered through 0.45 μm cellulose membrane filters and stored in LDPE bottles (500 mL). First, aliquot samples were analyzed for labile mercury (II) following the recommended procedures in section 2.2.4. Another aliquot

was subjected to UV radiation at 254 nm for 6h in presence of HCl (10%) and analyzed for total mercury(II). Based on these bases, the current of the first aliquot (i_1) will be a measure of free mercury (II) ions, while the current of the second aliquot (i_2) is a measure of total lead. Thus, the difference in current (i_2-i_1) is a measure of the complexed fractions of mercury in the water samples. The spiking method was also applied for mercury determination as follows: transfer known volumes (5.0 mL) of water sample adjusted to pH 7-8 into the cell and measure the peak current displayed before and after addition of various known volumes (0.2-1.0 mL) of standard mercury(II) ions. The linear plot of standard addition curve was successfully used for measuring mercury(II).

2.3. Results and discussion

2.3.1.Characterization of Hg-TAR

TAR is a well-known chelating reagent which is used as an indicator in acid–base titrations [45, 46]. The reagent TAR (Fig. 2.1) has three acidity constants, two of them are due to the two ionizable OH groups (k_{OH}) ($pK_a = 6.3$ and 9.8) [47] and the third one (k_{NH}) is due to the dissociation of the protonated species at pH lower than 1.0. Preliminary investigation on the interaction of TAR reagent with mercury(II) at various pH has revealed considerable color change in alkaline solution of pH 7-9 in good agreement with the results reported by . Karipcina, et al, 2009 [48]. The fact that, TAR reagent exists in the anionic form in basic solutions probably due to the deprotonation of phenolic group (Fig. 3). Thus, the electronic spectra of the reagent TAR and its mercury(II) complex were recorded to fully assign the chemical structure of mercury(II)-TAR complex in aqueous ethanol solution of pH 7-8. The electronic spectra of the reagent TAR and its mercury (II) chelate in aqueous media are demonstrated in Fig.2.2.

In the visible region, the spectrum of the TAR reagent *vs.* ethanol, showed one well defined peak at λ_{max} 443nm, while, the electronic spectrum of its mercury(II) complex *vs.* The reagent blank revealed one well defined absorption peak (λ_{max}) at 518 nm (Fig.2.2). The observed colour change and the progressive bathochromic shift in the electronic spectrum of Hg-TAR complex suggest complex formation of TAR with mercury. The observed enhancement in the molar absorptivity of the Hg(II)-TAR complex at peak maxima in the visible region added further confirmation of Hg-TAR complex. The stiochiometric of mercury(II) to TAR in the produced mercury(II)-TAR complex was determined by continuous variation and molar ratio methods via measuring the absorbance of the complex at λ_{max} 518 nm at various concentrations of mercury (II) and TAR [49]. The results of the two methods revealed formation of mercury (II): TAR at 1:2 molar ratios. These results suggest formation of Hg(TAR)₂ complex.

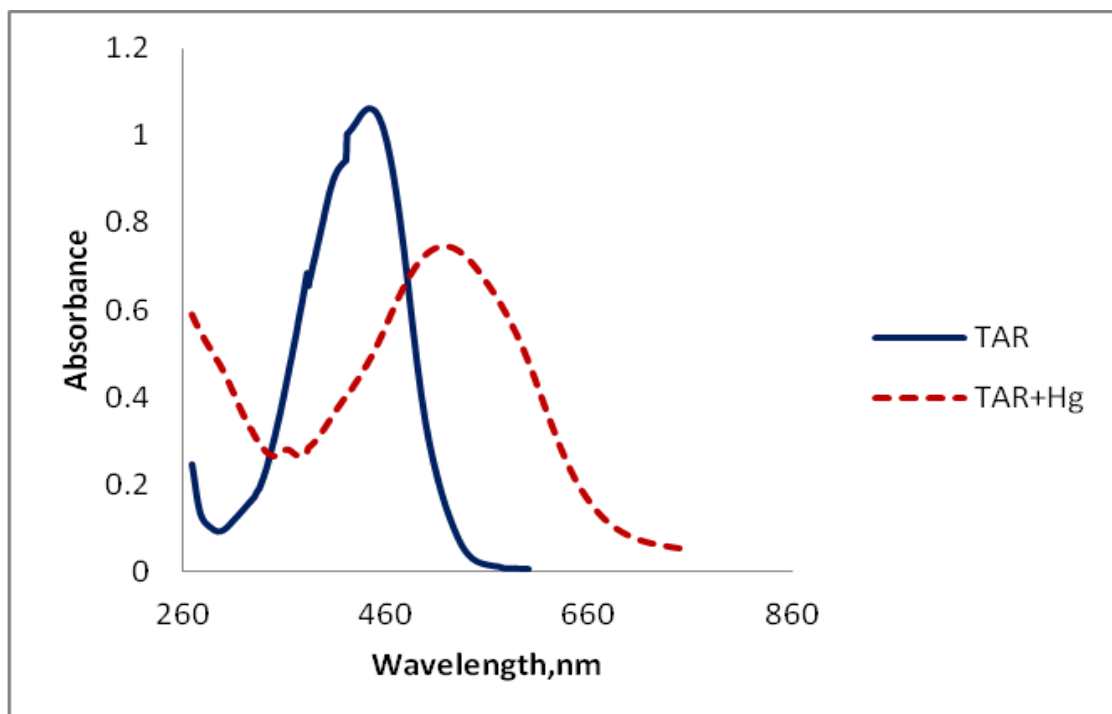


Fig.2.2. Electronic spectra of TAR and its mercury(II) complex in aqueous medium.

The binding sites of TAR reagent (Fig. 2.1) are due to the oxygen atoms of the two hydroxyl groups after de protonation, and the two nitrogen atoms of azo and pyridine nitrogen. Thus, the most probable binding sites of the free ligand (TAR) to Hg-TAR complex was assigned in the present study by recording FTIR spectra of the solid reagent and its solid mercury (II) complex in the 4000–400 cm^{-1} range (Fig. 2.3). In the FTIR spectrum of free TAR, the vibration modes at 3020 and 3080 cm^{-1} are assigned to $\nu(\text{C-H})$ [50]. These bands are stable in the position as well as more or less intensity when one goes from TAR to its mercury (II) complex indicating that these vibrations are purely due to $\nu(\text{C-H})$. The broad band appeared around 3331 cm^{-1} in the ligand spectrum is safely assigned to phenolic $\nu(\text{O-H})$ groups. In Hg(II)-TAR complex, this broad band is still broad, which renders it difficult to attribute to the involvement of phenolic OH group in coordination. The stretching vibration of $\nu(\text{C=N})$ of the thiazolylazo nitrogen is observed in the form of a strong intensity at 1644 cm^{-1} in the free TAR [50]. The spectral region at 1600–1400 cm^{-1} is complicated because of the stretching modes of $\nu(\text{C=N})$ – and $\nu(\text{N=N})$ – which are superimposed in the same region. The band at 775 cm^{-1} in the ligand is still in the same position in the Hg(II)-TAR complex indicating the non-involvement of the thiazole S in the coordination. The participation of the deprotonated phenolic OH group in chelation with mercury was confirmed by the blue shift of the $\nu(\text{C-O})$ stretching band at 1273 cm^{-1} in the free ligand to 1192 cm^{-1} in Hg complex [50]. This is supported by band observed at 597 cm^{-1} due to $\nu(\text{Hg-O})$ [50]. The $\nu(\text{-C=N-})$ band due to pyridine nitrogen at 1644 cm^{-1} in the free TAR remained in the same position in the Hg(II)-TAR complex indicating the non-involvement of the N atom of the thiazole moiety in coordination [48, 50, 51]. The band appearing at 1587 cm^{-1} was safely assigned to $\nu(\text{N=N})$ of the azo group of the ligand. The bands observed at 1401 and 1554 cm^{-1} in the free TAR due to azo group $\nu(\text{-N=N-})$ are shifted to 1499 and 1360 cm^{-1}

¹upon complex formation indicating participation of N atom of the azo group to mercury(II). This was confirmed by the weak vibration band observed at 418 cm⁻¹ in Hg complex due to ν (M-N)_{azo}. Therefore, the FTIR spectrum of the complex indicates that TAR behaves as monobasic acid bidentate fashion (NO) via Ar-OH and -N=N- [50, 51]. ¹H NMR spectra of the free ligand TAR and its mercury(II) complex in CDCl₃ were recorded. The chemical shift (ppm) of the proton of the hydroxyl group at 5.4 ppm of the free ligand was disappeared upon coordination confirming participation of the ligand via one of the phenolic hydroxyl groups. The thiazole C-H was noticed at 7.65 ppm. Thus, the reagent TAR coordinates to mercury in a bidentate fashion via azo and hydroxyl groups, hence the most probable structural formula of mercury(II)-TAR complex is proposed in Fig. 2.4. The data also suggested the possible use of TAR reagent as complexing agent for cathodic stripping voltammetric determination of mercury (II) in water samples in the subsequent work.

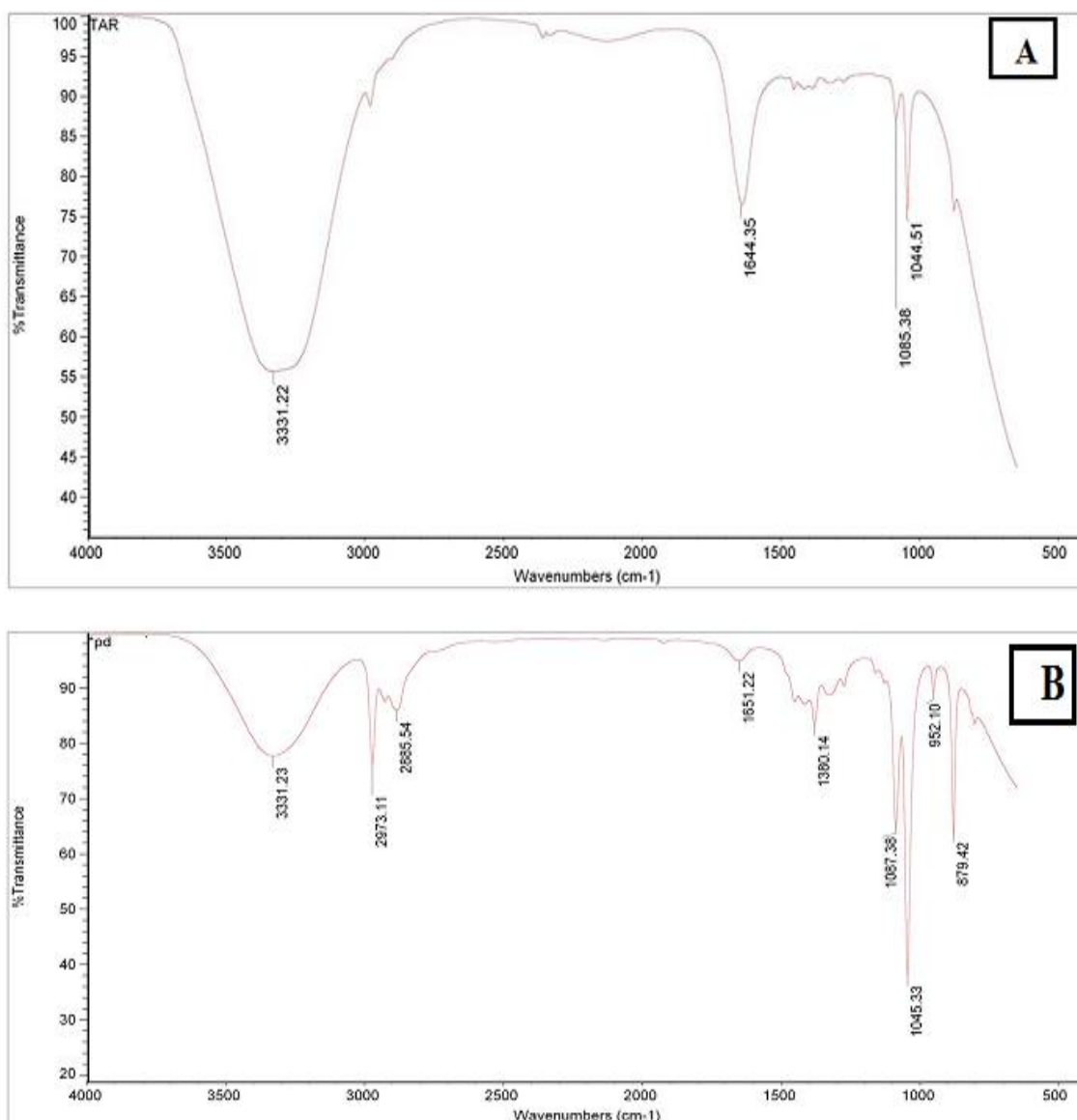


Fig. 2.3. FTIR spectra of TAR (A) and its mercury(II) complex (B).

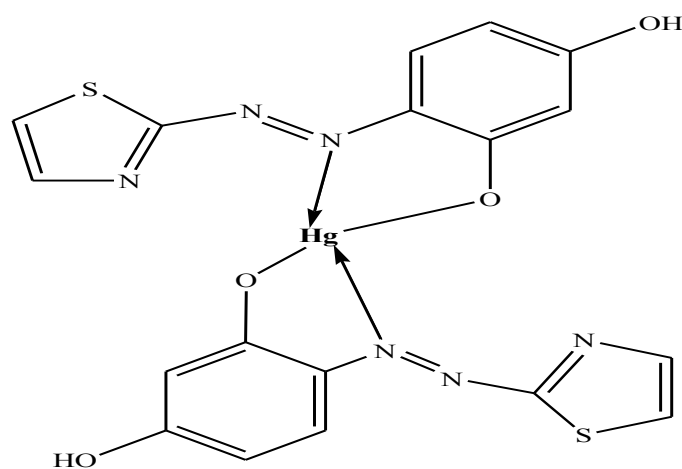


Fig.2.4 .Proposed chemical structural formula of mercury(II) – TAR complex.

2.3.2 Electrochemical behaviour of Hg (II) – TAR complex:

The pH of the electrolysis medium represents one of the most important parameter strongly control the shape of the DP-CSV, peak potential and peak current. Hence, the differential pulse cathodic voltammograms (DP-CSVs) of TAR in the absence and presence of mercury (II) ions at the HMDE over a wide range of pH 2.3-11 using Britton-Robinson (B-R) buffer solutions were critically carried out. The DP CSV of the supporting electrolyte i.e background, and the background with addition of TAR were recorded initially and the results revealed ill defined cathodic peaks. On the other hand, the DP CSV after addition of mercury (II) to the TAR solution at various pH (pH 2-11) well defined cathodic peaks were observed. The DP-CSV of the complex showed a well-defined reduction peak in the range -0.2 to - 0.55V vs. Ag/AgCl reference electrode. Representative data are shown in Fig.2.5. The observed cathodic peak was most likely belong to the reduction of the azo group (-N=N-) in the TAR reagent. The dependence of the cathodic peak potential ($E_{p,c}$) on the pH was explained by a direct exchange of four electrons in one step. On increasing the solution pH, the $E_{p,c}$, at -0.25 was shifted to more negative potential confirming the irreversible nature of the electrochemical reduction process and the electrode reaction involves hydrogen ions [52, 53]. The cathodic peak current ($I_{p,c}$) reached maximum at pH 5. However, in the subsequent work, buffer solution of pH 6 was selected since constant, reproducible and sharp cathodic peak at -0.38 V vs. Ag/AgCl reference electrode was observed.

Over the investigated pH range (pH 2.3-11), the DP-CSV of mercury (II) – TAR displayed one well defined cathodic wave in the range at - 0.18-0.54 V vs. Ag/AgCl reference electrode and is most likely assigned to reduction of the N=N group in TAR reagent. The observed dependence of the reduction peak on the pH can be explained by a direct exchange of four electrons in two successive two - electron steps with splitting of

the N=N group to form $-\text{NH}_2-\text{NH}_2$ [52]. In the DP-CSV, on raising the solution medium pH, the potential of the cathodic peak of mercury (II)-TAR chelate was shifted cathodically to more negative potentials. The plot of the change of the cathodic peak potential vs. pH was linear (Fig. 2.6) following the linear regression equation (2.2):

$$E_{p,c} = -0.078 \text{ pH} - 0.13 \quad (R^2 = 1.0) \quad (2.2)$$

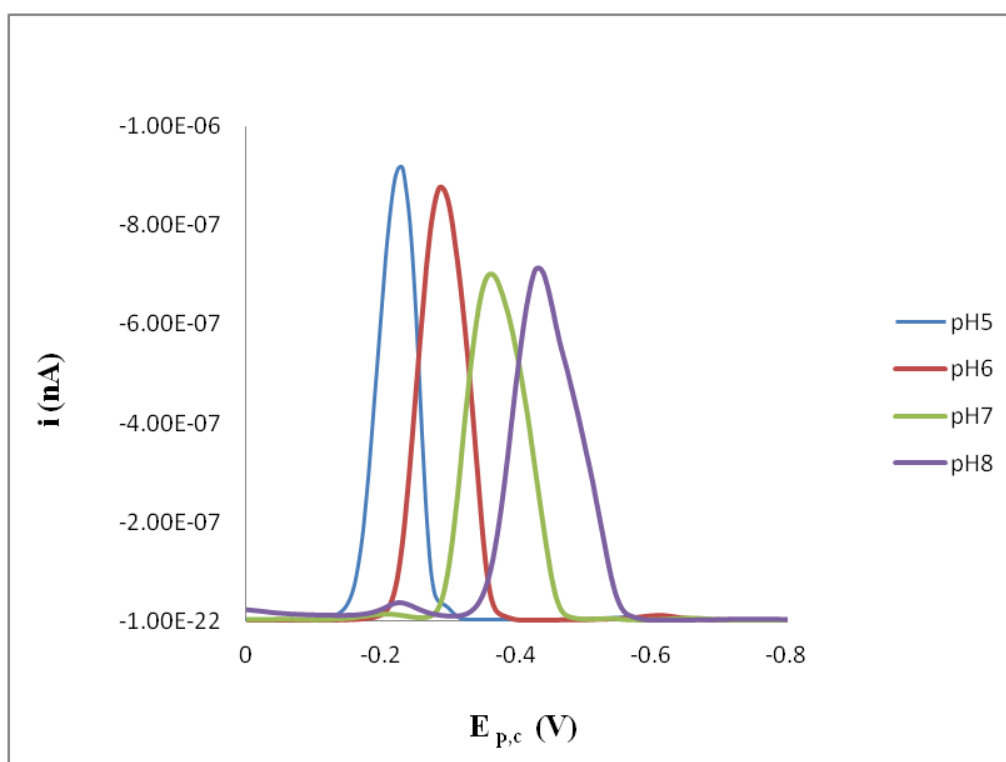


Fig.2.5 DP-CSVs of TAR(9.8×10^{-7} M) in presence of mercury (II) ions (4.9×10^{-7} M) at various B-R buffer solutions at the HMDE vs. Ag/AgCl reference electrode at 50 mVs^{-1} scan rate and 50 mV pulse amplitude.

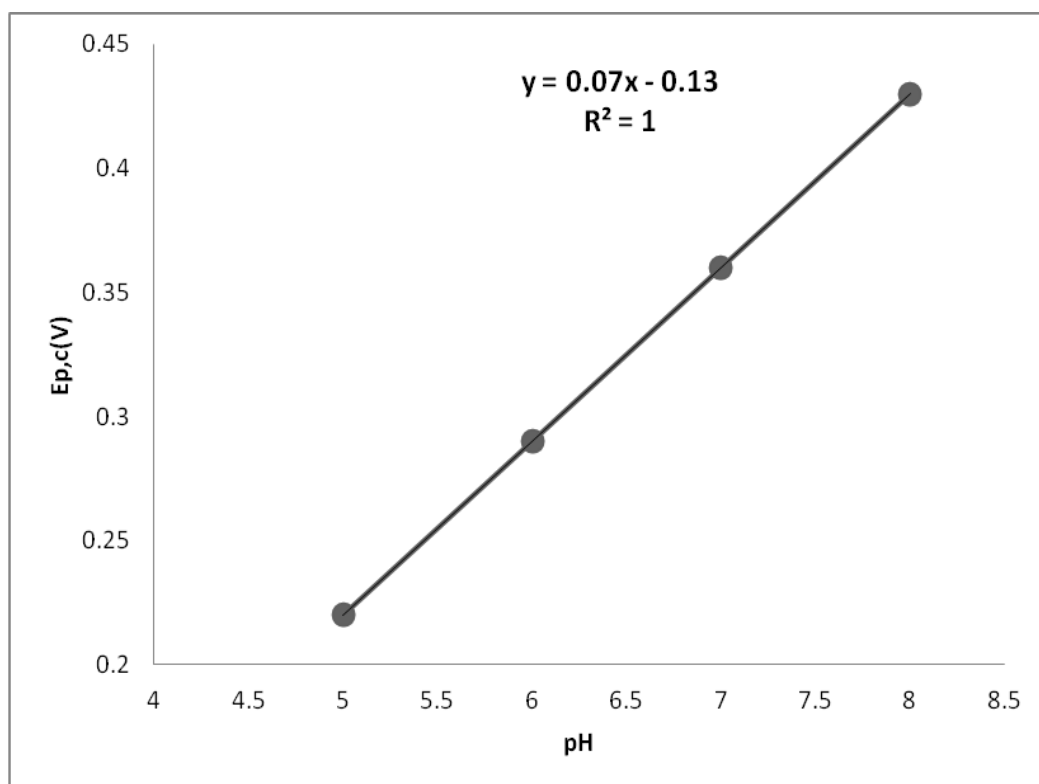


Fig.2.6 Plot of cathodic peak potential ($E_{p,c}$) of mercury (II)-TAR complex vs. solution pH at HMDE.

The cyclic voltammograms of mercury(II) – TAR complex at HMDE in B-R buffer of pH 6-7 at various scan rates ($20-1000 \text{ mVs}^{-1}$) vs. Ag/AgCl reference electrode were critically recorded. The results are demonstrated in Fig. 2.7. The CVs showed two well defined cathodic peaks in the range $E_{p,c1} = -0.64$ to -0.9 and $E_{p,c2} = -1.4$ to 1.47V . On the reverse scan, one ill defined anodic peak ($E_{p,a} = -0.3$ to -0.4V) was observed revealing the irreversible nature of the electrode process. This calculated value of peak –peak potential difference ($\Delta E_p = (E_{p,a} - E_{p,c1})$) was $> 200 \text{ mV}$ confirming the irreversible nature of the observed electrode couples.

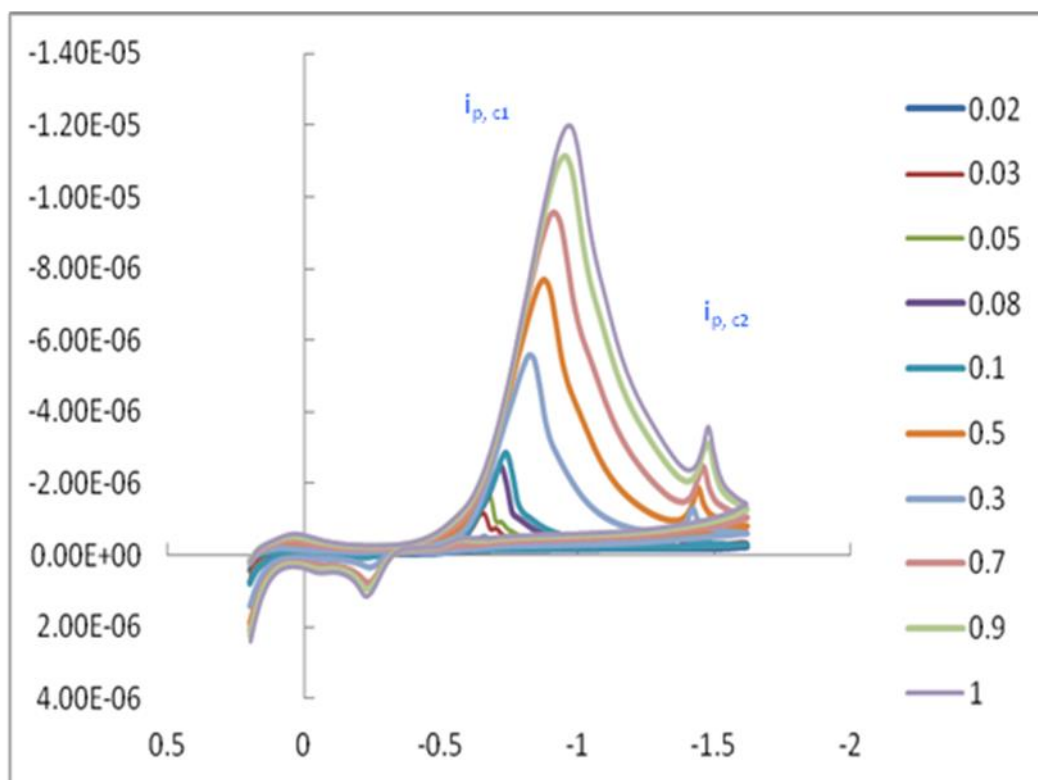


Fig.2.7 Cyclic voltammograms of mercury (II)-TAR at pH 6-7 at various scan rates (20-1000 mVs^{-1}) at HMDE vs. Ag/AgCl electrode.

The influence of the scan rate ($\nu=20-2000 \text{ mVs}^{-1}$) on $E_{p,c}$ and $I_{p,c}$ of mercury (II) - TAR complex at pH 6-7 was investigated on a freshly drop of the HMDE. On raising the scan rate, the potential of the cathodic peak ($E_{p,c1}$) was shifted cathodically (Fig. 2.8) confirming the irreversible nature of the electrochemical reduction process of Hg-TAR complex [52]. The $i_{p,c}$ increased linearly on raising the scan rate ($\nu^{1/2}$) indicating that, the reduction step is diffusion controlled electrochemical process (Fig.2.9) [52, 53]. The plot of $\log i_{p,c1}$ vs. $\log \nu$ at pH 6-7 at HMDE against Ag/AgCl was also linear (Fig. 2.10) with a slope > 0.5 ($R^2= 0.98$) and far from the theoretical value (1.0) expected when there is an adsorption process on the electrode of the HMDE confirming the irreversible nature of the electrochemical process [52].

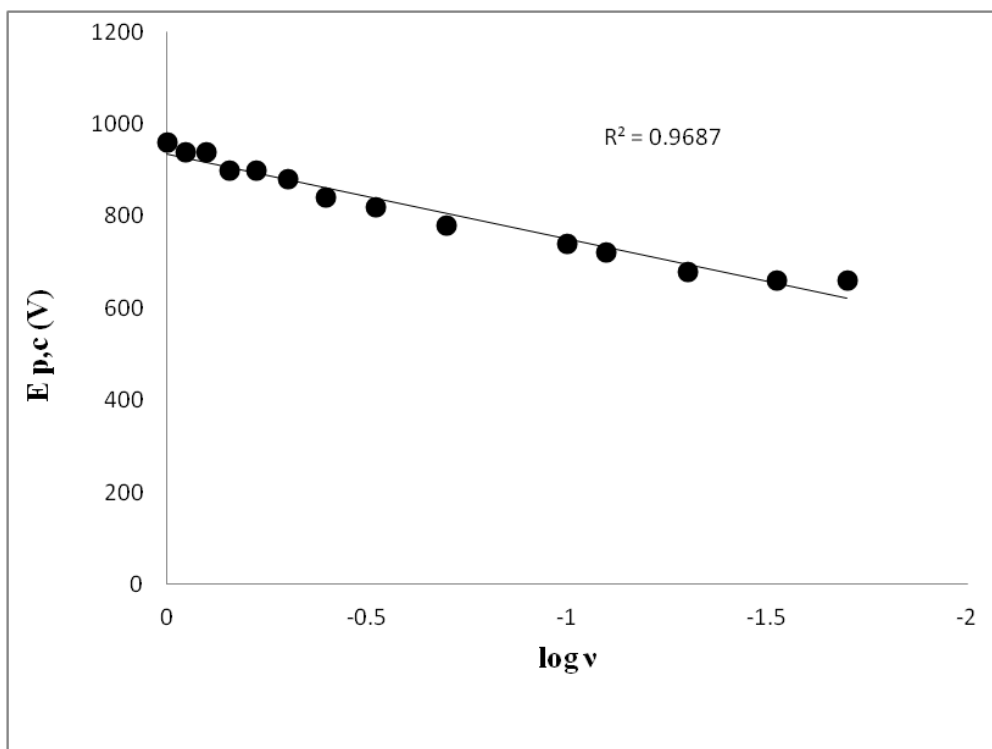


Fig.2.8. Plot of $E_{p,c}$ vs. $\log v$ of Hg-TAR complex at pH 6-7 at HMDE vs. Ag/AgCl reference electrode.

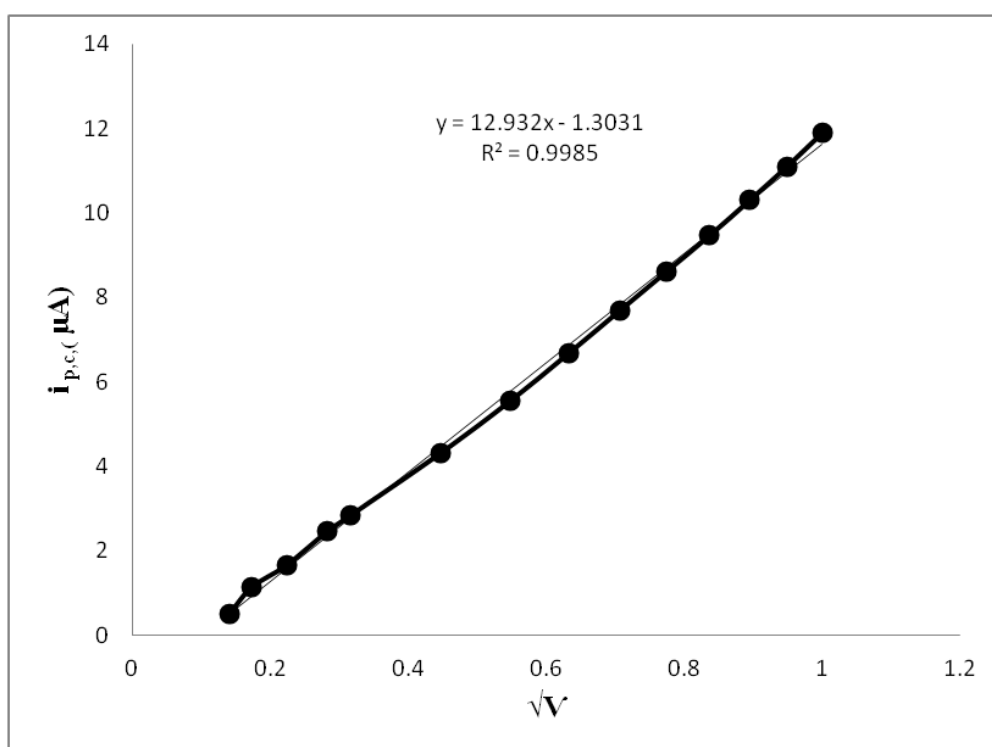


Fig.2.9 Plot of $i_{p,c}$ vs. square root of the scan rate (v) of Hg-TAR complex at pH 6-7 at HMDE vs. Ag/AgCl reference electrode.

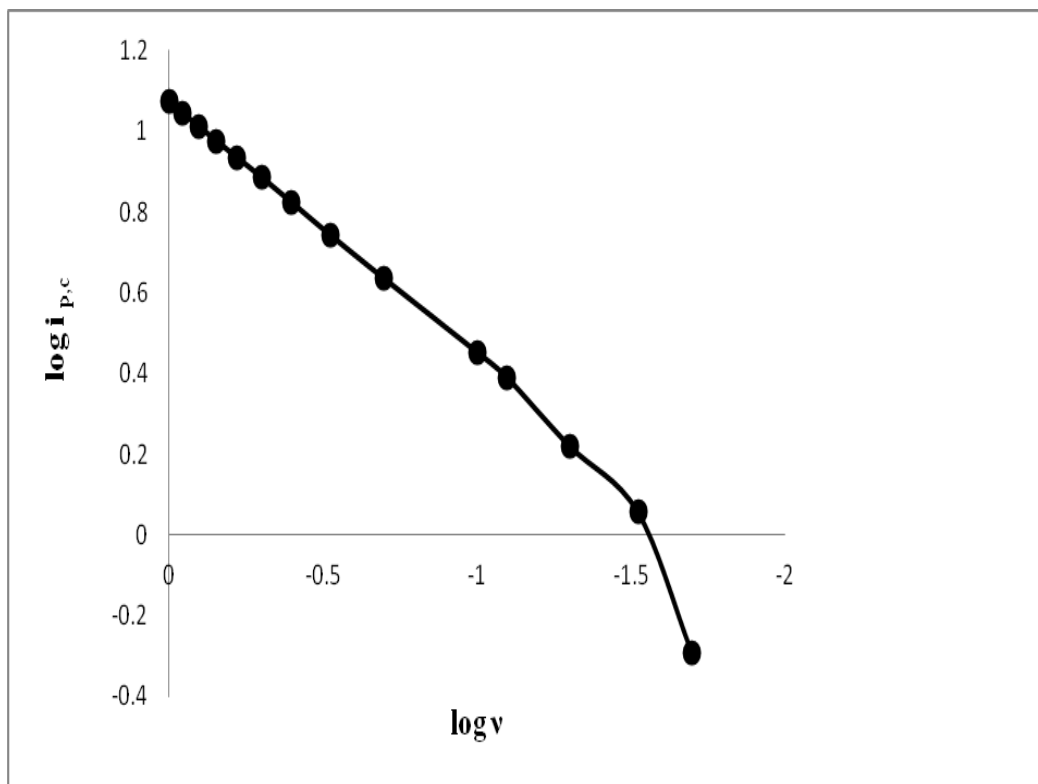


Fig.2.10. Plot of $\log i_{p,c1}$ vs. $\log v$) of Hg-TAR complex at pH 6-7 at HMDE vs. Ag/AgCl reference electrode.

The plot of the cathodic peak current function ($i_{p,c1} / v^{1/2}$) vs. scan rate is shown in Fig.2.11 The current function ($i_{p,c} / v^{1/2}$) increased continuously on increasing the v (Fig.2. 11) indicating that, the reduction process of the azo group (-N=N-) of Hg (II) - TAR complex do not favour the electrode- coupled chemical reaction mechanism of EC type [52]. The fact that, in an EC mechanism with an irreversible electrochemical process, the ratio $i_{p,c} / v^{1/2}$ should decrease continuously on raising the scan rate. The CVs also exhibited an ill defined cathodic peak in the range $E_{p,c2} = -1.4$ to $1.47V$ at scan rate $>80 \text{ mVs}^{-1}$. Thus, it can be concluded that the product of this reduction step undergoes a very slow follow-up chemical reaction and the electrode reaction favour EE type mechanism [52].

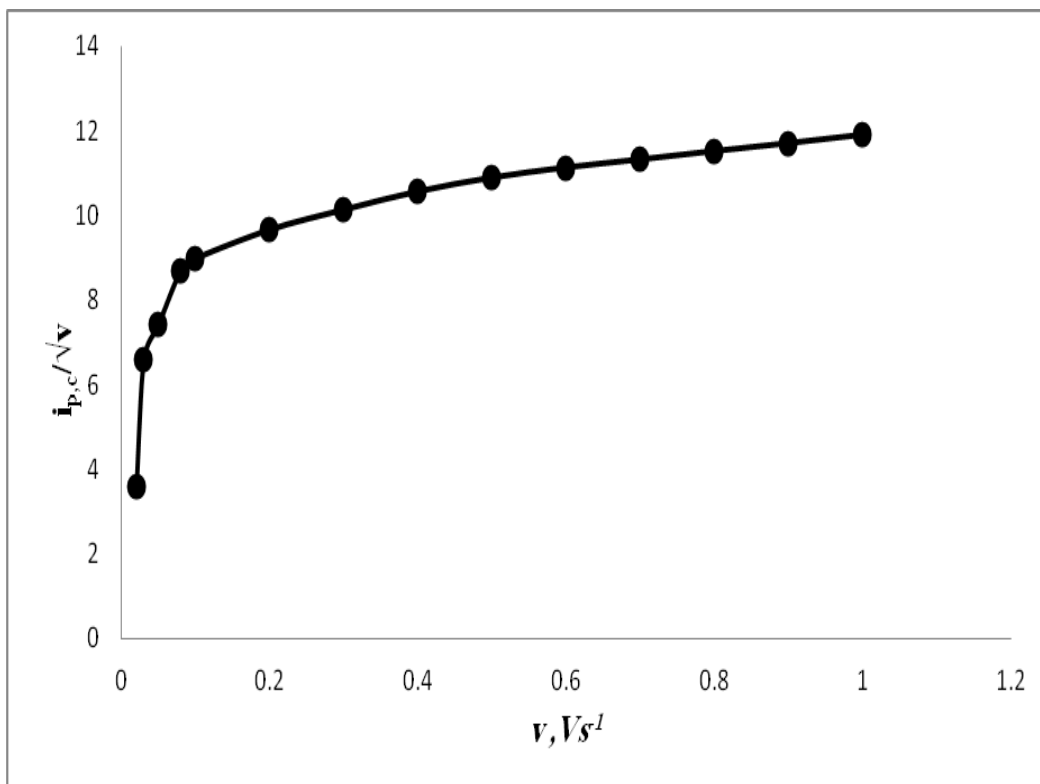


Fig.2.11. Plot of current function ($i_{p,c} / v^{1/2}$) vs. scan rate at HMDE vs. Ag/AgCl electrode.

The product of the number of the electron transfer in the rate-determining step (N_α) of the reduction process and the corresponding charge transfer coefficient (α) i.e. αN_α of the surface reaction of the adsorbed species were calculated at pH 6-7 from the slope of the linear plot of $E_{p,c}$ vs. $\log v$ (Fig. 2.8) employing the following equation:

$$\Delta E_{p,c} / \Delta \log v = - 29.58 / \alpha N_\alpha \quad (2.3)$$

Assuming $N_\alpha=2$, the value of α calculated from the slope of the straight line was in the 0.82 ± 0.03 confirming the irreversible nature of the two – electron reduction

electrode process. The value of α was also calculated from the influence of the scan rate on the CV of Hg(II)-TAR at pH6-7 employing the equations [49]:

$$E_{p,c} - E_{p,c/2} = - 1.857 (RT/\alpha N_{\alpha} F) \quad (2.4)$$

$$(E_{p,c})_2 - (E_{p,c})_1 = RT/\alpha N_{\alpha} F. \ln (V_1/V_2)^{1/2} \quad (2.5)$$

where, $E_{p,c/2}$ is the half peak potential in volt, T= absolute temperature, R is the gas constant = 8.3143 C/K.mol; F= Faraday constant =96.487 coul /equ and v_1 and v_2 are the scan rate (mVs^{-1}) at two different values. Assuming $N_{\alpha} = 2$, the value of α calculated from equations 2.4 and 2.5 were found < 0.5 confirming the irreversible nature of the electrode process.

The surface coverage of the electroactive species, Γ was calculated employing the equation [52]:

$$I_{p,c} = n^2 F^2 A \Gamma v / 4RT \quad (2.6)$$

where n represents the number of electrons involved in the electrochemical process, A is the geometric surface area ($3.8 \times 10^{-3} \text{ cm}^2$) of the HMDE and other symbols have their usual meaning. From the slope of $i_{p,c1}$ vs. sweep rate (Fig. 2.12), the calculated surface coverage of Hg(II)-TAR was $6.13 \times 10^{-5} \text{ mol/ cm}^2$ for $n = 2$ suggesting application of the reagent TAR for DP-CSV determination of trace concentrations of mercury in aqueous media.

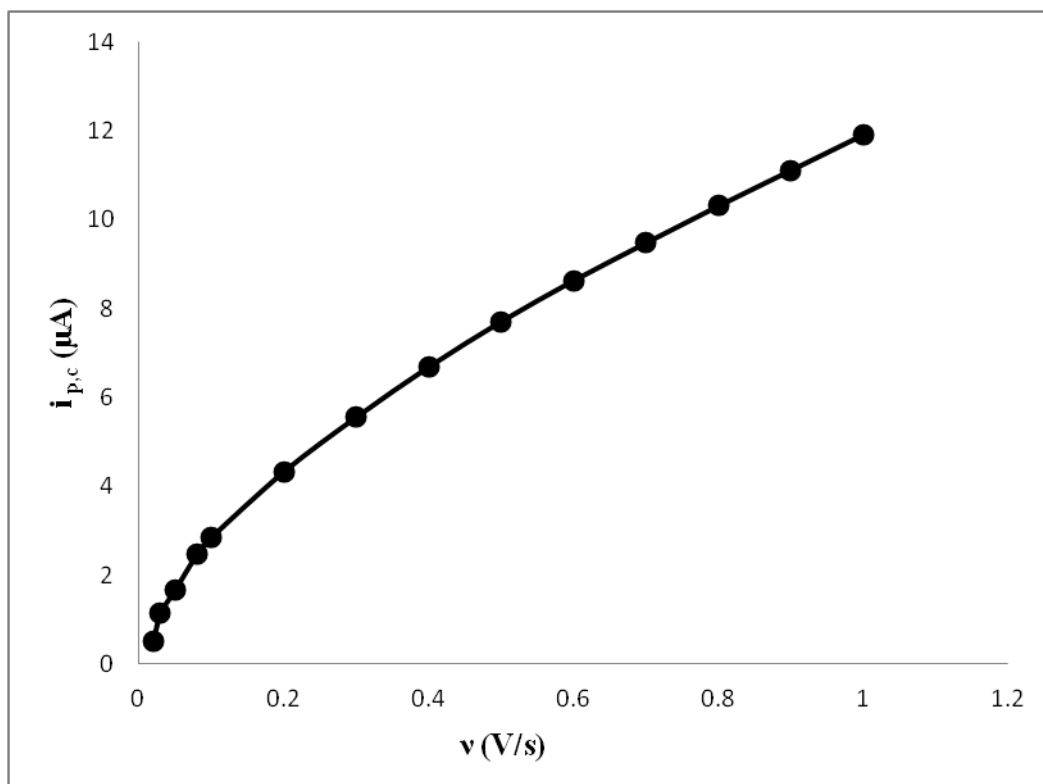


Fig.2.12 Plot of CV cathodic peak current ($i_{p,c}$) vs. scan rate at HMDE vs. Ag/AgCl electrode at pH 6-7 of Hg(II)-TAR complex.

2.3.3. Analytical parameters

The results of DP-CSV and CVs revealed high degree of adsorption and good sensitivity of the developed cathodic peak (-0.38 V) of mercury(III) –TAR. Thus, the reagent TAR was suggested as a complexing agent for DP-CSV determination of trace concentrations of mercury(II) ions in aqueous media. The influence of different parameters that control the cathodic peak current of the cathodic wave of mercury (III) – TAR complex was critically investigated at the HMDE vs. Ag/AgCl reference electrode. The influence of pH on the DP-CSV of Hg(II)-TAR employing B-R buffer on the peak current at- 0.38 V vs. Ag/AgCl was studied over a wide range of pH after 60 s preconcentration time. The plot of the cathodic peak current vs. pH is shown in Fig.2.13. Maximum enhancement of the cathodic peak current was observed at pH 5. However,

buffer solution of pH 6-8 was adopted in the next work. At this range of pH constant, selective, reproducible and sharp cathodic peak at -0.38 V vs. Ag/AgCl reference electrode was observed. At pH > 8 the cathodic peak current decreased due to formation of unstable or hydroxo species of mercury(II). Thus, , the solution pH was adopted at pH 6-7.

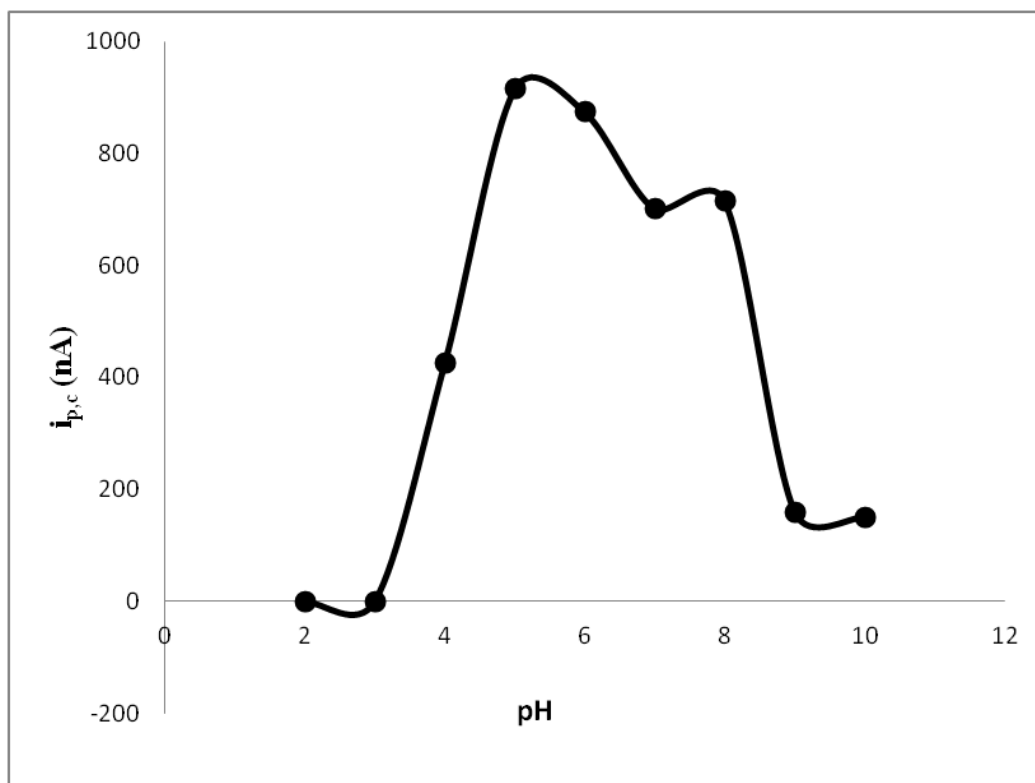


Fig.2.13. Effect of pH on peak current of Hg(II)-TAR. Conditions: [TAR], 9.8×10^{-7} M; $[Hg^{II}]$, 4.9×10^{-8} M; 50 mVs^{-1} scan rate and 50 mV pulse amplitude.

The accumulation times were examined in the range of 30 - 300s. Representative results are shown in Fig.2.14. Maximum peak current and well defined peaks were obtained at 60 s at $E_{p,c} = -0.38$ V. At longer time; the peak current began to decrease suggesting that the electrode surface was saturated with free TAR. The observed decrease in the cathodic current at longer deposition time is a characteristic feature of adsorptive stripping with the stirred solution. Hence, in the subsequent work, an accumulation time of 60s was adopted in the subsequent work for Hg determination by TAR reagent.

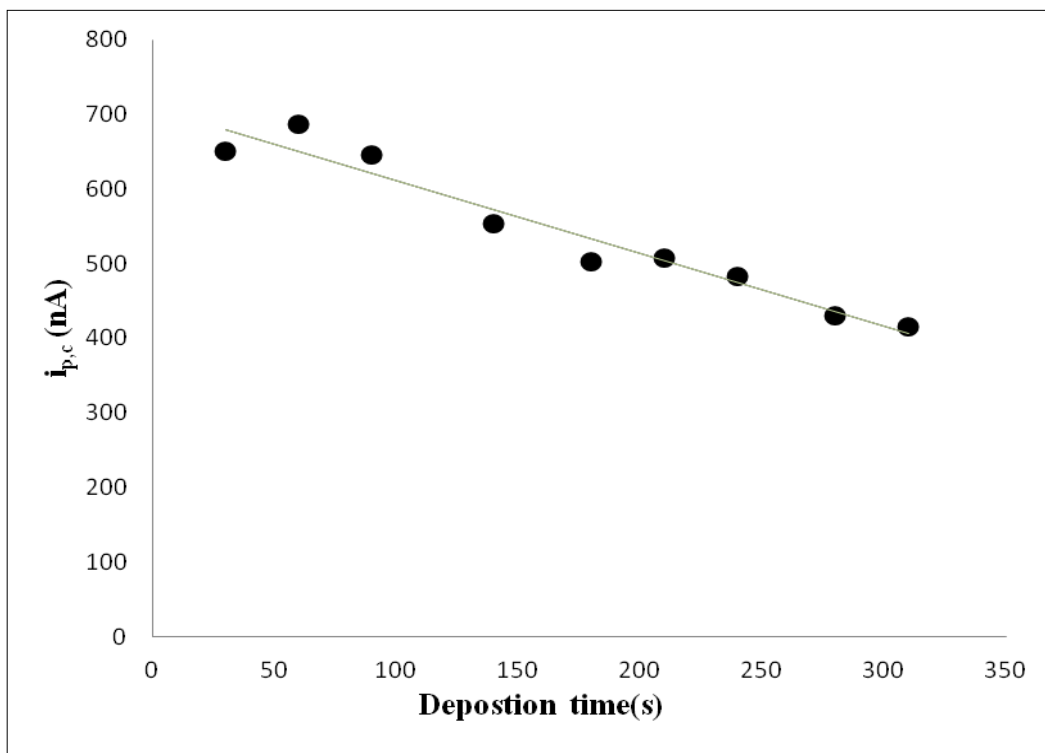


Fig.2.14. Plot of Effect of the cathodic peak current of Hg(II)-TAR vs. Accumulation time (s). Conditions: TAR concentration $=9.8 \times 10^{-7}$ M; $\text{Hg}^{2+} = 4.9 \times 10^{-11}$ M; deposition potential $= -0.45$ V, scan rate 60 mVs^{-1} and pulse amplitude of 60 mV.

The effect of deposition potential on the adsorptive cathodic stripping peak current of Hg-Tar complex was evaluated over a wide range of deposition potential (0.0 - -0.25 V) vs. Ag/AgCl reference electrode after 60s collection time. The results are shown in Fig.2.15. Maximum cathodic peak current was achieved at increased on decreasing the deposition potential and reached maximum at -0.04 V. Thus, a deposition of -0.04 V was selected in the subsequent work.

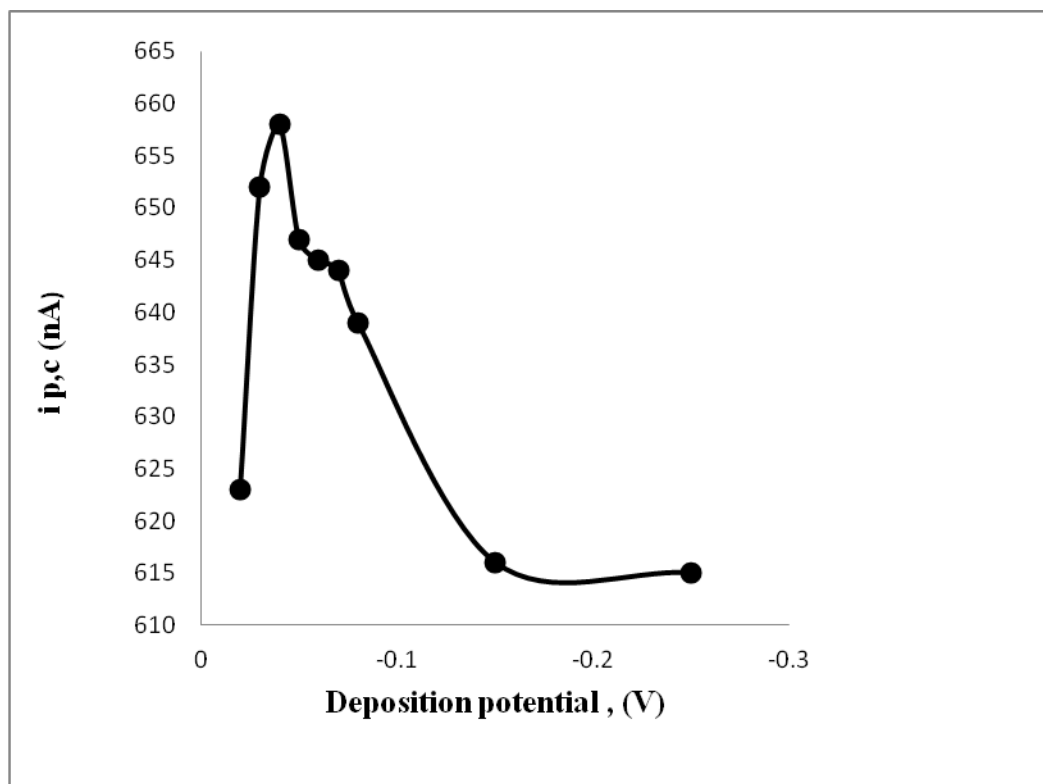


Fig.2.15. Plot of the cathodic peak current of Hg(II)-TAR vs. Deposition potential (V) Conditions: TAR concentration = 9.8×10^{-7} M; $\text{Hg}^{2+} = 4.9 \times 10^{-11}$ M; deposition time = 60s, scan rate 60 mVs^{-1} and pulse amplitude of 60 mV.

The influence of starting potential on the DP-CSV peak current of Hg(II)-TAR complex at pH 6-7 at peak potential of -0.38 V at the optimum experimental parameters was evaluated over a wide range of potential (0.0 – 0.1 V) at the HMDE. Maximum cathodic current was obtained at 0.0 V. Thus, in the subsequent work, a starting potential of 0.0 V was adopted in the next work.

The influence of scan rate ($5.0\text{-}800 \text{ mVs}^{-1}$) on the $i_{p,c}$ of Hg(II)-TAR at pH 6-7 ($9.8 \times 10^{-7} \text{ mol L}^{-1}$) in the presence of mercury (II) ions ($4.5 \times 10^{-7} \text{ mol L}^{-1}$) was investigated under the optimal operational parameters of accumulation time, deposition potential and starting potential. The results are demonstrated in Fig. 2. 16. The $i_{p,c}$ increased steadily on raising the scan rate from 5.0 to 800 mVs^{-1} . However, a scan rate of 60 mVs^{-1} was

selected in the subsequent work. At 60 mVs^{-1} scan rate, well defined and symmetric cathodic peaks, excellent background, accuracy and sensitivity were achieved.

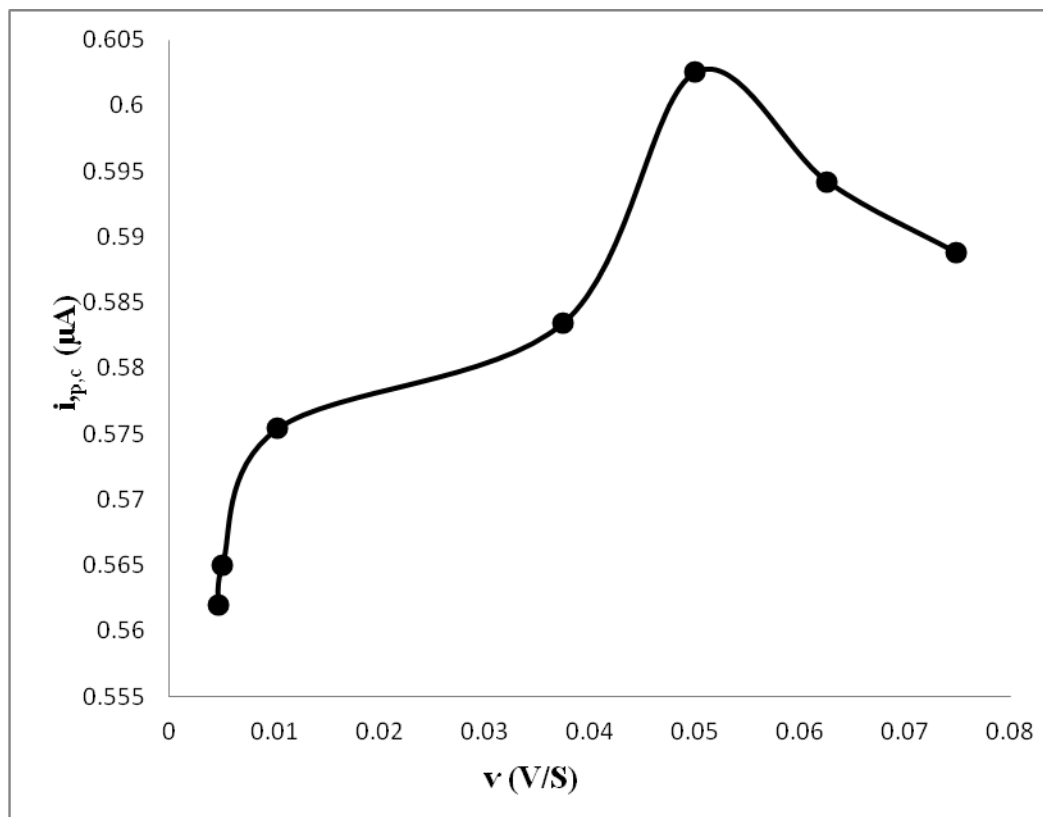


Fig.2.16 Effect of scan rate on the cathodic peak current of Hg(II)-TAR vs. Accumulation time (s). Conditions: TAR concentration $=9.8 \times 10^{-7} \text{ M}$; $\text{Hg}^{2+} = 4.9 \times 10^{-7} \text{ M}$; deposition potential $= -0.04 \text{ V}$, scan rate 60 mVs^{-1} and pulse amplitude of 60 mV .

mercury(II) was examined over a wide range (10 to 100 mV) under the optimal conditions. The data revealed excellent, symmetric cathodic peaks and maximum peak currents were achieved at 60 mV. Therefore, in the subsequent work, pulse amplitude of 60 mV was chosen as an optimum value.

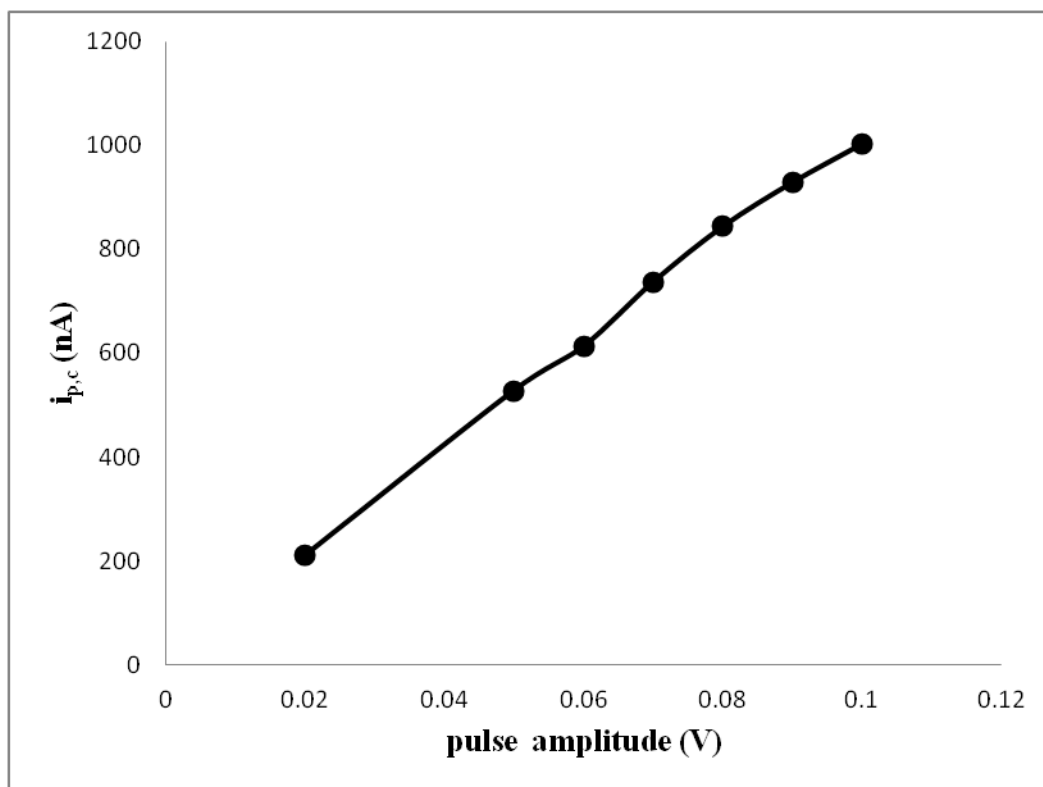


Fig.2.17 . Effect of pulse amplitude on peak current. Conditions: [TAR] 9.8×10^{-7} M; [Hg^{II}], 4.9×10^{-11} M; deposition potential, -0.04 V.

The influence of the TAR concentration (1.0×10^{-6} – 6.0×10^{-5} mol L⁻¹) on the cathodic peak current under the optimal experimental parameters was investigated. The results are demonstrated in Fig. 2.18 The cathodic current at $E_{p,c}$ of -0.38 V vs. Ag/AgCl electrode increase on increasing reagent concentration and remained constant at TAR concentration higher than 3.0×10^{-5} mol L⁻¹. At much higher concentration of TAR, the sensitivity of the cathodic peak current decreased and deteriorated gradually. This trend is most likely attributed to the competitive adsorption of free TAR. At the break point (3×10^{-5} mol L⁻¹) of TAR concentration, the molar ratio of mercury (II) to TAR was exactly 1:2 molar ratio. These data confirmed the proposed chemical structure given in Fig.2.4. These data added further confirmation that, the reagent TAR is coordinated to Hg²⁺ ion through one of the two phenolic hydroxy groups and the azo group of the reagent (Fig.

2.1). Therefore, in the subsequent work, a concentration of $3.5 \times 10^{-5} \text{ mol L}^{-1}$ of the reagent was selected.

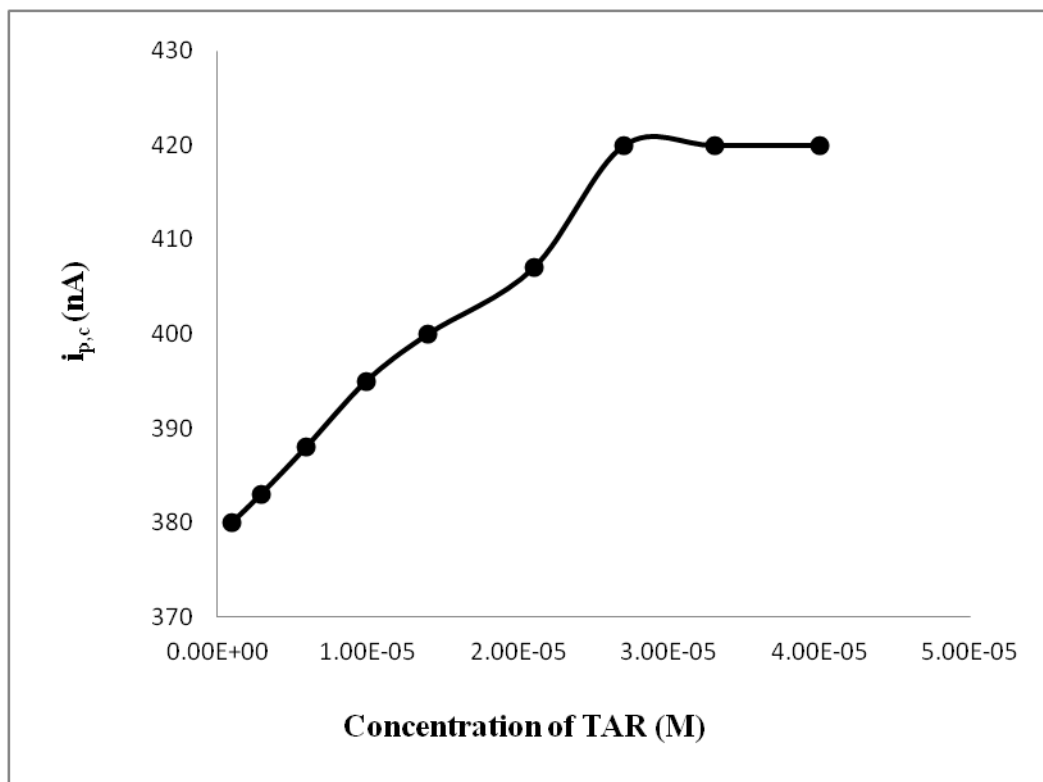


Fig.2.18. Influence of TAR concentration on the $i_{p,c}$ at -0.38 V of the DP-CSV of mercury(II)-TAR complex at pH 6-7 at HMDE vs. Ag/AgCl . Mercury (II) ions ($1.5 \times 10^{-5} \text{ M}$); E_{acc} -40 mV ; t_{acc} of 60 s ; V of 60 mVs^{-1} and 60 mV pulse amplitude.

2. 3.4. Analytical performance of the developed DP-CSV procedure:

The validation of the proposed DP-CSV procedures for mercury (II) determination under the optimized operational parameters was determined in terms of the limit of detection (LOD), limit of quantification (LOQ), linear dynamic range and relative standard deviation (RSD, reproducibility) .The DP-CSVs of Hg(II)-TAR at different concentrations of mercury(II) ions are shown in Figs.2.19 . The plot of $i_{p,c1}$ of the cathodic peak (at $E_{p,c}$ 0.38V) measured by the developed DP-CSV procedure vs. mercury(II) concentrations was linear over the concentration range 7.5×10^{-9} (1.5 ppb) –

5.25×10^{-7} (70.0 ppb) mol L^{-1} is shown in Fig.2.20. Above $5.5 \times 10^{-7} \text{ mol L}^{-1}$, the calibration curve tended to levelled off because of the adsorption saturation. The calibration plot have the following regression equations:

$$i_{p,c1} (\text{n A}) = 1.639 C (\text{n M}) + 2.0 \quad R^2 = 0.991 \quad (2.7)$$

According to IUPAC system[54], the values of the lower limits of detection (LOD) and limit of quantification (LOQ) were calculated using the following equations:

$$\text{LOD} = 3\sigma/b \quad (2.8)$$

and

$$\text{LOQ} = 10\sigma/b \quad (2.9)$$

where, σ is the standard deviation of replicate determination values of the blank under the same experimental conditions and b is the sensitivity, namely the slope of the calibration plot of the analyte. The values of detection (LOD) and quantification (LOQ) under the conditions established for mercury(II) was estimated using the equations (2.8) and (2.9) were found equal 2.25×10^{-9} (0.45 ppb) and 7.5×10^{-9} (1.5ppb) mol L^{-1} , respectively. Such limits could be improved to lower values by preconcentration of mercury(II) ions from large sample volumes onto polyurethane foam immobilized withTAR in a packed column mode followed by subsequent recovery (elution) and analysis by the developed method.

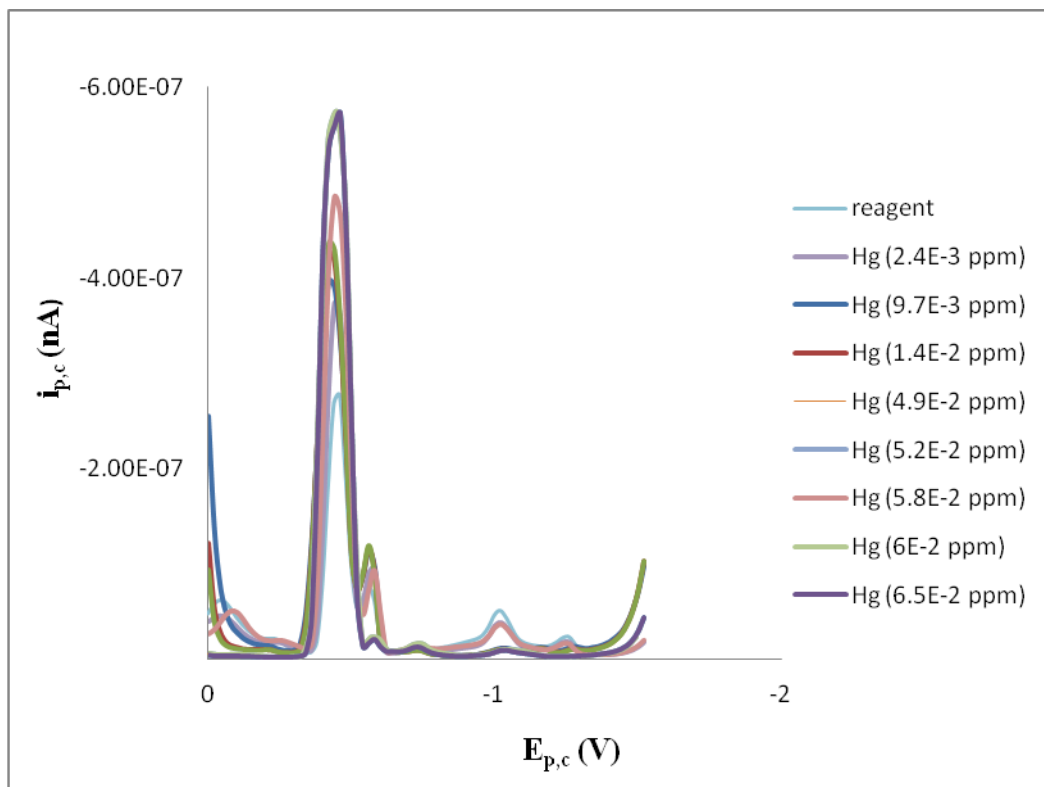


Fig.2. 19 DP-CSVs of Hg(II)-TAR complex in the presence of various concentrations of mercury ($7.5 \times 10^{-9} - 5.25 \times 10^{-7}$) mol L⁻¹) at HMDE vs. Ag/AgCl electrode at pH 6-7 under the optimum operational parameters.

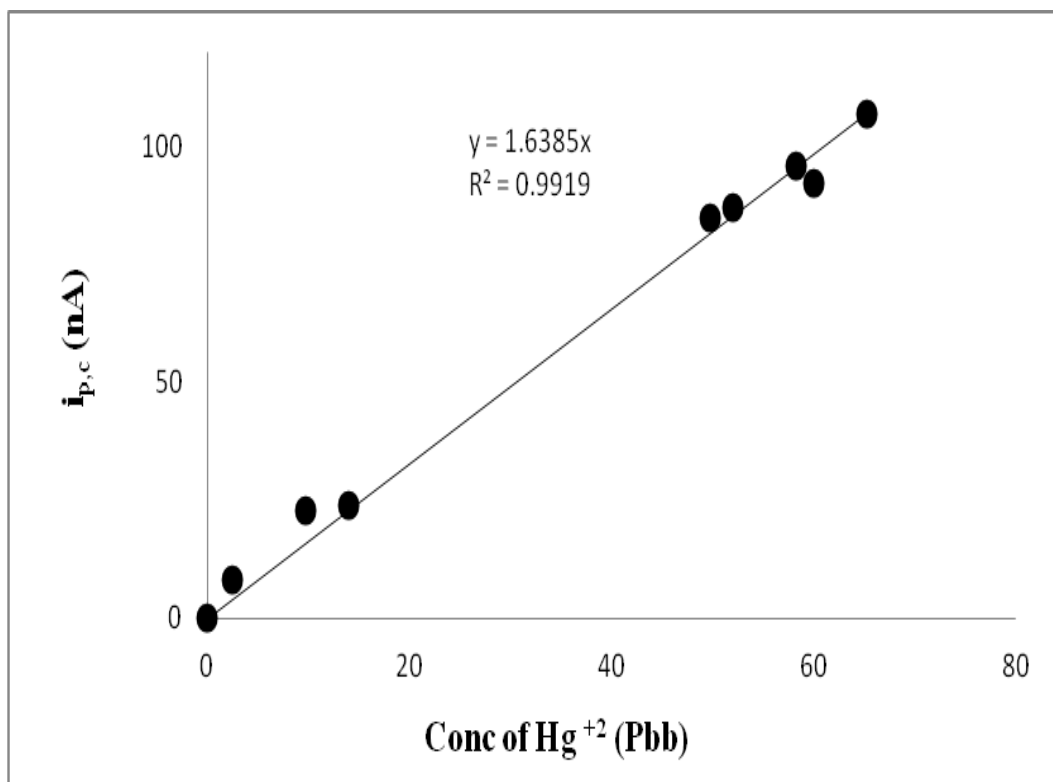


Fig.2.20 Calibration plot of Hg(II) -TAR complex in the presence of various concentrations of mercury ($7.5 \times 10^{-9} - 5.25 \times 10^{-7}$) mol L⁻¹) at HMDE vs. Ag/AgCl electrode at pH 6-7 under the optimum operational parameters.

The main analytical features (LOD, LOQ and the linear dynamic range) of the developed method were compared successfully with many of previously published electrochemical, chromatographic and spectrometric methods. The figure of merits of the developed DP-CSV are better than the corresponding values of the reported spectrophotometric [31- 34] and voltammetric methods [32,39-43]. The relative standard deviation (RSD) of mercury (II) based on five measurements of Hg (II) at 8.6×10^{-9} mol L⁻¹ was found equal to 2.8% confirming the precision of the method. The developed method is low cost, short deposition, selective and quite applicable for routine analysis.

2.3.5. Interference study:

Surfactants and metal ions are generally present in real samples and are more serious interferences in stripping analysis. Thus, the developed DP-CSV at -0.38 V procedure was applied for analysis of mercury (II) ions at concentration of 4.5×10^{-8} mol L⁻¹ under the recommended experimental procedures in the presence of a relatively high excess (1 mg mL⁻¹) of As(III), Zn(II), Cd(II), Co(II), Cu(II), Ca(II), Mn(II), Ni(II), Pb(II), and Sb(IV) ions. The tolerance limit was defined as the concentration of the foreign ion added causing a relative deviation within $\pm 5\%$ in the magnitude of the peak current (at -0.38 vs. Ag/AgCl) of the solution. Negligible interference of these ions was achieved and only slight shift in the potential of the cathodic shift and an ill defined new peak was noticed at potential higher than -0.6 of Hg (II)-TAR complex. Moreover, the linearity of the calibration curve of mercury was maintained also in the presence of the other ions in solution. The ions F⁻ and CN⁻, Br⁻, SO₄²⁻ and CO₃²⁻ was tested individually at 50 -100-fold mass concentration excess over mercury (III) ions and negligible interference of most of these ions was achieved .

2.3.6 Analytical applications:

2.3.6.1. Analysis of certified reference material (IAEA Soil-7)

The analytical utility of the proposed DP- CSV procedure was tested by analysis of mercury in the CRM sample (*IAEA Soil-7*) as described in the experimental section (2.2.5.1). An acceptable agreement between the results of the developed DP-CSV (45.2 ± 2.5 µg/kg) ICP-MS (40.9 ± 2.7 µg/kg), recommended value (40.0 µg/kg) and 95% confidence interval (30-70 µg/kg) confirming the precision of the developed method. The relative standard deviation (RSD) for triplicate voltammetric analysis was in the range ± 2.8 -3.8%, highlighting that good precision was maintained for the real

sample. The *F*- and *t*-tests at 95% confidence levels showed no significant differences between values achieved by the developed DP-CSV procedures ($45.2 \pm 2.5 \mu\text{g/kg}$) and the standard ICP-MS ($40.9 \pm 2.7 \mu\text{g/kg}$) method. The developed method is simple to operate and applicable for routine analysis of very low concentrations of mercury ions compared to other reported electrochemical methods.

2.3.6.2. Analysis of mercury (II) in tap- and drinking water samples:

The proposed DP-CSV procedure was assessed by performing analysis of mercury(II) species in tap and drinking water samples. Water samples were collected and filtered through a $0.45 \mu\text{m}$ cellulose membrane filter as described in the experimental section. The water samples were then analyzed by the developed DP-CSV method employing the standard addition procedure. The results of analysis of Hg (II) after spiking of tap- and drinking water samples ($n = 6$) showed acceptable results. Representative data in drinking water samples are summarized in Table 2.2. The results obtained are in good agreement with the values obtained using direct ICP-MS demonstrating the accuracy and suitability of the developed DP-CSV method. The *F* (1.2-2.33) test at 95% confidence levels did not exceed the theoretical ones 6.388 and no significant differences were observed between the developed and the standard ICP-MS methods. .

Table.2.2. Analysis of mercury spiked to drinking water samples (n=6) by the developed methods*

Sample	Added, ppm	Found \pm SD, mgL ⁻¹	Recovery \pm RSD,%
	--	0.0 \pm 0.003	--
Drinking water	0.039840637	0.028 \pm 0.0015	100 \pm 12.4
	0.0497	0.052 \pm 0.0023	104.52 \pm 10.24
	0.0596	0.059 \pm 0.0046	98.92333 \pm 0.76
	0.0695	0.068 \pm 0.0029	97.82286 \pm 4.86
	0.0793	0.086 \pm 0.003	108.36 \pm 2.16
	0.0891	0.094 \pm 0.002	105.3844 \pm 0.44
	0.0990	0.107 \pm 0.006	108.07 \pm 1.41

* Average recovery (n=6) \pm relative standard deviation

2. 3.6.3 Chemical speciation of mercury in drinking:

The use of the proposed DP – CSV method for the chemical speciation of labile and complexed fractions of mercury in the aqueous media at a total concentration \leq 10 $\mu\text{g L}^{-1}$ were attempted. The test aqueous solutions were analyzed following the recommended procedures for mercury (II) determination. Another aliquot sample was analyzed following the recommended procedures for Hg (II) determination after prior UV digestion in the presence of HCl (10%). Analysis of spiked Hg ions in the test solutions were then determined from the difference ($C_2 - C_1$) between the concentration of the first (C_1) and second (C_2) aliquots. Acceptable recovery percentage (95-103%) of Hg was successfully achieved and successfully compared with the results obtained by ICP-MS data (97-102 %) of Hg recovery.

2.4. Conclusion:

The developed method provides an excellent approach for determination of mercury because of its sufficient precision and simplicity without sample pre treatment. The method compares favourably with the reported spectrochemical [7-20], electrochemical [33-39] and other methods [22, 23]. The sensitivity and selectivity of the developed method could be improved to lower concentrations of Hg (III) by prior preconcentration of Hg ions from large sample volumes onto TAR or ditizone immobilized polyurethane foam packed column followed by elution with specific eluting agent. However, work is still continuing for i- on-line voltammetric stripping analysis for the chemical speciation of labile mercury (II) and complexed fractions in environmental samples; ii-investigating the influence of organic material present in natural water samples and finally iii- investigating the ligation capacity of some other the complexing agents which are most likely present in natural water e.g. phenols and other surfactants.

2. 5. References:

1. R.A. Gayer "Toxicological Effects of Methyl mercury" National Academy Press, Washington 2000.
2. L.D. Lacerda, W. Salomons, Mercury from Gold and Silver Mining, A Chemical Time Bomb, Springer, Berlin, Heidelberg, 1998, p. 146.
3. P.J. Craig, "Organometallic Compounds in the Environmental" Longman, Harlow (1986).
4. "Water Quality and Treatment" American Water Works Association, 4th edn. McGraw Hill Inc., New York, 1990.
5. European Commission DG ENV. Heavy Metals in Waste. E3 (2002).
6. Y.Wu., W.X.Wang, Environmental Pollution, 159 (2011) 3097.
7. M. Hussein, H. Moghaddam, Talanta 67 (2005) 555.
8. J. M. Schmit, M. Youla, Y. Gelinas, Anal Chim Acta 249 (1991) 495 .
9. D.E. Nixon, M.F. Burrit, T.P. Moyer, Atomic spectroscopy 54 (1999) 1141.
10. H. Shoaee, M. Roshdi, N. Khanlarzadeh, A. Beiraghi, Spectrochimica Acta Part A: Molecular and Biomolecular Spectroscopy 98 (2012) 70–75
11. M. Vijayakumar, T.V. Ramakrishna, G. Aravamudan, Talanta **27** (1980) 911.
12. E. Saouter, B. Blattmann, Anal. Chem. **66** (1994) 2031 - 2037.
13. A. Shafawi, L. Ebdon, M. Foulkes, P. Stockwell, W. Corns, Analyst **124** (1999) 185.
14. D.G. da Silva, L.A. Portugal, A. M. Serra, S. L.C. Ferreira , V. Cerdà, Food Chemistry 137 (2013) 159–163
15. V. Červený, M. Horváth, J.A.C. Broekaert, Microchemical Journal 107 (2013)10.

16. E. Saouter, B. Blattmann, *Anal. Chem.* **66** (1994) 2031 - 2037.
17. E.M. Martine, P. Berton, R.A. Olsina, J.C. Altamirano, R.G. Wuilloud, J. hazardous materials in press 45(2009)2343.
18. J.L. Manzoori, M.H. Sorouraddin, A.M.H. Shabani, J. *Anal. Atomic Spectrom.* **13** (1998) 305.
19. J. Nevado, R.C. Marti-Domeadios, F.J. Bernado, M.J. Moreno, *journal of Chromatography A* 1093 (2005) 218.
20. Z. Zhang, H. Liu, H. Zhang, Y. Li, *Anal. Chim. Acta* **333** (1996) 119.
21. C. Faller, N.Y. Stojke, G. Henze, K.Z. Brainina, *Anal. Chimica Acta* 396 (1999) 195.
22. L. Bennun, J. Gomez, *Spectrochim. Acta* **52B** (1997) 1195 .
23. P.R. Devi, T. Gangaiah, G.R.K. Naidu, *Anal. Chim. Acta* **12** (1991) 533.
24. M. Tuzen, M. Soylak, *Bulletin Environ. Contam. Toxicology*, 74 (2005) 968 972.
25. M. Tuzen, I. Karaman, D. Citak, M. Soylak, *Food. Chem. Toxicology*, 47 (2009) 1648.
26. M. Tuzen, A. Sari, D. Mendil, M. soylak, *J. Hazard. Mater.*, 169 (2009) 263.
27. M. Tuzen, I. Karaman, D. Citak, M. Soylak, 169 (2009) 345.
28. S. Suresha, M.F. Silwadi, A.A. Syed, *International J. Environmental Analytical Chemistry* 82 (2002) 275.
29. A.Y. El- Sayed, *Analytical Letters* 31 (1998) 1905.
30. Xiao - Ling He, Yong - Qiu Wang, K.Q. Ling, *Talanta* 72 (2007) 747.
31. S. Chatterjee, A. Pillai, V. K. Gupta, *Talanta*, 57 (2002) 461.
32. A. Giacomino., O. Abollino., M. Malandrino., E. Mentasti, *Talanta*,75 (2008) 266.

33. S. Chatterjee., A. Pillai., V.K.Gupta, *Talanta*, 57 (2002) 461–465.
34. L.Sipos., H.W. Nürnberg., P. Valenta., M. Branica, *Analytica Chimica Acta*, 115 (1980) 25.
35. J.M. Pinilla., L. Hernández.,A.J. Conesa, *Analytica Chimica Acta* ,319 (1996) 25.
- 36 Y.Bonfil., M. Brand., and Kirowa-Eisner, *Analytica Chimica Acta*,424(1) (2000) 65.
37. E. A.Osipova., V. E. Sladkov., A.I. Kamenev., V. M. Shkinev., K. E.Geckeler, *Analytica Chimica Acta*, 404 (2000) 231.
- 38.N.Yang., Q. Wan, and J. Yu, *Sensors and Actuators B: Chemical*,110 (2005) 246.
39. F. Okc.,H. Ertas.,F. Nil Ertas, *Talanta*,75 (2008) 442–446.
40. E. Bernalte., C. Marín Sánchez., E.P. Gil , *Analytica Chimica Acta*, 689 (2011) 60.
41. A.M.Ashrafi, K. Vytřras, *Talanta*, 85 (2011) 2700.
42. A.A. Ensafi., A.R.Allafchian ., M. Saraji., B. Farajmand , *Talanta* ,99 (2012) 335.
- 43.T.Hezard, K. Fajerweg, D. Evrard., V. Collière., P. Behra.,P. Gros, *Journal of Electro - analytical Chemistry*, 664 (2012) 46.
44. A.I. Vogel "Quantitative Inorganic Analysis"^{3rd} edn, Longmans Group Ltd., England, 1966.
45. K. Ueno, T. Imamura, K.L. Cheng, *CRC Handbook of Organic Analytical Reagents*, CRC Press, 1992 P. 227.
46. E. Bishop, *Indicators*, Pergamon Press Ltd, Oxford, 1972, P. 300.
47. A. Benvidi, F. Heidari, M. M. Ardakani, A. M. Hajishabani, J. Ghasemi, *Chinese Chemical Letters* 21 (2010) 725.

48. F. Karipcina, E. Kabalcilara, S. Ilican, Y. Caglarb, M. Caglar, *Spectrochimica Acta Part A* 73 (2009) 174.
49. D. Sawyer, W.R. Heinemann, J. Beebe, "Chemistry Experiments for Instrumental Methods", John Wiley & Sons, New York, 1984.
50. K. Nakamoto "Infrared and Raman Spectra of Inorganic and Coordination Compounds" Wiley Interscience, New York 222 (1971).
51. M.M. Omar, G.C. Mohamed, *Spectrochimica Acta Part A* 61 (2005) 929.
52. A.J. Bard, L. Faulkner, L., "Electrochemical Methods: Fundamentals and Applications", John Wiley & Sons, New York, (1980) p. 218.
53. R.S. Nicholson, I. Shain, *Anal. Chem.*, 36 (1964) 706.
54. Miller, J. and Miller, N. " Statistics for

Chapter III

Direct Determination of Trace Concentration of Palladium in water by Square Wave Adsorptive Cathodic Stripping Voltammetry Using 4-(2- Thiazolylazo)–Resorcinol Reagent.

3.1 Introduction

Recently, interest in the development of analytical techniques for analysis of precious group elements (PGEs) i.e. platinum group metals (PGMs) comprises Pt, Pd, Rh, Ir, Os and Ru is growing because of their applications in chemical engineering, micromechanics and medicine [1, 2]. The significance of palladium as a transition metal lies in its corrosion resistant nature and alloying ability. Thus, it is an important element in metallurgy [3] and hence it has a wide spectrum of applications in catalytic converters in motor vehicles and in some other industrial processes e.g. electrical and electronic industries, brazing alloys, petroleum, and catalytic chemical reactions, dentistry and medical devices, jewelry, surgical instruments, and as nano-particles for the development of new active catalysts [4, 5]. Although the benefits of car catalysts are indisputable, the emission of Pd into the environment is largely associated with the production and recycling of catalytic converters in the metal finishing industry as well as the operation of vehicle catalysts. Hence its concentration has been rapidly increasing in the environment [3].

Palladium is found at low concentrations in several matrices [5]. Some of Pd compounds have been reported as potential health risks to humans, causing asthma, allergy, rhino conjunctivitis and other serious health problems [7]. Thus, palladium is a new contaminant to the environment with the introduction of automobile catalyses containing elements of the PGEs. Because of its toxicity [6], its monitoring at trace level in surface waters, soil surfaces, plant and particular matter samples has been getting increasingly important [6, 7]. Hence, the development of a simple, sensitive and selective analytical method for Pd determination has been a challenge for researchers [8]. In few cases palladium has tested by the medical field to be used as possible new antitumor drug [9 -11].

The development of analytical methods for Pd determination is important for effective monitoring of pollution levels of this metal in our environment. Although the concentration of Pd in different compartments of environment continuously increases, it is still at the level of ng g^{-1} (or ngmL^{-1}) [12]. Numerous interactions between the analyte and the matrix constituents can significantly influence both the limit of detection and the accuracy of the analytical method. Many spectrochemical methods e.g. atomic absorption spectrometry (AAS) e.g. atomic absorption (AAS) [12, 13], both flame (FAAS) [14-16] and electrothermal spectrometry (GFAAS). [17-20], inductively coupled plasma optical emission spectrometry (ICP-OES) or inductively coupled plasma mass spectrometry (ICP-MS) [21-24] has been developed for Pd determination in real samples. Neutron activation analysis (NAA)[25-27], optical emission spectrometry (OES)[28], X-ray fluorescence (XRF)[29] and sensor membrane [11] have been also developed for pD determination. Although most of these methods have good sensitivity, they are usually difficult and an initial sample pretreatment such as preconcentration of the analyte and matrix separation is often necessary [22], well-controlled experimental conditions and a profound sample preparation are of prime importance. Other main disadvantages e.g. the complexity, the high cost of the instruments and the need of some degree of expertise for their proper operation [7].

Recently, voltammetric techniques involving stripping voltammetry [30] are of great concern in r[30]. Stripping voltammetry represents the most popular, thanks to such unquestionably features as excellent sensitivity and selectivity, low detection limits, good accuracy and precision, and inexpensive and portable instrumentation [30 -32].

Square-wave voltammetry (SWV) represents one of the most popular and most exploited technique in the family of the pulse voltammetric techniques [32 -36] and it is considered as “electrochemical spectroscopy” due to its ability to provide closer insight into various redox mechanisms [37] A literature survey on the Pd determination by different voltammetric methods from different matrices is demonstrated in Table 3.1. Square wave –cathodic stripping voltammetric (SW-CSV) is based upon the accumulation of the analyte on a suitable working electrode by potential controlled adsorption and subsequent electrochemical reduction of the preconcentrated species. A recent literature has revealed no study on the use of 4-(2-Thiazolylazo) resorcinol as chelating agent for analysis of Pd in complex matrix e.g. wastewater, etc. by SW-CSV . Thus, the work presented in this chapter reports : i redox behavior of palladium (II) - TAR chelate in B-R buffer in an attempt to develop a low cost, convenient and simple square wave adsorptive cathodic stripping voltammetry method for palladium determination in complex matrices e.g. tap- and industrial wastewater and certified reference. The work also includes a proper assignment of the most probable electrochemical mechanism and nature of electrode reactions and finally chemical speciation of Pd in complex matrices e.g. water samples and certified reference materials.

Table 3.1 Voltammetric methods for palladium (II) determination

Technique	Complexing agent	Working electrode	Limit of detection, (LOD)	Reference
ASV	DMG	HMDE	0.02 $\mu\text{g L}^{-1}$	[35]
LSP	DMG	HMDE	0.744 $\mu\text{g L}^{-1}$	[36]
ASV	—	MCPE with crown ethers	2.76 $\mu\text{g L}^{-1}$	[37]
DP-ASV	—	MCPE with thioridazine	0.5 $\mu\text{g L}^{-1}$	[38]
DP-CSV	DMG	Mixed binder carbon paste electrode containing DMG	0.1 $\mu\text{g/g}$	[39]
DP-ASV	DMG	HMDE	0.05 $\mu\text{g/L}$ (liquid) 0.05 $\mu\text{g/g}$ (solid)	[40]
LSASV	—	MCPE with sodium humate (NaA-CMCPE)	—	[41]

Table 3.1. Continued

Technique	Complexing agent	Working electrode	Limit of detection, (LOD)	Reference
DP-CSV	DMG	HMDE	2.13 $\mu\text{g L}^{-1}$	[42]
LSV			0.5 $\mu\text{g L}^{-1}$	
AC-SWV			0.085 $\mu\text{g L}^{-1}$	
AdSV	BINPHT	HMDE	2 $\mu\text{g L}^{-1}$	[43]
DPV	—	HMDE	40 $\mu\text{g L}^{-1}$	[44]
SWAdSV	DMG in HCl	HMDE	0.075 $\mu\text{g L}^{-1}$	[45]
SWV	Hydroxylamine	HMDE	0.77 $\mu\text{g L}^{-1}$	[46]
SWAdSV	DMG in acetate buffer pH 3.5	HMDE	0.049 $\mu\text{g L}^{-1}$	[47]
SWAdSV	DMG in HCl	HMDE	0.019 $\mu\text{g L}^{-1}$	[48]
DPAdSV	DMG	HMDE	0.042 $\mu\text{g L}^{-1}$	[49]
AdSV	DMG	GC modified with array of Hg nanodroplets	1.6 μM	[53]
SWAdSV	DMG	Silver amalgam film electrode(Hg(Ag)FE)	0.15 $\mu\text{g L}^{-1}$	[54]

3.2 Experimental

3.2.1 Reagents and materials

All chemicals used were of analytical reagent grade and were used as received. Plastics and glassware's were cleaned by soaking in dilute HNO_3 (10% w/v) and were rinsed with distilled water prior to their use. A series of Britton-Robinson (B-R) buffer (pH 2.5-11) as reported [50].. A BDH stock solution (1000 mgL^{-1}) of palladium (II) was used for the preparation of more diluted solutions in de-ionized water. A stock solution ($1 \times 10^{-6} \text{ mol L}^{-1}$) of the selected TAR, (TAR), was used as a complexing agent acid was prepared by dissolving an accurate weight of the reagent in Ethanol. The reagent solution was kept on the refrigerator. BDH standard solutions of some diverse ions which are commonly in association with palladium e.g. aluminium, copper, chromium, iron and magnesium (1000 mgL^{-1}) were also used.

3.2.2 Apparatus

The cyclic, linear and differential pulse cathodic stripping voltammetric measurements, double beam spectrophotometer (190-1100 nm) with 1cm (path width) quartz cell, FTIR spectrometer 100 series (Beaconsfield, Bucks, and UK and a Perkin Elmer inductively coupled plasma- mass spectrometer (ICP-MS) (Sciex model Elan DRC II, USA) were used as described in chapter 2. A CEM microwave system (Mars model, 907500, USA), a three-compartment borosilicate (Metrohm) voltammetric electrochemical cell (10 mL) configuration incorporating hanging mercury dropping electrode (working electrode), double-junction Ag/AgCl,(3M) KCl, (reference electrode) and Pt wire (counter electrode) and digital pH-meter

(model MP220, Mettler Toledo) for pH measurements were used as mentioned in chapter 2. A digital-micro-pipette 10 -100 μ L (Volac) was used and the electrochemical data were then recorded at room temperature and the peak current heights were measured as described earlier.

3.2.3 General recommended procedures

An accurate volume (10 mL) of B-R buffer (or ammonia solution) of pH 7-8 was transferred into the electrochemical cell where the electrodes are immersed in the test solution through which pure nitrogen stream was passed for 15 min before recording voltammograms. The scans were initiated in the negative direction of the applied potential from 0.0 V to -1.5 V vs. Ag/AgCl reference electrode. After recording the voltammogram of the supporting electrolyte, an accurate volume (100.0 μ L) of the TAR reagent (1.0×10^{-5} mol L⁻¹) was transferred into the electrochemical cell to provide a final concentrations of 1.0×10^{-7} mol L⁻¹. A stream of pure nitrogen was passed through the test solution through for 5 min before recording voltammogram. The stirrer was then stopped and after 10s quiescence time, the voltammogram was recorded by applying a negative potential scan from 0.0 to -1.5 V vs. Ag/AgCl at 180 s accumulation time, 0.15 V deposition potential, 0.0 V starting potential, 50 mV pulse amplitude and 60 mVs⁻¹ scan rate. The background SW-CSV voltammogram of the supporting electrolyte and the blank solution was recorded. An accurate volume (20 μ L) of palladium (II) solution (1.2×10^{-6} mol L⁻¹) was added to the electrochemical cell. The SW-CSV was repeated with a new mercury drop under the same experimental conditions in the presence of various concentrations of palladium. (20-100 μ L). The peak current of Pd was measured at -

0.47 V vs. Ag/AgCl. Palladium concentration was then determined from the difference between the cathodic peak current before and after adding palladium to the reagent solution corresponding cathodic peak current at -0.47 V. Following these procedures, the effect of diverse ions also investigated. Cyclic voltammetry at HMDE and Pt working electrodes at various scan rates (20 - 2000 mVs⁻¹) and at different Pd²⁺ concentrations at the same pH was critically investigated to assign the most probable electrochemical reduction mechanism.

3.2.4 Analytical applications

3.2.4.1 Analysis of certified reference materials

An accurate weight (0.13 – 0.15±0.01g) of the CRM sample (*IAEA-Soil-7*) was digested as reported earlier in chapter 2 [51]. The solid residue was re dissolved in dilute HNO₃ (5.0 mL, 1.0 mol L⁻¹) and the resulting mixture was filtered through a Whatman 41 filter paper, transferred to volumetric flask (25.0 mL). The solution was completed to the mark with deionized water and an accurate volume of the digested sample was adjusted to pH 7-8 (5.0 mL) with few drops of NaOH (1.0 mol L⁻¹) and B-R buffer of pH 7-8. The solution transferred to the volumetric cell and the SW-CSV voltammograms were recorded by applying a negative potential scan from 0.0 to -1.5 V vs. Ag/AgCl at various additions of standard Pd concentration at the optimized experimental conditions. The peak current at ~ -0.47 V was measured and the change in the peak current was used for constructing a linear plot of standard addition of Pd. The content of Pd in the CRM sample was computed from the linear plot of the standard addition plots.

3.2.4.2 Analysis of palladium in water samples

The standard addition (spiking) method was used for the analysis of palladium(II) in drinking water or Red sea water samples (100.0 mL) as follows: Water samples were initially filtered through 0.45- μm cellulose acetate membrane filter and subjected to UV mineralization for 6 h. Transfer known volume (5.0 mL) of the water sample adjusted to pH 7 to the electrochemical cell followed by adding few drops of EDTA (2% m/v). The current height displayed by the test solution before and after addition of various volumes (10-20 μl) of standard palladium (II) was then measured and used for determining palladium (II) via the linear plot of the standard addition. For validation, the samples were also analyzed using ICP-MS as standard method.

3.3 Results and Discussion

3.3.1 Characteristics of the palladium (II) – TAR

Preliminary investigation involving the reaction of TAR with palladium (II) was critically investigated by visible and IR spectra. In the visible region, the spectra of TAR and its palladium complex showed one well defined absorption peak at λ_{max} 443 and 459 nm, respectively (Fig. 3.1). The observed color change and the progressive bathochromic shift in the electronic spectra of Pd-TAR complex suggest complex formation of palladium with TAR. Molecular structure of Pd(II)-TAR was determined via continuous variation method at 459 nm at various concentrations of palladium (II) and TAR [52]. The data indicated formation of Pd (II): TAR at 1:2

molar ratios. Thus, the most probable chemical structure of palladium (II) with TAR is $\text{Pd}(\text{TAR})_2$.

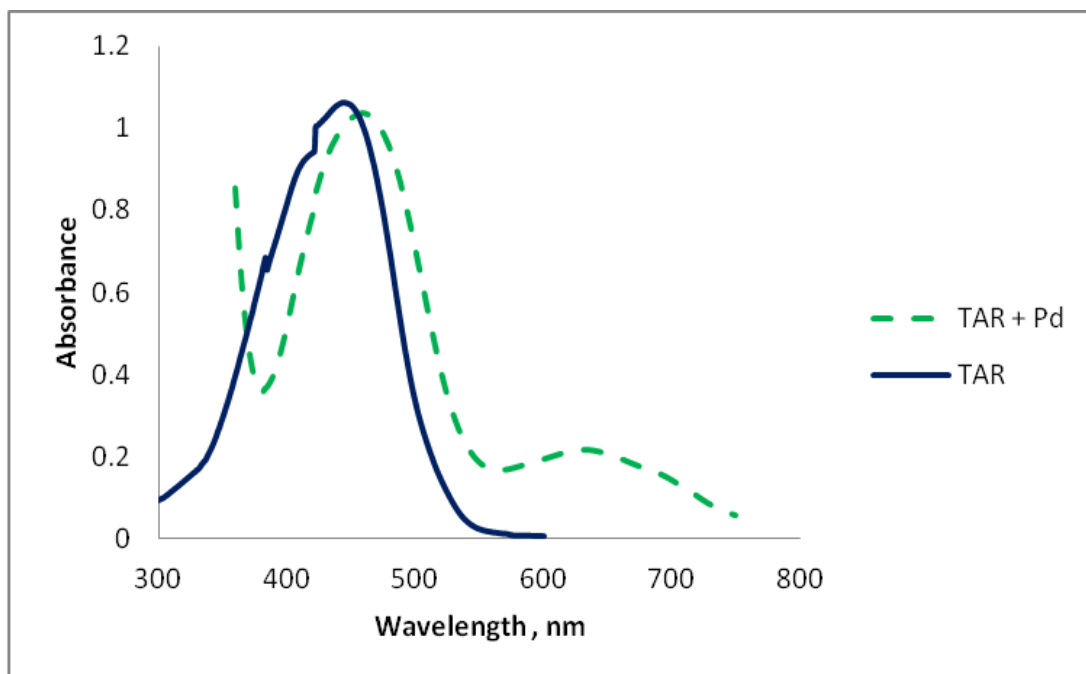


Fig.3.1. Visible spectra of the reagent TAR and its Pd (II)-TAR complex.

The IR spectra of the free ligand and its Pd-TAR complex were carried out in the region $4000\text{--}400\text{ cm}^{-1}$. In the IR spectrum of the ligand (Fig. 2.3), the broad band observed at 3316.63 cm^{-1} due to the phenolic OH group is still broad and decreased in the IR spectrum of the complex (Fig. 3.2). The -(C=N) stretching vibration of the thiazolylazo nitrogen is observed in the form of a strong-intensity band at 1644.35 cm^{-1} in the free ligand. This band not affected upon complex formation suggesting no participation of S atom to palladium upon complex formation. The band observed at 1587 cm^{-1} assigned to $(\text{N}=\text{N})$ of the azo group in the free TAR is shifted to lower frequency by value 56 cm^{-1} upon complex formation indicating coordination of azo group on complex formation to palladium. This is further

supported by the appearance of the band corresponding to the M-N stretching vibration at 452–531 cm^{-1} in the complex. The participation of the deprotonated phenolic OH group in complex formation is confirmed by the blue shift(63cm^{-1}) of the $-(\text{C}-\text{O})$ stretching band in the complex. This is further supported by the appearance of the band at 527–530 cm^{-1} due to metal–oxygen stretching vibration (M-O). Thus, TAR coordinates to palladium in a bidentate fashion via azo and hydroxyl group, hence the structure of the formed chelate is most likely as shown in Fig. 2.3. Thus, the reagent TAR is suggested for square wave cathodic stripping voltammetric determination of palladium (II) in water samples in the subsequent work.

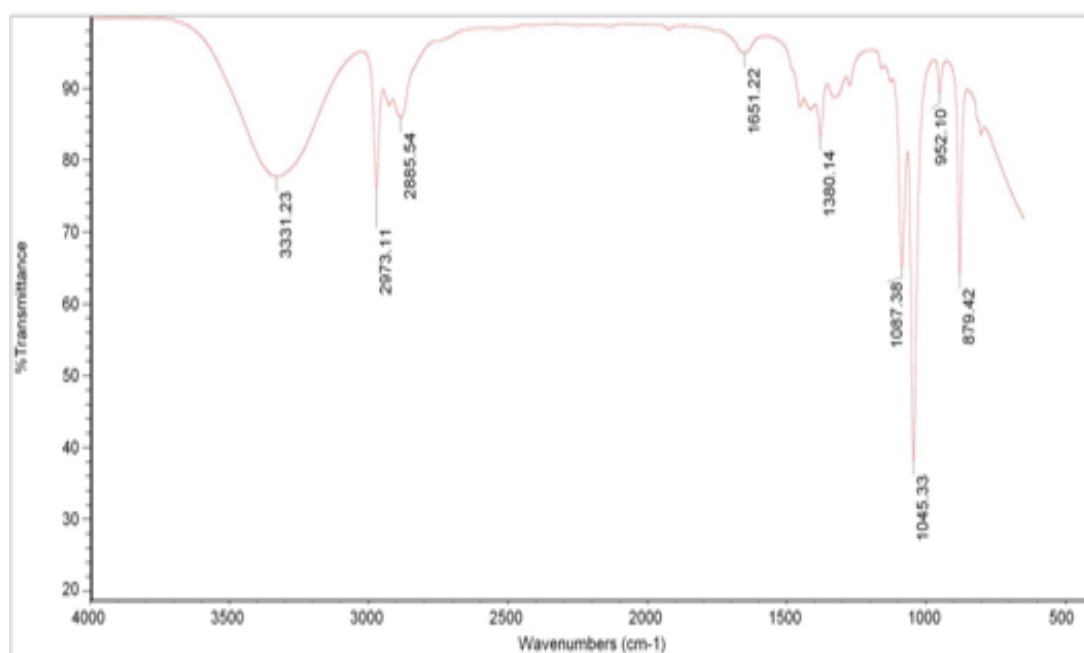


Fig. 3.2 IR spectrum of palladium-TAR chelate.

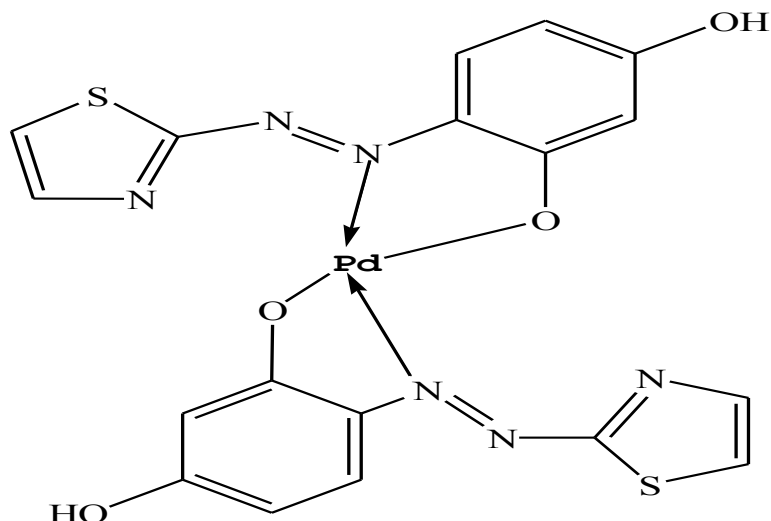


Fig. 3.3 Proposed chemical structure of Pd(II)-TAR complex.

3.3.2 Electrochemical behaviour of palladium (II) – TAR complex

Based on the electronic spectra of the reagent TAR and its Pd(II) complex, detailed investigation involving the redox characteristics of the reagent TAR (8.9×10^{-8} M) with Pd (II) (1.6×10^{-8} M) in B-R buffer (pH 2.5- 11) was carried out using square wave –cathodic stripping voltammetry at the HMDE vs. Ag/AgCl electrode. The voltammogram of the supporting electrolyte i.e background, and the background with addition of TAR were recorded initially and the results revealed ill defined cathodic peaks. At various pH 2-11, addition of palladium (II) to the TAR solution, well defined cathodic peak was observed in the range -0.2 to - 0.55V vs. Ag/AgCl reference electrode. Representative data are shown in Fig.3.4. This cathodic peak is most likely assigned to the reduction of the azo group (-N=N-) in the TAR reagent. On increasing the solution pH, the $E_{p,c}$ at -0.23 was shifted to more negative value showing the irreversible nature of the electrochemical reduction process and the electrode reaction involves hydrogen ions [53]. The cathodic peak current ($I_{p,c}$) increased on increasing pH and reached maximum at pH 7-8. Hence, in the

subsequent work, buffer solution of pH 7-8 was selected since constant, reproducible, sharp and high cathodic peak current at -0.47 V vs. Ag/AgCl reference electrode.

The observed dependence of the reduction peak on the pH can be explained by a direct exchange of four electrons in two successive two - electron steps with splitting of the N=N group to form $-\text{NH}_2-\text{NH}_2$ [53]. In the SW-CSV, on raising the solution pH, the potential of the cathodic peak of Pd (II)-TAR chelate was shifted cathodically to more negative potentials. The plot of the change of the cathodic peak potential vs. pH was linear (Fig. 3.5) following the linear regression equation (3.1)

$$E_{p,c} = 0.0716x + 0.1306, \quad (R^2 = 0.953) \quad (3.1)$$

At pH <6, the poor adsorption of the reduced species and hydrogen at the surface of the HMDE may also account of the observed trend [53]. At $7 < \text{pH}$, the observed cathodic peak was disappeared due to the instability of the electrogenerated Pd-TAR species and the possible of the electroactive species.

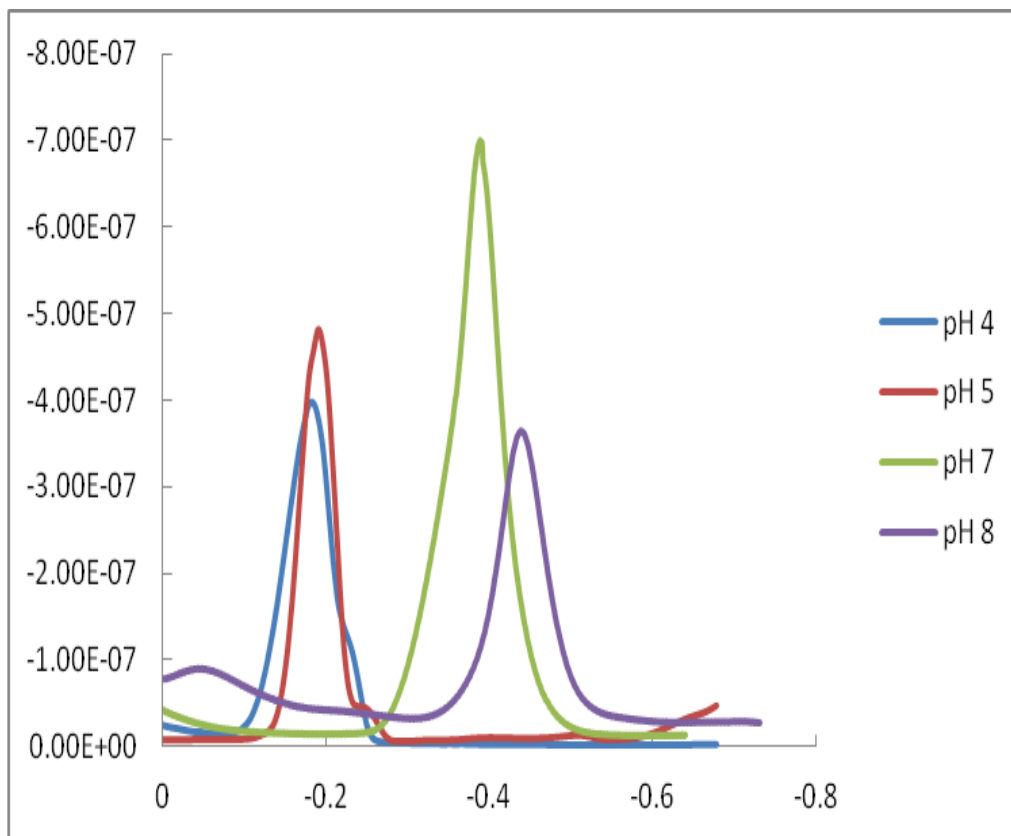


Fig.3.4. Square wave -CSV of palladium (II)-TAR complex species in various B-R buffers of pH 4, 5, 6, 7.04 and 8.1 at the HMDE vs. Ag/AgCl. P, [TAR] = 8.9×10^{-8} M; [Pd^{II}], 1.6×10^{-8} M; scan rate = 100 mV/s; pulse amplitude of 60 mV

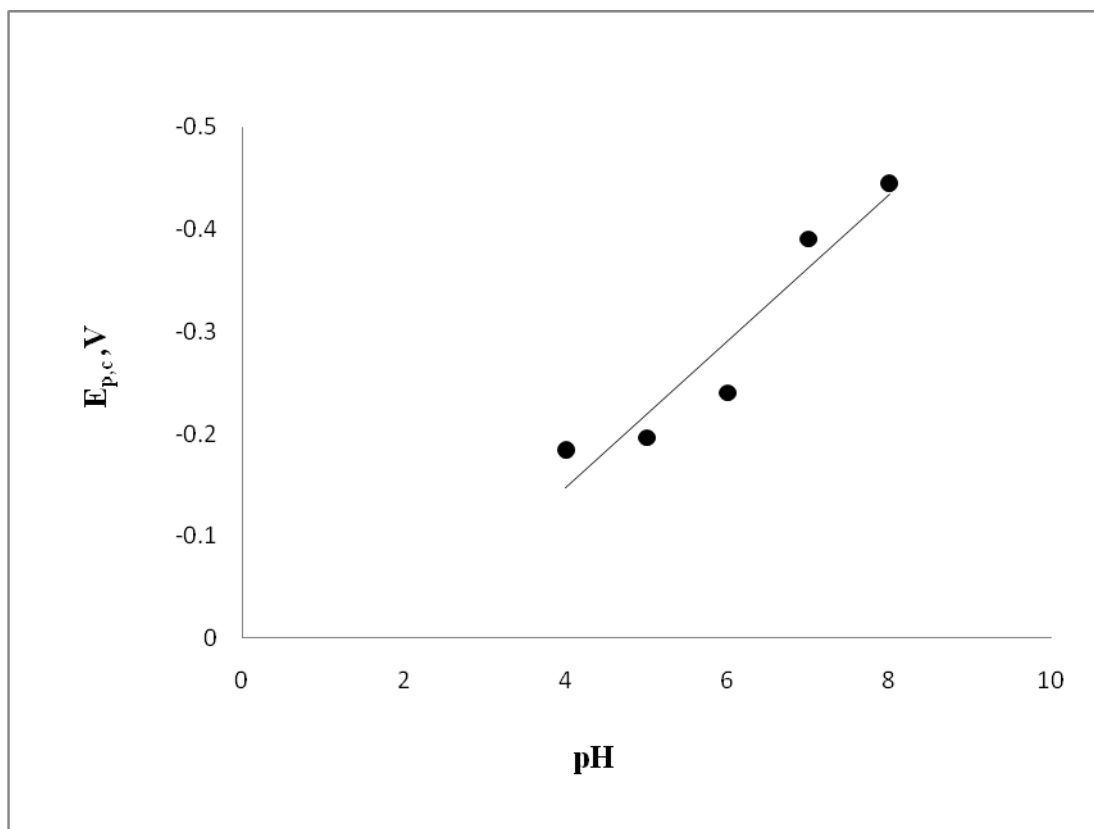


Fig.3.5. Plot of cathodic peak potential of palladium (II)-TAR at 100 mVs⁻¹ scan rate and 50 mV pulse amplitude.

The cyclic voltammograms of Pd(II) – TAR complex at HMDE in B-R buffer of pH 7-8 at various scan rates vs. Ag/AgCl reference electrode were recorded. Representative voltammograms are shown in Fig. 3.6. At scan rate < 100mv/s, the CV showed one well defined cathodic peak in the potential range -0.35-0.40 V and another ill defined cathodic peak in the range -0.65-0.75 vs. Ag/AgCl reference electrode. At scan rate 100 mV/s, on the reverse scan one well defined adsorption peak at -0.37 V more or less mirror image to the cathodic peak at -0.35-0.40 V indicating that, this peak is adsorption peak. Another ill defined anodic peak at -0.1 V was noticed at sweep rate 100 mV/s revealing the irreversible nature of the electrode process at which $E_{p,a} = -0.1$ and $E_{p,c} = -0.7$ V. The calculated value of

peak –peak potential difference ($\Delta E_p = (E_{p,a} - E_{p,c1})$) was > 600 mV confirming the irreversible nature of the observed electrode couples.

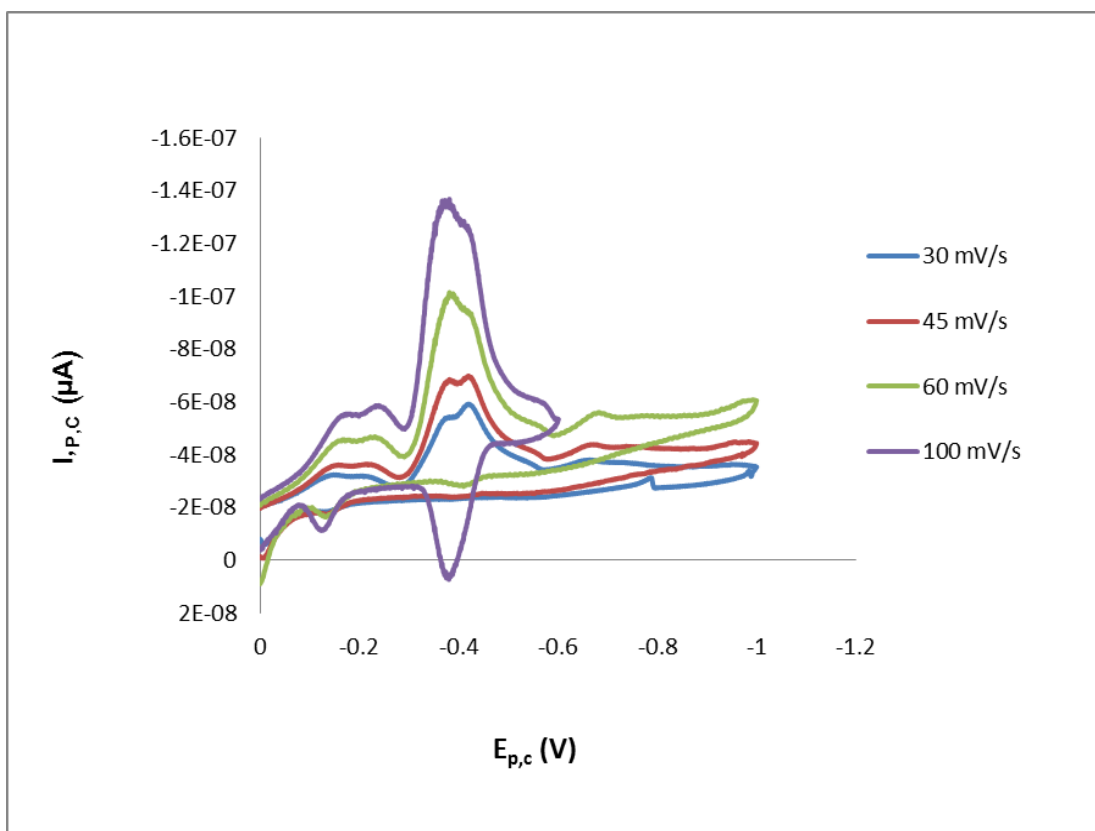


Fig.3.6. Cyclic voltammograms of palladium (II) - TAR at various scan rates (30 – 100 mV s^{-1}) at pH 7 at HMDE vs. Ag/AgCl. $[\text{TAR}] = 4.9 \times 10^{-7} \text{ mol L}^{-1}$ and palladium (II) concentration = $9 \times 10^{-8} \text{ mol L}^{-1}$

The influence of the scan rate on $E_{p,c}$ of Pd (II) - TAR complex at pH 7-8 was investigated on a freshly drop of the HMDE. The plot of \log scan rate (ν) versus second cathodic peak potential is shown in Fig. 3.7. The potential of the cathodic peak ($E_{p,c1}$) at 0.65 — 0.75 V was shifted cathodically on increasing the scan rate (Fig. 3.6) confirming the irreversible nature of the electrochemical reduction process of Pd-TAR complex [52]. This conclusion was confirmed from the slope of the linear

plot of $\log i_{p,c}$ vs. $\log v$ at pH 7 at HMDE against Ag/AgCl (Fig. 3. 8). The slope of the linear plot was 0.446 and far from the theoretical value (1.0) expected when there is an adsorption process on the electrode of the HMDE confirming the irreversible nature of the electrochemical process [52]. The cathodic peak current ($i_{p,c}$) at high scan rate increased linearly with square root of scan rate ($v^{1/2}$) (Fig. 3. 9) showing that, the reduction step is diffusion controlled electrochemical process [52, 53].

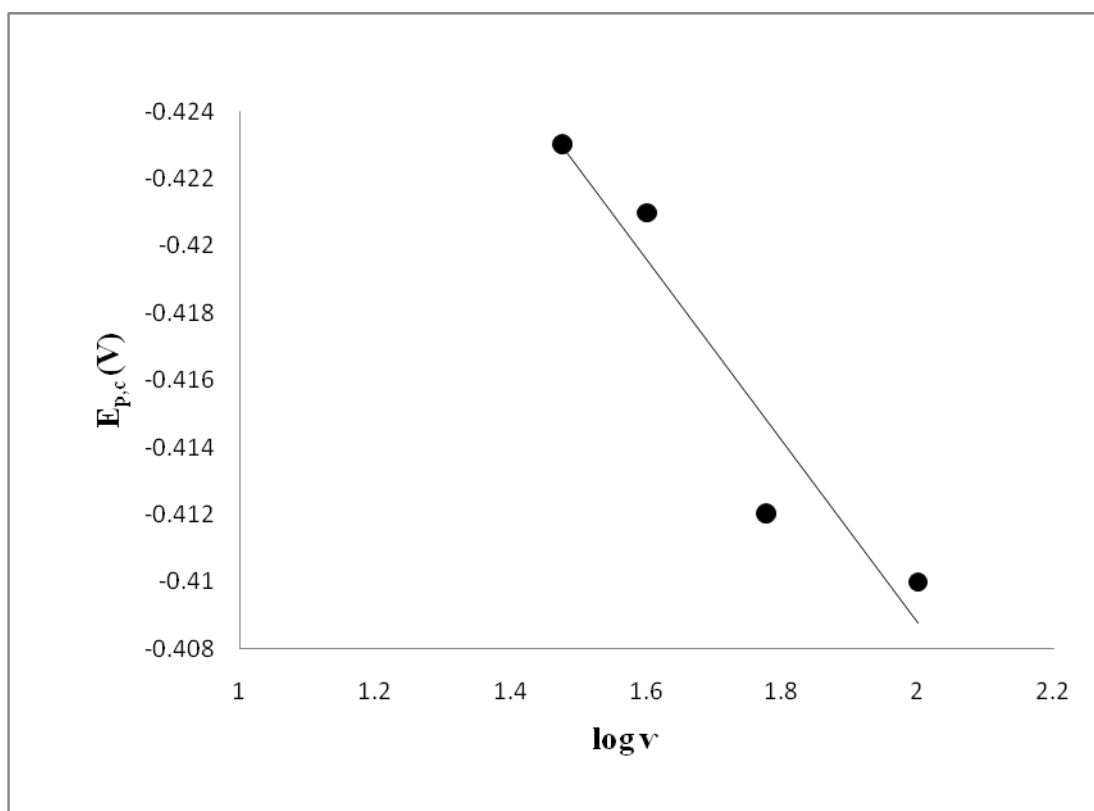


Fig.3.7 Plot of $E_{p,c}$ vs. $\log v$ of Pd(II)-TAR complex at pH 7-8 at HMDE vs. Ag/AgCl reference electrode.

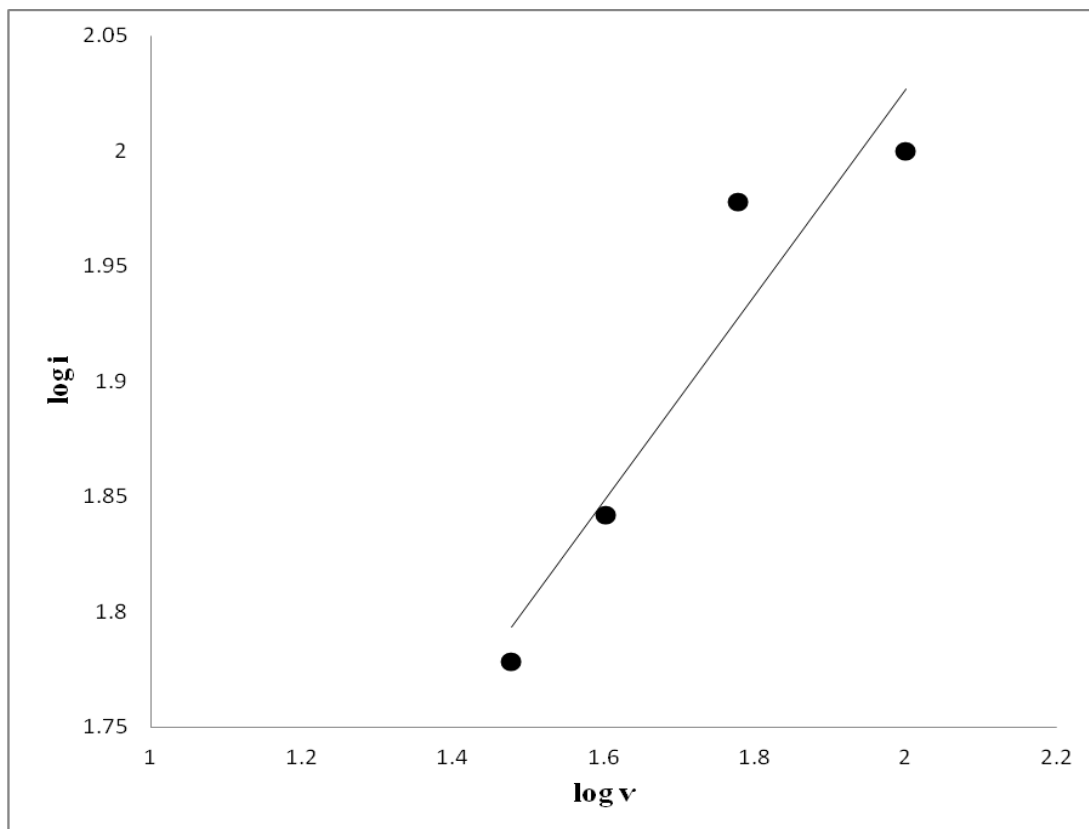


Fig.3.8 Plot of $\log i_{p,c}$ vs. $\log v$ of Pd-TAR complex at pH 7-8 at HMDE vs. Ag/AgCl reference electrode.

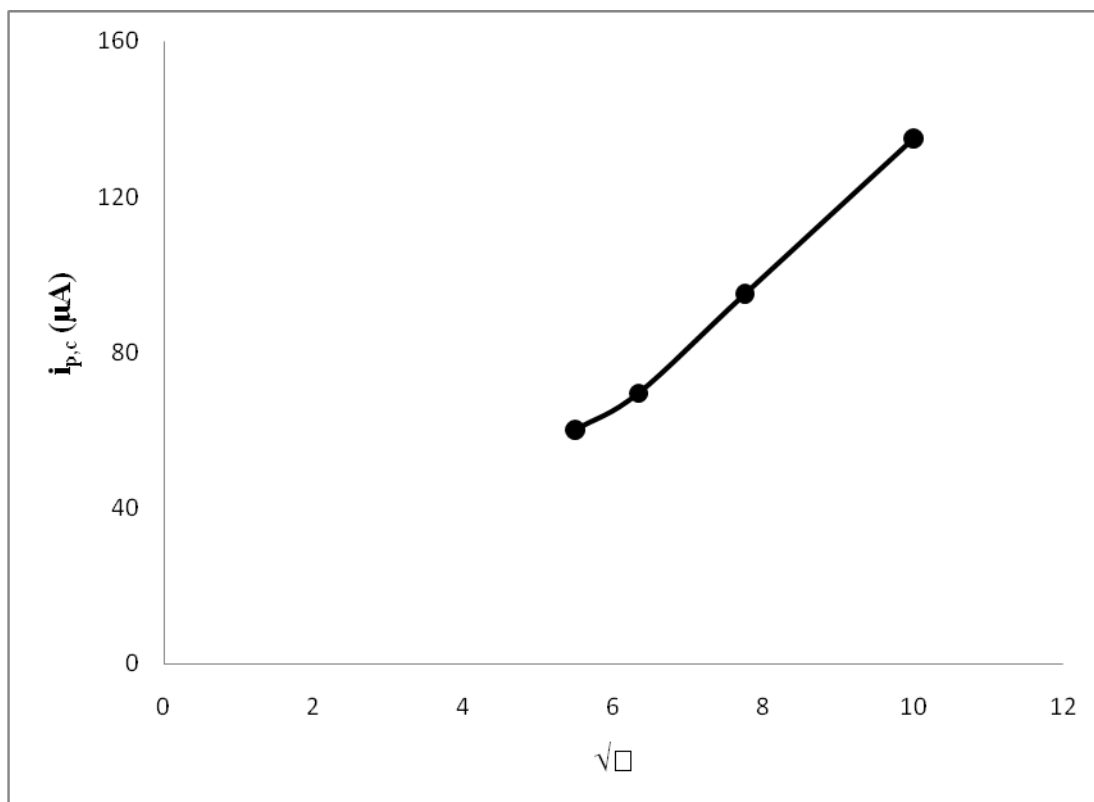


Fig.3. 9 Plot of $i_{p,c}$ vs. square root of scan rate (v) of palladium (II)-TAR complex at pH 7-8 at HMDE and Ag/AgCl reference electrode.

The variation of current function ($i_{p,c}/v^{1/2}$) with the scan rate is an important diagnostic criterion for distinguishing between two types of mechanism by cyclic voltammetry; i. chemical reaction coupled between two charge – transfer processes (ECE) and ii. Two successive one electron charge transfer processes (EE). In the ECE process with an irreversible chemical reaction the current function $i_{p,c}/v^{1/2}$ should decrease with increasing the scan rate [53]. Plot of the current function ($i_{p,c}/v^{1/2}$) vs. v of Pd(II)-TAR complex increased continuously on increasing v (Fig.3.10) indicating that, the reduction process of the azo group (-N=N-) of Pd (II) - TAR complex do not favor ECE [52]. The CVs also exhibited an ill defined cathodic peak in the range $E_{p,c2} = -1.4$ to 1.47V at scan rate $>80 \text{ mVs}^{-1}$. Thus, the product of this

reduction step undergoes a very slow follow-up chemical reaction and the electrode reaction favor EE type mechanism [52] and the protonation reaction is very fast and / or complete in solution medium.

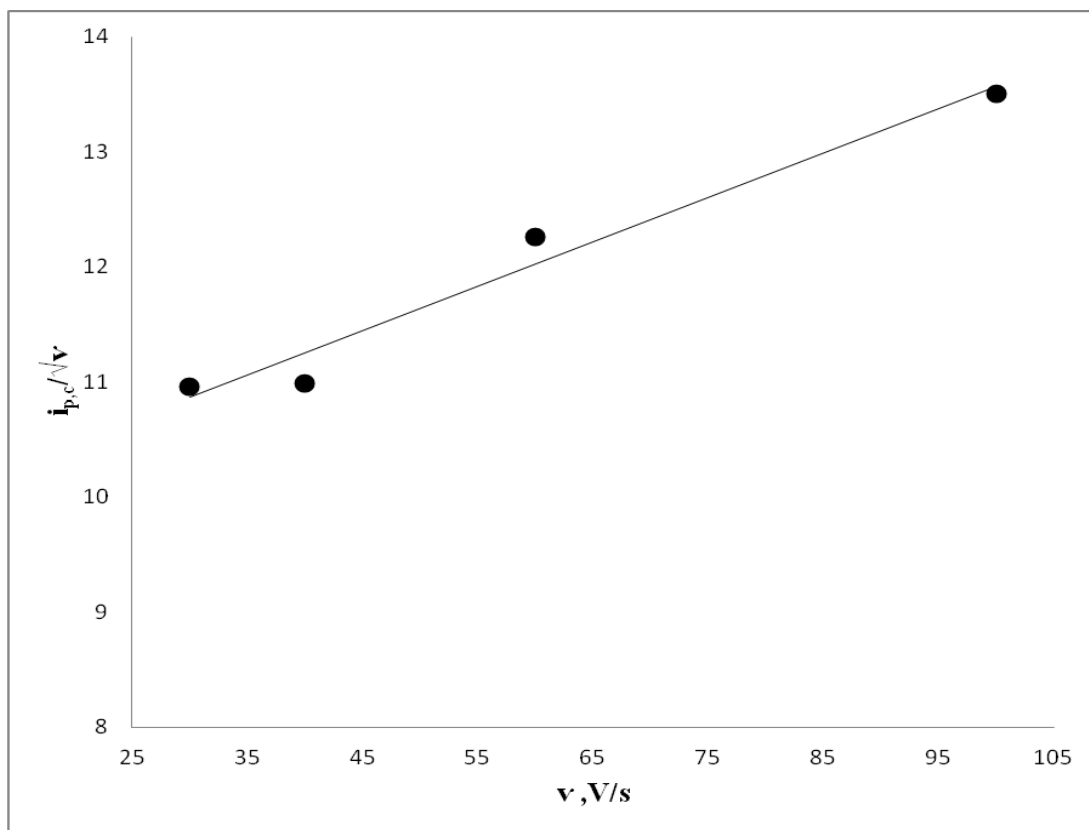


Fig.3.10 Plot of current function ($i_{p,c} / v^{1/2}$) vs. scan rate of Pd(II)-TAR complex at HMDE vs. Ag/AgCl electrode.

3.3.3 Influence of analytical parameters

The high degree of adsorption of Pd(II)-TAR at pH 7-8 and the sensitivity of the developed cathodic peak at -0.43 V of palladium(II)-TAR complex at HMDE vs. Ag/AgCl electrode recommended the possible use of TAR as a proper complexing agent for developing a low cost, precise and convenient square wave-differential

pulse adsorptive cathodic voltammetric method for palladium (II) determination in various matrices. Therefore, the influence of pH employing B-R buffer on the peak current height at $-0.43\text{ V vs. Ag/AgCl}$ electrode was critically investigated over a wide range of pH (2.0 - 11) after 180 s preconcentration time of the Pd (II)-TAR chelate onto the HMDE. The results are demonstrated in Fig.3.11, where maximum cathodic peak current at -0.43 was achieved at pH 7-8. At pH > 9 the reagent TAR dissociated easily and easily participated in the complex formation with palladium (II). Therefore, in the subsequent work, the solution pH was adjusted at pH 7-8 employing Britton-Robinson as supporting electrolyte.

The influence of deposition potential ($- 0.1 - 0.2\text{ V}$) on the adsorptive cathodic stripping peak current response for palladium(II)-TAR complex at HMDE vs. Ag/AgCl after deposition time of 200 s was critically investigated. The results are demonstrated in Fig. 3.12. As can be seen, the peak current increased as the potential of the electrode became more negative up to 0.15 V , levelled off and decreased at more positive value of deposition potential. The fact that, at the pH employed, the palladium (II)-TAR complex could bears two negative charges. Thus, the adsorption of Pd (II)-TAR is most likely favoured at potential less than this value. However, the peak current drops rapidly as the potential are more positive than 0.15 V . Therefore, in the subsequent work a preconcentration potential of 0.15 V was chosen versus Ag/AgCl reference electrode.

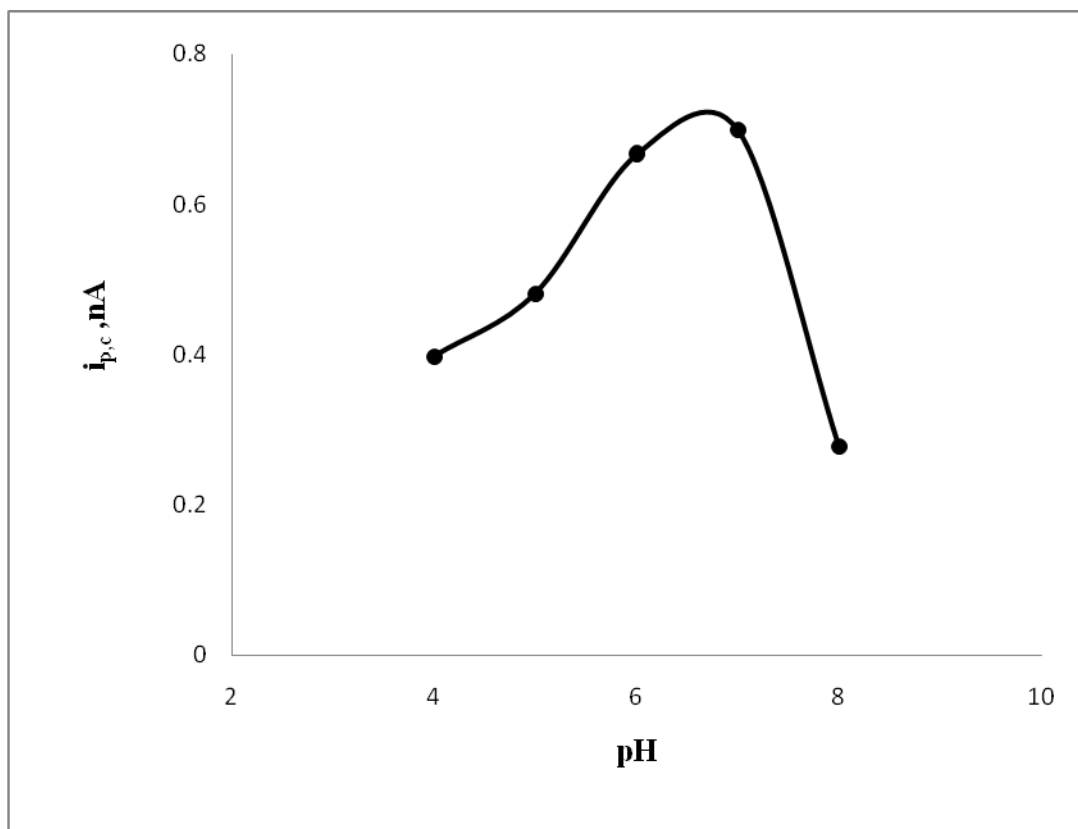


Fig.3.11 Influence of pH effect on the cathodic peak current of Pd(II)-TAR complex at HMDE vs. Ag/AgCl reference electrode. Conditions: [TAR], 9×10^{-8} M; 8.9×10^{-8} M; [Pd^{II}], 1.6×10^{-8} M; deposition potential, -0.1V; deposition time, 180 s; pulse amplitude, 0.05 V; scan rate, 50 mV s^{-1} .

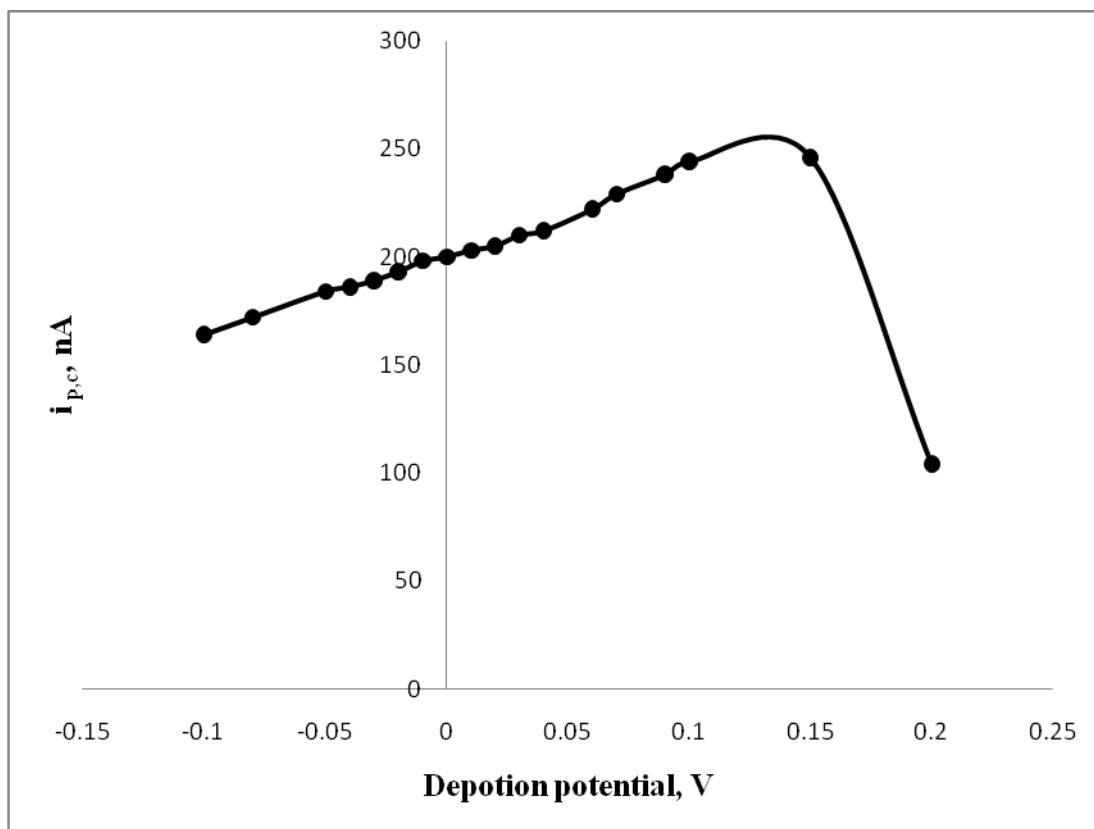


Fig.3.12 Influence of deposition potential on the cathodic peak current of Pd(II)-TAR complex at HMDE vs. Ag/AgCl reference electrode. Conditions: [TAR] = 8.9×10^{-8} M, $[Pd^{II}]$, 1.6×10^{-8} M, accumulation time, 180 s, pulse amplitude = 50 mV and scan rate of 50 mV s^{-1} .

The most important criteria in stripping procedures are the accumulation time that has a pronounced effect on both sensitivity and linear dynamic range. Hence, the influence of deposition time (100-400 s) on the cathodic peak current at -0.43 V was critically studied at HMDE. The results are shown in Fig.3.13 The peak current increases as the preconcentration time increases up to 200 s, levelled off at accumulation time >200 s and remained constant at longer time confirming the chemical equilibria between the electrode and the complex species of palladium(II)

at the employed pH 7-8. Thus, in the next work, an accumulation time of 200 s was generally adopted.

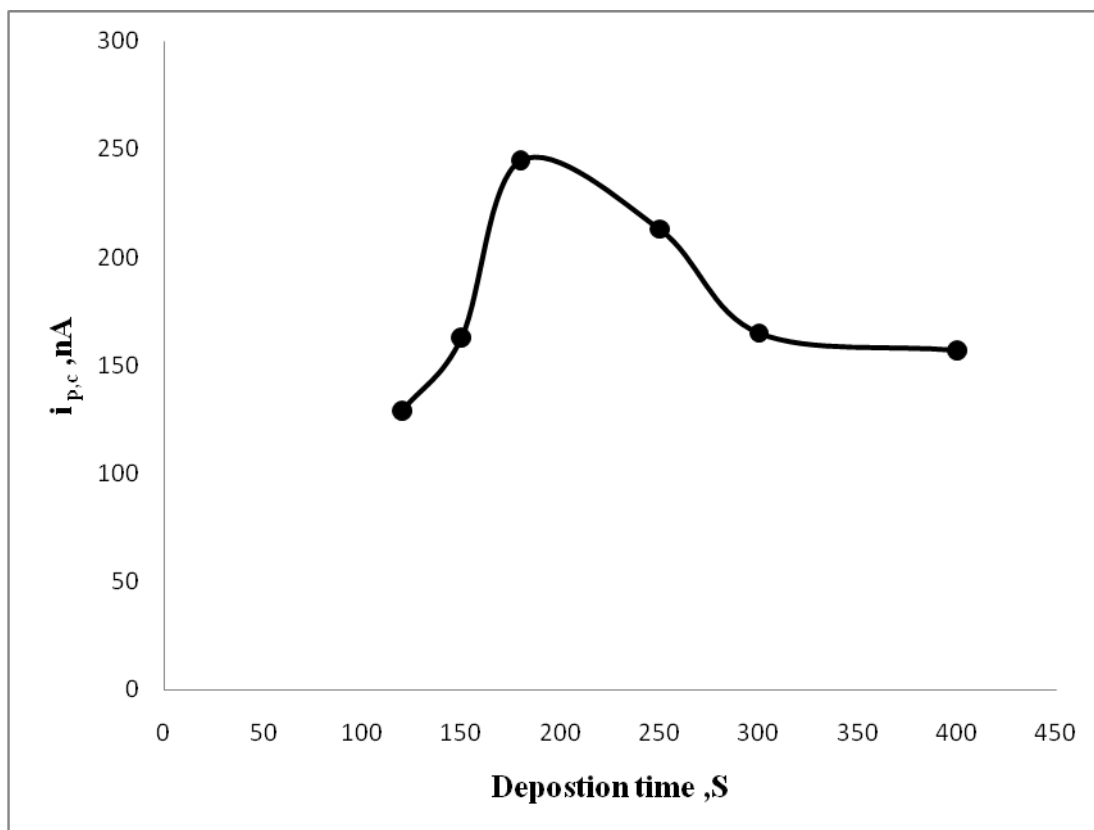


Fig.3.13 Effect of deposition time on on the cathodic peak current of Pd(II)-TAR complex at HMDE vs. Ag/AgCl reference electrode.. Conditions: TAR], 8.9×10^{-8} M; $[Pd^{II}]$, 1.6×10^{-8} M; deposition potential, 0.15 V, pulse amplitude, 0.05 V and scan rate of 50 m V s^{-1} .

Pulse amplitude represents an effective factor in stripping procedures since it has an excellent and interrelated effect on the cathodic peak current. Thus, detailed investigation involving the influence of pulse amplitude (10-80 mV) on the cathodic peak current at pH 7-8 and under the optimum parameters of deposition time and potential was critically investigated. The results are demonstrated in Fig.3.14. The

cathodic peak current increased steadily on increasing the pulse amplitude up to 50 mV and levelled off at more pulse amplitude. Thus, it can be concluded that, at pulse amplitude > 50 mV the capacitive current and a sloping background current signal renders the measurements. At this value of amplitude best sensitivity and instrumental setting of the cathodic peak current to background current characteristics at -0.43 V was achieved. Thus, in the subsequent work pulse amplitude of 50 mV was selected.

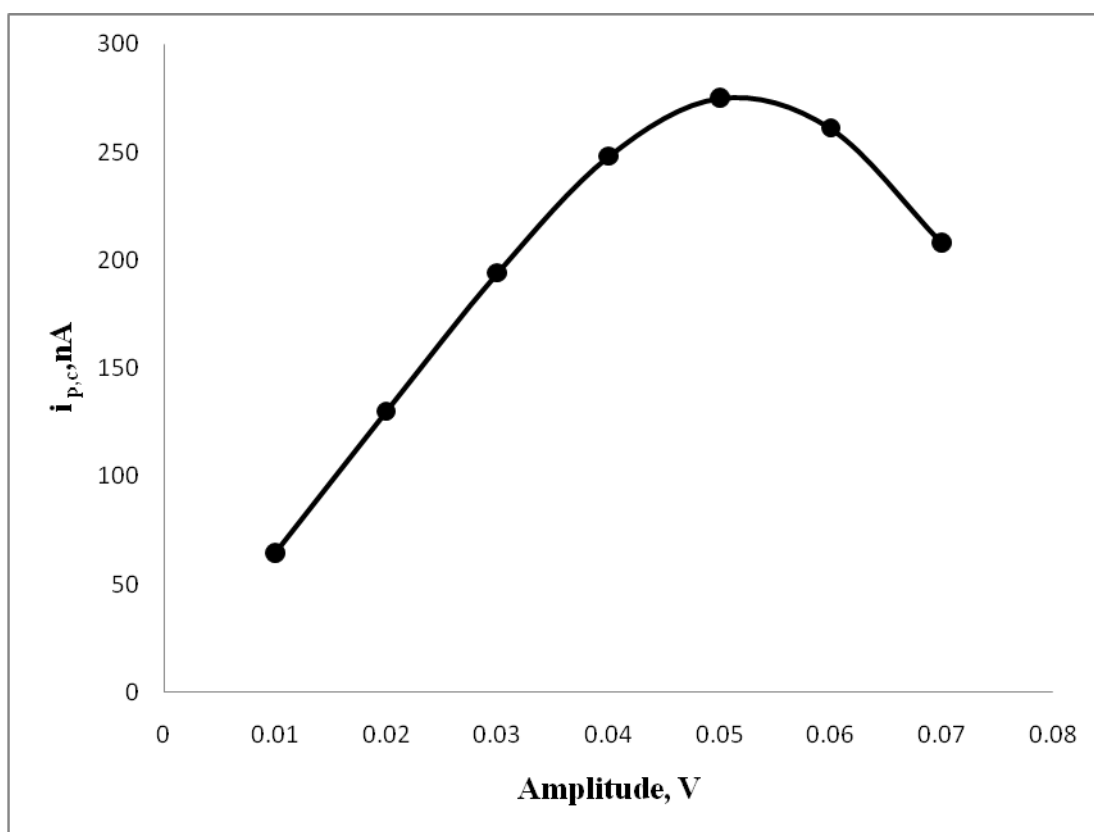


Fig.3. 14 Plot of pulse amplitude on the cathodic peak current. Conditions: [TAR] = 8.9×10^{-8} M, $[Pd^{II}] = 1.6 \times 10^{-8}$ M, deposition potential = -0.15 V, deposition time = 200 s and 55 mV/s scan rate.

Scan rate is an important parameter in stripping voltammetry. Thus, the influence of scan rate (30- 100 mVs^{-1}) on the cathodic peak current was critically studied at peak potential of -0.47 V. The data are shown in Fig.3.15. The cathodic peak current increased steadily. However, in the subsequent work, a scan rate of 50 mV/s was adopted. At this value of scan rate best signal to background current characteristics and peak symmetry were achieved.

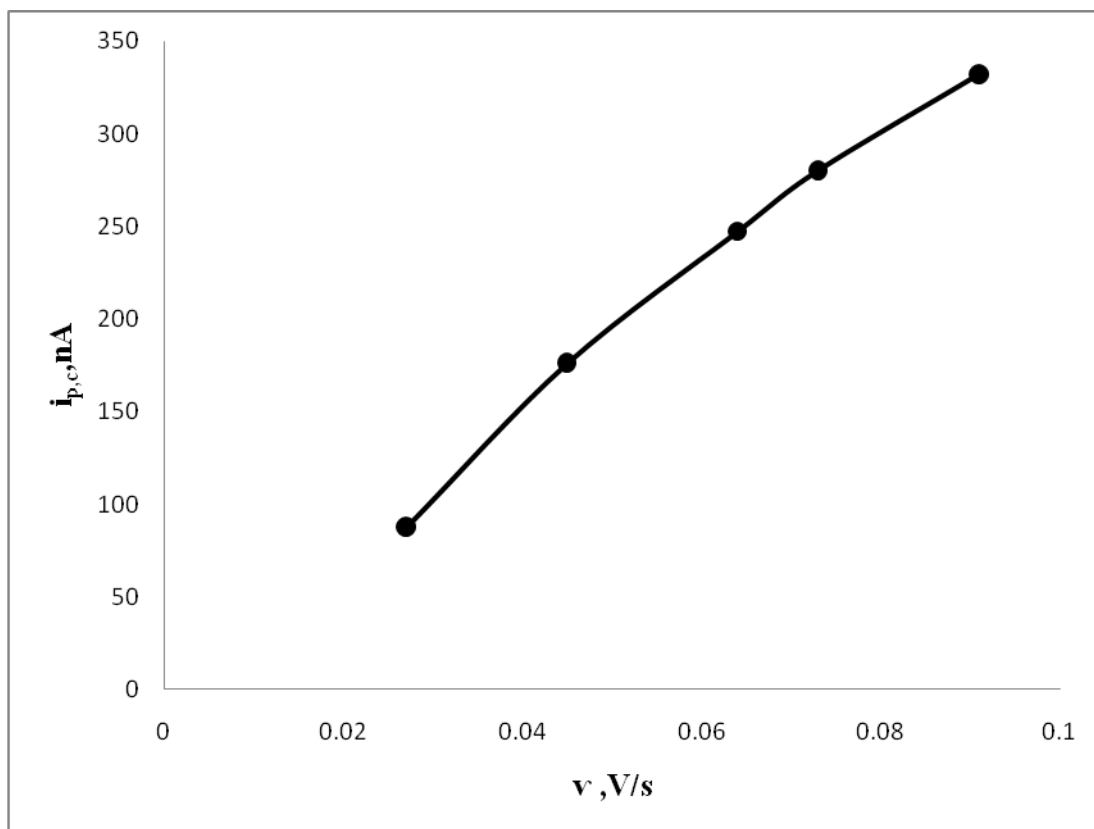


Fig.3.15 Effect of scan rate (mV/s) on the cathodic peak current. Conditions: TAR , $8.9 \times 10^{-8} \text{ M}$; $[\text{Pd}^{\text{II}}]$, $1.6 \times 10^{-8} \text{ M}$; deposition potential, 0.15 V; deposition time, 180 s; pulse amplitude, 0.05 V.

The influence of TAR concentration (1.0×10^{-9} - 1.6×10^{-7} M) on the cathodic peak current height at pH 7-8 under the optimal operational parameters was critically investigated (Fig. 3.16). On increasing TAR concentration, the $I_{p,c}$ increased linearly up to 6.0×10^{-8} mol L⁻¹ and distinct break point was achieved at higher reagent concentration (Fig. 3.15). At the observed break point (6.0×10^{-8} mol L⁻¹), the reagent TAR concentration was just twice palladium (II) ions concentration in the electrochemical cell confirming that, the adsorbed species has a palladium to reagent 1:2 molar ratio i. the complex has the structure of Pd(TAR)₂. At reagent TAR concentration higher than 6.0×10^{-8} mol L⁻¹, the specific adsorption of excess TAR species at concentration higher may account for the observed trend, whereas a non-adsorptive Pd (II) species is formed at lower TAR concentration. Thus, a 10×10^{-8} mol L⁻¹ of TAR was selected in the subsequent work as a compromise between good sensitivity and complex stability.

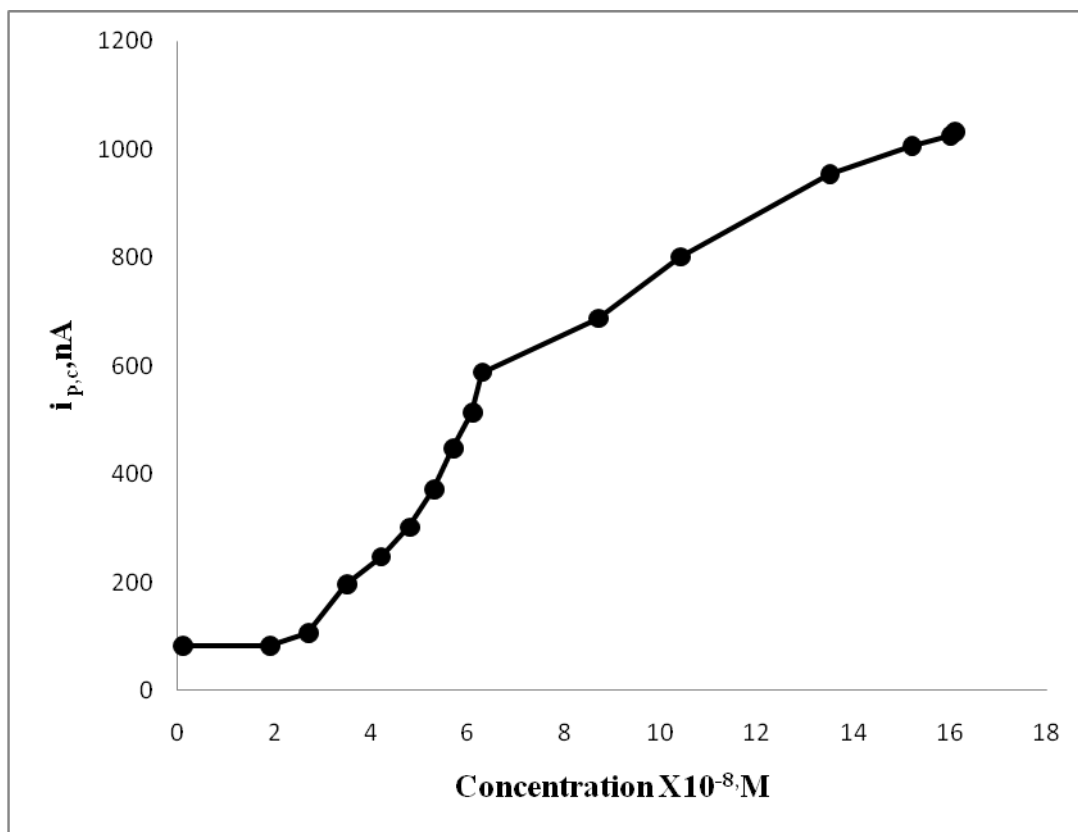


Fig. 3.16 Plot of TAR concentrations versus cathodic peak potential at pH 7-8 at HMDE vs. Ag/AgCl reference electrode. Conditions: Deposition potential =0.15V, deposition time =200 s; scan rate 50 M/s and pulse amplitude of 50 mV.

3.3.4 Analytical performance of the developed SW-CSV method

The performance of the developed square wave –CSV for palladium determination using TAR was determined in terms of the figure of merits (LOD, LOQ and linear dynamic range and reproducibility) under the optimized experimental conditions of pH 7-8, preconcentration potential of 0.15 V, deposition time of 200s, 100 mV/s scan rate, pulse amplitude of 60 mV and TAR concentration (6.0×10^{-8} mol L⁻¹). The square voltammograms and the corresponding calibration plot are demonstrated in Figs.3.17 & Fig. 3.18, respectively. The plot of Pd

concentration vs. cathodic peak current at -0.43 V vs. Ag/AgCl reference electrode was found linear in the concentration range 5.0 – 53.0 μgL^{-1} of palladium (II) and it was leveled off at concentrations higher than 53 μgL^{-1} of palladium (II) because of the adsorption saturation [54]. The linear plot can be expressed by the following regression equation:

$$i_{p,c} \text{ (nA)} = 4.64 C \text{ (}\mu\text{gL}^{-1}\text{)}, \quad R^2 = \mathbf{0.9779} \quad (3.2)$$

Based on Miller and Miller, 1991 [55], the calculated values of LOD and LOQ using the formulas $\text{LOD} = 3S_{y/x}/b$ and $\text{LOQ} = 10S$ where $S_{y/x}$ is the standard deviation of y- residual and b is the slope of the calibration plot were found equal to 1.63 and 5.0 μgL^{-1} , respectively. The main analytical features (LOD, LOQ and the linear dynamic range) of the developed method are better than the corresponding values of the reported methods reported spectrophotometric and voltammetric methods summarized in Table 3.1. Some of these methods are also exhibited high LOD and serious interferences by halide ions e.g. F^- , Cl^- , Br^- and I^- . The relative standard deviation (RSD) of palladium (II) based on five measurements of Pd (II) at 5.0 μgL^{-1} was found equal to $\pm 3.6\%$ confirming the precision of the method. The developed method is low cost, short deposition, selective and quite applicable for routine analysis. The sensitivity could be improved to pico molar palladium by on-line preconcentration from large sample volumes onto polyurethane foam packed column followed by elution prior determination.

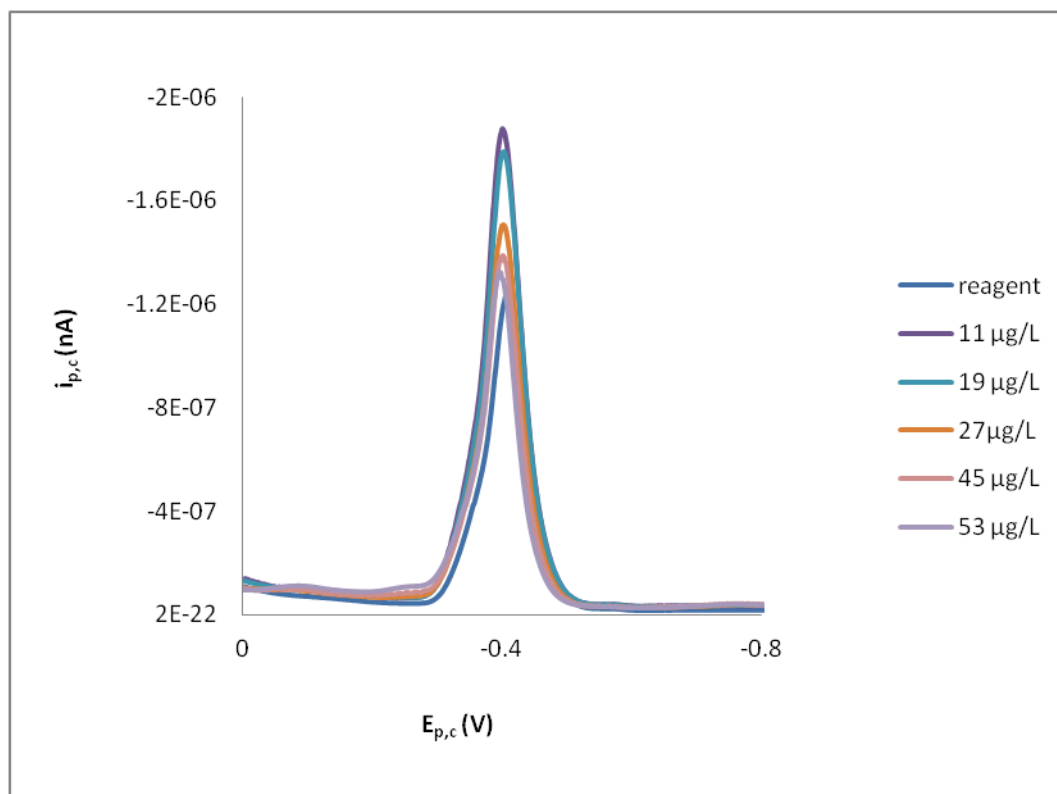


Fig.3. 17 SW-CSVs of Pd(II)-TAR complex in the presence of various concentrations of palladium (5.0- 53 $\mu\text{g/L}$) at HMDE vs. Ag/AgCl electrode at pH 6-7 under the optimum operational parameters

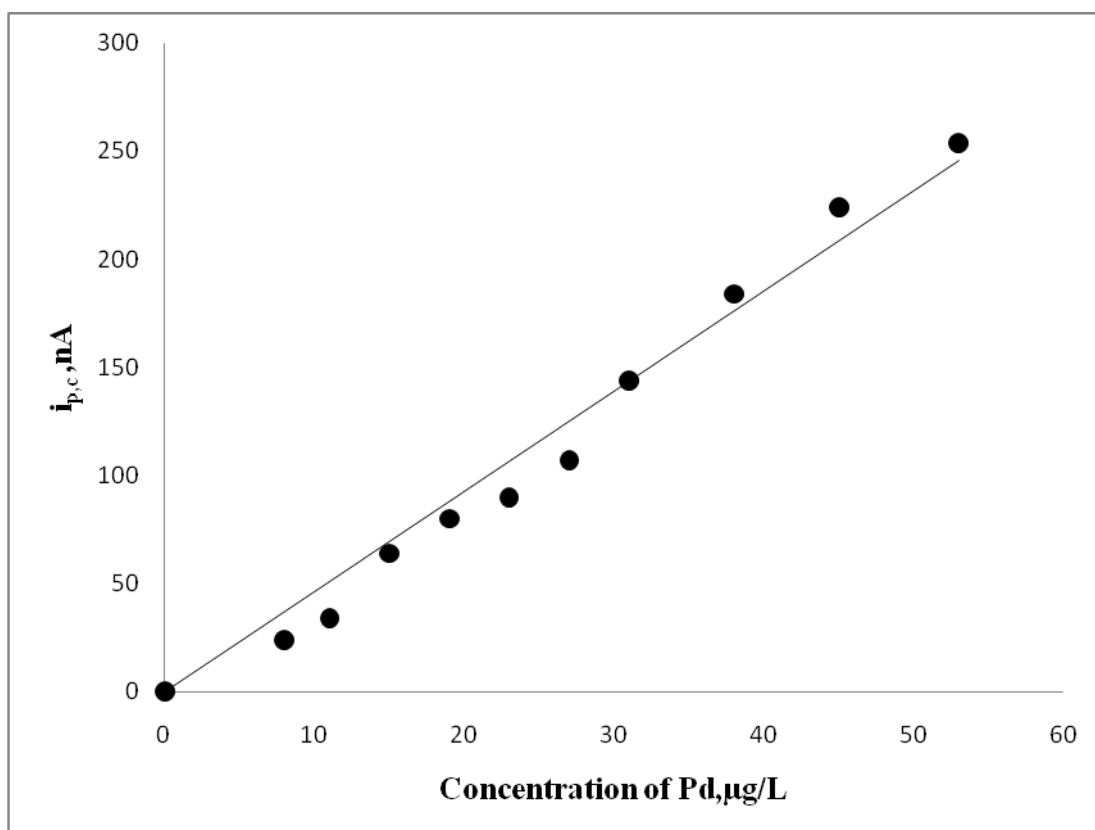


Fig.3.18 Calibration plot of palladium(II) -TAR complex in the presence of various concentrations of palladium ($7.5 \times 10^{-9} - 5.25 \times 10^{-7}$) at HMDE vs. Ag/AgCl electrode at pH 6-7 under the optimum operational parameters.

3.3.5 Influence of diverse ions on the sensitivity of the developed method

The influence of a series of interfering species e.g. Ca^{2+} , Co^{2+} , Cu^{+2} , Mg^{+2} , Zn^{+2} , As^{3+} , Sb^{+5} at a relatively high excess (100 fold excess) on the analysis of standard palladium (II) ions at concentration ($1.6 \times 10^{-8} \text{ mol L}^{-1}$) was studied individually by the developed SW-CSV. The tolerance limit was defined as the concentration of the foreign ion added causing a relative deviation within $\pm 4\%$ in the magnitude of the peak current at $-0.43 \text{ V vs. Ag/AgCl}$ electrode. The ions

Co^{2+} , Ni^{+2} and Sb^{5+} interfered seriously on the cathodic peak current of Pd(II)–TAR complex, while the ions Zn^{2+} decreased the current of Pd(II)–TAR complex with a formation of new peak confirm more shift at cathodic side. At 10 fold high excess of the ions Cu^{+2} , Ca^{2+} , Mg^{+2} and As^3 , no significant change in the the cathodic peak was noticed.

3.3.6 Analytical applications

3.3.6.1 Analysis of Pd in CRM (IAEA Soil-7)

The validation of the SW- CSV procedure was performed by the analysis of palladium in the CRM sample (*IAEA Soil-7*) as described in the experimental section before. An acceptable agreement between the results of the developed DP-CSV and ICP-MS and the certified value of palladium.

3.3.6.2 Analysis of palladium in water sample

The developed method was applied for the analysis of palladium (II) in tap water sample by the standard addition method. The current of the observed cathodic peak shifted cathodically to -0.5 V vs. Ag/AgCl reference electrode increased linearly on spiking palladium to the real water sample. The results of palladium (II) determination by the spiking method is demonstrated in Fig. 3.19. The data revealed the absence of palladium in the tested water sample in good agreement with the results achieved by the standard addition employing th standard ICP-MS confirming the suitability of the method compared the ICP-MS.

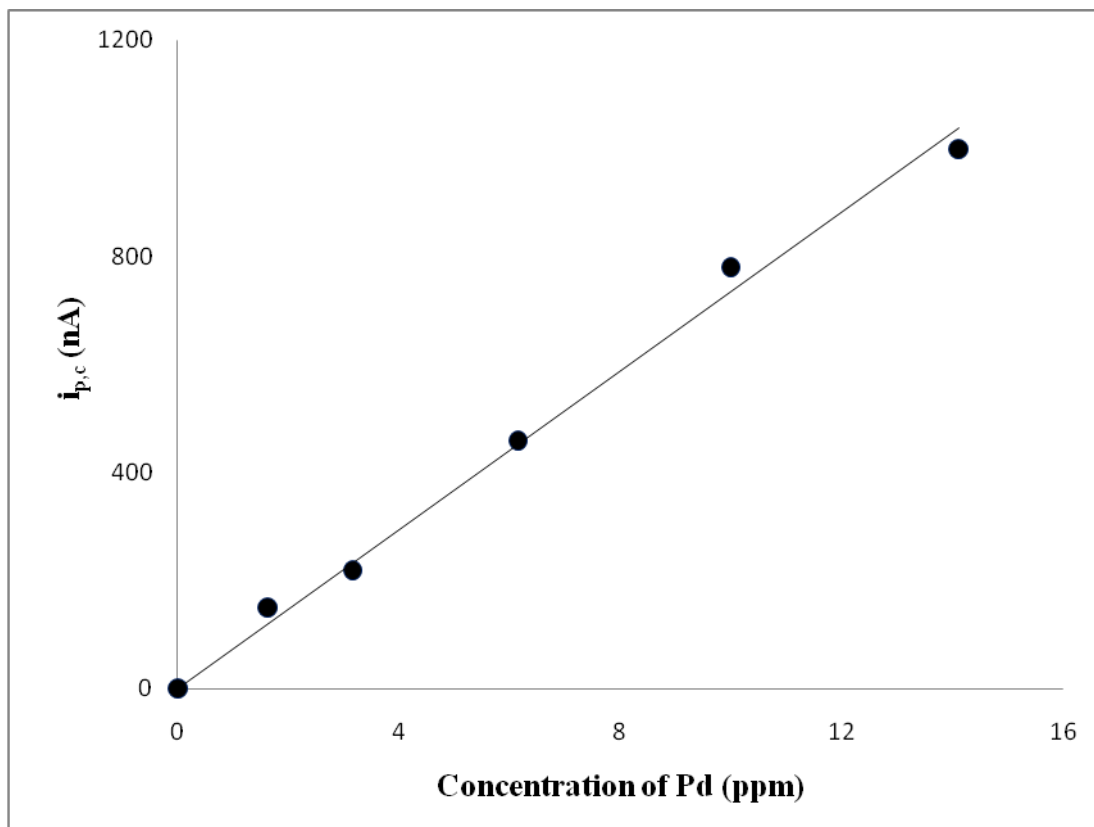


Fig.3. 19 Typical calibration plot for the analysis of palladium (II) in drinking water at pH 7-8 at HMDE vs. Ag/AgCl reference electrode.

3.4 Conclusion

The developed SW-CSV method compares favorably with many spectrophotometric and electrochemical methods. The method could be extended for the analysis of palladium in wastewater and other environmental water samples at ultra trace concentration after preconcentration of palladium from the test solution at TAR immobilized polyurethane as reported earlier by El-shahawi et al [56, 57]. Thus, work is continuing for: the possible application of on-line SW-CSV determination of palladium after masking and / or minimization of the interferences present in various environmental water samples. The method could be extended to pico molar level after on-line prior pre concentration from large sample volumes onto solid sorbent packed column followed by elution and subsequent determination of Pd.

3. 5 References

1. C. Locatelli, *Electroanalysis* 19 (2007) 2167 and references therein.
2. Z. Marczenko, M. Balcerzak, *Separation, Preconcentration and Spectrophotometry in Inorganic Analysis*, El- Sevier, Amsterdam, 2000.
3. A. Tunceli and A.R. Turker, *Anal. Sci.*, 16 (2000) 81.
4. Hesse, Rayner W. "Palladium". *Jewelrymaking through history: an encyclopedia*. Greenwood Publishing Group. (2007) 146.
5. R. R. Barefoot, J. C. Van Loon, *Talanta* 49 (1999) 1.
6. R. Merget, G. Rosner, *Sci. Total Environ.* 270 (2001) 165-173.
7. K. Ravindra, L. Bencs, R.V. Grieken, *Sci. Total Environ.* 318 (2004) 1–43 Review.
8. X. Wang, M. Wu, W. Tang, Y. Zhu, L. Wang, Q. Wang, P. He, Y. Fang , *J. Electroanal. Chem.*, 695(2013) 10-16 .
9. H. Tavallau, M. Jahromi, *J. Serb. Chem. Soc.* ,74 (3) (2009) 311–315 .
10. R.R. Barefoot and J.C. Van Loon, *Talanta*, 49, (1999) 1–14.
11. D. Afzali, R. Jamshidi, S. Ghaseminezhad, Z. Afzali , *Arabian Journal of Chemistry*, 5 (2012) 461–466
12. H. Zheng, H. Li, Y. Zeng, L. Ma, *Yankuang Ceshi*, 24, (2005) 299-302.
13. Pei Liang*, Ehong Zhao, Feng Li , *Talanta* 77 (2009) 1854–1857
14. B. Goldlewska-Zylkiewicz, M. Zaleska, *Anal. Chim. Acta*, 462 (2002) 305-312.
15. M. Iglesias, E. Anticó, V. Salvadó, *Talanta*, 59 (2003) 651-657.
16. R. R. Barefoot, J. C. Van Loon, *Talanta* 49 (1999) 1

17. B. A. Lesniewska, B. Godlewska-Zylkiewicz, A. Hulanicki, *Chem. Anal. (Warsaw, Pol.)*, 50 (2005) 945-950.
18. Y. C. Sun and C. H. Hsieh, *J. Anal. At. Spectrom.*, 17 (2002) 94–98.
19. C. P. R. Morcelli, A. M. G. Figueiredo, J. E. S. Sarkis, J. Enzweiler, M. Kakazu, J.B.Sigolo, *Sci. Total Environ*, 345 (2005) 81-91.
20. B. Godlewska-Zylkiewicz, *Microchim. Acta*, 147 (2004) 189–210.
21. M. Schwarzer, M. Schuster, R. Von Hentig, *Fresenius J. Anal. Chem.*, 368 (2000) 240-243.
22. S. Posta, F. Kukula, *Radioisotope*, 17 (1976) 559-576.
23. A R. Byrne, *Mikrochim. Acta (Wien)*, I (1981) 323-329.
24. M. Geldmacher-von Mallinckrodt, M. Pooth, *Arch Toxicol*, 25 (1969) 5-18.
25. G. Asimellis., N. Michos., I. Fasaki., M. Kompitsas, *Spectrochim. Acta*, B 63 (2008) 1338.
26. D. Afzali., R. Jamshidi., S. Ghaseminezhad., Z. Afzali, *Arabian Journal of Chemistry*, 5 (2011) 461-466.
27. Y-Q. Ye, X.-Z Yang, X-S.Li, F.-Q Yao, Q.-F Hu, *Asian Journal of Chemistry*, 24 (11) (2012) 4967.
28. C. Van Der Horst, B. Silwana, E. Iwuoha, V. J. Environ, *Sci. Health - Part A Toxic/Hazardous Substances and Environmental Engineering*, 47 (13) (2012) 2084.
29. A.A. Ensafi, T. Khayamian, M. Atabati, M.M. Ardakani, *J. Can., Anal. Sci. Spectro*, 49 (1) (2004) 8.
30. A.Bagheri., M.Taghizadeh., M.Behbahani., A.A.Asgharinezhad, A., Salarian, A. MiDehghani, H. Ebrahimzadeh., M. Amini, *Talanta*, 99 (2012) 132–139.

31. V.Mircesk., R.Gulaboski, *Electroanalytical*, 13 (2001) 1326–1334
32. J.G.Osteryoung., R.A.Osteryoung , *Anal. Chem*, 57 (1985) A101–A110
33. F.Scholz., U.Schröder., R.Gulaboski, (2005), *Electrochemistry of Immobilized Particles and Droplets*, Springer, Berlin.
34. .R.Gulaboski., L. Mihajlov, *Biophysical Chemistry*, 155 (2011) 1-9
35. A. Messerschmidt., R. Huber., K.Wieghardt., T. Poulos, *Handbook of Metalloproteins* Wiley (2001).
36. J.Wang., K. Varughese, *Anal. Chim. Acta*, 199 (1987) 185.
37. .Z. Zhao, Z. Gao, *J. Electroanal. Chem*, 256 (1988) 65.
38. K.J.Stetzenbach., M.Amano., D.K. Kreamer and V.F.Hodge , *Ground Water*, 32(1994) 976-985.
39. G.Raber, K.Kalcher, C.Neuhold, C.Talaber , *Electroanalysis*,7 (1995) 138-142.
40. Z-Q.Zhang, H.Liu.,H. Zhang, and Y-F.Li, *Anal. Chim. Acta.*, 333(1996) 119-124.
41. M. Georgieva, B. Pihlar,J. Fresenius , *Anal Chem*, 357 (1997) 874.
42. C-Y.Su., B-S. Kang. , T-B. Wen., Y-X. Tong., X-P. Yang., C. Zhang , H-Q. Liu ., J. Sun, *Polyhedron*, 18 (1999) 1577–1585.
43. N.B. Silverberg., L.K.Lim., A.S.Paller, and A.J.Mancini, *J. Am, Acad.Dermatol.*, 42(2000) 803
44. S.Kim, and K.W.Cha, *Talanta*, 57(2002) 675

45. V. T. Aher., M. M. Palrecha., A. V. Kulkarni., G. C. Shah1, Journal of Radioanalytical and Nuclear Chemistry, 252 (3)(2002) 573–576.
46. C. Locatelli, D. Melucci, G. Torsi, Anal. Bioanal. Chem, 382(2005) 1567.
- 47.C. Locatelli, Electroanalysis, 17(2005) 140.
48. C. Locatelli, Anal. Chim. Acta, 557(2006) 70.
49. C. Locatelli, Electrochim. Acta, 52(2006) 614.
50. 44. A.I. Vogel "Quantitative Inorganic Analysis"3rd edn, Longmans Group Ltd., England, 1966.
51. I. Narin, M. Soylak, M. Dogan, Fresenius Environ. Bull. 6 (1997)749.
52. D. Sawyer, W.R. Heinemann, J. Beebe, "Chemistry Experiments for Instrumental Methods", John Wiley & Sons, New York, 1984.
53. A.J. Bard, L. Faulkner, L., "Electrochemical Methods: Fundamentals and Applications", John Wiley & Sons, New York, (1980) p. 218.
54. M. Odabasoglu, G. Turgut, H. Kocaokutgen, Phosphorous, Sulfur, Silicon and Related Compound 152 (1999) 27-34.
55. J.C. Miller, J. N. Miller "Statistics for Analytical Chemistry" Ellis-Horwood, New York, 4th edn., 1994
56. M.S.El-Shahawi, M.A.El-Sonbati, Talanta 67(2005) 806.
57. A.B. Farag, M.H. Soliman, O.S. Abdel-Rasoul, M.S. El-Shahawi, Anal. Chim. Acta 601 (2) (2007) 218.

Chapter IV

**Chemical Speciation of Trace
Concentrations of Arsenic(III & V) in
Water and Wastewater Samples by Local
Clay of Saudi Arabia Prior inductively
coupled plasma–optical emission
spectrometry**

4.1.Introduction:

Heavy metals are introduced into the aquatic environment through, dumping wastes, effluents from runoff of terrestrial system (Industrial and domestic effluents) and geological weathering [1-3]. Cadmium, arsenic, copper, mercury and others have the ability to accumulate in bottom sediments. Due to various processes of remobilization, these metals may be released and moved into the biological or food chain and concentrate in fish and other edible organisms, thereby reaching humans and causing chronic or acute disease [2]. Heavy metals occur in a minute concentration in natural biological systems and exert beneficial or harmful effects on plant, animal and human life [3]. Detailed investigation will be focused on the use of clay as solid sorbent in liquid-solid separation.

Arsenic has trace abundance in the Earth's crust, yet it occurs widely in the environment, with localized high concentrations found in certain rocks, soils and waters. In nature, arsenic exists essentially in four oxidation states: arsine (-III), arsenic (0), arsenite (III) and arsenate (V) [4]. Arsine is mainly present as inorganic arsenite (As^{3+}) and arsenate (As^{5+}) [2] while, organic arsenic species are negligible [5]. In ground water inorganic arsenic species are found at levels higher than the maximum contaminant level ($10 \mu\text{g L}^{-1}$) recommended by WHO [6]. Chronic and acute poisoning of arsenic due to exposure to elevated concentrations has been reported worldwide. The worst arsenic calamity in groundwater has been reported in West Bengal and Bangladesh, where groundwater is the main source for drinking water [6]. In West Bengal and Bangladesh, drinking water contains arsenic above $50 \mu\text{g L}^{-1}$ [7]. Arsenic is a naturally occurring element widely distributed in the earth's crust. Inorganic compounds are mainly used to preserve wood. Ingesting very high levels

of arsenic result in death. Exposure to lower levels can cause nausea and vomiting, decreased production of red and white blood cells, abnormal heart rhythm, damage to blood vessels, and a sensation of “pins and needles ” in hands and feet [7, 8]. Ingesting or breathing low levels of inorganic arsenic for a long time can cause a darkening of skin and the appearance of small “corns ” or “warts ” on the palms, soles, and torso [8].

Arsenic and its compounds are toxic pollutants for environment and all living organisms [9]. The toxicity of arsenic derived from several natural phenomena and anthropogenic activities [10]. Arsenic (III, V) species mainly reach humans through water supplies depending on the solution pH and redox conditions [11, 12]. Typical concentration of arsenic in natural water can raise up to 3.0 mgL^{-1} [13]. Arsenate species predominate in aerobic and oxidizing conditions while, arsenic species prevail in anaerobic and moderately reducing conditions [11]. Due to the high toxicity of arsenite and arsenate species and the widespread of their emission, arsenic and its compounds are strictly controlled by environmental regulations [12]. Arsenic (III) has been reported to be 25-60 times more toxic than arsenic (V) and organoarsenic [14-16].

A wide variety of methods e.g. spectrophotometry, atomic absorption spectrometric (AAS) methods e.g. coupled to hydride generation (HG-AAS), graphite furnace atomic spectrometry (GFAAS); atomic fluorescence spectrometry (AFS); inductively coupled plasma-optical emission spectrometry (ICP-OES); inductively coupled plasma-mass spectrometry (ICP-MS), X-ray spectrometry; neutron-activation analysis (NAA); and capillary electrophoresis have been reported [14-19]. Chemical speciation of As(III) and As(V) in water, food and biological samples has been reported by Tuzen et al., 2010 [19]. Arsenic(III) ions have been quantitatively

extracted and recovered on *Alternaria solani* coated Diaion HP-2MG resin at pH 7 using HG-AAS. Arsenic (V) in the test solution containing arsenic(III &V) has been reduced to arsenic(III) by KI -L(+) ascorbic acid solution. Traces of arsenic(V) have been calculated as the difference between the total arsenic content and As(III) content. A preconcentration factor of 35 and a detection limit of 11 ng L^{-1} for As(III) ($n = 5$) were achieved. The relative standard deviation and relative error of arsenic(III) determinations were lower than 7% and 4%, respectively [19].

Preconcentration methods combined with instrumental analysis have frequently been used for arsenic determination in complex matrix samples [20, 21]. A novel method has been reported for determination of ultra trace arsenic species in water samples by hydride generation atomic absorption spectrometry (HGAAS) [21]. The method has been based upon the use of pyronine B as chelating agent in presence of sodium dodecyl sulfate (SDS) at pH 10.0 and extraction into olyethylene glycol tert-octylphenyl ether (Triton X-114) non-ionic surfactant. Under the optimized conditions, a preconcentration factor of 60 and a detection limit of $0.008 \mu\text{g L}^{-1}$ with a correlation coefficient of 0.9918 has been achieved with a calibration curve in the range of $0.03\text{--}4.00 \mu\text{g L}^{-1}$ [21]. A simple and sensitive method has been reported for chemical speciation of arsenic (III& V) [22]. The method was based upon extraction of arsenic(III) complex with pyrolidinedithiocarbonate (PDC) of the general formula As(PDC)_3 into methyl isobutyl keton (MIBK) and subsequent determination by electrospray ionization mass spectrometry (ESI-MS). Arsenate ions were also determined after reduction to arsenic (III) with thiosulfate and determined by ESI-MS [22]. The limit of detection of As was $0.22 \mu\text{g L}^{-1}$ using $10 \mu\text{L}$ of sample solution, and it is far below the permissible limit of As in drinking water, $10 \mu\text{g L}^{-1}$,

recommended by the WHO [6]. Total inorganic arsenic (III) and (V) in urine was also determined in urine samples.

Electrochemical methods offer excellent possibilities for determination of arsenic in arsenic compounds present at trace and ultra trace concentrations in various matrices [23]. Electrochemical techniques offer many advantages e.g. simple instrumentation and operation; low cost; high sensitivity and excellent selectivity which allow the chemical speciation of trace metal ions including arsenic. Potentiometric methods have rarely been used for analysis of arsenic in its compounds by developing a series of arsenate-ion selective electrodes [24, 25]. A novel method has been reported by Xu et al.2008 [26, 27] for determination of trace and ultra trace concentrations of arsenite on highly ordered platinum-nanotube array electrodes (Pt NTAEs). Stripping analysis techniques have been successfully reported as readily amendable for on-site analysis for accurate measurements of low concentrations of arsenic with rapid analysis and low cost/weight instruments in natural water [28, 29]. Several stripping voltammetric methods have been published for analysis of arsenic (III) at trace levels at hanging mercury dropping electrode (HMDE) [30 -32]. Macro- sized gold film electrodes [33 -35] and solid gold electrode substrates [36-38] have been also reported for analysis of arsenic (III and V) species.

Chemical speciation and determination of trace amounts of arsenic(III & V) in seawater have been reported by Zhang, et al, 2004 [39]. Arsenic (III) has been coprecipitated quantitatively with a Ni–ammonium pyrrolidine dithiocarbamate (APDC) complex at the pH 2–3, while arsenic (V) was hardly coprecipitated under the same pH condition The coprecipitates arsenic(III) species have been directly measured by electrothermal atomic absorption spectrometry (ETAAS) and used the

solid sampling technique [39]. Trace concentration of arsenic (V) has been calculated by difference in concentration between arsenic(III) and total arsenic in the sample solution. The concentration factor by co-precipitation has been reached at about 40 000 when 2 mg of nickel as a carrier element added to 500 mL of water sample [38]. A detection limit for arsenic (III) of 10 ng L^{-1} was achieved [39]. X-ray fluorescence spectrometry (TXRF) with L-cysteine followed by solid phase extraction after complex formation with sodium The procedure allowed analysis of As in the presence of V, Fe, Ni, Cu, Zn, Pb, and U ions in seawater [40].

The application of low-cost adsorbents as a replacement for costly conventional methods of removing heavy metal ions from wastewater has been reviewed [41]. On the other hand, the significant growth in Saudi Chemical industries requires efficient and cost-effective processes to phase out water and air pollution that is caused by these industrial activities. A promising strategy is to make use of cheap local materials in a simple technological ways to hamper the accumulation of these pollutants and to prevent their subsequent effects in Saudi inhabitants. Research in heavy metal removals became a public health concern because of its non-biodegradable and persistent nature. The toxicity of these metals is enhanced through accumulation in living tissues and consequent biomagnification in the food chain [42]. Several methods have been used for removal of heavy metals from water and wastewater using chemical precipitation, physical treatment such as ion exchange, solvent extraction, reverse osmosis and adsorption [43 -46]. Natural clays as the adsorbent with a low cost have received much attention on heavy metals sorption from contaminated water [47, 48].

Recently, the use of clay minerals for sorption and / or removal of heavy metals in industrial effluents has been object of study in a great deal of research due to its

several economic advantages [49 -54]. The cost of these adsorbents is relatively low when compared to other alternative adsorbents, including activated coal, natural and synthetic zeolites, ion-exchange resins and other adsorbent materials. Clay minerals as Montmorillonite, Vermiculite, Illite and Kaolinite are some natural materials that are being studied as heavy metal adsorbents [55, 56]. Another advantage of using clay as an adsorbent is related to its intrinsic properties such as: great specific surface area, excellent physical and chemical stability and several other structural and surface properties [57-60]. Thus, the development of low cost and selective method for separation and / or determination of trace and ultra trace concentrations of arsenic in various matrices e.g. drinking, marine waters and industrial wastewater represent a vital task for human health in recent years. Hence, the overall objectives of the work presented in this chapter are focused on: i developing precise, low cost procedure for removal of arsenic (III & V) by local clay as solid sorbent; ii studying the kinetics and thermodynamic characteristics of arsenic (III) sorption by clay; iii investigating the retention mechanism of arsenic (III) by the clay and finally iv developing a low cost clay packed column for chemical speciation of arsenic (III, V) in different water samples.

4.2 Experimental:

4.2.1. Reagents and materials:

All chemicals used were of analytical reagent grade quality and were used without further purification, unless stated otherwise. All solutions were prepared in de - ionized water, and were kept in a refrigerator. All the plastic and glassware bottles were cleaned by soaking in dilute HNO₃ (10% w/v) and were rinsed with distilled water prior to use. Most of the chemicals were provided by Merck

(Darmstadt, Germany). All solutions were made up by doubly demonized distilled water throughout the work. Stock solutions of sodium arsenite (NaAsO_2) and sodium arsenate (NaAsO_3) ($1000.0\mu\text{g mL}^{-1}$) were prepared by dissolving the required weight of each compound separately in deionized water. More diluted solutions ($0.01\text{-}10\mu\text{g mL}^{-1}$) of arsenic (III) and (V) were freshly prepared daily in doubled distilled water. The following salts NaCl , LiCl , KCl and NH_4Cl (BDH, Poole, UK) (1-2 % w/v) were prepared separately by dissolving an accurate weight of each compound in water. Universal buffer solutions were prepared by mixing equimolar concentrations of acetic acid, phosphoric acid and boric acid (0.12 mol L^{-1}) and adjusting the solution pH to the required value with NaOH (0.2M) [61].

4.2.2 Apparatus

A Perkin Elmer inductively coupled plasma – optical emission spectrometer (ICP- OES, Optima 4100 DC (Shelton, CT, USA) was used and operated at the optimum operational parameters for arsenic determination. A Perkin Elmer ICP – MS Sciex model Elan DRC II (California, CT, USA) was also used to measure the ultra trace concentrations of As in the effluent of the developed clay packed column at the operational parameters of the manufacture. The ICP-MS instrument is optimized daily before measurements and operated as recommended by the manufacturer. A Philips X-ray diffractometer Model PW/840/20 was used to identify the clay minerals present in the ore samples at the optimum operational parameters (KV 40, MA 30, $\text{Cu } \alpha$ radiation, and $2\theta/1\text{ min/cm}$) of the instrument. Perkin-Elmer arsenic and multi-element standard solutions were used for analytical verification of the developed method. Ore samples were also analyzed for major oxides and trace elements after microwave

digestion using concentrated acid $\text{HNO}_3\text{-HCl-HF}$ mixture using the optima ICP-OES (4100 DV) spectrometer. If the resulting concentration of trace elements lies below $1.0 \mu\text{g mL}^{-1}$, ICP-MS is performed on the sample solution to determine the concentration of the element with great accuracy. A Corporation Precision Scientific mechanical shaker (Chicago, CH, USA) with a shaking rate in the range 10 – 250 rpm and glass columns (5.0 cm x 10.0 mm i.d) (Fig. 4.1) were used, respectively. A Milli-Q Waters Plus system (Milford, MA, USA) and a Thermo Fisher Scientific Orion model 720 pH Meter (Milford, MA, USA) were also used. A CEM microwave system (Mars model, 907500, USA) was used for the digestion of the certified reference material (CRM, *IAEA-soil-7*). A Teflon digestion vessel (HP 500) was used for the digestion of the food stuffs in the microwave system.

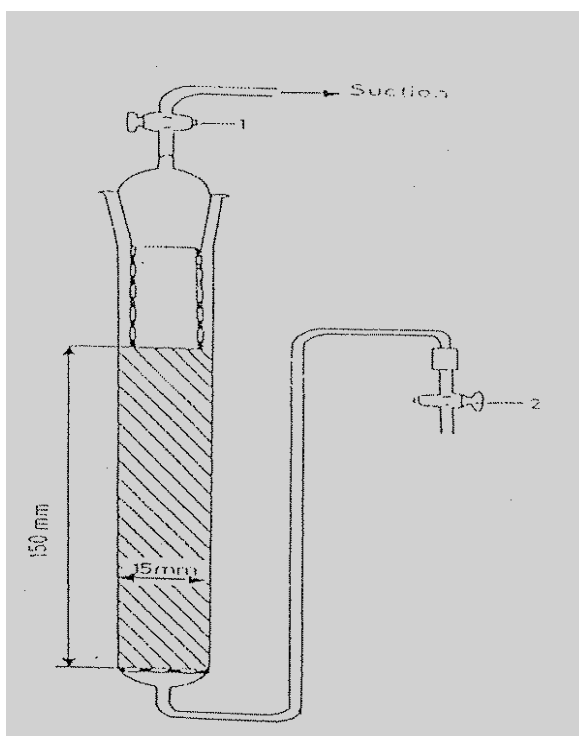


Fig.4.1 Preparation of polyurethane foam packed column.

4.2.3 Clay deposits

Clay deposits constitute a major component of the Tertiary sedimentary rocks exposed in Makkah and Rabigh quadrangles along the Red Sea coast in the west central part of the Arabian Shield between latitudes 21° and 23° N and longitudes $38^{\circ} 50'$ and $40^{\circ} 30'$ E (Fig.4.2) and were successfully collected by A.A. Eldougdoug and H. M. Harbi (Department of Mineral Resources and Rocks, Faculty of Earth Sciences, King Abdulaziz University, P.O. Box 80206, Jeddah, 21589, Saudi Arabia). The area is covered mainly by Precambrian basement rocks which is unconformably overlain by the Tertiary formations in the west and by the basalt flows in the north. Quaternary surficial sands and gravels cover extensive areas along the coastal plain and the wadis. Lithologically, the Tertiary formations consist mainly of siliciclastic rocks (sandstones, siltstones, and clays) and are usually capped with the basaltic flows. These rocks are best preserved and exposed when they are covered with the Tertiary basalt flows (Fig.4.3) and occur as low lying hills rising above the coastal plain.

Clay deposits vary from one area to the another and are mainly composed of montmorillonite and kaolinite with minor illite and chlorite in addition to some percentages from calcite and quartz and other non - clay minerals. Clay deposits near Khulays village are bedded and multicolored with some beds. The beds are almost composed of montmorillonite and are chocolate brown in color (Figs. 4. 4 & 4.5). The mineralogy of these clayey deposits was studied by Basyoni et al.2002 [62] and Taj et al., 2002 [63] and have concluded that the clay deposits are of three types. The 1st is highly montmorillonitic, the 2nd is a mixture of montmorillonite, kaolinite, and illite, and the 3rd is highly kaolinitic with minor montmorillonite. The 1st type is

widely distributed around Khulays village. Other minerals which may occur in the deposits were not identified, e.g. calcite, quartz, gypsum, magnetite, chromite. These minerals will affect the chemistry of these deposits (major oxides and trace metals).

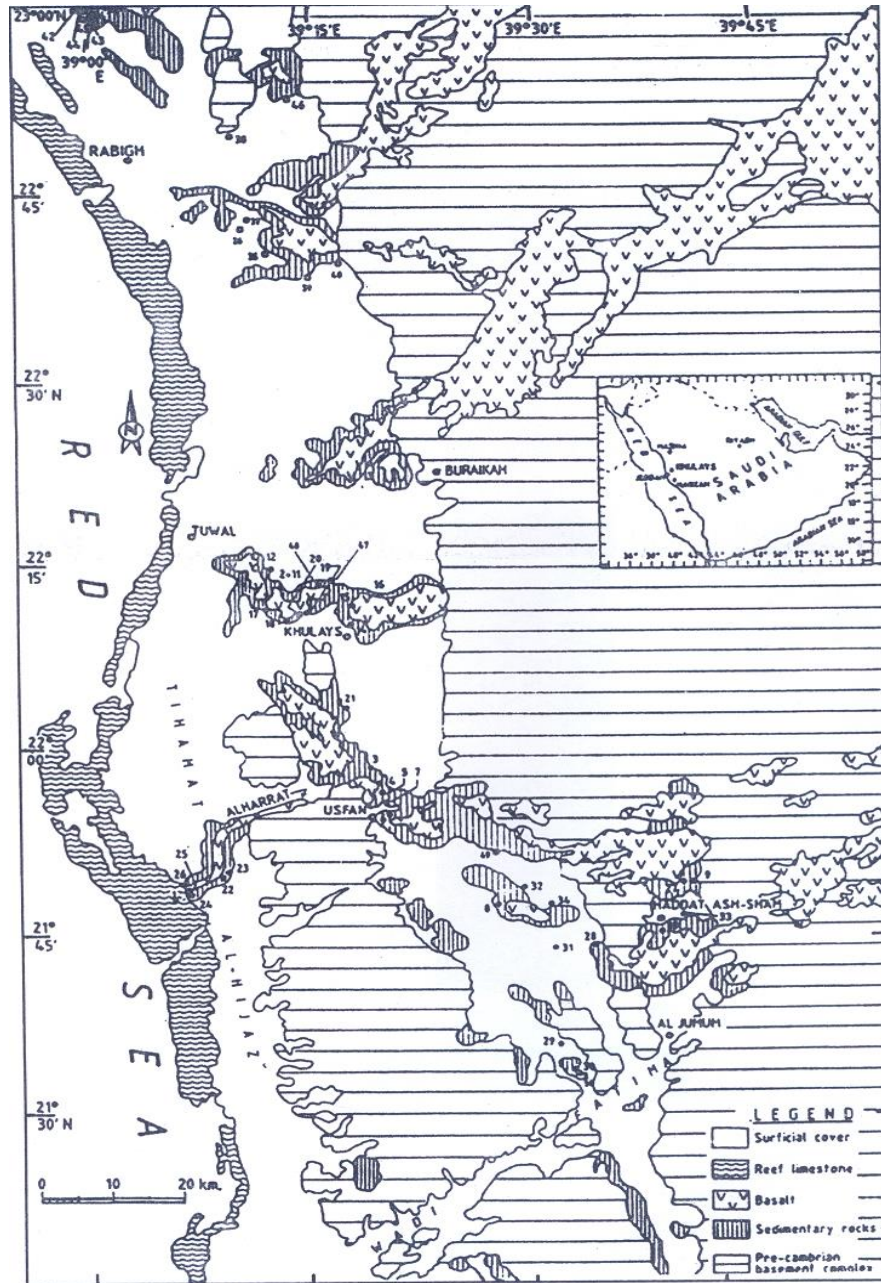


Fig. 4.2 Simplified geological and location map of the sedimentary clay deposits in Makkah and Rabigh quadrangles.

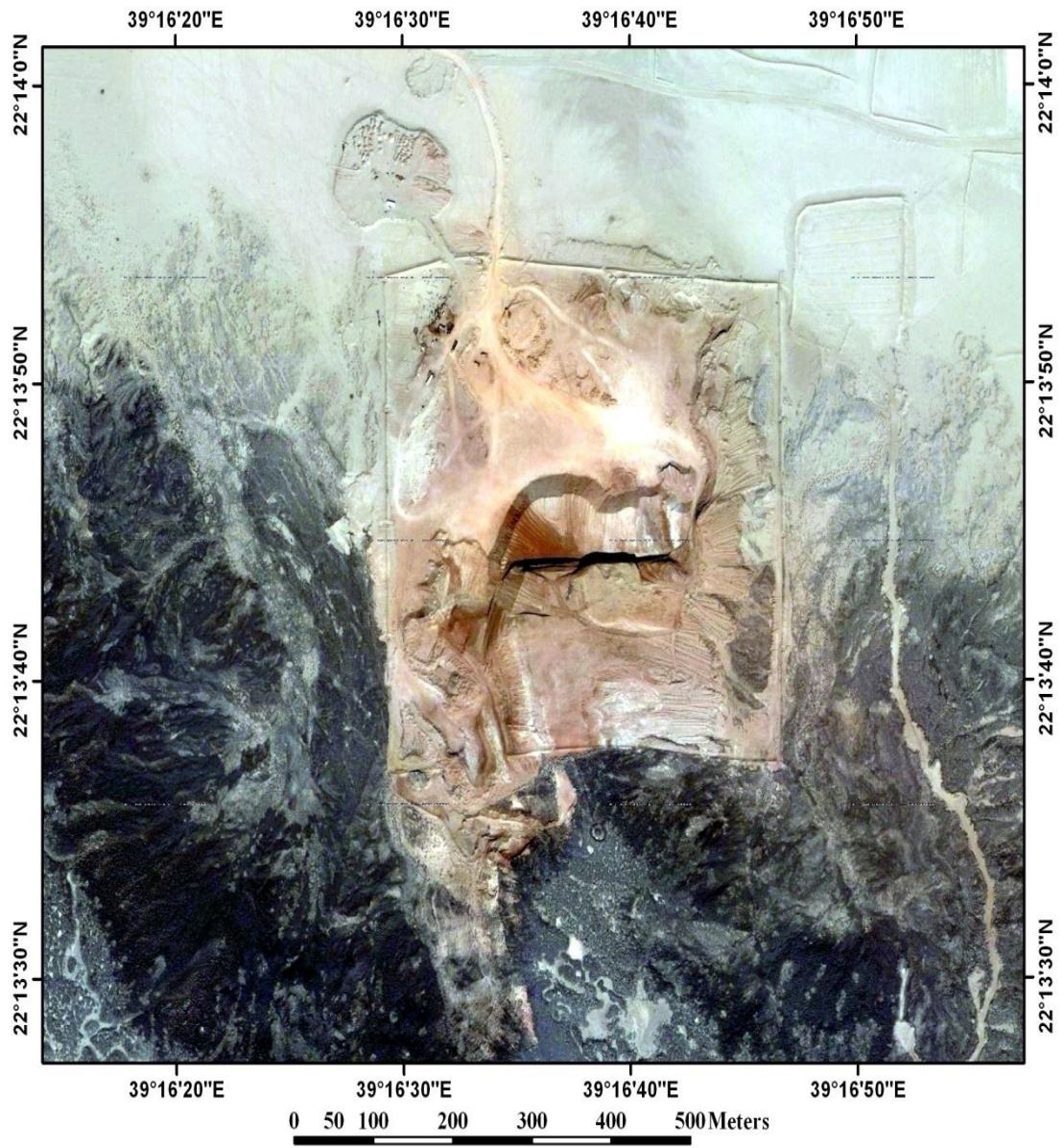


Fig.4.3. A landsat image showing Al – Khyat clay quarry, Khulays area. Basalt flows at the top (dark black areas).

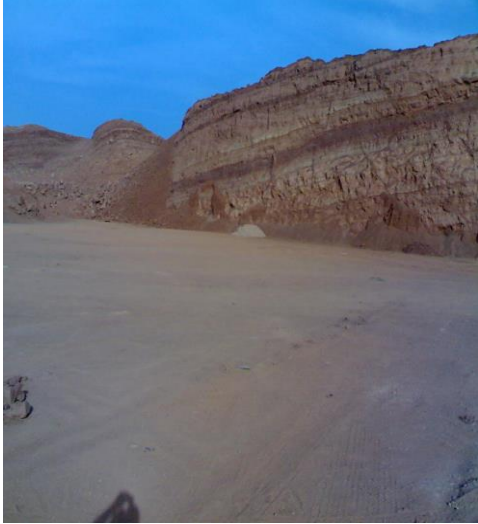


Fig.4.4 Bedded clay deposits with Harrat basalt at the top (Right top).



Fig.4.5 Bedded multicolored clay deposits with montmorillonite rich beds (chocolate brown).

The chemistry (major oxides and trace metals) of the bulk samples from some of these clay deposits has been studied [63] and some examples of major oxides for representative bulk samples (1-3) are given in Table 4.1. These data do not show distribution of the major oxides and the trace metals between the clay and non-clay fraction have been reported [62]. Most of the trace metals are associated with the clay minerals, and there is a positive correlation between the Fe_2O_3 content and trace metals (Mn, Cr, Ni, Cu, Zn).

Five samples representing the different clayey beds were collected from the face of Al-Khyat quarry which is located to the north of Khulays village (Fig. 4.2). The clay fraction from the different samples was separated according to the following procedure [62, 63]:

- i. An approximate weight (200 g) of each bulk ore sample (samples 1-5) collected from five different locations (Al – Khyat clay quarry, Khulays area) based on the map shown in Fig. 4.1 is placed in a glass beaker (400 mL) and mixed well with distilled water with constant stirring until complete disintegration of the sample.
- ii. Hydrogen peroxide (15%, 20 mL) was added to the sample solution to remove organic materials (Possibly present) and the sample was left for 24 hours.
- iii. The fine fractions were transferred to graduated cylinder (1000.0 mL) and few drops of NH_4OH were added to dissolve salts (if present).
- iv. Add acetic acid was then added to dissolve the carbonates (if present). Some of the upper turbid part of the solution was transferred to three glass slides and were left to dry at room temperature.
- v. The 1st glass slide was left without treatment; the 2nd glass slide was heated at 550°C for two hours, and finally the 3rd glass slide was placed in a glycerin bath until saturation. The three glass slides were finally subjected to X-ray diffraction technique to fully identify the clay minerals {(Montmoillonite, $\text{Al}_2(\text{OH})_2\text{Si}_4\text{O}_{10}$; Illite, $\text{K}_{0-2}\text{Al}_4(\text{Si}_{8-6}\text{Al}_{0-2})\text{O}_{20}(\text{OH})_4$ and Kaolinite, $\text{Al}_2\text{Si}_2\text{O}_5(\text{OH})_4$)} present.

Table 4.1. Represented major and trace constituents of bulk samples (1-3) from Khulays Formation (KH) [63]

Station	KH ₁			KH ₂							KH ₃	
	No.	1	2	3	F1	F2	P3	7	8	9	10	13
SiO ₂ %	54.7	57.3	51.7	75.7	51.6	51.6	45	49.2	65.6	51.1	51	51.1
Al ₂ O ₃	16.2	17.8	16.1	7.8	19	19	18	19.9	14.2	19	14.1	16.7
Fe ₂ O ₃	6.7	6.2	6.3	3.7	10.7	12.5	11.7	9.3	4.1	10	8.1	8.6
CaO	1.3	1.0	1.7	1.1	1.2	1	5.3	2.2	1.1	1	4.6	1.2
MgO	2.1	1.4	*2.1	1.1	1.4	1.4	1.7	1.8	1.2	1.3	1.4	1.8
K ₂ O	<0.5	0.5	<0.5	0.6	0.6	1.6	<0.5	<0.5	0.5	0.5	<0.5	<0.5
MnO	0.02	0.01	0.01	0.07	0.04	0.04	0.05	0.03	0.02	0.02	0.02	0.02
TiO ₂	1.14	1.11	1.1	0.62	1.27	1.28	1.14	1.27	0.87	1.25	0.87	0.96
P ₂ O ₅	0.125	0.061	0.297	0.076	0.289	0.205	0.551	0.215	0.051	0.101	0.061	0.158
Na ₂ O	1.8	0.95	2.1	1.44	0.81	0.77	0.8	0.88	0.81	0.86	1.17	1.51
SO ₃			<0.0	<0.0					<0.0	<0.0	<0.0	<0.0
	<0.05	<0.05	5	5	<0.05	<0.05	<0.05	<0.05	5	5	5	5
LiO.	15.22	13.7	17.5	7.35	13.22	12.4	15.83	15.54	11.22	14.62	17.93	17.19
Total	99.9	100.1	99.5	99.6	100.2	100.9	100.6	100.9	99.9	99.8	99.8	99.76

4.2.4 Preparation of clay packed column:

An accurate weight (0.4±0.02 g) of powdered clay mineral was packed in the glass columns (Fig.4.1) by applying the vacuum method of sorbent packing as described earlier [64] as follows: After introducing Cotton wool into the column by glass rod, clay powder was homogeneously packed in the column by applying gentle pressure with a glass rod to reduce the volume of the clay powder as much as

possible. During packing step, tap (1) in Fig (4.1) was connected to a suction pump, while tap (2) is closed to avoid air bubbles. After 20 min of evacuation, doubly distilled water was allowed to fill the column gradually through tap (2) while tap 1 is closed.

4.2.5 General batch experiments:

In a series of conical flasks (250 mL), an accurate weight ($0.2 \pm 0.001\text{g}$) of the clay mineral of sample 5 was mixed with an aqueous solution (200 mL) containing arsenic (III) at concentration level of $20 \mu\text{g mL}^{-1}$ at various pH (pH 2.2-11.4) using Britton-Robinson buffer and also with acetic acid acetate buffer (pH 2.2-5.7). The solutions were shaken for 60 min at $25 \pm 1^\circ \text{C}$ on a mechanical shaker. After phase separation, the aqueous phase was separated out by decantation and the concentrations of arsenic remained in the aqueous phase was determined with ICP-OES and I or ICP-MS (At concentrations below $1.0 \mu\text{g/mL}$). The concentration of arsenic (III) retained on the clay solid sorbent was determined from the difference between the concentration of arsenic (III) solution before (C_o) and after (C_a) shaking with the clay. The amount of arsenic (III) retained at equilibrium, q_e , the extraction percentage ($\% E$) and the distribution ratio (D) of the arsenic(III) uptake by the used clay were finally calculated, respectively employing the following equations, respectively:

$$q_e = \frac{(C_b - C_a) \times V}{W} \quad (4.1)$$

$$\%E = (C_o - C_a) / C_a \times 100 \quad (4.2)$$

$$\%E = 100D / D + (V / W) \quad (4.3)$$

$$D = \frac{\% E}{100 - \% E} \times \frac{V(ml)}{W(g)} \quad (4.4)$$

where, V is the sample volume in mL and W is the weight of the clay mineral in grams. Following these procedures, the effect of other parameters e.g. shaking time, temperature, and arsenic (III) concentration ($1.0 \times 10^{-4} - 20 \times 10^{-4} \text{ mol L}^{-1}$) on the arsenic (III) uptake was carried out. The extraction percentage, D , q_e , and the amount of arsenic (III) retained at time t (q_t) are the average of three independent measurements and the precision in most cases was $\pm 2\%$.

4.2.6. Flow experiments:

4.2.6.1 Retention and recovery of arsenic (III)

In aqueous solution (0.1 L) spiked with arsenic(III) at concentration ($20 \mu\text{g/m}$) at pH 6-7 and was percolated through the $\text{THA}^+.\text{Br}^-$ or PUFs ($0.40 \pm 0.01\text{g}$) packed columns at $2\text{-}3 \text{ mL min}^{-1}$ flow rate. A blank experiment was also carried out in the absence of arsenic (III) ions. The sample and the blank clay packed columns were then washed with 100 mL of an aqueous solution. Complete retention of arsenic (III) ions took place as indicated from ICP-OES analysis of arsenic species in the effluent. Complete recovery of arsenic from clay packed column was achieved by percolating HNO_3 (10 mL, 1.0 mol L^{-1}) at 5 mL min^{-1} flow rate. Equal fractions of the eluate were then collected and analyzed for arsenic. The height equivalent to theoretical plates (HETP) and the plate numbers (N) were calculated from the output of the

chromatograms. The HETP and N were also determined from the breakthrough capacity experiments of arsenic(III) species at $\mu\text{g/ml}$ under the optimum conditions of arsenic (III) retention.

4.2.6.2. Extraction procedures of arsenic (V) species

Arsenic (V) was successfully reduced to arsenic (III) following the work reported [65]. In this experiment, an accurate weight (0.05 g) of sodium arsenate was allowed to react with an approximate weight (0.1 g) of sodium sulfite in the presence of hydrochloric acid (2.0 mol L^{-1}). The solution was then allowed to boil for 30 min to release all unreacted sulfur dioxide and left to cool. The solution was finally diluted with de ionized water and quantitatively transferred to volumetric flask. Different concentrations ($5.0\text{-}15\mu\text{g mL}^{-1}$) were transferred to the conical flask (50 mL capacity) were adjusted to pH 6-7 and percolated through clay packed column as described for As(III) retention. The retained arsenic (III) species was then recovered with HNO_3 (10 mL, 1.0 mol L^{-1}) at 5 mL min^{-1} flow rate. The concentration of the produced arsenic ions was then determined with ICP-OES using calibration curve of arsenic.

4.2.7. Analytical applications:

4.2.7.1. Analysis of arsenic(III) in tap and wastewater samples

Tap and/ or industrial wastewater samples (0.1 - 1.0 L) were collected, filtered through a $0.45 \mu\text{m}$ membrane filter and the solutions pH were adjusted to pH 6-7. To each sample solution an accurate concentration of arsenic (III) species at the concentration range $5.0\text{-}25.0 \mu\text{g L}^{-1}$ was added. The samples solutions were percolated through clay packed columns at 5 ml min^{-1} flow rate. Complete sorption

of arsenic (III) ions was achieved as indicated from the analysis of As in the effluent solutions. The retained arsenic species was then recovered quantitatively with nitric acid (10 mL, 1.0 mol L⁻¹) at 5 mL min⁻¹ flow rate as noticed from analysis of eluate by ICP-OES.

2.7.2 Analysis of arsenic (V) in tap and wastewater samples

Tap and/ or industrial wastewater samples (0.1 - 1.0 L) were collected and filtered through a 0.45 µm membrane filter as described before. The sample solutions were then spiked with different concentrations (5.0-25.0 µg L⁻¹) of NaAsO₃. The sample solutions were then reduced to arsenic(III) as described in section 4.2.6.2. The pH of the solutions was then adjusted to optimum pH and the sample solutions were then percolated through clay packed columns at 5 mL min⁻¹ flow rate. Complete sorption of arsenic(III) ions was achieved as indicated from the analysis of As in the effluent. The retained arsenic species was then recovered quantitatively with nitric acid (10 mL, 1.0 mol L⁻¹) at 5 mL min⁻¹ flow rate.

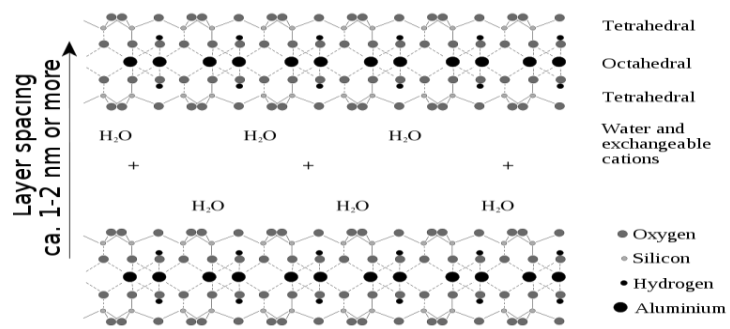
2.7.3. Recovery and determination of total inorganic arsenic(III & V) in water samples

Aqueous solutions (100 mL) containing the binary mixture of arsenic (III) & (VI) species at a total concentration ≤10 µg/mL were totally reduced to arsenic(III) with Na₂SO₃-HCl and heating for 15 min. The solutions were then percolated through clay packed column at 5 mL min⁻¹ flow rate at pH 6-7. Complete sorption of arsenic species took place as indicated from analysis of As in the effluent solution. The retained arsenic species were then recovered quantitatively with HNO₃ (1.0 mol L⁻¹) at 3.0 mL min⁻¹ flow rate and analyzed by ICP-OES.

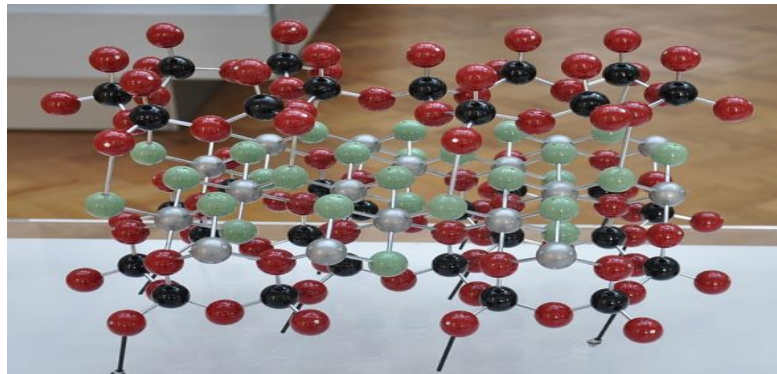
4.3. Results and discussion

4.3.1 Characterization of clay minerals

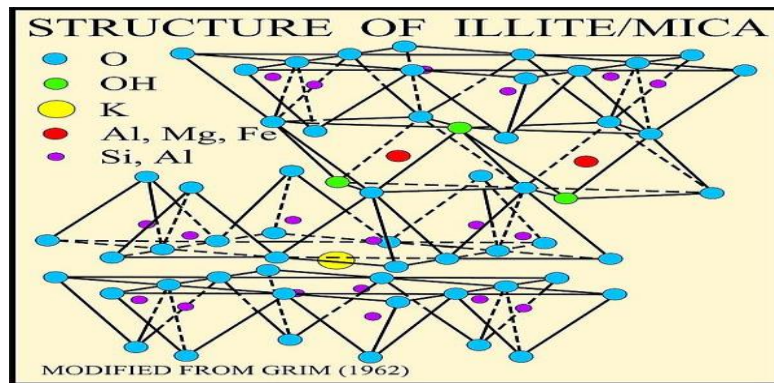
Clay deposits vary from one area to another area and they are mainly composed of clay minerals namely montmorillonite (I), kaolinite (II) with minor illite (III) (Fig. 4.6) in addition to some percentages from chlorite, calcite and quartz. Thus, five bulk samples representing the different clayey beds were collected from the face of Al-Khayat quarry which is located to the North of Khulays village (Fig. 4.1). Preliminary study on bulk samples were carried out by taking few grams of each bulk sample and pulverizing them in an agate mortar. The samples were mounted on a glass slide and analyzed by XRD to identify the clay minerals present. XRD patterns of the five samples are shown in Figs. 4.7-4.11. The results of XRD patterns of the samples revealed that, the samples consist mainly of quartz (major), montmorillonite (I) (trace), kaolinite (II) (minor), and illite (rare) (Fig. 4.11). On the other hand, samples 3 & 5 are disintegrated easily and are rich in clay fractions compared to other bulk samples 1, 2 and 4. Thus, detailed identification of clay fractions of samples 3 & 5 was carried out by XRD. The XRD patterns of clay fractions of untreated and treated clay minerals of samples 3 & 5 are demonstrated in Figs. 4.12 and 4.13. The XRD patterns show that the relative abundance of the clay minerals montmorillonite (minor), Kaolinite (II) (major) and illite (trace) are noticed in clay fractions. Thus, in the subsequent work clay minerals of sample 3 was selected for chemical separation and determination of traces of arsenic.



I



II



III

Fig. 4. 6 Chemical structures of clay minerals (Montmorillonite (I), Kaolinite (II) and illite (III)).

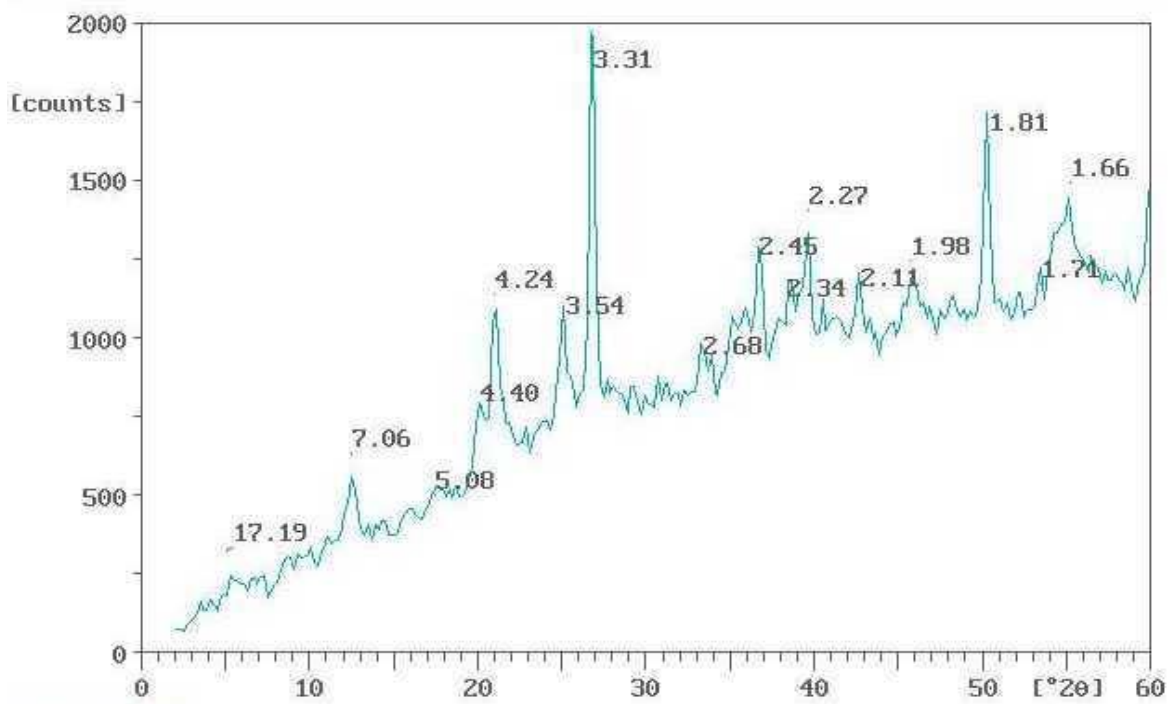


Fig.4.7 XRD pattern of bulk sample number 1.

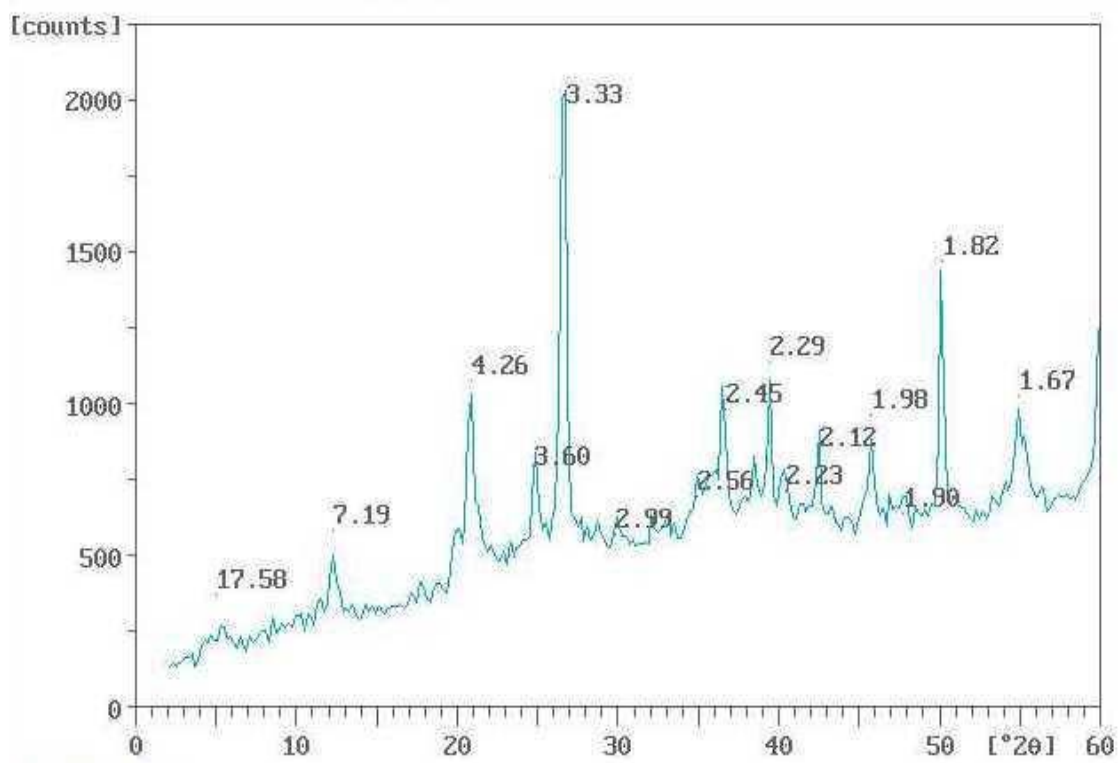


Fig.4.8 XRD pattern of bulk sample number 2.

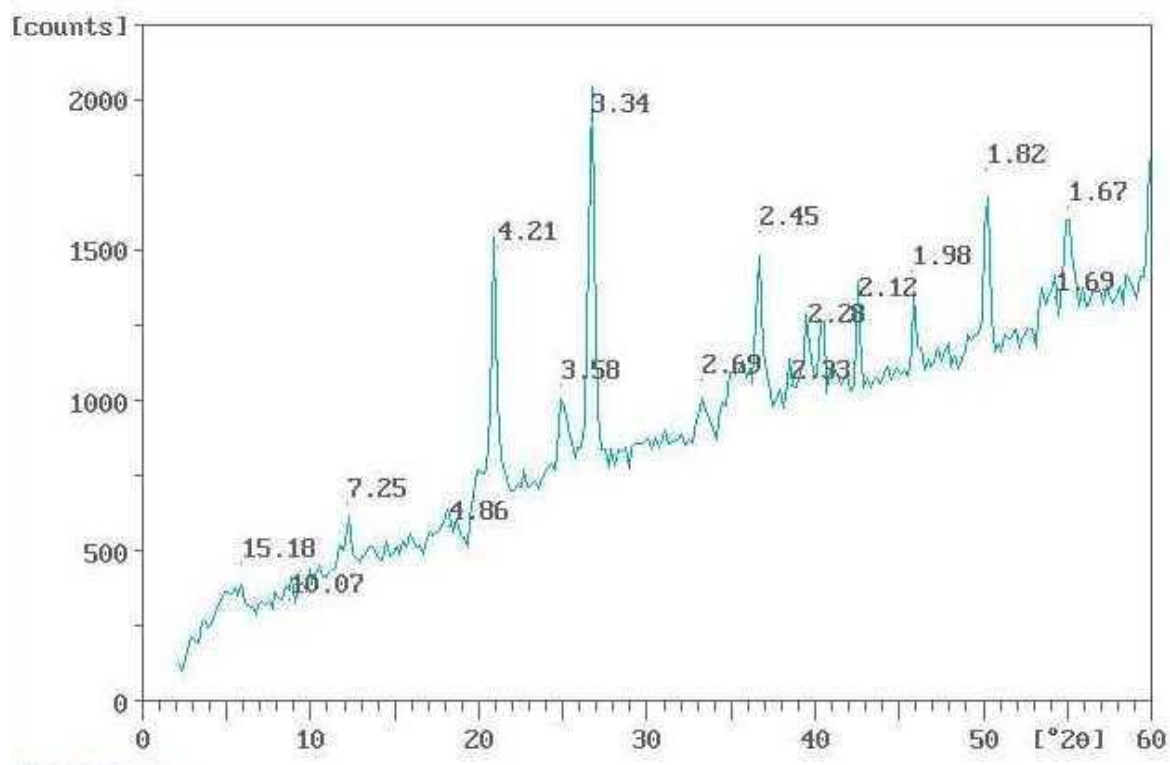


Fig.4.9 XRD pattern of bulk sample number 3.

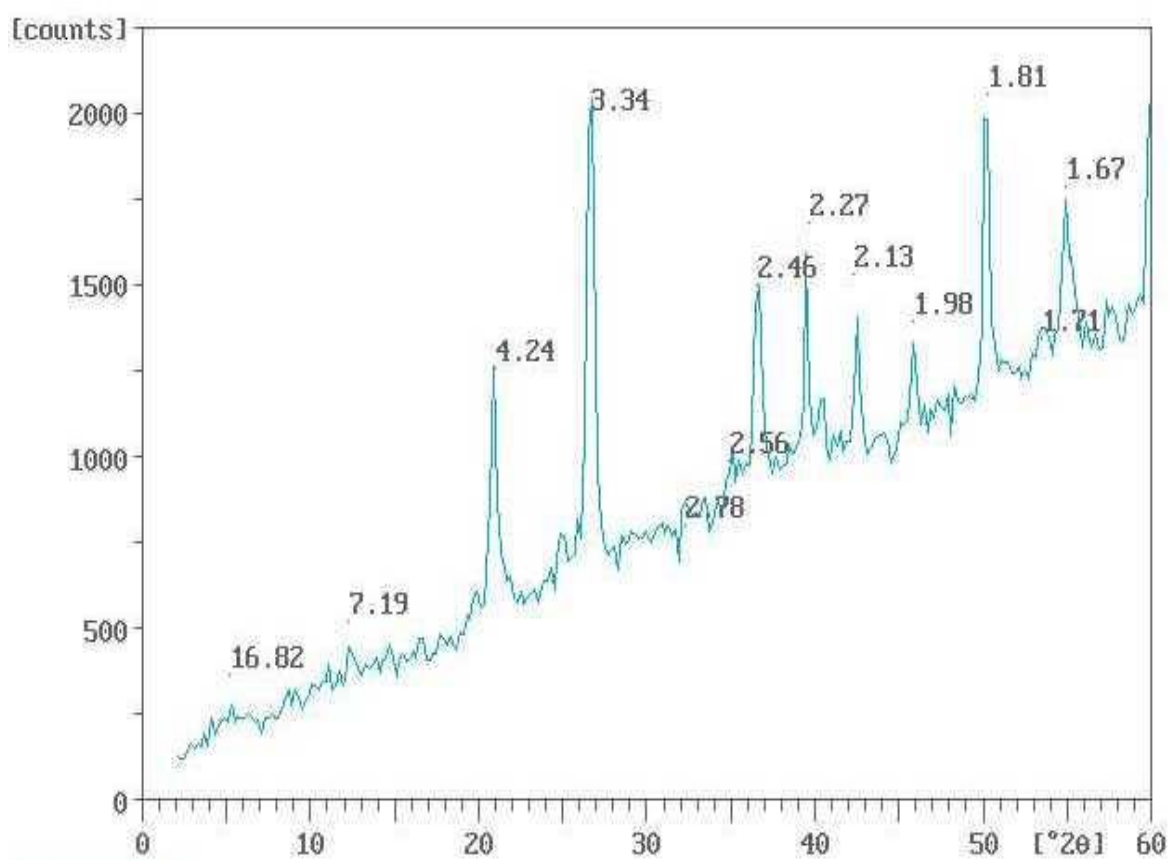


Fig.4.10. XRD pattern of bulk sample number 4.

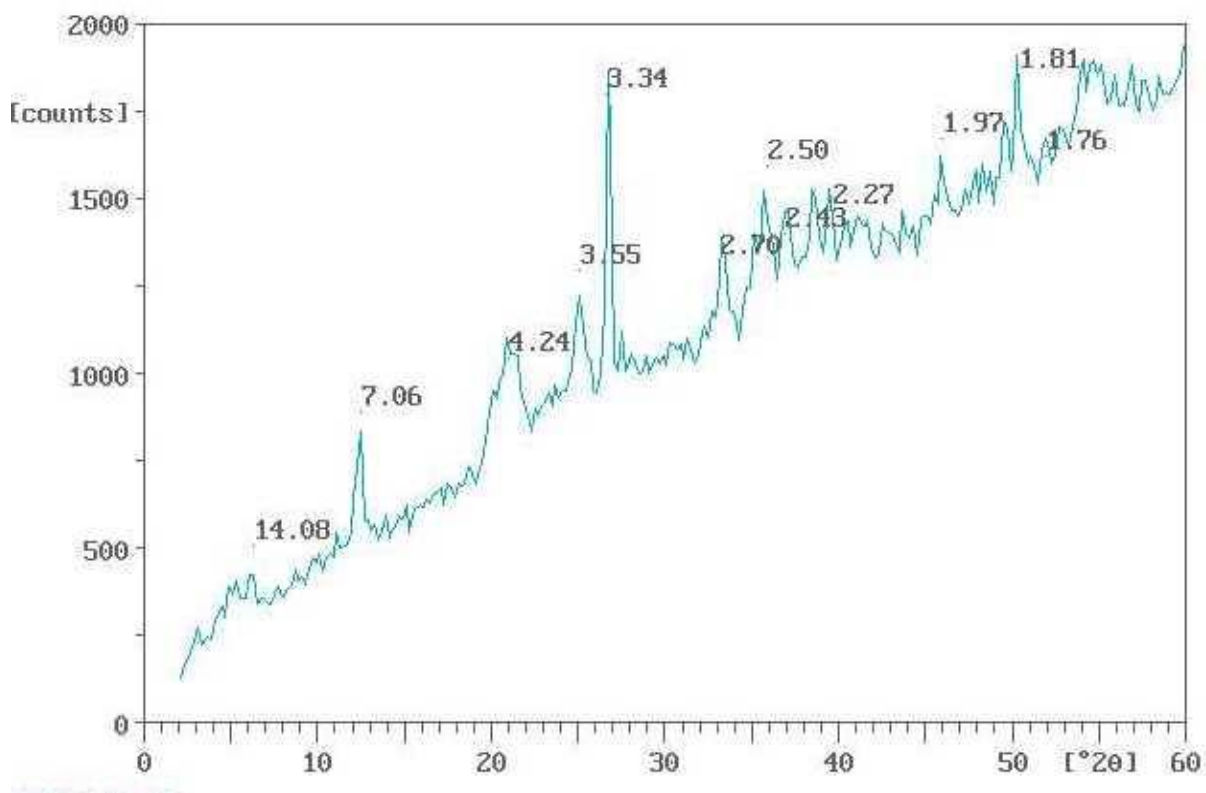


Fig.4.11. XRD pattern of bulk sample number 5.

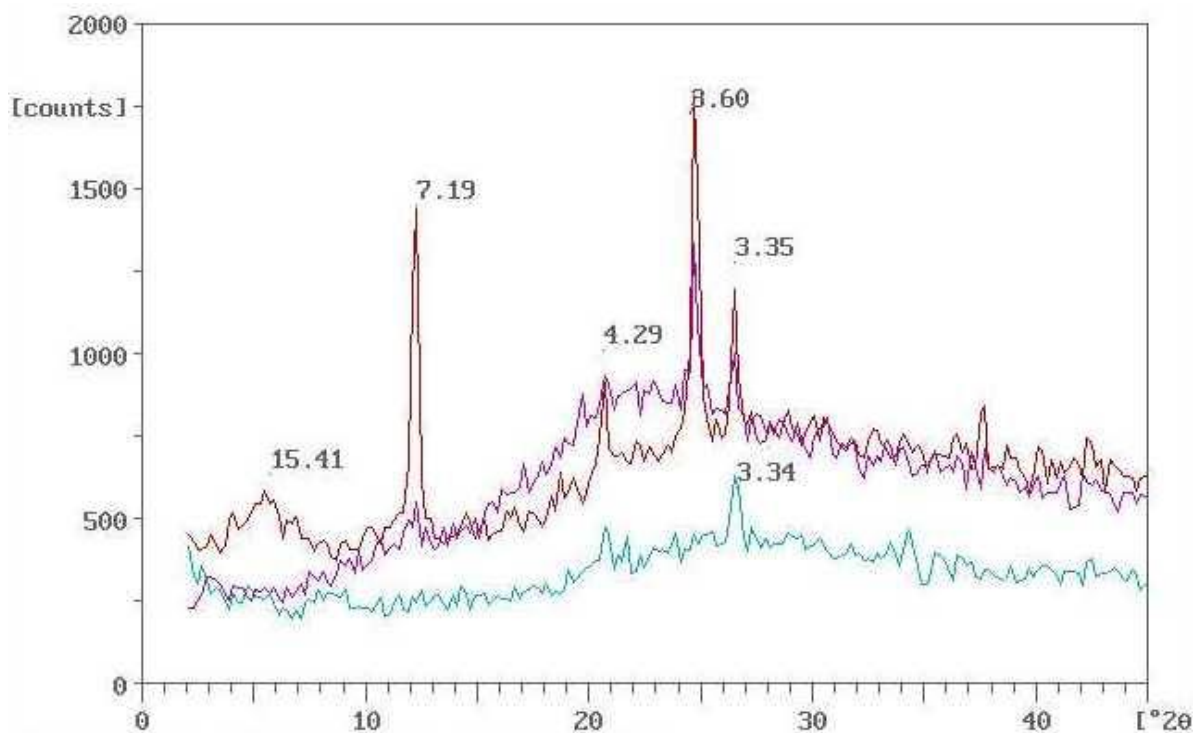


Fig.4.12. XRD pattern of untreated (Red); glycolated (Violet) and heated sample 3 at 550 °C (Green).

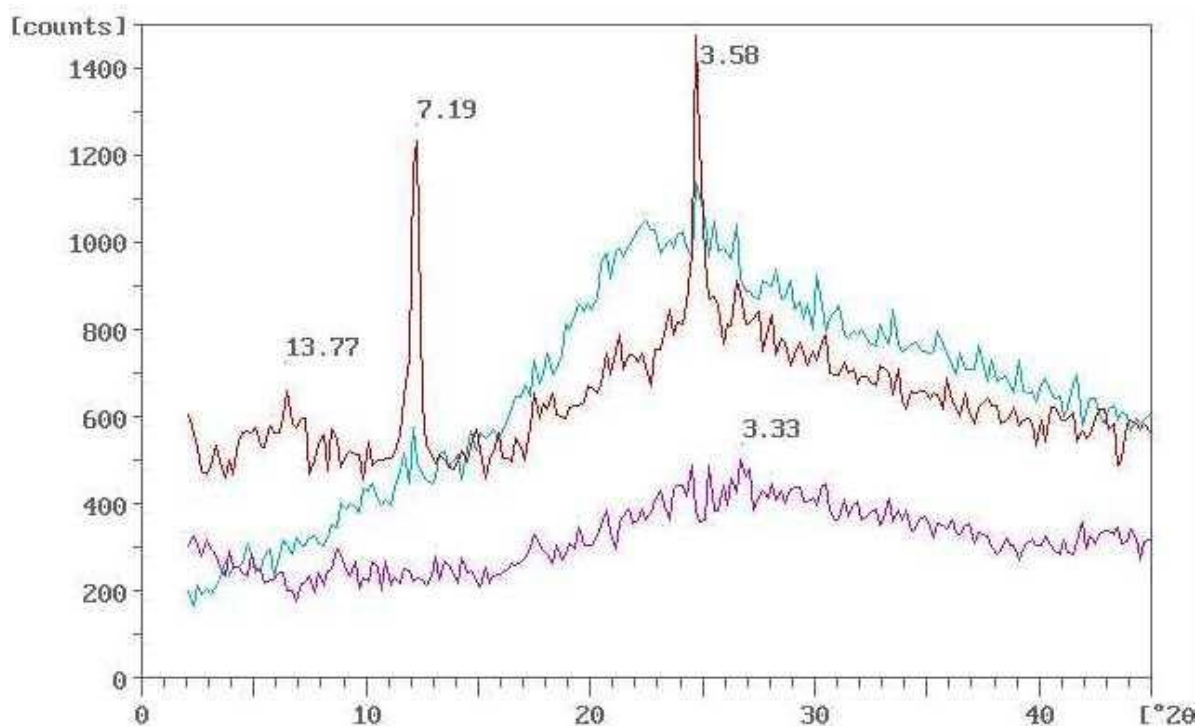


Fig.4.13. XRD pattern of untreated (Red); glycolated (Violet) and heated sample5 at 550 °C (Green).

4.3.2. Retention profile of arsenic(III) on local clay minerals

The development of a suitable pre concentration and separation procedures for subsequent determination of traces and ultra traces of arsenic (III) in industrial wastewater and / or natural water samples are becoming increasingly important [42, 65]. The most commonly methods used for arsenic determination are based upon spectrometric after liquid-liquid and / or solid phase extraction procedures with expensive solid sorbents. Thus, recent years have seen considerable progress on developing sorbent for effective separation of arsenic such as clay minerals [42]. Clay minerals e.g. mont - mor illonite, kaolinite, with minor illite (Fig. 4.6) concentrate inorganic and organic substances from different media by the phase distribution mechanism rather than adsorption [42].

The chemical structure of the clay minerals together with the efficient ion exchange properties offer higher concentrating ability and flow rate compared with other solid supports. Sorption preconcentration under static and dynamic conditions is particularly attractive because of its speed, easily be controlled and high preconcentration coefficients per unit time. Preliminary investigations have shown that, clay minerals retained considerable amount of arsenic (III) species from aqueous media. Clay minerals combines both the advantages of rapidity of kinetic process and selectivity for sorption of arsenic(III) from the aqueous phase. Thus, the analytical utility of such processes for the separation, chemical speciation and sequential determination of total inorganic arsenic(III) & (V) was critically investigated in the subsequent sections in more details using batch and flow modes of separation.

The amount of arsenic (III) ions extracted from the aqueous solution by clay minerals was found to depend on the aqueous solution pH. Thus, the sorption profile of arsenic (III) ($20\mu\text{g mL}^{-1}$) from the test aqueous solutions at different pH by clay ($0.2 \pm 0.01\text{g}$) was critically investigated employing Britton-Robinson (B-R) buffer (pH 2-11) .After shaking the test solutions with clay for 1.0 h, the amount of arsenic(III) remained in the aqueous solution was then measured via ICP-OES at the optimum operational parameters. The uptake percentage (%E) of arsenic (III) species from the aqueous solution onto the clay sorbent was then calculated by difference between arsenic concentration in the aqueous solution before and after extraction employing equation 4.2. Representative results are shown Fig. 4. 14. The sorption profile of arsenic (III) by clay minerals slightly increased on increasing the solution pH and reached maximum at pH 6-7 and decreased progressively on raising the solution pH. The observed decrease on the arsenic(III) uptake at $\text{pH} \geq 7$ is most likely attributed to the

instability or the hydrolysis of the produced complex species formed between arsenic (III) complex species and the sorbent and subsequent hydrolysis.

In acidic $\text{pH} \leq 6$, the uptake of arsenic(III) species was low by the solid sorbents. This behavior is most likely attributed to the occurrence of arsenic(III) species as anionic complex species $[\text{AsCl}_4]^-$ which minimizes the performance of the sorbent to act as good cation ion exchange. Similar retention profile for the extraction of aurocyanide ion-pairs with alkali metal ions into long chain poly ethers has been reported [66, 67]. The change of the environment around arsenic(III) ions and the available binding sites of the clay became more hydrophilic. These two factors are most likely to diminish the need for solvating water molecules and reduce the arsenic (III) uptake onto the sorbent. Thus, in the subsequent work solution pH was adopted at pH 6-7.

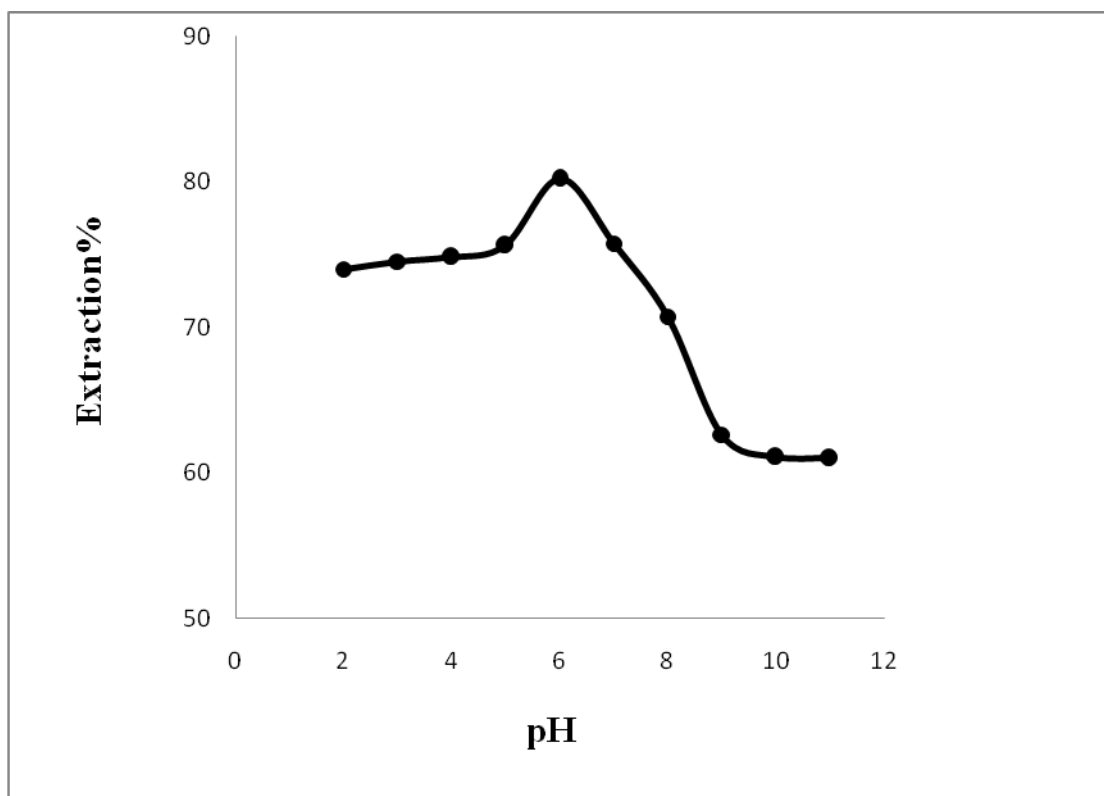


Fig . 4. 14 .Effect of pH on the sorption percentage of arsenic(III) from the aqueous solutions onto clay minerals at 25 ± 1 °C after 1 h shaking time.

The influence of shaking time (0- 100 min) on the separation of arsenic (III) from the aqueous media of pH 6-7 was carried out by clay sorbent. The results are summarized in Fig. 4.15. The extraction was found fast in the beginning up to 20 min, followed a first-order rate equation. The overall equilibrium of arsenic(III) retention onto the sorbents was attained in ~80 min (Fig. 4.15) and the uptake percentage (E) and D of arsenic (III) retention onto clay sorbent were better than that obtained by other solid sorbent. The half-life time ($t_{1/2}$) of the equilibrium sorption of arsenic (III) as calculated from the plot of $\ln C/C_0$ versus time (Fig.4.16) onto the sorbent from the aqueous media to reach 50% saturation of the sorption capacity was found in the range 3.9 ± 0.2 min . The sorption of arsenic (III) ions was fast within the first 25 min and slightly increased up to a constant value less than 80 min shaking time of both sorbents towards arsenic (III) retention. Thus, a shaking time of 80 min was adopted in subsequent experiments.

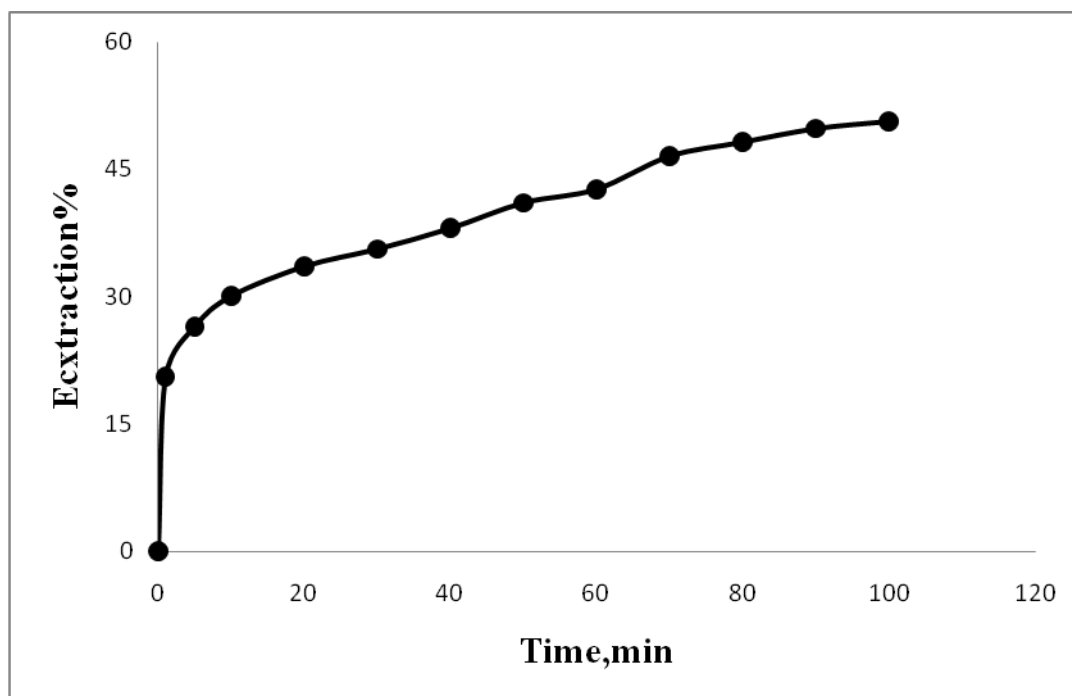


Fig . 4. 15 Influence of shaking time on the percentage uptake (%) of arsenic (III) from the aqueous solutions at pH 6-7 onto clay minerals at 25 ± 1 °C.

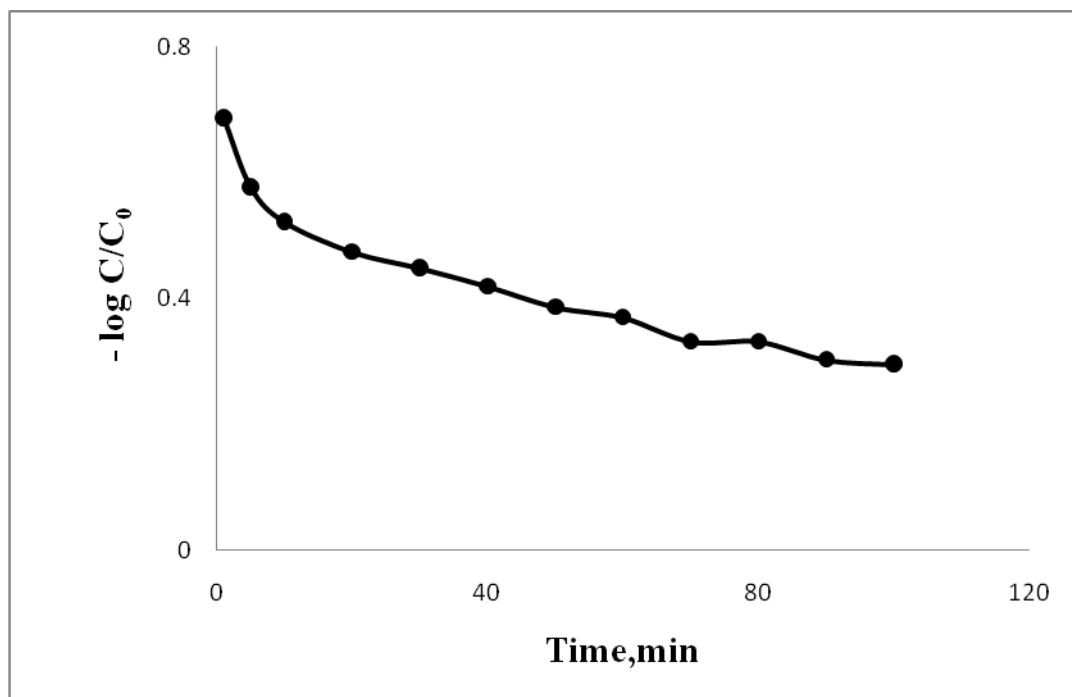


Fig . 4. 16 Rate of arsenic(III) retention from the test aqueous solution of pH 6-7 onto clay minerals at 25 ± 1 °C.

The effect of the sorbent doze (w) and batch factor (v/w) on the arsenic (III) retention at $10 \mu\text{g mL}^{-1}$ onto clay sorbent was investigated. The uptake of arsenic increased on increasing the sorbent doze up to 0.2g of the sorbent. Therefore, in the subsequent work, $0.2 \pm 0.03\text{g}$ of the solid sorbents was adopted. The sorption percentage of arsenic (III) onto the sorbent decreased up to $45.4 \pm 2.7\%$ and $55 \pm 3.6\%$, respectively on increasing the sample volume from 100.0 mL to 1000 mL.

4.3.3 Kinetic behavior of arsenic (III) sorption onto local clay sorbent

The sorption of arsenic (III) ions onto clay mineral sorbent was fast and the equilibrium was attained a constant value within 80 min shaking time (Fig. 4. 15). This conclusion was supported by the value of $t_{1/2} = 3.9 \pm 0.2$ min of arsenic (III) sorption by the clay sorbent. Thus, gel diffusion is not only the rate-controlling step for both sorbents as in the case of common ion exchange resins [69]. Therefore, the kinetic behavior of arsenic (III) sorption onto clay sorbent depends on film diffusion and intraparticle diffusion, and the more rapid one will control the overall rate of transport. Hence, the retained arsenic (III) species onto the used solid sorbent was subjected to Weber – Morris model [70, 71]:

$$q_t = R_d (t)^{1/2} \quad (4.5)$$

where, R_d is the rate constant of intra-particle transport in mmol g^{-1} and q_t is the sorbed arsenic(III) concentration (mmol.g^{-1}) at time t . Representative results are shown in Fig.4. 17. The plot of q_t vs. time was found linear ($R^2=0.975- 0.980$) in arsenic (III) retention onto the clay sorbent up to 25.3 ± 1.1 min and deviate on increasing the shaking time. In the initial stage, the diffusion rate was found high and decreased on passage of time indicating that the rate of the retention step is film diffusion at the early stage of extraction [72, 73]. The values of R_d computed from the two distinct slopes of the Weber- Morris plots for the unloaded clay were found equal $0.703 \pm 0.03 \text{ mmol g}^{-1}$ with $R^2 = 0.998$ towards arsenic (III) in the initial stage up to 25.3 min of agitation time and reduced beyond time higher than 30 min, respectively. The change in the slope for the clay mineral is most likely due to the existence of different pore sizes [73]. The R_d value indicated that intra-particle diffusion step can be considered as the rate controlling step. The line does not pass

through the origin confirming particle film diffusion along with intra-particle diffusion [72, 73].

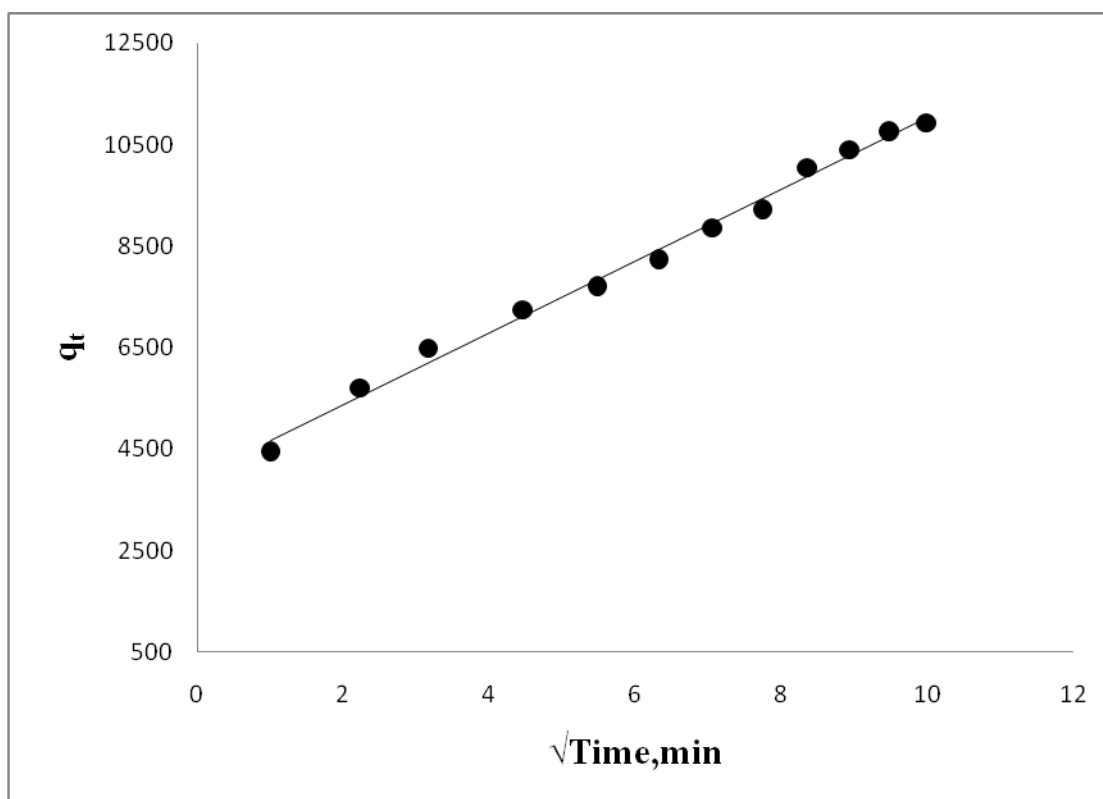


Fig. 4. 17 Weber-Morris plots of the sorbed arsenic(III) concentration from aqueous solution of pH 6-7 vs. square root of shaking time onto clay minerals at 25 ± 1 °C .

Moreover, the rate constant for the retention step of arsenic (III) retention onto the tested solid sorbent was also evaluated in the light of Lagergren rate equation [74]:

$$\log(q_e - q_t) = \log q_e - \frac{K_{Lager}}{2.303} t \quad (4. 6)$$

where, q_e is the amount of arsenic (III) sorbed at equilibrium per unite mass of sorbent (mmol.g^{-1}) and k_{Lager} is the first order overall rate constant for the retention process, s^{-1} and t = time, s. The plot of $\log (q_e - q_t)$ vs. time was linear (Fig. 4. 18) with a correlation coefficient (R^2) of 0.90. The value of K_{lager} calculated from the slope was found 3.3 s^{-1} for clay minerals towards sorption of arsenic. These data suggested first

order kinetics for arsenic (III) retention towards the used sorbent. On the other hand, the influence of adsorbate concentration on the values of K_{lager} was investigated. The value of k_{lager} increased on increasing adsorbate concentration confirming formation of monolayer arsenic (III) species onto the surface of the used adsorbent as well as the first order kinetic nature of the retention processes [74]:

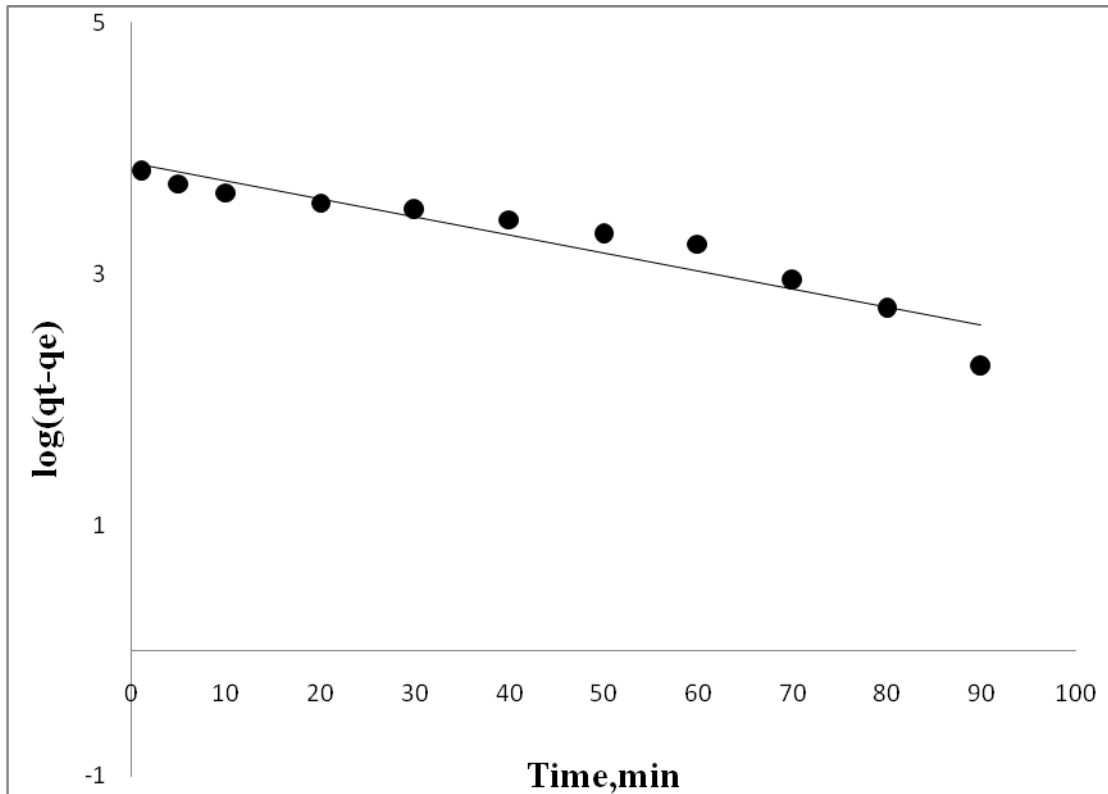


Fig. 4. 18 Lagergren plot of the kinetics of arsenic (III) sorption from the aqueous solution of pH 6-7 onto unlo clay minerals at $25 \pm 0.1^\circ\text{C}$.

In the light of Lagergren kinetic model, the results were further confirmed by Bhattacharya- Venkobachar kinetic model [75, 76]:

$$\log_{10}(1-u_{(t)}) = \frac{-K_{Bhatt}}{2.303} t \quad (4.7)$$

where, $u(t) = \frac{C_o - C_t}{C_o - C_e}$, K_{Bhatt} = overall rate constant, s^{-1} , t = time, s, C_o =

concentration of the metal ion at time t mg L^{-1} , C_e = concentration of the arsenic(III) at equilibrium, mg L^{-1} . Plot of $\log(1 - u_t)$ vs. time for clay sorbent is demonstrated in Fig.

4. 19. Based on this model, the value of K_{Bhatt} at the optimum conditions of arsenic(III) retention from aqueous solution of pH 6-7 on to the clay sorbent was $2.95 \pm 0.1 \text{ s}^{-1}$.

The value is close to the value deduced from Lagergren model confirming first order kinetics for arsenic retention towards clay sorbent. Thus, the overall uptake of arsenic(III) onto the used sorbent is most likely involved three steps: i- bulk transport of arsenic species in solution, ii-film transfer involving diffusion of arsenic ions within the pore volume of the clay minerals and/or along the pore wall surface to the active sorption sites of the sorbent and finally iii- exchange between arsenic(III) complex ion with the counter of the clay sorbent. Therefore, the actual sorption of arsenic onto the interior surface is rapid and hence it is not the rate determining step in the sorption process. Thus, one may conclude that, film and intra-particle transport might be the two main steps controlling the sorption step. Thus, "solvent extraction" or a "weak base ion exchanger" mechanism is not only the most probable participating mechanisms and most likely, some other processes like specific sites on the clay minerals are possibly involved simultaneously in the arsenic (III) retention from the bulk aqueous solution on the tested the solid sorbent.

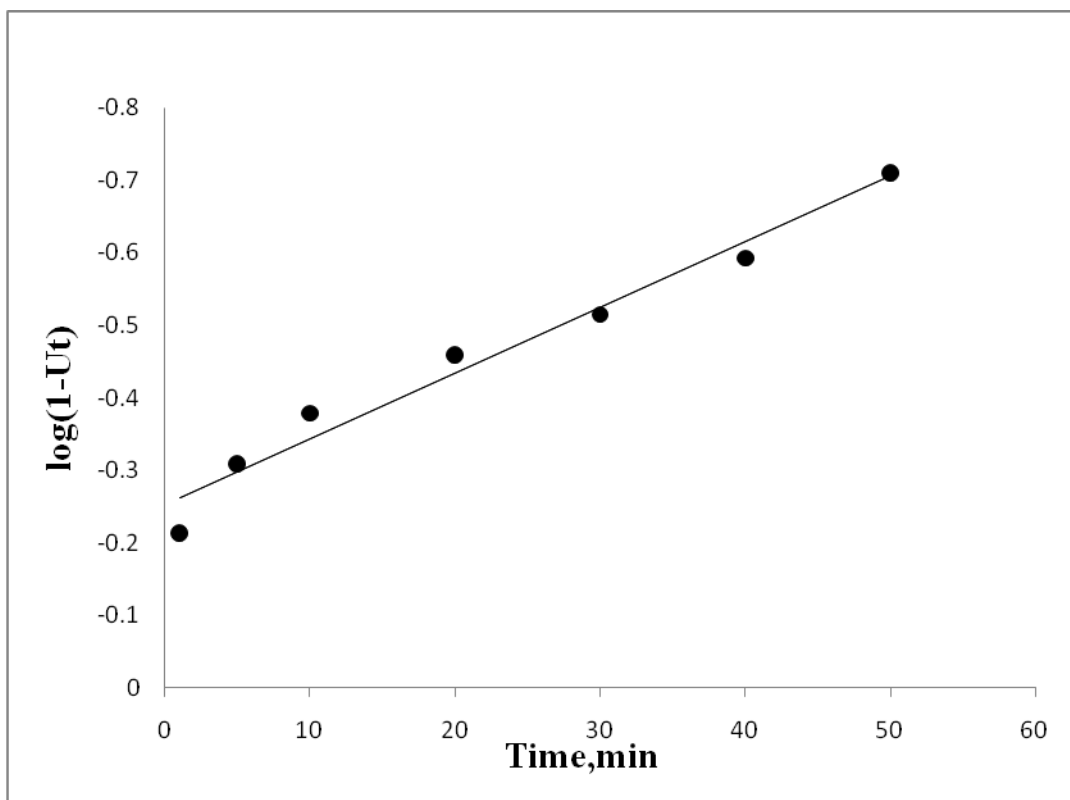


Fig. 4.19. Bhattacharya- Venkobachar plots of arsenic(III) uptake from aqueous solution of pH 6-7 onto clay sorbent at $25\pm 0.1^\circ\text{C}$.

4.3.4 Sorption isotherms of arsenic(III) species onto clay sorbent

The sorption characteristics of arsenic (III) over a wide range of equilibrium concentrations $10.0\text{-}100\ \mu\text{g mL}^{-1}$ from the aqueous solution of pH 6-7 onto the clay sorbent was studied. The plots of the amount of arsenic(III) ions retained onto the sorbent vs. their equilibrium concentrations in the bulk aqueous solution are shown in Fig. 4. 20. The data revealed that, at low or moderate analyte concentration, the amount of arsenic retained on the sorbent varied linearly with the amount of arsenic remained in the bulk aqueous solution. The equilibrium was also approached only from the direction that of arsenic (III) ions rich aqueous phase confirming first-order sorption kinetics of

the sorption step. A relatively reasonable sorption capacity of arsenic(III) ions towards clay sorbent as predicted from the sorption isotherm was found greater than $78.4 \pm 0.7 \text{ mg g}^{-1}$ of clay sorbent.

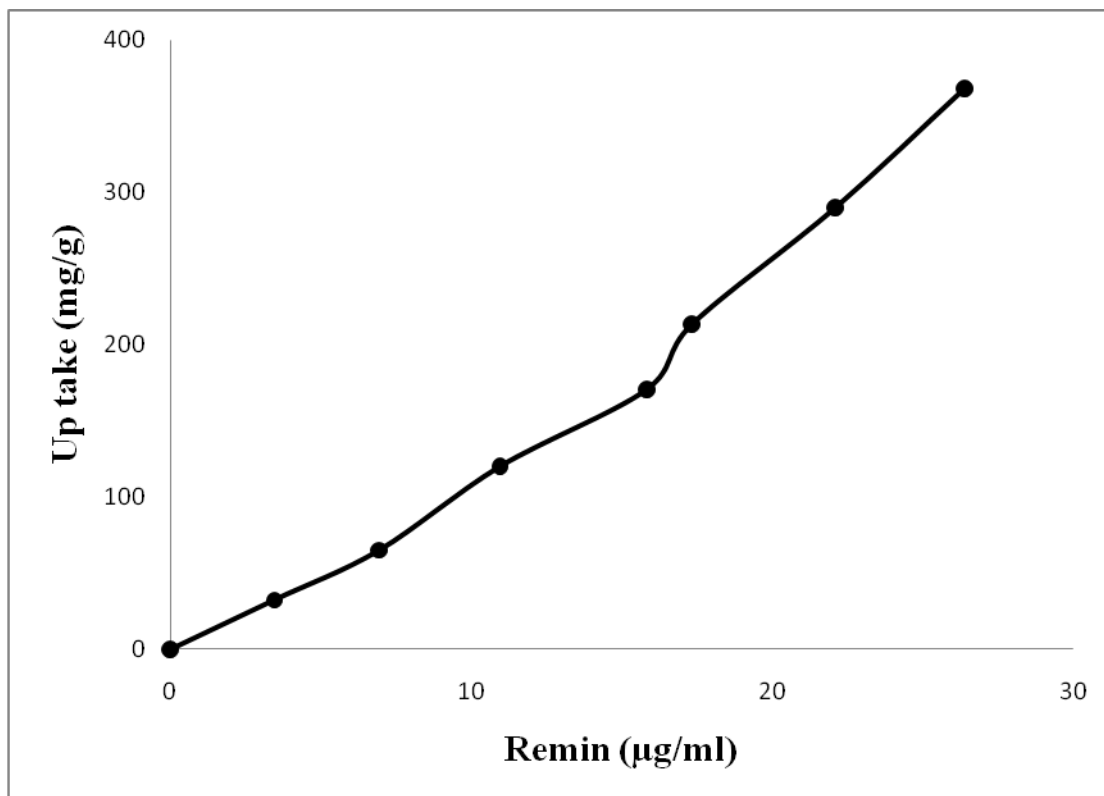


Fig.4.20 Sorption isotherms of arsenic (III) uptake from the aqueous solution of pH 6-7 onto clay sorbent at $25 \pm 0.1^\circ\text{C}$.

The most favorable distribution ratio (D) of arsenic (III) retention onto the used sorbents was achieved from diluted (10-100 µg/mL) solutions of arsenic.

On increasing arsenic concentration from 10µg/mL to 100 µg/mL of arsenic, the value of D increased from 2070 to 3066.7 mL/g (Fig. 4. 21). The fact that, clay minerals montmorillonite, kaolinite and illite (Fig. 4.6) contain large number of accessible active sites and many pores in their chemical structure (Fig. 4.6) [76, 77]. Therefore, in the sorption steps of arsenic(III) from the aqueous solution diffusion of the solute through a hypothetical film or hydrodynamic boundary layer took and both

intra-particle transport and the film diffusion may be the tow steps controlling the molecular diffusion at the macro pores of the sorbent [76, 77].

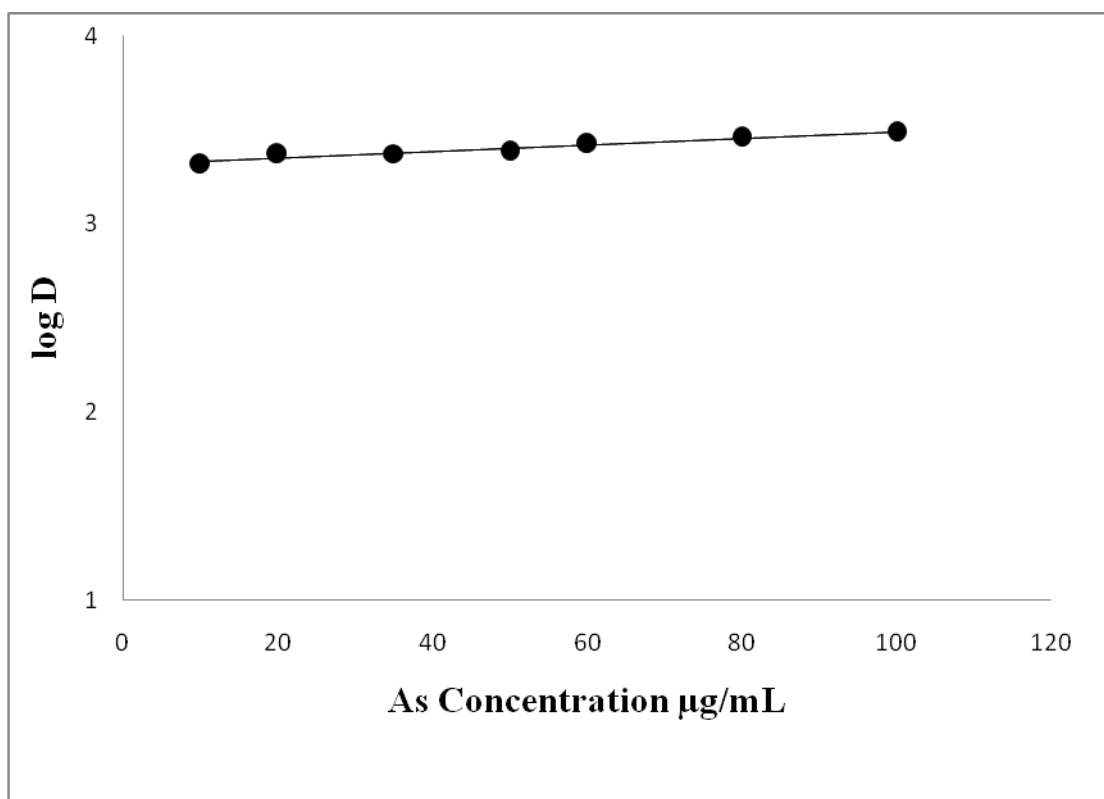


Fig.4.21 Plot of D of arsenic sorption vs. As concentration in the bulk aqueous solutions of pH 6-7 onto clay minerals at $25\pm 0.1^\circ\text{C}$.

The retention profile of arsenic(III) from the aqueous solution onto the used sorbents was subjected to Freundlich, Langmuir and Dubinin-Radushkevich (D-R) isotherm models [76] over a wide range of equilibrium concentration through linear regression in a condition of best fit.

The Freundlich model [78] is expressed in the following form:

$$\log C_{ads} = \log A + \frac{1}{n} \log C_e \quad (4.8)$$

where, A and $\frac{1}{n}$ are Freundlich parameters related to the maximum sorption capacity of solute (mol g^{-1}) and C_{ads} is the sorbed arsenic (III) concentration onto the per unit

mass of the clay sorbent (mol g^{-1}) at equilibrium. Plot of $\log C_{\text{ads}}$ vs. $\log C_e$ (Fig.4.22) for the arsenic (III) retention onto clay was linear ($R^2=0.994$) over the entire concentration range of the analyte indicating a better fit for the experimental data. The Freundlich sorption isotherm encompasses the heterogeneity of the surface and exponential distribution of the sites and their energies. The characteristics Freundlich constants $\log A$ and $1/n$ computed from the intercept and slope of the linear plot (Fig. 4.22) were found equal $31.78 \pm 0.1 \text{ mmol.g}^{-1}$ and 0.87 for arsenic sorption onto clay sorbent, respectively. The value of $1/n < 1$ indicates favorable sorption of arsenic (III) onto clay sorbent. The sorption capacity is slightly reduced at lower equilibrium concentration and the isotherm does not predict any saturation of the clay by the adsorbate. Thus, infinite surface coverage is predicted mathematically and physisorption on the surface of the both sorbents is expected.

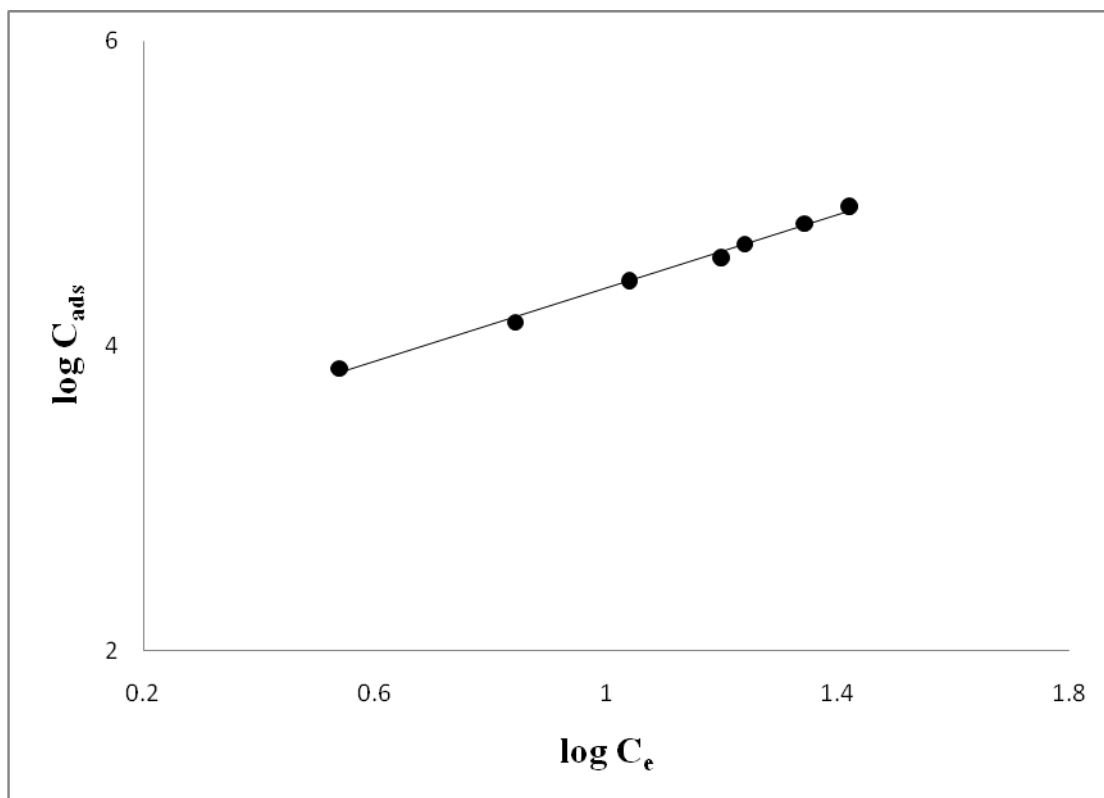


Fig.4.22 Freundlich sorption isotherm of arsenic(III) retention from the aqueous solution of pH 6-7 onto clay minerals at 25±0.1°C.

The results were also subjected to Langmuir isotherm model [79]. This model in the aqueous phase is expressed by the following linearized equation [79]:

$$\frac{C_e}{C_{ads}} = \frac{1}{Qb} + \frac{C_e}{Q} \quad (4.9)$$

where, C_e and C_{ads} are the concentration of sorbate (mmol L^{-1}) in solution and at the sorbent surface at equilibrium, Q is the Langmuir parameter related to maximum adsorption capacity of solute per unite mass of adsorbent required for monolayer coverage of the sorbent surface and b represents the binding energy of solute sorption that is independent of temperature, respectively. The Langmuir isotherm assumes that, ions are sorbed on definite sites that are monoenergetic on the sorbent surface and each site can accommodate only one molecule or ion and the sorbed ions cannot

migrate across the surface or interact with neighboring ions or molecules. The plot of C_e / C_{ads} vs. C_e over the entire range was linear (Fig. 4.23) ($R^2 = 0.9853$) confirming that, the adsorption characteristics of arsenic onto clay sorbent obeyed Langmuir model which represents the presence of monolayer adsorption. The maximum adsorption capacity parameters (Q) and the Langmuir constant (b) evaluated from the slope and intercept of Langmuir plot (Fig. 4. 23) were found equal $320.06 \mu\text{mol.g}^{-1}$ and $0.439 \pm 0.012 \text{ L}/\mu\text{mol}$, respectively. These data indicate that, the surface of the clay sorbent posses good mass transfer which facilitating diffusion of arsenic to the bulk of the binding sites. Thus, an added component for "surface adsorption participates in the arsenic (III) uptake.

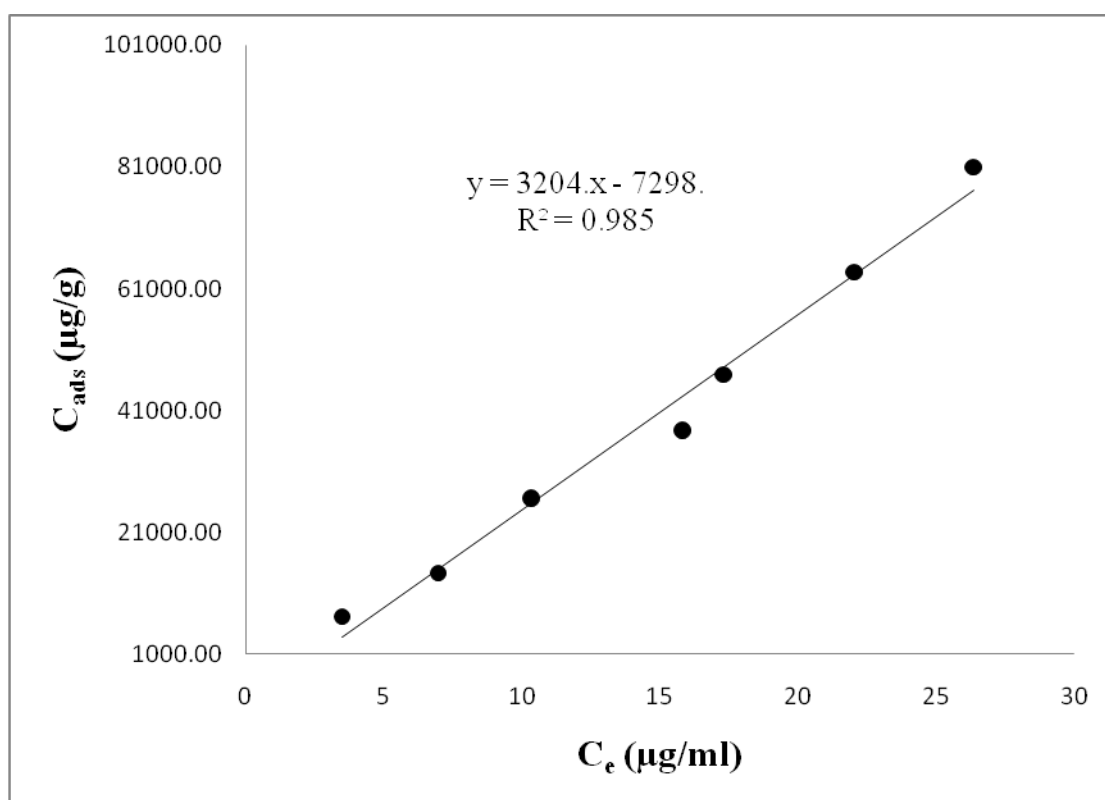


Fig.4.23 Langmuir sorption isotherms of arsenic(III) uptake from the aqueous solutions of pH 6-7 onto clay sorbent at $25 \pm 0.1^\circ\text{C}$.

Assuming the surface of the clay sorbent is heterogeneous and an approximation to a Langumir isotherm model is chosen as a local isotherm for all sites that energetically equivalent, the quantity β can be related to the mean free energy (E) of the transfers of one mole of arsenic from infinity to the clay surface. This quantity can be expressed by the equation.

$$E = 1/ \sqrt{-2} \beta \quad (4.10)$$

The value of E was found in range of 0.8 ± 0.07 kJ/mol for arsenic towards clay sorbent. Based on these results and the data reported earlier [80, 81], a dual retention mechanism involving absorption related to “weak-base ion exchange” and an added component for “surface adsorption” is the most probable mechanism for arsenic (III) uptake by clay sorbent. Such proposed model can be expressed as follows:

$$C_r = C_{abs} + C_{ads} = DC_{aq} + \frac{SK_L C_{aq}}{1 + K_L C_{aq}} \quad (4.11)$$

where, C_r and C_{aq} are the equilibrium concentrations of arsenic (III) ions onto the solid sorbent and in aqueous solution, respectively. The parameters C_{abs} and C_{ads} are the equilibrium concentration of arsenic(III) ions retained onto the used solid sorbents as an absorbed and adsorbed species, respectively, S and K_L are the saturation value for the Langmuir adsorption.

4.3.5. Thermodynamic characteristic of arsenic(III) retention onto clay sorbent

The nature of the retention process of arsenic (III) by the clay sorbent at pH 6-7 was determined by studying the retention behavior of arsenic(III) over a wide range of temperature (298.-353 k). The thermodynamic parameters (ΔH , ΔS , and ΔG) of arsenic (III) uptake onto clay were determined employing the following equations:

$$\ln K_c = \frac{-\Delta H}{RT} + \frac{\Delta S}{R} \quad (4.12)$$

$$\Delta G = \Delta H - T \Delta S \quad (4.13)$$

$$\Delta G = -RT \ln K_c \quad (4.14)$$

where, ΔH , ΔS , ΔG and T are the enthalpy, entropy, Gibbs free energy changes and temperature in Kelvin, respectively and R is the gas constant ($\approx 8.3 \text{ j mol}^{-1}$). K_c is the equilibrium constant depending on the fractional attainment (F_e) of the sorption process The values of K_c for the retention of arsenic(III) ions from the aqueous media of pH 6-7 at equilibrium onto clay was calculated employing the equation:

$$K_c = \frac{F_e}{1 - F_e} \quad (4.15)$$

The plot of $\ln K_c$ vs. $1/T$ (Fig.4. 24) was linear over the investigated temperature range (300-353 K). The numerical values of ΔH , ΔS and ΔG as calculated from the slope and intercept of Fig.4. 24 were found equal $- 21.74 \pm 0.6 \text{ kJmol}^{-1}$, $-3.25 \pm 0.32 \text{ Jmol}^{-1} \text{ K}^{-1}$ and $-975.3 \pm 3.8 \text{ kJmol}^{-1}$ (at 298 K), respectively with a correlation factor of 0.9998.

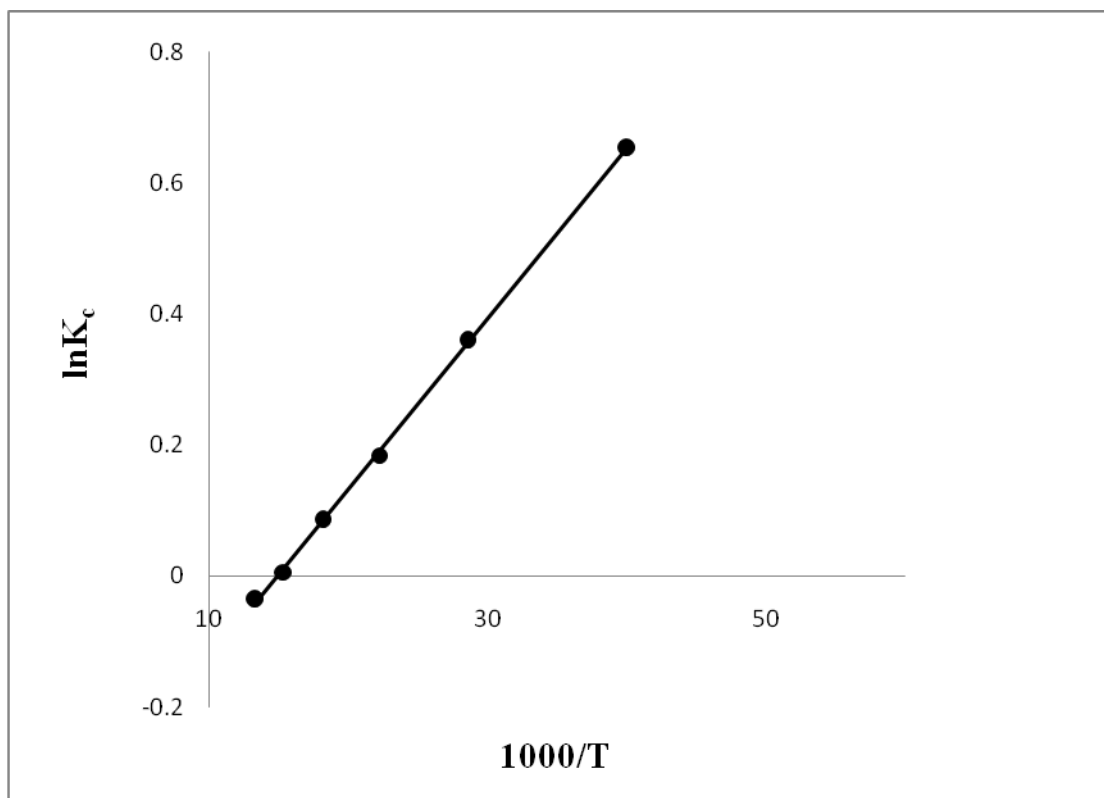


Fig.4.24. Plot of $\ln K_c$ of arsenic(III) sorption versus $1000/T$ (K^{-1}) from the aqueous solutions of pH 6-7 onto clay sorbent.

Considering the Van't Hoff equation and writing it in terms of the distribution ratio of arsenic, D , the following expression is obtained:

$$\log D = \frac{-\Delta H}{2.30 RT} + C \quad (4.16)$$

where, C is a constant. The values of D of arsenic (III) retention from aqueous media of pH 6-7 onto clay sorbent decreased on raising temperature. The plots of $\log D$ vs. $1000/T$ for the arsenic (III) retention onto clay sorbent was linear (Fig. 4. 25). The calculated value of ΔH for arsenic (III) sorption was found equal $-18.9 \pm 0.9 \text{ kJmol}^{-1}$ in good agreement with the data obtained from the equations 4.12.

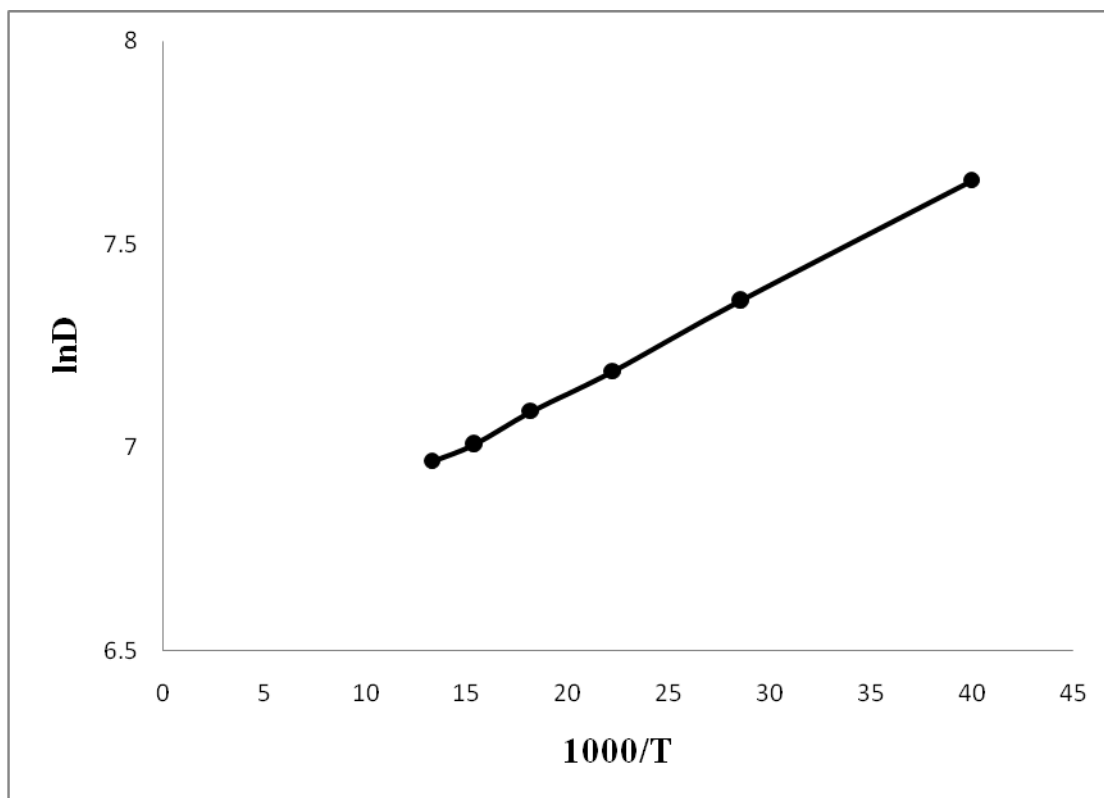


Fig.4. 25 Vant-Hoof plot of the distribution ratio (log D) vs. 1000/T (K⁻¹) for arsenic (III) retention onto clay sorbent.

The negative value of ΔH reflected the exothermic behavior of arsenic (III) uptake by the clay sorbent and non- electrostatics bond formation between the adsorbent and the adsorbate. The negative value of ΔS may be indicative of : i. moderated sorption step of arsenic(III) and ordering of ionic charges without a compensatory disordering of the sorbed ion associate onto the sorbent; ii. the freedom of motion of arsenic (III) is more restricted in the clay structure than in solution. Increasing temperature may affect the physical structure of clay and the strength of the intermolecular interactions between the clay structure and arsenic (III) ions. For example, igher temperature may cause the membrane matrix to become more unstructured and affect the ability of the polar segments to engage in stable hydrogen bonding with arsenic (III) ions, which would result in a lower extraction. The negative values of ΔG at 295 K indicate spontaneous and physico sorption nature of retention onto clay. The increase in the ΔG value with

temperature may be due to the spontaneous nature of sorption and is more favorable at low temperature confirming the exothermic sorption process. The energy of the active sites of clay minerals provided by raising temperature is most likely minimizes the possible interaction between the active sites of the clay and the complex arsenic(III) ions resulting a lower sorption percentage of the analyte. Thus, a dual-mode sorption mechanism involves both absorption related to “weak ion exchange” and an added component for “surface adsorption” seems a more probable model for arsenic(III) uptake. These results suggest the possible use of clay in packed mode for quantitative collection and chemical speciation of arsenic (III &V) after reduction of arsenic(V) to trivalence state.

4.3.6 Chromatographic separation of arsenic (III) by clay packed column

The kinetics and the sorption results of arsenic (III) towards clay suggested the application of clay packed column for chromatographic separation of arsenic (III) from distilled water samples. Thus, an aqueous solution (100 mL) of deionized waters at pH 6-7 arsenic(III) species at 0.01- 10 $\mu\text{g L}^{-1}$ concentration was percolated through the clay packed column separately at 5 mL min^{-1} flow rate. Analysis of arsenic in the effluent solutions against reagent blank under the same experimental condition revealed the absence of arsenic species indicating complete sorption of arsenic onto the clay packed column. A series of eluting agents e.g. HNO_3 , HClO_4 , HCl , thiourea (1.0 mol L^{-1}) and acetone was tested as proper eluting agents for arsenic (III) from clay packed column. Complete recovery (95.05-99.3 \pm 2.1 %) of the retained arsenic(III) species from the foam packed columns employing HNO_3 (1 mol L^{-1}) at 5 mL min^{-1} flow rate. Representative data of the extraction and recovery of arsenic(III) species

employing clay packed columns are summarized in Table 4.2. Thus, in the subsequent work nitric acid (1 mol L⁻¹) system was selected as a proper eluting agent for recovery of arsenic (III) from clay packed column. With HNO₃ (1 mol L⁻¹), the recovery percentage of arsenic was reproducible even at trace arsenic (III) concentrations in the test solution.

Table 4.2. Average recovery percentage (%) of arsenic(III) ions from deionized water by the developed clay packed column at 5 mL min⁻¹ flow rate[†]

As(III) added, µg L ⁻¹	Average As found, µg L ⁻¹	Average recovery [†] , %
0.05	0.051± 0.005	102± 2.9
1.0	1.03± 0.04	103 ± 3.9
5.0	5.1± 0.1	102.0 ± 2
10.0	9.8± 0.2	98.0 ± 2.0

[†] Average recovery (n=5) ± relative standard deviation.

The proposed clay packed columns was also tested for the collection and recovery of arsenic (V) species (0.01-10 µg mL⁻¹) from aqueous solutions after reduction to arsenic(III). A series of reducing agents such as KI-L-ascorbic acid [19]; sodium thiosulfate [22] and sodium sulphite- HCl was tested as proper reducing agents for complete reduction of arsenic(V) species to tri valent arsenic species. Among of these reducing agents, Na₂SO₃-HCl (1.0 molL⁻¹) system and boiling the aliquot of arsenic(V) species for five min was found the most suitable reducing system for arsenic (V) to arsenic (III). The extraction and recovery of arsenic(V) at concentration levels 1.0-10 µg mL⁻¹ (200 mL) after reduction with Na₂SO₃-HCl (1.0

molL⁻¹) system to arsenic (III) were tested employing clay packed column. The test solutions after adjustment of the pH 6-7 were percolated through the packed columns at 5 mL min⁻¹ following the recommended extraction procedure for arsenic(III) extraction and recovery. The results are summarized in Table 4.3. Satisfactory results were achieved with a recovery percentage in the range of 98±-105.0±2.4 %, n=5.

Table 4.3. Average recovery percentage (%) of arsenic(V) ions from deionized water by the developed clay packed column at 5 mL min⁻¹ flow rate[†]

As(III) added, µg L ⁻¹	Average As found , µg L ⁻¹	Average recovery [†] , %
0.01	0.011	110.0± 2.9
0.05	0.052± 0.005	104 ± 3.9
1.0	1.05± 0.04	105.0 ± 4
5.0	5.2± 0.1	104 ± 2.0

[†] Average recovery (n=5) ± relative standard deviation.

The extraction and recovery of the total inorganic arsenic(III) and arsenic(V) ions in their binary mixtures in the aqueous media by the developed clay packed columns were carried out. Satisfactory recovery percentage of various gold (I) and gold (III) species was obtained in the range 95.3 ±5.2- 104.3 ±3.7%.

The effect of flow rate (2-110 mL min⁻¹) on the uptake and recovery of arsenic (III) by clay packed column was examined by percolating 100 mL of distilled water spiked with arsenic (III). Complete retention of arsenic (III) was achieved quantitatively (>96%) at flow rate ≤ 5 mL min⁻¹. At flow rate higher than 5mL min⁻¹, the sorption performance of arsenic (III) ions decreased. The effect of the sample volume (0.1- 1.0

L) on arsenic(III) uptake was also investigated at 5 mL min⁻¹ flow rate. Complete retention (98.0±4.5 %, n=5) was achieved.

4.3.7 Analytical performance of the developed clay packed columns

The performance of clay packed column was generally determined via number (N) and the height equivalent to the theoretical plate (HETP). Thus, the performance (HETP& N) of clay packed columns (0.5 0g) was critically determined by passing an aqueous solution (1.0 L) containing arsenic (III) at 5 µg mL⁻¹ concentration levels at the optimum condition through the packed column at 5 mL min⁻¹. Complete sorption of arsenic (III) took place as indicated from ICP-OES analysis of arsenic in the effluent. The retained arsenic(III) species were then eluted from the clay packed column with nitric acid (20mL, 1.0 molL⁻¹). A series of fractions (10.0 x 2mL) of the eluent solutions at 3 mL min⁻¹ were then collected and analyzed for arsenic. The results are shown in Fig.4.26. The HETP and the number of theoretical plates N were then evaluated from the elution curve employing Gluenkauf equation [82]:

$$N = \frac{8 V_{\max}^2}{W^2} = \frac{L}{\text{HETP}} \quad (4.17)$$

where, V_{\max} = volume of eluate to peak maximum, W = width of the peak at 1/e times the maximum solute concentration and L is the length of the foam bed in mm. The N and HETP values were found equal 91 ± 2 and 1.05 ± 0.03 mm, respectively. The N and HETP of clay packed column were also calculated from the breakthrough capacity curve. method. The values of N and HETP were in the range 80 ± 4 and 1.27 ± 0.04 mm, respectively in good agreement with the results obtained from the chromatogram method (Fig. 4.27). The critical and breakthrough capacity of arsenic(III) retained onto clay packed column were 1.64 and 1.9 mg/g of arsenic (III)

uptake per one gram of the sorbent at flow rate of 5 mL min^{-1} . The lower limits of detection (LOD) and quantification (LOQ) [83] under the optimum experimental conditions were found 0.03 and $0.099 \text{ }\mu\text{g/mL}$, respectively. Such limits could be improved to lower value by increasing the volume of the aqueous phase containing ultra trace concentration of arsenic (III) at the optimum condition.

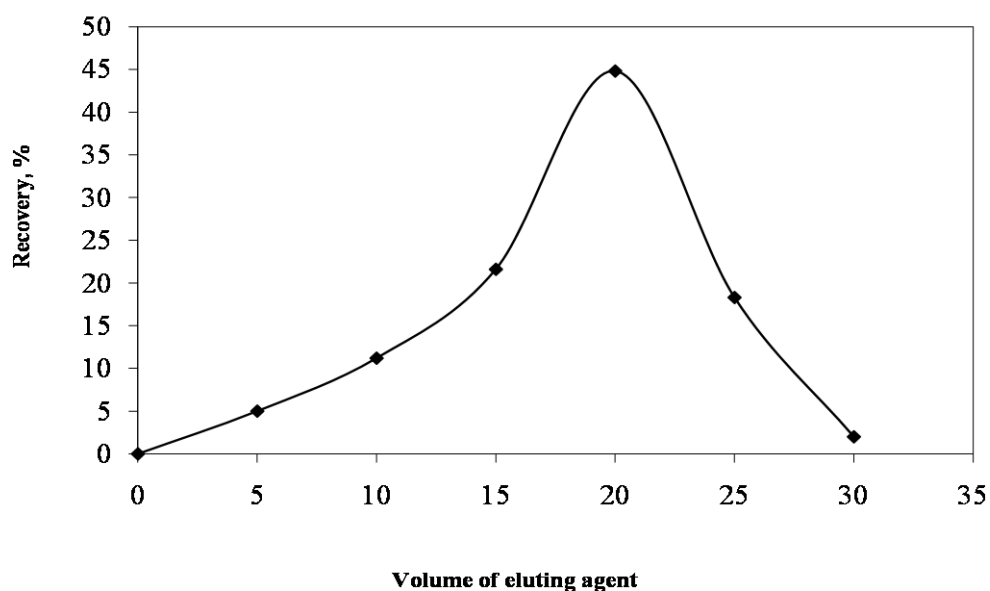


Fig.4.26. Chromatogram of recovery of arsenic (III) recovery from the aqueous solution by clay packed column using nitric acid as eluting agent at 3 mL min^{-1} flow rate.

4.3.8 Analytical applications of clay packed column

The accuracy of the developed method was successfully assessed by performing the recovery tests in the spiked tap- and wastewater samples with arsenic (III) ions. The water samples were first acidified with phosphoric acid and filtered through a 0.45 μ m cellulose membrane filter. An aqueous solution (1000 mL) of the water sample was then spiked with arsenic (III) & (V) species at a total concentration of 5 μ g/mL. The test solutions were then percolated through clay packed columns at 5 mL min⁻¹ at the optimum conditions described earlier for arsenic(V). Arsenic species were retained quantitatively as indicated from the analysis of arsenic in the effluent solution. The retained arsenic species were then recovered with nitric acid at 5.0 mL min⁻¹ as described and subsequently determined by ICP-OES. A comparison between the concentrations of arsenic obtained and that expected in the tested tap- and wastewater samples revealed satisfactory recovery percentage in the range 97.2-101.7% of arsenic ions. The acceptable agreement between arsenic concentration found and the expected value demonstrates the accuracy of the developed clay packed column towards arsenic for analysis of real samples. Clay packed column was also applied for the collection and recovery of arsenic (V) at concentrations 10 μ g L⁻¹ in tap water samples. The aliquot samples were first collected, filtered through a 0.45 μ m cellulose membrane filter and spiked with arsenic (III). The test solutions were then reduced as described, percolated through clay packed column at flow rate of 5 mL min⁻¹ and finally analyzed by ICP-OES as described for arsenic (III). A reasonable recovery percentage of 94.5 \pm 3.5 was achieved.

4.4. Conclusion:

Application of preconcentration/separation procedures is able to minimize limitations related to sensitivity and selectivity for arsenic determination in complex matrixes. The retention profile of arsenic onto clay sorbent revealed excellent sorption of arsenic(III) ions even at ultra concentrations in the aqueous phase. The kinetic data confirmed the intra-particle diffusion and the first order model for the retention step. The sorption step followed Langmuir and Freundlich adsorption isotherms. Clay packed column can be reused many times without loss in the column performance (N, HETP). The membrane-like structure of the clay is superior compared to any other known rigid or granular solid sorbent and permit rapid separation at relatively flow rate. The developed method is simple, reliable and low cost for the chemical speciation of arsenic (III) & (V). However, work is still continuing for investigating the influence of memory effect, organic material present in the investigated fresh water samples and competitive complexing agents in addition to the possible on-line chemical speciation of arsenic (III) and & (V) after reduction of the latter to arsenic (III).

4.5 References

1. M.L. Davis, D.A. Cornwell, McGraw-Hill. 2nd edn. (1991)
2. R.S. Oremland, P.R. Dowdle, S. Hoefy, J.O. Sharp, J.K. Schaepfer, L.G. Miller, J.S. Blum, R.L. Smith, N.S. Bloom, D. Wallschlaeger, *Geochimica and Geochimica Acta*, 64 (2000) 3073.
3. Forstner, U., Wittman, G.T., (1981) Springer-Verlag.
4. A. Gonzalez, M.L. Cervera, S. Armenta, M. de la Guardia, *Anal. Chim. Acta* 636 (2009) 129.
5. S. Wang, C.N. Mulligan, *Science of The Total Environment*, 366 (2006) 701.
6. D. Mohan, C.U. Pittman, *J. Hazard. Mater.* 142 (2007) 1.
7. D.P.L. Smedley, D.G. Kinniburgh, *Applied Geochemistry* 17 (2002) 517.
8. ATSDR “(2007), Division of Toxicology and Environmental Medicine ToxFAQs™, Atlanta, GA: U.S. Department of Public Health and Human Services, Public Health Service.
9. C.K. Jain, I. Ali, *Water Res.* 34 (2000) 4304.
10. D.B. Singh, G. Prasad, D.C. Rupainwar, V.N. Singh, *Water, Air, Soil Pollut.* Vol. 42 (1988) 373.
11. L. Lorenzen, J.S.J. Van Deventer, W.M. Landi, *Miner. Eng.* 8(4) (1995) 557 .
12. D. Mohan, C.U. Pittman *Hazard Mater.* 142 (2007) 1.
13. P. Mondal, C.B. Majumder, B. Mohanty, *Hazard Mater.*, 137 (2006) 464.
14. M. Kumaresan, P. Riyazuddin, *Curr. Sci* 80 (2001) 837.
15. M. Burguera, J.L. Burguera, *Talanta*, 44 (1997) 1581.
16. G.M.P. Morrison, G.E. Batley, T.M. Florence, *Chem. Brit.*, 25 (1989) 791.
17. Z.L. Gong, X.F. Lu., M.S. Ma, C. Watt, X.C. Le, *Talanta*, 58 (2002) 77.
18. H. Huang, P.K. Dasgupta, *Anal. Chim. Acta.* 380 (1999) 27.

19. M. Tuzen, K.O. Saygi, I. Karaman, M. Soylak, *Food and Chemical Toxicology*, 48 (2010) 41.
20. N.B. Issa, V.N. Rajaković-Ognjanović, A.D. Marinković, L.V. Rajaković, *Analytica Chimica Acta*, 706 (2011) 191.
21. K. Minakata, M. Suzuki, O. Suzuki, *Anal. Chim. Acta*, 631 (2009) 87.
22. N. Dirilgen, N. Dogan, H. Ozbal, *Anal. Lett.*, 39 (2006) 127.
23. R.A. Meyers, "Encyclopedia of Environmental Analysis and Remediation", John Wiley and Sons Inc., 1998.
24. R. Feeney, S.P. Kounaves, *Talanta*, 58(1) (2002) 23.
25. T.M. Florence, *Talanta*, 29 (1982) 345.
26. H. Xu, L. Zeng, S. Xing, G. Shi, J. Chen, Y. Xian, L.J. Jin, *Electrochem. Commun.*, 10 (2008) 1893.
27. H. Xu, L. Zeng, S. Xing, G. Shi, J. Chen, Y. Xian, L.J. Jin, *Electrochem. Commun.*, 10 (2008) 551.
28. E. Munoz, S. Palmero, *Talanta*, 65 (2005) 613.
29. G. Cepria, N. Alexa, E. Cordos, J.R. Castillo, *Talanta*, 66 (2005) 875.
30. H. Li, R. Smart, *Anal. Chim. Acta*, 325 (1996) 25.
31. W. Holak, *Anal. Chem.*, 52 (1980) 2189.
32. M D.S. Pereira, E. Winter, J.R. Guimaraes, S. Rath, *Environ. Chem. Lett.*, 5 (2007) 137.
33. Y. Sun, J. Mierzwa, M. Yang, *Talanta*, 44 (1997) 1379.
34. E. Viltchinskaia, L. Zeigman, D. Garcia, P. Santos, *Electroanalysis*, 9 (1997) 633.
35. P. Davis, G. Dulude, R. Griffin, W. Matson, E. Zink, *Anal. Chem.*, 50 (1978) 137.
36. C. Hua, D. Jagner, L. Renman, *Anal. Chim. Acta*, 201 (1978) 263.

37. F. Bodewig, P. Valenta, H. Nurnberge, Fresenius' Z, anal.Chem., 311(1982)187.
38. G. Forsberge, J. O'Laughlin, R. Megargle, S. Koirtyohann, Anal.Chem., 47 (1975)1586.
39. O. Zhang , H. Minami, S. Inoue , I. Atsuya, Analytica Chimica Acta, 508 (2004) 99.
40. B. Staniszewski ,P. Freimann, Spectrochimica Acta Part B. 63 (2008)1333.
41. A. Arafat, J.C. Jansen, A.K. Barakat, H. van Bekkum, In Synthesis of Zeolite Y with Different Aluminium Content Using Microwave Technology., Proceedings of the 9th International Zeolite Conference, July 5-10, Montreal, Canada., 1992.
42. H. OMRI, N. H. BAT Chem Sci Trans., 2(2) (2013) 357-366
43. H. Shibata, R. Brand, G. Mul, J.A. Moulijn, Surface Science and Catalysis 172 (2007) 249-252.
44. S.A. Tromp, G. Mul, Y. Zhang-Steenwinkel, M.T. Kreutzer, J.A. Moulijn, Catalysis Today 126 (2007)184-190.
45. T. Van Gerven, G. Mul, J. Moulijn, A. Stankiewicz, Chemical Engineering and Processing 46 (2007) 781-789.
46. W. Wei, M.S. Hamdy, J.C. Jansen, J.A. Moulijn, G. Mul, Surface Science and Catalysis 170B (2007) 1190-1196.
47. K.S. Yang, G. Mul, J.A. Moulijn, Electrochimica Acta 52 (2007) 6304
48. O. Berg, M.S. Hamdy, T. Maschmeyer, J.A. Moulijn, M. Bonn, G. Mul, J. Phys. Chemistry C 112 (2008) 5471.
49. P.Du, A. Bueno-Lopez, M. Verbaas, A.R. Almeida, M. Makkee, J.A. Moulijn, G.J. Mul, J. Catalysis 260 (2008) 75.

50. S. Telalovic, S.; Ramanathan, A.; Mul, G.; Hanefeld, U. J. Mater, J. Materials Chemistry(2010), 20, 642-658.
51. G. Mul, M.A. Banares, G. Garcia Cortez, B. van der Linden, S.J. Khatib, J.A. Moulijn, Phys. Chem. Chem. Phys. 5 (2003) 4378.
52. G. Mul, M.A. Banares, B. van der Linden, B.M. Weckhuysen, J.A. Moulijn, Abstracts of Papers, 226th ACS National Meeting, New York, NY, United States, September 7-11,(2003) .
53. G. Mul, I.E. Wachs, A.S. Hirschon, Catalysis Today 78 (2003) 327.
54. J. Perez-Ramirez, F. Kapteijn, J.C. Groen, A. Domenech, G. Mul, J.A. Moulijn, J. Catalysis 214 (2003) 33.
55. J. Perez-Ramirez, G. Mul, F. Kapteijn, J.A. Moulijn, Kinetics and Catalysis (Translation of Kinetika i Kataliz) 44 (2003) 639.
56. A. Anjum, P. Lokeswari, M. Kaur, M. Datta, J. Analytical Sciences, Methods and Instrumentals, 1 (2011) 25.
- 57.X. Jing,W. Feng, P. hong, Research J. Chem. Environ., 17 (2013) 41.
58. J. Hizal, R. Apak, J.Colloid and Interface Science 295 (2006) 1.
59. J. Perez-Ramirez, G. Mul, J.B. Taboada, F. Kapteijn, J.A. Moulijn, 2001 Clay Odyssey, Proc. Int. Clay Conf., 12th, Bahia Blanca, Argentina, July 22-28, (2001) (2003), 631-638.
60. A.R. Vaccaro, G. Mul, J. Perez-Ramirez, J.A. Moulijn, Applied Catalysis, B: Environmental 46 (2003) 687.
61. H.T.S. Britton, Hydrogen Ions.,_113-117,4th edn., London: Chapman and Hall, (1952).

62. M.H. Basyoni, M.A. El-Askary, N.A. Saad and R.J. Taj, *J. Sci. Res. Sultan Qaboos Univ.*, 7 (2002) 259.
63. R.J. Taj, M.A. El-Askary, N.A. Saad and M.H. Basyoni, *J. Marine Sci. Kau.*, 13 (2002) 93.
64. M. S. El-Shahawi, M.A. Othman , M. A. Abdel-Fadeel, *Anal. Chim. Acta*, 546 (2005) 221.
65. R. Feeney, S.P. Kounaves, *Talanta*, 58 (2002) 23-31.
66. K. Rzeszutek, A. Chow, *J. Membr. Sci.* 181 (2001) 265.
67. M.H. Mashahadziadeh, R. Mohyaddini, M. Skamsipur, *Sep. Purif. Technol.* 39(2004)161.
68. M. Bagheri, M.H. Mashahadziadeh, S. Razee, *Talanta* 60(2003)839.
69. S.Palagyi, T.Braun, Z.Homonnay and A.Vertes, *Analyst*, 117 (1992) 1537.
70. W.J.Weber Jr and J.C.Morris, *J.Sanit.Eng.Div.Am.Soc.Civ.Eng.*, 89 (SA2) (1963) 31.
71. W.J.Weber Jr and J.C.Morris, *J.Sanit.Eng.Div.Am.Soc.Civ.Eng.*, 90 (SA3) (1964) 70.72.
72. M.M.Saeed, A.Rusheed, *Radiochim. Acta*, 90(1) (2002) 35.
73. S.L.C.Ferreira, H.C.dos Santos, M.S.Fernandes, *J.Anal.At.Spectrom.*, 17 (2002) 115.
74. S. Lagergren, B.K. Sven, *Vatenskapsakad. Handl.*, (1898)24.
75. A.K. Bhattacharya, C.V`enkobachar, *J.Gviron. Eng.*, 110(1984)
- 110.S.Bhattacharya,
76. S.K.Roy and A.K.Chakraborti, *Anal.Chim.Acta*, 257 (1992) 123.
76. C.H.R.Nambiar, B.Narayana, B.Rao, R.Mathew, B.Ramachandra, *Microchem. J.*, 53 (1996) 175.

77. G.A.Somorjai” Introduction to Surface Chemistry and Catalysis” John Wiley& Sons, INC, 1994.
78. H. Freundlich "Colloidal Capillary Chemistry" Methuen, London, 1926.
79. L. Langmuir, J.Am. Chem.Soc., 40(1918) 136.
80. M.S.El-Shahawi, M.A.El-Sonbati, Talanta 67(2005) 806.
81. M.H.Cordoba, P.N.Navarro, I.L.Garcia, Intern.J. Environ. Anal.Chem. 32 (1988) 97.
82. A.B. Farag, M.H. Soliman, O.S. Abdel-Rasoul, M.S. El-Shahawi, Anal. Chim. Acta 601 (2) (2007) 218.
83. J.C.Miller, J. N. Miller "Statistics for Analytical Chemistry" Ellis-Horwood, New York, 4th edn., 1994.

Conclusion and concluding remarks

Within the frame work of the present thesis , the following remarks can be concluded:

- i. A favorable and highly stable stripping response peak for mercuric determination employing DP-CSV and TAR reagent was achieved with good precision, low detection limit and good linear dynamic range.
- ii. A low cost, precise and selective SW-CSV method for Pd determination at HMDE was developed. The method was free from most of the interferences present in chromatographic, spectrofluorimetric and spectrophotometric methods.
- iii. The potential usage of Saudi Arabia clay mineral in removal and chemical speciation of arsenic(III, V) fom aqueous solution by static and dynamic modes was carried out.
- iv. The adsorption capacity of As towards clay minerals was good compared to other conventional solid sorbents.
- v. Retention and kinetic processes of arsenite species in aqueous media towards clay minerals are mostly likely fitted on Langmuir-typr isotherm and first order reaction kinetics.
- vi. Local clay minerals can be used after modification with selective complexing agent and/ or nano particles of metal oxides for removal, separation and/ or chemical speciation of AS and other heavy metal ions in aqueous environment.
- vii. Research regarding the use of clay minerals either modified or not modifiedd is limited .

Future work

- i . The problem of environmental protection and pollution control has become one of modern man's precautions. Thus, primary and secondary prevention needs to be pursued through public health policy initiatives in future.
- ii. Preparation of modified clay minerals from local resources in Saudi Arabia with selective chromogenic agents to be used as low cost solid sorbent for minimizing pollution of industrial effluent should be investigated.
- iii. Preparation of nano clay minerals physically treated with nano particles e.g TIO_2 , Fe_3O_4 and other nano metal oxides for removal of hazardous heavy metals and organic compounds is of great importance to be examined.
- iv. Preparation of solid phase microextraction (SPME) system using modified nanoclay minerals for improving LOD and LOQ for ultra trace heavy metal ions in marine water, sediment and industrial wastewater is of great importance to be tested.
- v. Pre- concentration of ultra trace concentrations of the tested heavy metal ions by modified clay minerals followed by on-site DP-CSV and SW-CSV analysis will be tested. Such modification most likely provide short analytical time, ruggedness and precise to the analytical methodology.
- vi. Preparation of electrochemical nano sensors involving graphene/nanoclay; graphene/nafion, graphene/ multiwallcarbon nanotubes for improving LOD, LOQ, selectivity in stripping voltammetry and SWV SV for ultra trace metal analysis is of great importance to be tested in future.
- vii. In the quest of development of selective and low cost procedures for speciation of As, Hg and Pd by electrochemical nano sensors employing graphene-nafion, graphene-multiwall nanotubes and/ or graphene-hydroxy apatite nano particles should be ongoing.

Publications

List of articles, revised, submitted and under preparation from this work

1. M.S. El-Shahawi, A. Hamza and A.A. Bahaffi “ Characterization of Saudi Clay minerals and their Analytical Applications” J. Clay Minerals, 2013.
2. M.S. El-Shahawi, A. Arafat, A. Hamza and A.A. Bahaffi” Thermodynamics and Kinetic of Arsenic(III) Retention rom aqueous Media onto Saudi Arabia Clay Minerals. Submitted to Chemical Engineering Journal, 2013.
3. M.S. El-Shahawi, A. Hamza, and A.A. Bahaffi Sorption Characteristics and Chemical Speciation of Arsenic(III & V) in Water employing Clay Minerals Packed Column, Revised by Analytica Chimica Acta. to Chemical Engineering Journal, 2013.
4. M.S. El-Shahawi, A. Hamza, A. Al-Attas and A.A. Bahaffi Trace determinación of palladium in wáter by Square wave Direct adsorptive cathodic stripping voltammetry using 4-(2-thiazolylo) – resorcinol” submitted to Electroanalysis.
5. M.S. El-Shahawi, A. Hamza, A. Al-Attas and A.A. Bahaffi Trace Chemical Speciation of Mercury in Water by Direct adsorptive cathodic stripping voltammetry using 4-(2-thiazolylo) – resorcinol” To be submitted to J. Electroanalytical Chemistry.

نتائج الدراسة :

توصلت الدراسة إلى نتائج التالية :

1. امكن استحدث طريقة جديدة سهلة وفعالة لتقدير وتصنيف أيونات الزئبق الثنائي باستخدام تقنية الفولتامترية النزعي الكاثودي و ذلك بتفاعل الكاشف المخليبي (TAR) مع ايونات الزئبق الثنائي حيث تم اختزال المتراكب المتكون عند رقم هيدروجيني (pH 7.8) على قطب قطرة الزئبق المعلقة ،ومن ثم امكن تحديد الظروف المثالية باستخدام DPV differential pulse voltammetry بالنسبة للزئبق
2. أمكن دراسة السلوك الكهربى لمتراكب الزئبق مع المركب المخليبي قيد دراسته كما تم حساب العديد من الدوال المعيرة على كفاءة الطريقة قيد الدراسة $1.97 \times 10^{-10} \text{ mol L}^{-1}$.
3. استحداث طريقة فولتامترية انتقائية بسيطة في تقدير أيونات البلاديوم الثنائية بعد تكوينها متراكب مع المركب المخليبي (TAR) حيث تم اختزال المتراكب المتكون عند رقم هيدروجيني مناسب. تم تحديد الظروف المثالية للطريقة المقترحة وقد أظهرت هذه الطريقة استجابة خطية سريعة لمدى واسع من تراكيز أيونات البلاديوم الثنائية كما امكن حساب أقل تركيز وأمكن الكشف عن بداية التقدير LOQ ونهاية التقدير LOD لأيونات البلاديوم كما تم مقارنة نتائج الطريقة قيد الرسالة مع نتائج ICP-MS وقد أظهرت توافقاً جيداً ز
4. امكن دراسة السلوك الأستقبائى والسلوك الحركى (Kinetic Behavior) لأيونات الزرنيخ الثلاثى على الطين المحلى كصنف ثابت. امكن ايضا تحديد ميكانيكية عملية الفصل (Retention Mechanism) ودراسة تأثير درجة الحرارة على عملية الأستبقاء و من ثم تم حساب العديد من الدوال الدينامكية (Thermodynamic Parameters, ΔG , ΔS , ΔH) لأستبقاء ايونات لأيونات الزرنيخ الثلاثى باستخدام النمط الاستاتيكي
5. أمكن ايضا حساب السعه لأيونات الزرنيخ الثلاثى على الصنف الثابت كما تم تحضير عمود معبأ بالطين المحلى واستخدامه فى فصل وتقدير ايونات الزرنيخ الثلاثى والخماسى بعد اختزال الأخير .

الملخص العربي (Arabic Summary)

عنوان الرسالة:

زيادة التركيز والتقدير والتصنيف الكيميائي لتركيزات متناهية الصغر لبعض الملوثات غير العضوية في الأوساط المائية

هدف الدراسة:

في الآونة الأخيرة زاد الاهتمام بدراسة امكانية تحديد وإزالة العديد من العناصر الثقيلة من الأوساط المائية البيئة لما لها من خطورة عالية على صحة الإنسان و على النظام البيئي ومن ثم أصبحت حماية البيئة من مثل هذه الملوثات يعتبر من أهم القضايا الملحة في السنوات الأخيرة. في العصر الحالي . و مما لا شك فيه أن استخدام تقنيات رخيصة الثمن و دقيقة وتتميز بانتقائية عالية في تقدير وفصل العديد من الملوثات غير العضوية يعتبر إضافة جيد في مجال مجال الفصل الكيميائي و الكيمياء البيئية يعتبر إضافة و لهذا استهدفت الدراسة الآتي:

1. - استخدام طريقة جديدة لتقدير أيونات الزئبق الثنائي و البلاديوم الثنائي في عينات مياه بواسطة طرق الإمتزاز الكاثودي النزعي (Differential Pulse Adsorptive-Cathodic Voltammetry) و تقنية square wave (الموجة المربعة في النزح الفولتامترى الكاثودي Square Wave Adsorptive-Cathodic Voltammetry على قطب الزئبق المعلق).
2. - دراسة ميكانيكية عملية الإختزال بواسطة طريقة الإمتزاز الفولتامترى النبضي لأيونات الزئبق الثنائي و البلاديوم الثنائي مع المرتبط قيد الدراسة.
3. استحداث طرق جديدة سهلة و رخيصة للفصل والتصنيف الكيميائي لأيونات الزرنيخ الثلاثي والخماسي في الأوساط المائية المختلفة مثل مخلفات الصرف الصناعي السائلة كنواتج للعديد من العمليات الصناعية بواسطة استخدام طرق الإدمصاص على سطح صلب من الطين اوالطين المحلى (Local Clay) بعد فصله وتجهيزه باستخدام طرق التعويم المعروفة. ولاشك ان هذا النوع من الطين متوفر في المملكة العربية السعودية كخامات أولية.

إجراءات الدراسة:

تضمنت الدراسة الفعاليات التالية:

- 1- دراسة العوامل المختلفة على تقنية الفولتامترى النزعي المهبطي (CSV) على قطب قطرة الزئبق المعلقة لتقدير الزئبق الثنائي و البلاديوم الثنائي باستخدام أحد مركبات الأزو و من ثم دراسة إمكانية تقدير الزئبق و البلاديوم في عينات المياه.
- 2- دراسة إمكانية استخدام الطين المحلى في فصل و تقدير أيونات الزرنيخ الثلاثي والخماسي من الأوساط المائية باستخدام النمط الاستاتيكي و كرماتوجرافيا العمود.

المستخلص العربي (Arabic Abstract)

عنوان الرسالة:

زيادة التركيز والتقدير والتصنيف الكيميائي لتركيزات متناهية الصغر لبعض الملوثات غير العضوية في الأوساط ألمانية

تضمنت الدراسة الأتي:

من المعروف إن العيد من مركبات الأزو والمحتوية على أكثر من مركز نشط مثل مجموعة الهيدروكسي لها المقدرة الفائقة لتكوين العديد من المركبات المخليبية مع العديد من العناصر الفلزية السامة في الأوساط المائية ذات الأرقام الهيدروجينية ومن ثم تضمنت الدراسة الأتي: إمكانية وتقدير ايونات الزئبق على قطب قطرة الزئبق المعلق في محلول منظم من بروتين - روبنسون والحصول على قمة اختزال غير عكسية وذلك باستخدام الفولتامترى النزعي الكاثودي النبضي التفاضلي عن طريق تكوين معقد فلزي مع الكاشف المخليبي TAR و أيضا تحديد أفضل الظروف لزيادة حساسية الطريقة المقترحة و إثبات أن عملية الاختزال غير عكسية وقد أمكن الحصول على نهاية كشف ونهاية تقدير عالية في تقدير ايونات الزئبق في الأوساط المائية. اضافة الى ذلك تم استحداث طريقة لتقدير البلاديم باستخدام الفولتامترى النزعي الكاثودي بتكوين متراكب مخليبي مع الكاشف العضوي TAR. تم دراسة تأثير معدل المسح في تقنية الفولتامترى الدائري ومن ثم تم تحديد ميكانيكية تفاعل القطب الكاثودي على قطب الزئبق المعلق. أمكن ايضا فصل واستخلاص ايونات الزرنيخ الثلاثي في مخلفات مياه الصرف الصناعي بتطبيق طريقة مستحدثة يتم فيها ادمصاص ايونات الزرنيخ بواسطة الطين المحلى (Local Clay) كصنف صلب ثابت ,ومن ثم دراسة السلوك الأستبقائي لايونات الزرنيخ الثلاثي والخماسي بالطرق الأستاتيكية كما تم ايضا استخدام كروماتوجرافيا العمود على الصنف الثابت المستخدم.

زيادة التركيز والتقدير والتصنيف الكيميائي لتركيزات

متناهية الصغر لبعض الملوثات غير العضوية في

الأوساط المائية.

أمل علي محمد باحفي

(ماجستير علوم – كيمياء تحليلية)

بحث مقدم لنيل درجة الدكتوراة في العلوم- الكيمياء

(الكيمياء التحليلية)

إشراف

أ.د. أميرة العطاس

أ.د. عبد الغني حمزة

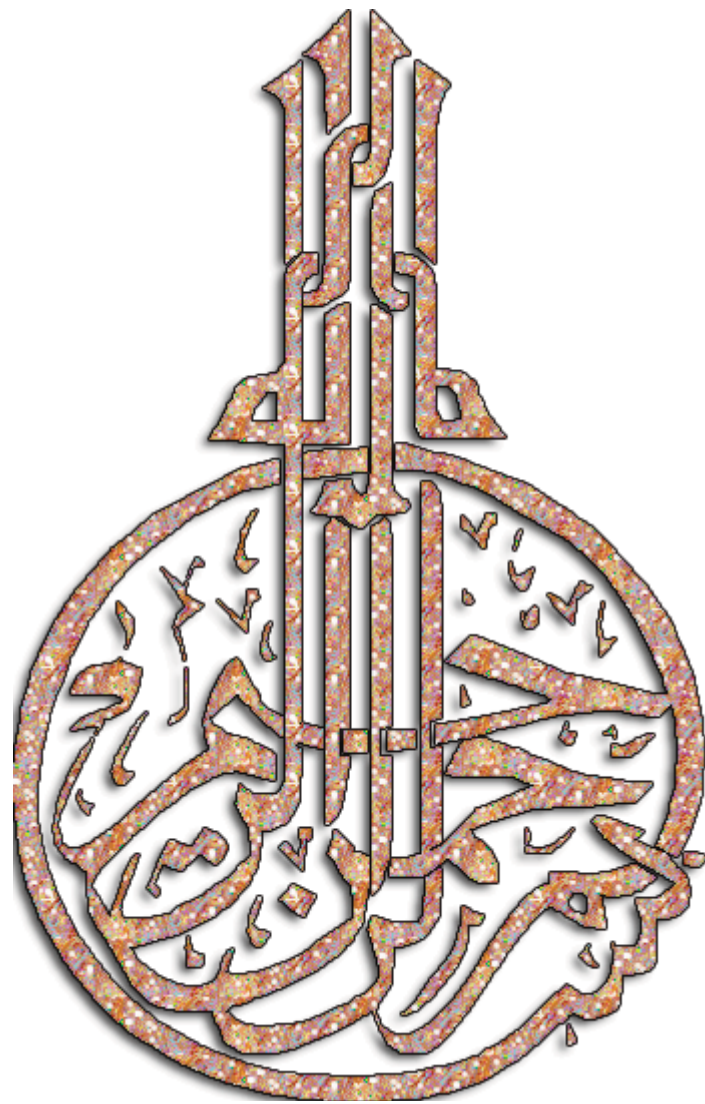
أ.د. محمد سرور الشهاوي

كلية العلوم

جامعة الملك عبد العزيز

جده- المملكة العربية السعودية

رجب 1434 هـ - مايو 2013 م



زيادة التركيز والتقدير والتصنيف الكيميائي لتركيزات

متناهية الصغر لبعض الملوثات غير العضوية في

الأوساط المائية.

أمل علي محمد باحفي

(ماجستير علوم – كيمياء تحليلية)

بحث مقدم لنيل درجة الدكتوراة في العلوم- الكيمياء

(الكيمياء التحليلية)

كلية العلوم- قسم الكيمياء

جامعة الملك عبد العزيز

جدة – المملكة العربية السعودية

رجب 1434 هـ - مايو 2013